Strategies for improved enzymatic hydrolysis of lignocellulose

Thesis submitted under the Faculty of Science of the
Cochin University of Science and Technology
For the award of degree of

Doctor of Philosophy

In

BIOTECHNOLOGY

Vani Sankar

Reg. No. 4352

Centre for Biofuels

Biotechnology Division
CSIR-National Institute for interdisciplinary Science and technology
Thiruvananthapuram 695019, India
November 2015

Council of Scientific and Industrial Research, Government of India
National Institute for Interdisciplinary Science and Technology
Pappanamcode, Thiruvananthapuram 695019, Kerala, India
Phone: +91 471 2515368, Fax: +91 471 2491712
Email: rajeevs@niist.res.in | rajeev.csir@gmail.com

Centre for Biofuels
Biotechnology Division

Dr Rajeev K Sukumaran, MSc, PhD, PGDBi
Senior Scientist & Head
Biofuels and Biorefineries Section

19 November 2015

DECLARATION

I hereby declare that the work presented in this thesis entitled "**Strategies for improved enzymatic hydrolysis of lignocellulose**" is a *bona fide* record of the research carried out by **Ms Vani Sankar** (Reg No. 4352) under my guidance and supervision and under the co-supervision of Dr S Savithri, Senior Principal Scientist of Computational Modeling and Simulation Section, of the Process Engineering and Environmental Technology Division, at the Centre for Biofuels, Biotechnology Division, CSIR-National Institute for Interdisciplinary Science and Technology, Thiruvananthapuram, India. I declare that all suggestions made by the audience during pre-synopsis seminar and recommended by the Doctoral committee have been incorporated in the thesis. I also declare that this work or no part of it has been submitted elsewhere for the award of any Degree, Diploma, Associate ship or any other title or recognition

Rajeev Kumar Sukumaran

Dr S Savithri
Senior Principal Scientist
Computational Modeling & Simulation Section
Process Engineering and Technology Division
Phone: +91 471 2515264, Fax: +91 471 2491712
Email: sivakumarsavi@gmail.com

Thiruvananthapuram
19 November 2015

CERTIFICATE

This is to certify that the work embodied in the thesis entitled "**Strategies for improved enzymatic hydrolysis of lignocellulose**" has been carried out by Ms. Vani Sankar (Reg. # 4352) under my supervision at the Centre for Biofuels, Biotechnology Division of CSIR – National Institute for Interdisciplinary Science and Technology, Thiruvananthapuram, and the same has not been submitted elsewhere for a degree.

(S. Savithri)

Thesis Co - Supervisor

Thiruvananthapuram

19 November 2015

DECLARATION

I hereby declare that the work presented in this thesis entitled **"Strategies for improved enzymatic hydrolysis of lignocellulose"** is original work done by me under the supervision of Dr Rajeev Kumar Sukumaran and co-supervision of Dr S Savithri, at the Centre for Biofuels, Biotechnology Division of CSIR – National Institute for Interdisciplinary Science and Technology, Thiruvananthapuram, India. I also declare that this work did not form part of any dissertation submitted for the award of any degree, diploma, associateship, or any other title or recognition from any University/Institution.

Vani Sankar

Acknowledgements

Words would fail to express my gratitude to my research supervisor, Dr Rajeev K Sukumaran, Senior Scientist, Centre for Biofuels, Biotechnology Division, CSIR - National Institute for Interdisciplinary Science and Technology (NIIST), Trivandrum. His research strategies, scientific and professional ethics, vision, dynamic attitude, quest for perfection and most importantly the work-freedom he provided, all have helped me shape this thesis the way it is now. If it was not for him, I do not think I could have completed my thesis in a successful manner.

Now, it is with a deep sense of gratitude I acknowledge my research co-supervisor, Dr S Savithri, Senior Principal Scientist, Computational Modeling Section (CMS), Process Engineering and Environmental Technology (PEET) Division, NIIST. Without her support, I could never have had the confidence to pursue research in an area that I had never heard of earlier. The passion with which she has corrected this thesis is just unique to her. I thank her for being a caring and wonderful person brimming with optimism that she has been to me always.

More to this, I owe my gratitude to Dr R Panneerselvam, DST Fast Track Scientist, CMS Section, PEET Division, NIIST for helping me with computational fluid dynamics modeling. Had it not been for his patient help and guidance, I would never have been able to complete my work on time.

Again, here go my sincere thanks to Dr Ashok Pandey, Head, Centre for Biofuels and Biotechnology Division, NIIST, for the support and help he provided throughout the course of my stay at NIIST. I really admire him for efficiently managing all his professional activities with an unparallel zeal and commitment.

It is now my privilege to acknowledge Dr A Ajayaghosh and Dr Suresh Das (present and former directors of NIIST respectively), for providing me the necessary research facilities at the institute. I also thank Dr Gangan Prathap (former acting director of NIIST) for being the chairperson during my pre-synopsis presentation and for giving valuable suggestions that helped me improve a lot thematically and systematically.

I would also like to acknowledge the Council for Scientific and Industrial Research (CSIR), New Delhi, for providing me financial assistance in the form of Senior Research Fellowship.

I need to take this opportunity to be grateful to scientists and technical staff at Biotechnology Division as well for their valuable support and comments during my research. Special thanks to Dr Leena and Dr Anil for helping me with HPLC analysis of my samples.

Here, I would like to thank Dr KSMS Raghavarao, chief scientist, Department of Food Engineering and Mr Dhaneesh, technical assistant, CSIR - Central Food Technological Research Institute (CFTRI), Mysore, for helping me with particle size analysis. I would also like to thank Amrutha and Hrishi (Senior Research Fellows at CFTRI) for making my stay there a pleasant one.

I extend my heartfelt gratitude to Ms Minu M, Senior Design Engineer, BiOZEEN, Bangalore, for her valuable help during fixing of reactor dimensions, while I would also like to thank Mr Tinu V G, Technical Leader, CADD Centre, Trivandrum, for his patient help in drawing the reactor designs.

I also extend my sincere thanks to Dr Sarita G Bhat, Associate Professor, Department of Biotechnology, CUSAT, expert member of my Doctoral Committee for providing valuable comments and suggestions that helped in improving the quality of my work immensely.

I am here to extend my gratefulness to Mr Peer Muhammad, Mr M R Chandran, Mr Ashwin, technical staffs at NIIST for helping me with various analyses. I would also like to be grateful to Mr Nagendra Baku, Mr George, Ms Vineetha, Ms Linsha, Mr Sreejith, Mr Prakash S P, Ms Divya Phillips, Ms Vindhya, Ms Arya, Mr Shaban and other friends at NIIST for helping me in my work.

I owe my passion for research and understanding of scientific temperament to my Professor, Dr K Murali Manoj, Former Head of the Department, METS School of Engineering, Thrissur.

Further, I am indebted to my friends at Biotechnology Division, NIIST for their support during my stay there. In particular, to Meena, Sabeela, Aravind, Leya, Rajasree, Arya, Akanksha, Varsha and Vaisakhi for all the good times that we shared together and support extended to me in the form of fruitful discussions. I would also like to thank Vishnu, Dileep and Sujith for helping me with the laborious milling and pretreatment of biomass. I am also indebted to Bimal for helping with formatting of thesis chapters.

And for sure I need to extend my gratitude to my in-laws as well for their support during my stay at their place.

I can't now leave this opportunity to thank my sister Veena, for being my emotional support throughout these years. I can never explain how a heartwarming gossip with her used to rejuvenate me at the end of a tiring day.

All said, I don't think I can thank Vivek, my better half, enough for being there whenever I needed a help. Thanks for always being my one point solution for all problems. I don't think not many, like him, can stay awake till 3.00 am after a long day at work, and give a company when I was writing thesis.

Finally, my words fall short, if I have to thank my parents. I could never have reached where I am today without their constant encouragement and belief in me. It is their dream that builds my life.

LIST OF PUBLICATIONS

SCI Journals

1. **Vani S**, Sukumaran RK, Savithri S. Prediction of sugar yields during hydrolysis of lignocellulosic biomass using artificial neural network modeling. Bioresource Technol. 2015. http://dx.doi.org/10.1016/j.biortech.2015.01.083.

2. **Vani S**, Binod P, Kuttiraja M, Sindhu R, Sandhya SV, Preeti VE, Sukumaran RK, Pandey A. Energy requirement for alkali assisted microwave and high pressure reactor pretreatments of cotton plant residue and its hydrolysis for fermentable sugar production for biofuel application. Bioresource Technol. 112 (2012) 300-307.

Book Chapters

1. Rajeev K. Sukumaran, **Vani Sankar**, Aravind Madhavan, Meena Sankar, Vaisakhi Satheesh, Ayman Salih Omar Idris, Ummalyama Sabeela Beevi. Enzyme Technologies: Current and Emerging Technologies for Development of Novel Enzyme Catalysts. In: Chandrasekaran M (Eds), Enzymes in Food and Beverage Processing, CRC Press, ISBN: 13: 978-1-4822-2128-2, (2015), 39-66.

Conference Papers/Presentations/Posters

1. **Best Poster award:**
   Sankar Vani, Sivaraman Savitri, Rajeev K Sukumaran. An Artificial Neural Network model for predicting the effect of substrate loading and particle size on sugar yields during enzymatic biomass hydrolysis. Poster presented in International conference on Emerging Trends in Biotechnology 2014, held at Jawaharlal Nehru University, Delhi from 6-9th November 2014.

2. **Sankar Vani**, Sivaraman Savitri, Rajeev K Sukumaran. Design of enzyme cocktails for biomass deconstruction: A model for predicting sugar yields of lignocellulose saccharifying enzyme blends. Poster presented in International conference on Industrial Biotechnology 2012, held at Panjabi University, Patiala, from 21-23rd November 2012.

CONTENTS

Chapter 1
Introduction and Review of Literature

1. Introduction

The energy consumption of a nation is by large an indicator of its progress and the rapid industrialization and steadily increasing world population has led to an overwhelming rise in energy consumption. The major resources catering to this increased energy demand is fossil fuels, including crude oil, coal and natural gas. As a result of increasing fossil fuel usage, these resources would be exhausted in the near future (Wyman, 2001). Campbell and Laherrere (1998) had used various techniques to estimate the current known crude oil reserves and the reserves as yet undiscovered and had concluded that the decline in worldwide crude oil production would begin before 2010. They also predicted that annual global oil production would decline from the current 25 billion barrels to approximately 5 billion barrels in 2050.

Apart from depletion of fossil fuels, increased usage of these resources leads to enhanced greenhouse gas (GHG) emission. Greenhouse gases (GHGs) such as carbon dioxide (CO_2) from fuel combustion contributes to global warming, with the 2010 global CO_2 emissions from fuel combustion estimated at 35.3 giga-tonnes CO_2 (68% increase from 21.0 Gt CO_2 in 1990). This amount of emitted CO_2 is spread among fuels such as coal at 43%, oil at 36%, and natural gas at 20%. CO_2 emissions from the transportation sector were estimated to be 22% of the total CO_2 emissions in 2010 and the current trends can also be expected to be similar. Higher GHG emissions have lead to a rise in global average temperature to the tunes of 3.6 °C above pre-industrial levels (IEA, 2012a; IEA, 2012b).

To mitigate the adverse effects of greenhouse gas (GHG) emissions on the environment and declining petroleum reserves, alternative energy sources that are sustainable and environmentally friendly have to be found out (Mabee et al., 2005). As a result, there is renewed interest in the production and use of fuels from plants or organic waste.

India is the world's fourth largest energy consumer and the largest consumer of crude and petroleum products after the United States, China and Japan. The net oil imports of the country rose from 43% in 1990 to 71% in 2012. Transport sector is the major consumer (around 51%) of petroleum products. Nearly 70% of diesel is consumed by the transport sector and the demand is expected to grow at 6–8% in the coming years parallel with a steady increase in vehicle ownership. Crude oil prices have been fluctuating and have increased to more than $140 per barrel (National Policy on Biofuels, 2015).

Bioethanol is considered as an important renewable fuel capable of at least partly replacing fossil-derived fuels (Sheehan et al., 1998; Caledria et al., 2003; Demain et al., 2005; Hill et al., 2006; Ragauskas et al., 2006). The world production of bioethanol increased from 50 million m^3 in 2007 to over 100

million m^3 in 2012 (Kang et al., 2014). The agreement implemented by Policy Energy Act (2005) followed by the Energy Independence and Security Act (EISA, 2007) aims to reach 36 billion gallons of bioethanol by the year 2022.

1.1. Global status of bioethanol research and production

In the U.S., major source of bioethanol is corn starch while in Brazil biofuel is mainly produced from sugarcane juice and molasses. Together, these two countries account for 89% of the global bioethanol production. There is a worldwide increase in research to develop alternative fuel from feed stocks to replace gasoline (Goldemberg, 2007). Bioethanol is chiefly extracted from starch sources such as corn in the North America whereas in South America, biofuel is produced from sugars including sugarcane and sugar beets (Wheals et al., 1999). European biofuel production is just 5% of the worldwide bioethanol production (Gnansounou, 2010). France and Germany are pioneers in biodiesel production and their combined annual production is approximately 56% of the global production mainly because of the rising importance of diesel engines and feedstock opportunity costs (European Union, 2009). Although other countries in the world collectively account for only 5% of the global bioethanol production, China, Thailand and India are directing research towards agricultural biotechnology and are emerging as potential biofuel producers (Swart et al., 2008).

In the U.S., biofuel is mostly derived from corn (Department of Energy, 2009). According to the renewable fuels association (2010) statistics, the production of bioethanol reached highest in the U.S. by year 2009 with capacity reaching 10.9 billion gallons (41.26 billion liters) representing 55% of the worldwide production. In the year 2010, corn-based ethanol production reached 12.82 billion gallons (48.52 billion liters) with the largest capacity in Iowa (28%) followed by Nebraska (13%) (Official Nebraska Government website, 2009).

Corn and sugar based first generation ethanol are not sufficient to replace a considerable portion of the one trillion gallons of fossil fuel presently consumed worldwide each year (Bell and Attfield, 2006). Ethical concerns about the use of food as raw materials for fuel production have encouraged research efforts to be directed to develop processes for bioethanol production from inedible feedstock alternatives (Taherzadeh, 1999; Sun and Cheng, 2002).

1.2. Advantages of lignocellulosic ethanol over first generation biofuel and petroleum products

The major advantage of lignocellulosic biomass materials over first generation biofuel substrates is that this is a renewable substrate for bioethanol production that does not compete with food production and animal feed. Apart from this, these lignocellulosic materials also contribute to environmental sustainability (Demirbas, 2003). The ready availability of lignocellulosic biomass from different low-cost raw materials such as municipal and industrial wastes, wood and agricultural residues also favor second generation bioethanol production (Cardona and Sanchez, 2007). At present, the most promising lignocellulosic feed stocks in the U.S., South America, Asia and Europe are corn stover, sugarcane bagasse, rice and wheat straws, respectively (Kadam and McMillan, 2003; Knauf and Moniruzzaman, 2004; Kim and Dale, 2005; Cheng et al., 2008b).

Figure 1.1: Comparison of petroleum based fuel, first and second generation biofuels

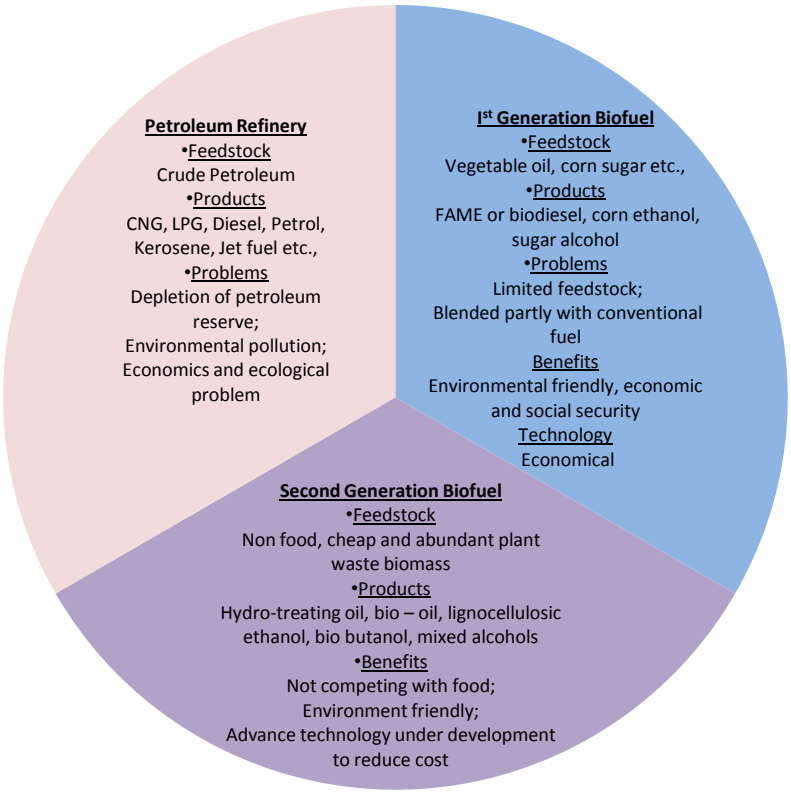

Apart from these, other major benefits of biofuels are lower emissions of green house gases, sustainability, consumption of waste, biodegradability, lower strain on earth by reducing requirement for mining, increased employment, reduced dependence on foreign sources for energy as feed stocks are

generally locally available resources; etc. The comparative advantages of second generation biofuel over petroleum and first generation fuel are as shown in Figure 1.1.

On a full fuel-cycle basis, corn ethanol has the potential to reduce GHG emissions by as much as 52% over petroleum-based fuels. Ethanol made from cellulosic biomass has the potential to reduce greenhouse gas emissions by as much as 86% (Wang et al., 2007). The comparative greenhouse gas emission reductions upon first and second generation biofuel usage are represented in Figure 1.2. Production of ethanol fuel requires less fossil energy than its petroleum-based counterpart. Cellulosic ethanol requires only ten percent of the fossil energy required to deliver a gallon of liquid transportation fuel on an energy equivalent basis compared to gasoline.

Figure 1.2: Green house gas emission reductions

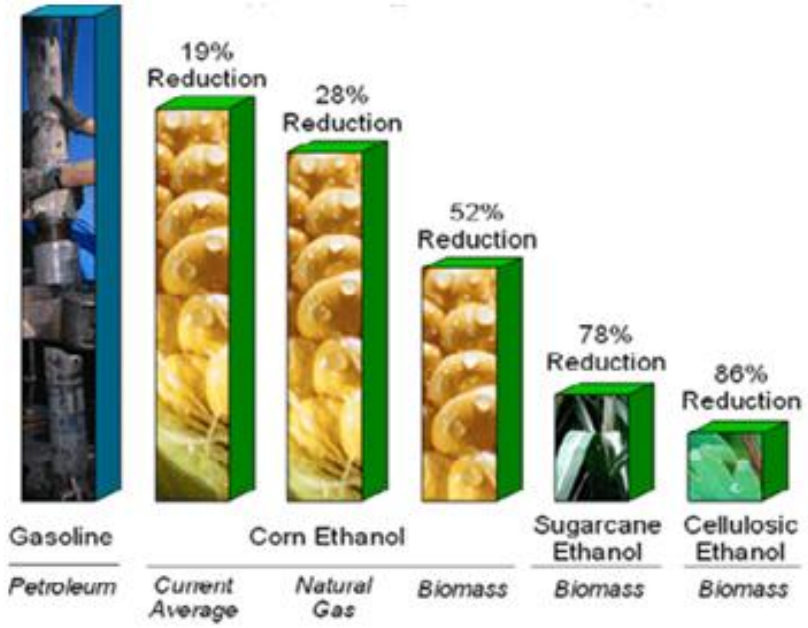

(Source; Wang et al., 2007)

The main reasons for the enhanced development of bioethanol are its use as a favorable and near carbon neutral renewable fuel, thus reducing CO_2 emissions and associated climate change. Its use as octane enhancer in unleaded gasoline and its use as oxygenated fuel-mix for a cleaner combustion of gasoline reduce tailpipe pollutant emissions and improve the ambient air quality. The largest single use of ethanol is as engine fuel and fuel additive. Fuel properties of ethanol are given in Table 1.1. High octane number and energy density make it ideal for use in engines.

Table 1.1: Fuel properties of ethanol

Fuel Characteristic	Methanol	Ethanol	Gasoline
Energy Density (MJ/L)	16	19.6	32
Air-Fuel ratio	6.5	9.0	14.6
Heat of vaporization (MJ/Kg)	1.2	0.92	0.36
Research octane number	136	129	91-99
Motor octane number	104	102	81-89

(Source: Lee et al., 2008)

Liquid biofuels for motor vehicles use biomass feed stock that have captured atmospheric CO_2, and therefore acts as a sink rather than a source for further CO_2 emissions. Table 1.2 details the relative reductions in GHG and other emissions in ethanol blends of gasoline. Ethanol is also used as octane number enhancer in place of MTBE, the latter considered as causing carcinogenic emissions upon fuel combustion.

Table 1.2: Reductions in Emission in Ethanol Blends of Gasoline

Emission	Low-level Blends (i.e., E10)	High-level Blends (i.e., E85)
Carbon Monoxide (CO)	25-30% decrease	25-30% decrease
Carbon Dioxide (CO_2)	10% decrease	Up to 100% decrease (E100)
Nitrogen Oxides (NO_x)	5% decrease	Up to 20% decrease
Volatile Organic Carbons (VOC's):	7% decrease	30% or more decrease
Exhaust Evaporative	No change	Decrease
Sulfur Dioxide (SO_2) and Particulate Matter	Decrease	Significant decrease
Aldehydes	30-50% increase (but negligible due to catalytic converter)	Insufficient data
Aromatics (Benzene and Butadiene)	Decrease	More than 50% decrease

(Source: Farrell et al., 2006; Dutcher et al., 2011; Graham et al., 2008)

1.3. Bioethanol from lignocellulosic biomass: Indian Scenario

India is the 4th largest petroleum consumer in world, 5th largest primary energy consumer in the world and stands 6th in energy demand in the world. India is also the world's 4th largest contributor to carbon emissions. Also, on-road vehicle population in India has increased from 49 million to more than 65 million vehicles over the last five years and is expected to grow annually by 8 to 10 per cent.

To develop alternative biofuel, India does not have surplus molasses to meet fuel demand (National Policy on Biofuel, 2015). Edible sugar sources (Grains, Cane, Tubers etc.) cannot be used for fuel. As of present day, 5% blending of ethanol with gasoline is mandatory in 9 states (demand 0.59 billion liters). The demand for ethanol is 1.17 billion liters if a 10% blend is used. Oil marketing companies have managed to achieve only 1.37% blending of ethanol with gasoline as compared to the 5% they are mandated to blend in the current year. 5% blending target would mean about 2.2 billion litres of ethanol would be required by 2017.

Even if the entire available molasses is made into ethanol, it can barely support the current demand and will not be able to support the future demands on ethanol. Alternative feedstock needs to be investigated for a self reliance on this future fuel. So to provide energy security to the country which produces only 23% of its petroleum requirements indigenously and reduce its GHG emissions, a national biofuel policy was framed by Ministry of New and Renewable Energy (MNRE), Government of India. The major objectives of the policy are as given below:

- Indicative target of 20% by 2017 for the blending of biofuels – bioethanol and bio-diesel. But it was revised to 5% blending due to lower ethanol production rates.
- Envisage development of next-generation, more efficient biofuel conversion technologies based on new feed stocks.
- Minimum Support Price (MSP) mechanism to ensure a fair price for bio-diesel oilseed growers.
- Minimum Purchase Price (MPP) for the purchase of bio-ethanol by the Oil Marketing Companies (OMCs).
- Bio-diesel production to be taken up from non-edible oil seeds in waste / degraded / marginal lands (National Policy on Biofuels, 2015).

1.3.1. Lignocellulose Biomass availability in India

India does not have surplus vegetable oil and biodiesel production should depend on imported oil. The nation does not have land resources to support the cultivation of oil crops or any energy crops at levels which can meet the production demand. More than 90% of the cereal crop residues are used domestically. 51% of the total land area in India is cultivated off which majority is rain fed. India generates ~600 MMT of agricultural residues annually and this could be a potential feedstock for fuel production (Sukumaran and Pandey, 2010). Surplus residues are sufficient to support projected demand for 2020 even with the most pessimistic conversion figures. Figure 1.3 shows the annual surplus availability of biomass residues in India.

Figure 1.3: Annual surplus availability of biomass residues in India (MMT)

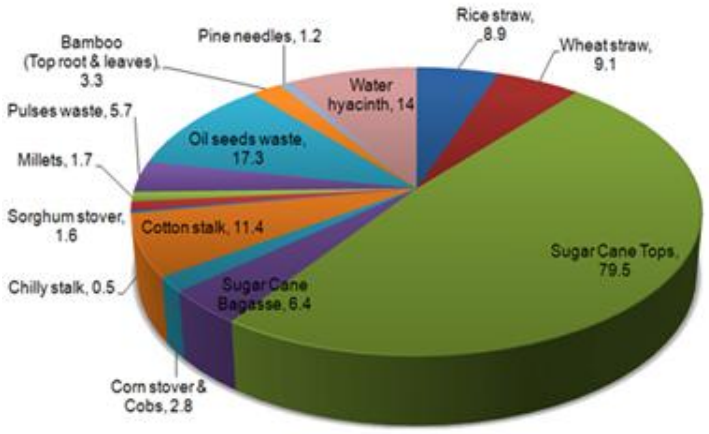

(Source –Pandey et al., 2009)

1.4. Lignocellulosic Biorefineries

1.4.1. General concept of biorefinery

National Renewable Energy Laboratory (NREL) defines biorefinery as a facility that integrates biomass conversion processes and equipments to produce fuels, chemicals and power from biomass. The goal of a biorefinery is to transform biomass into useful products using technology and processes. Biomass conversion requires deep understanding of production technology, chemistry, conversion technology of biomass, economics and environmental related issues (www.NREL.com). Biorefinery is the sustainable

processing of biomass into a spectrum of marketable products (food, feed, materials, and chemicals) and energy (fuels, power, heat) - IEA Bioenergy Task Force 42 Definition (IEA, 2012a). This means that biorefinery can be a concept, a facility, a process, a plant, or even a cluster of facilities. Main driver for biorefineries is the need for sustainability.

A biorefinery can use all kinds of biomass including wood & agricultural crops, forest residues, organic residues (both plant and animal derived), aquatic biomass (algae & sea weeds) and industrial wastes. A biorefinery should sustainably produce a spectrum of marketable products and energy. The products can be intermediates or final products, such as food, feed, materials and chemicals. Energy produced in biorefinery could be fuels, power and heat. The main focus of biorefinery systems which will come into operation within the next years is on the production of transportation biofuels (i.e. biofuel driven biorefineries). The co-produced bio-based products provide additional economic and environmental benefits.

Biorefinery concepts can be classified according to platforms, products, feedstocks and processes. Platforms may be defined based on 1) intermediates from raw materials towards the final biorefinery products, e.g. 'sugar' or 'lignin platform' 2) linkages between different biorefinery concepts and 3) final products of a biorefinery. Combined platforms are possible (e.g. C6 & lignin, C5 & C6). Intermediates from biomass can be substances such as syngas, biogas, sugars, lignin, organic juice and pyrolysis-oil. These intermediates are building blocks for the final products of the biorefinery including fuels, chemicals and (performance) materials. Other platforms can be hydrogen and electricity and heat (FitzPatrick et al., 2010; Jungmeier, 2010). A biorefinery should produce a spectrum of marketable products in order to maximize its economic sustainability and to aim for zero waste. Biorefineries may be configured around a large volume product to maximize economies of scale

1.4.2. Lignocellulosic biomass based biorefinery

The lignocellulose biorefinery system is based on biomass as processing input (feedstocks) for production of multiple bio-based products. The function of biorefinery system is to produce biofuel and platform chemicals from lignocellulosic biomass. A lot of research is now being focused on developing biorefineries for production of bio based products (Fernando et al. 2006; Kamm et al. 2006; Hatti-Kaul et al., 2007). Biorefinery is also being developed based on different feedstocks such as crops and crop residues, forest residues, green grasses, lignocellulosic biomass and industrial waste (Koutinas et al., 2007; Chew and Bhatia, 2008). Figure 1.4 shows the various platforms from lignocellulose based biorefinery. The various platforms are C5, C6 sugars, lignin and pyrolysis oil. In order to make biofuel

production viable, the inputs should be low cost and economic values need to be derived from the co-products.

Figure 1.4: Various platforms from lignocellulosic biorefinery

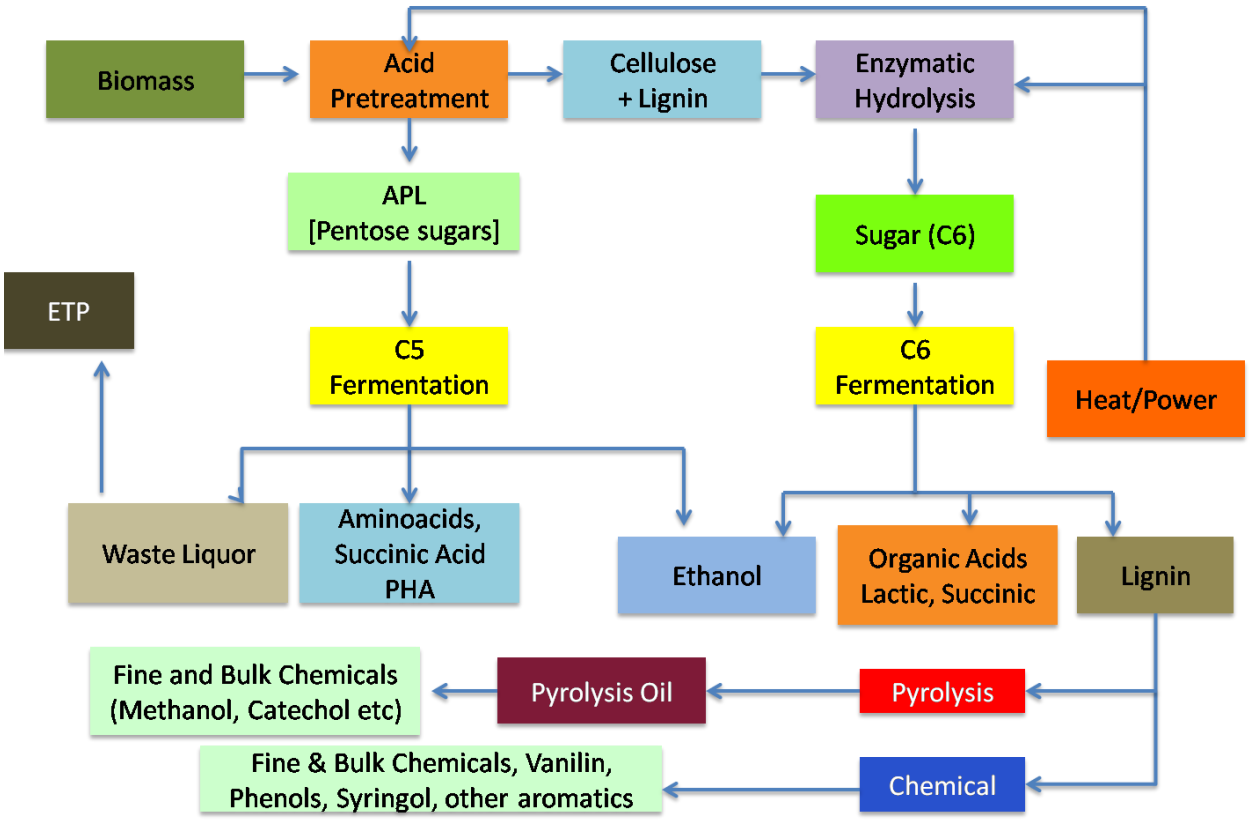

(Adapted from Howard et al., 2003)

Several bio based products are possible from lignocellulosic biomass in a biorefinery approach. Currently, products made from biological processes represent only a minor fraction of products from chemical industry. The first step in a biorefinery scheme involves biomass processing. Usually this is done by biomass pretreatment through physical, biological and chemical methods. The outputs from pretreatment step are platform molecules or streams that can be used for further processing (Cherubini & Ulgiati, 2010). Table 1.3 details the various bio products possible from lignocellulose biorefinery and the various classifications of biorefinery. Several reports describe the various value added chemicals that can be produced from biomass (Werpy, 2004; Demirabas, 2008; Bozell & Petersen, 2010; Güllü, 2010). Producing such high value low volume products along with bioethanol can offset the high costs incurred in biofuel production from lignocellulosic biomass.

Table 1.3: Various products from lignocellulosic biomass based biorefinery

Lignocellulose Biorefinery	
Orientation	Biofuels
Platform	C6, C5, Lignin, Syngas
Products	Bioethanol, sorbitol Fine chemicals (Amino acids, organic acids, Polyols, Vitamins, HMF), PHA, Cheto compounds, levulinic acid, xylitol Lignin, Aromatics (phenol, toluene, xylene), Vanilin FT diesel
Feedstock	Straw, Corn Stover, Bagasse, Woodchips, Energy Grasses
Processes	Biochemical, Thermo chemical, Chemical

1.4.2.1. Different platforms from lignocellulose biorefinery and their features

Different Platforms exist for the conversion of biomass to biofuel and other products, the most prominent of them being the syngas platform, sugar platform, lignin platform, pyrolysis platform etc. A detailed discussion of this can be found in Jungmeier et al., (2010). While different platforms approach the conversion of lignocellulose to fuel differently, bioethanol production is achieved most efficiently through the biochemical /sugar platform which incidentally is also the one with lowest energy consumption.

1.4.2.1.1. C6 and C6/C5 sugar platform

Six carbon sugar platforms are based on glucose polymers (starch, cellulose) which yield glucose, which in turn can serve as the platform for fermentative production of several chemicals and building blocks. It can also be converted chemically to useful building blocks like sorbitol (Bozell & Petersen, 2010). This platform relies on the biochemical conversion of biomass. Mixed C6 and C5 platforms are derived through lignocellulose hydrolysis – primarily hemicellulose. C6/C5 can technically yield the same products as C6 through fermentation. However, the technical, biological and economic barriers are much tougher here. Xylan/xylose contained in hemicelluloses can be thermally transformed into furans (2-furfuraldeyde, hydroxymethyl furfural), short chain organic acids (formic, acetic and propionic acids) and cheto compounds (hydroxy-1-propanone, hydroxy-1-butanone) (Bozell & Petersen, 2010; Güllü, 2010). Furfural can be processed to form building blocks of innovative polymeric materials (i.e. 2, 5-

furandicarboxylic acid). In addition, levulinic acid could be formed by the degradation of hydroxymethyl furfural (Demirabas, 2008). Another product prepared either by fermentation or by catalytic hydrogenation of xylose is xylitol (Bozell & Petersen, 2010).

1.5. Major steps in lignocellulosic biomass to ethanol conversion process

Lignocellulose is highly recalcitrant and its break down to component sugars though is a natural process is particularly challenging when it needs to be completed at the shortest time with minimal energy consumption. While lignocellulose can be digested using dilute acid, this has several problems including requirement of higher temperatures, corrosiveness of the catalyst, challenges in acid neutralization or recovery and environmental issues related to disposal of used acid. Due to the above, enzymatic conversion of biomass is the preferred strategy worldwide since it is most efficient, and can be performed under ambient conditions. Seemingly the only serious limitations here are the enzyme cost and long term stability of the enzyme which impedes repeated use.

Major steps involved in the conversion of lignocellulosic biomass are: (1) pre-treatment process which reduces the lignin content in biomass and increases the susceptibility of cellulose and hemicellulose to enzymatic degradation (2) enzymatic hydrolysis of polysaccharides to simple sugars (3) production of ethanol from sugars by fermentation (4) distillation of the produced ethanol (5) drying of the ethanol to remove moisture content (Wyman, 1999). Figure 1.5 illustrates the broad outline of major steps involved in lignocellulose conversion to bioethanol. After pretreatment of lignocellulosic biomass, there are mainly 3 different ways to achieve ethanol from the solid fraction containing celluloses.

1) *Separate hydrolysis and fermentation (SHF):* In this process, pretreated biomass is hydrolyzed to sugars and these sugars are fermented to ethanol in separate unit operations. The major advantage of this process is that each unit operation can be carried out at its own optimum condition. For example hydrolysis can be carried out at 45 – 50 °C which is the temperature optimum for cellulolytic enzymes (Saha et al., 2005; Olsson et al., 2006) and fermentation can be carried out at 30 - 37 °C which is the optimum temperature for ethanol producing organisms. The major drawback of this mode of operation is the inhibition of hydrolytic enzymes by the end product, glucose. Another major problem is contamination of hydrolysis operation (Taherzadeh and Karimi, 2007).

2) *Simultaneous Saccharification and Fermentation (SSF):* This process combines hydrolysis and fermentation in a single unit operation. Since the glucose produced by hydrolysis is immediately consumed by the fermentative microorganism, end product inhibition of enzymes could be reduced

(Krishna et al., 2001). Also, SSF gives higher ethanol yields at lower enzyme loadings in comparison with SHF (Sun and Cheng, 2002; Demain et al., 2005; Karimi et al., 2006). The major drawback of this process is the difference between optimum temperature of enzymes and ethanol producing organism.

3) *Consolidated Bioprocessing (CBP):* In this mode of ethanol production, cellulase production, hydrolysis and fermentation are carried out in a single unit operation (Lynd et al., 2005; Cardona and Sanchez, 2007). In CBP, only one microbial consortium or an engineered single organism is used for the production of cellulase and fermentation. The major advantage is lower production cost due to simpler lignocellulosic processing and lower energy input (Demain et al., 2005). The major strategies for attaining CBP is to modify excellent cellulase producers to produce high amounts of ethanol or vice – versa (Lynd et al., 2005).

Figure 1.5: Overview of steps involved in lignocellulose to ethanol conversion

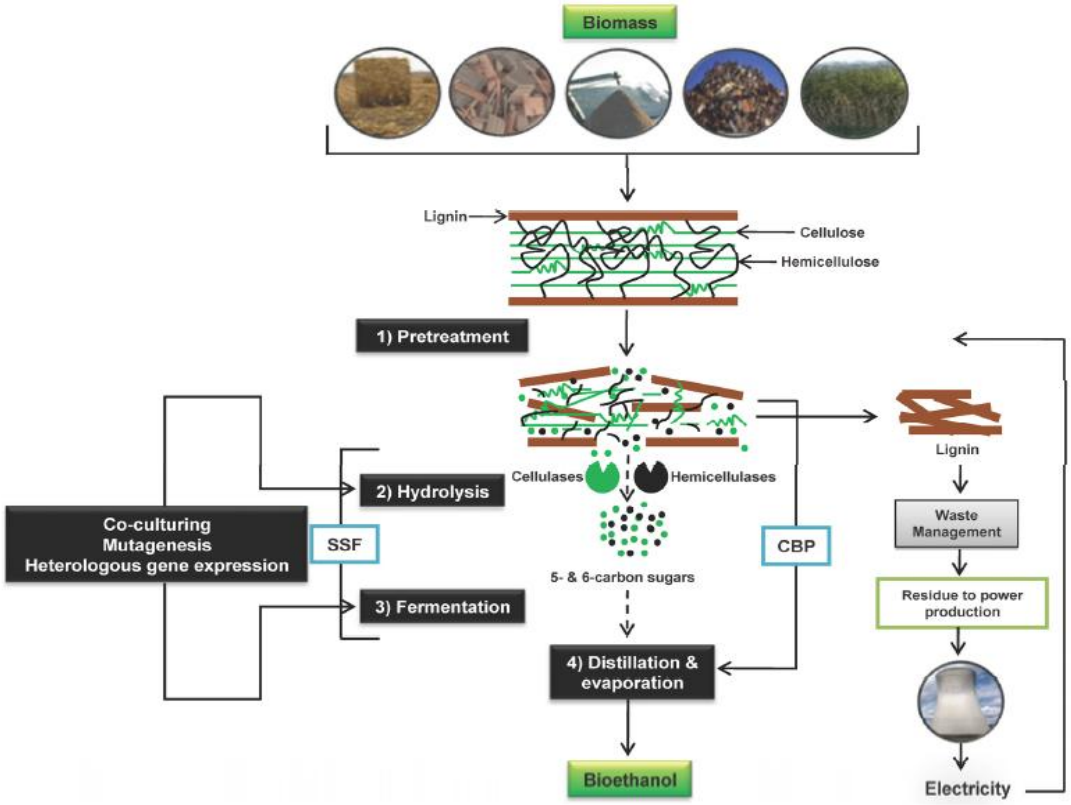

(Source: Anwar et al., 2014)

In addition to these modes, conversion of C5 and C6 sugars is achieved together in a unit operation. This is called simultaneous saccharification and co-fermentation (SSCF). In this process, polysaccharide containing biomass is subjected to cellulolytic and hemicellulolytic enzymes that produces C6 and C5 sugars. These sugars are then fermented together in one step to ethanol (Teixeira et al., 2000). One major drawback is that even the pentose utilizing organisms have a preference for hexoses. This problem is solved by sequential fermentation or by using genetically modified organisms that can utilize both sugars.

The flowchart for a typical lignocellulosic biomass to bioethanol process with alkali pretreatment is given in Figure 1.6. As is evident from the flowchart, multiple numbers of smaller operations are present in each unit operation in biomass to bioethanol conversion. This is one reason that contributes to the high cost of bioethanol from lignocellulosic biomass.

Figure 1.6: Unit operations in lignocellulosic biomass to ethanol conversion process

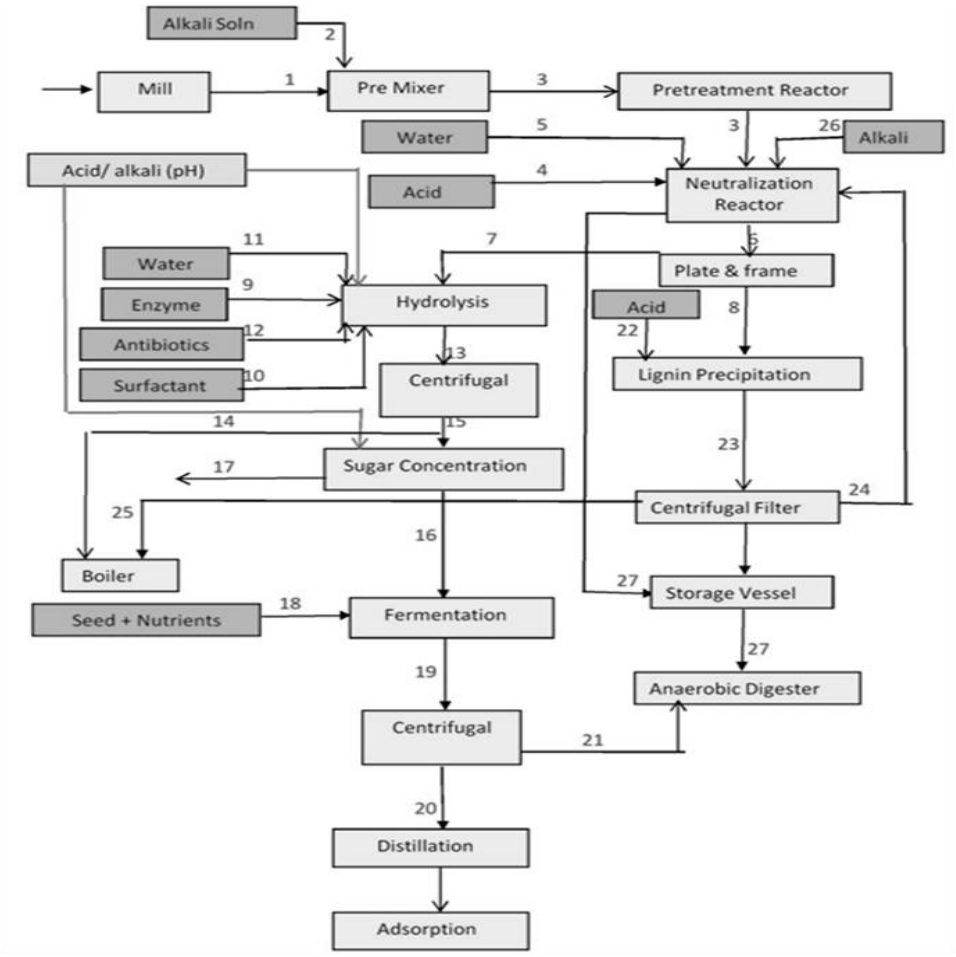

1.5.1. Challenges in lignocellulose to ethanol conversion process

In addition to the high cost of second generation bioethanol production process, there are several other challenges that need to be addressed for economical bioethanol production. An overview of a few of these challenges is given in Figure 1.7. The recalcitrant structure and complexity of lignocellulosic biomass remains a major economic and technical obstacle in biofuel production (Zhang et al., 1995). Effective pretreatment requires redistribution of lignin and improving cellulose accessibility to enzymes by increasing the available surface area on biomass. Presence of celluloses and hemicelluloses and the high degree of cross linking in the lignocellulose necessitate the requirement of various enzymes to cleave the biomass to sugars that adds to the cost of hydrolysis. In addition to that, xylooligosaccharides produced from hemicellulose hydrolysis inhibits cellulase (Yang et al., 2004). Soluble xylo-oligomers are most inhibitory to cellulase and substantially influence enzymatic hydrolysis (Qing et al., 2010; Ximenes et al., 2010). The most significant step in the process is hydrolysis which accounts for almost 50% of the total cost of bioethanol production. Hence strategies need to be devised to make this unit operation economical.

Figure 1.7: Challenges in second generation bioethanol production

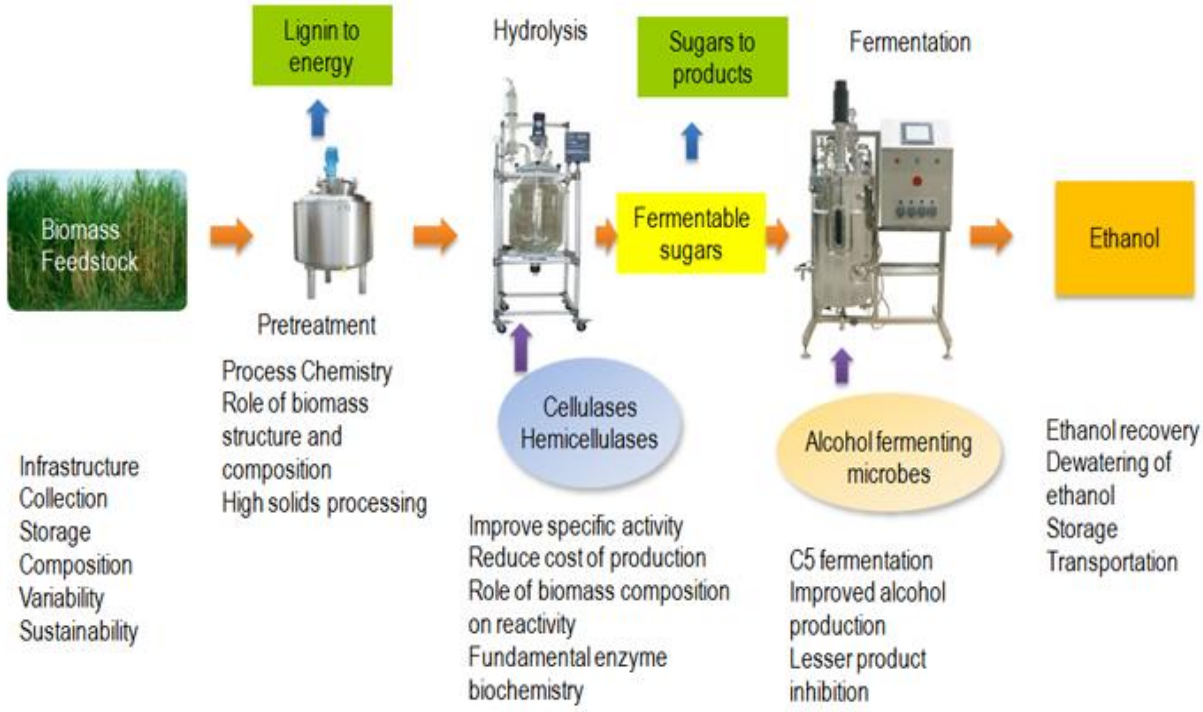

1.6. Hydrolysis of lignocellulosic biomass

Hydrolysis is the most important unit operation in lignocellulose to bioethanol conversion. The efficiency of this step determines the overall efficiency and economics of the whole process. Hydrolysis may be carried out either by enzymatic method or by acid hydrolysis. Dilute acid hydrolysis is carried out in two steps: step one is carried out at lower temperatures to maximize the yield of C5 sugars from hemicellulose; step two is carried out at higher temperatures to generate maximum C6 sugars from cellulose. Concentrated sulphuric acids are also used to hydrolyze the lignocellulosic biomass. The reaction is carried out at mild temperatures and pressure and yields very high sugar release efficiency. But the use of highly concentrated acids limits the applicability of this process (Idi and Mohamad, 2011).

Enzymatic hydrolysis of lignocellulosic biomass offers several advantages over acid hydrolysis: high specificity, lower by-product formation, milder operation conditions, lower energy consumption, lower undesired impact on environment, higher sugar yield, non requirement of corrosion resistant processing equipment due to non usage of acid, less acid waste and the potential for almost complete conversion (Wyman et al., 2005). Glucose gets dehydrated to 5-hydroxymethylfurfural (HMF) in the presence of acids. HMF further inhibits the subsequent microbial fermentation (Klinke et al., 2004; Binder and Raines, 2010). Hence, enzymatic hydrolysis is the preferred route for production of sugars from lignocellulosic biomass.

Enzymatic hydrolysis of lignocellulosic biomass is catalysed by cellulases, i.e. glycosyl hydrolases (GH) specialized in the hydrolysis of the 1,4-β-glycosidic bonds. In the total hydrolysis, cellulases are generally applied as cocktails of different cellulase activities. Usually, three cellulase activities have been considered: endoglucanases, which catalyse the random cleavage of the cellulose chains especially in the amorphous regions, causing rapid reduction in the cellulose degree of polymerization (DP) while liberating cello-oligomers in the process; cellobiohydrolases (exoglucanases), which catalyze the cleavage of cellobiose from the cellulose chain ends; and β-glucosidases which catalyse the hydrolysis of the liberated cello-oligomers to glucose (Wahlström and Suurnäkki, 2015).

Rigid and compact structure of lignocellulosic biomass acts as a limiting factor in hydrolysis of lignocellulosic biomass. This property of biomass is termed biomass recalcitrance. Biomass recalcitrance is closely related to the chemical and physical features of the plant cell wall. The presence of lignin, hemicelluloses, pectin, ash, etc., act as physical barriers to protect cellulose from hydrolytic enzymes. The major substrate factors affecting enzymatic hydrolysis of lignocellulose include lignin, hemicelluloses, and acetyl group contents, cellulose crystallinity, degree of polymerization, specific surface area, pore volume and particle size (Chang and Holtzapple, 2000; Sun and Cheng, 2002; Zhu et al., 2008; Zheng et

al., 2009). Hence, a detailed understanding of biomass structure is necessary to devise efficient strategies for lignocellulosic hydrolysis.

1.6.1. Structure of lignocellulosic biomass

Lignocellulosic biomass has a complex structure and consists of three major components including cellulose, hemicelluloses, and lignin (Hendriks and Zeeman, 2009). Cellulose is a linear polymer of anhydro D-glucose units linked by β-1-4 glycosidic bonds. Formation of cellulose chains due to β-1-4 glycosidic bonds and the interactions among the cellulosic chains via inter molecular and intra molecular hydrogen bond leads to highly ordered microfibrils known as crystalline cellulose. A small portion of cellulose structure can be amorphous. Crystallinity of cellulose is the most significant factor that negatively affects enzymatic hydrolysis of biomass to produce bioethanol.

Hemicelluloses are heteropolysaccharides and contain a wide variety of sugars. They are mainly composed of hexoses (D-glucose, D-mannose, and D-galactose), pentoses (D-xylose, L-arabinose, and D-arabinose), and deoxyhexoses (L- rhamnose or 6-dexoy-L-mannose and rare L-fucose or 6-deoxy-L-galactose) with small amounts of uronic acids present. The chemical composition and structure of hemicelluloses vary for different types of cellulosic biomass. Arabinoxylan and glucomannan are abundant in herbaceous biomass. Lower chemical and thermal stability of hemicelluloses is due to the lower degree of polymerization and lack of crystallinity (Beg et al., 2001; Koukiekolo et al., 2005).

Lignin is the largest non-carbohydrate fraction in lignocelluloses. Its structure is very complex compared to that of celluloses or hemicelluloses. Presence of lignin strongly inhibits enzyme adsorption during enzymatic hydrolysis of biomass. Lignin is a phenyl propane-based polymer that cannot be depolymerized to its original monomers. Three types of monolignols including *p*-coumaryl alcohol, coniferyl alcohol and synapyl lignin are present in lignin. Various types of carbon-carbon and ether bonds formed between monolignols results in a complex lignin structure. The complex lignin structure along with cellulose crystallinity and the sheath formed by lignin and hemicellulose, contributes to the recalcitrance of lignocellulosic biomass that inhibits the activity of hydrolytic enzymes during hydrolysis of lignocelluloses (Himmel et al., 2007)

In the lignocellulosic biomass, cellulose is entrenched in a matrix of hemicellulose, pectin and lignin (Raven et al., 1999; Eriksson and Bermek, 2009). Lignin and hemicellulose are found in the spaces between cellulose microfibrils in primary and secondary cell walls, as well as the middle lamellae (Eriksson and Bermek, 2009). The detailed structure of lignocellulosic biomass is given in Figure 1.8.

Figure 1.8: Structure of lignocellulosic biomass

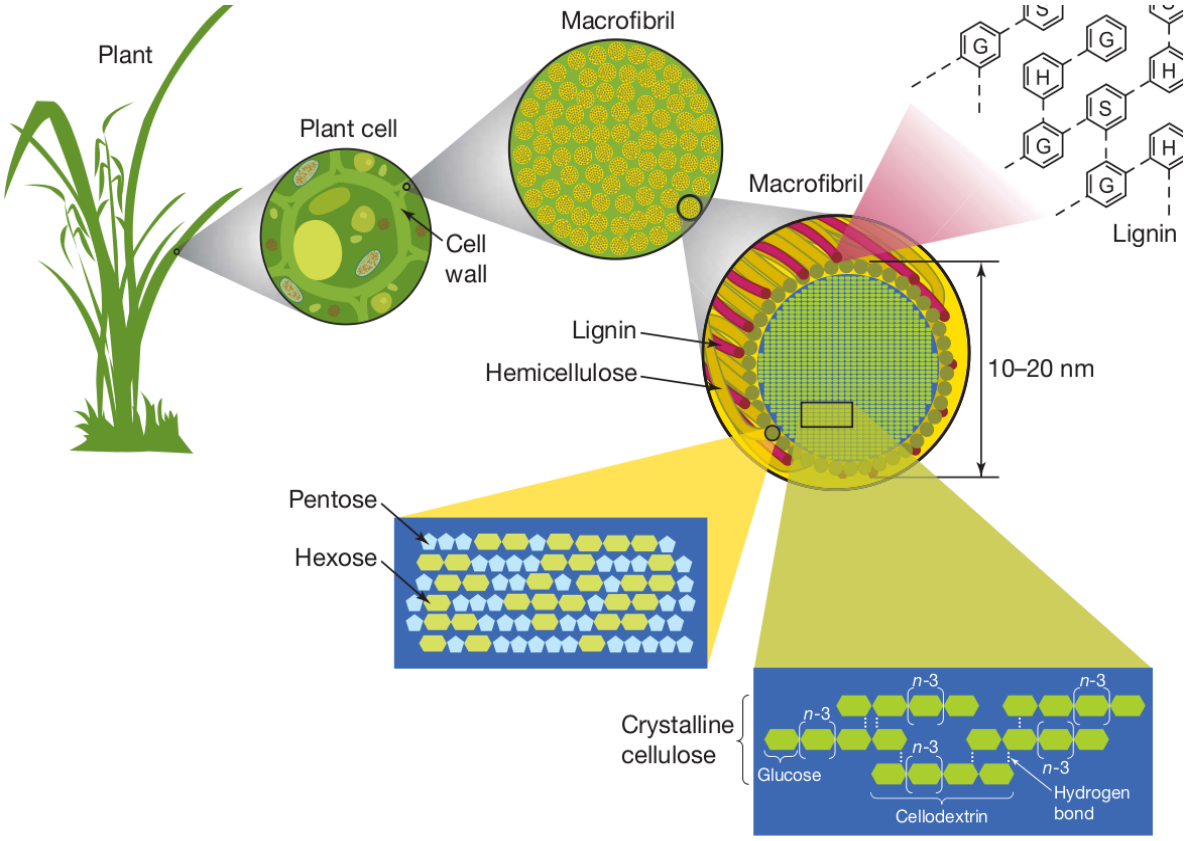

1.6.2. Effects of lignocellulosic substrate features on enzymatic hydrolysis of biomass

Understanding the substrate factors that contribute to enzymatic hydrolysis of lignocellulosic biomass would help in devising suitable strategies to overcome these limitations. Table 1.4 lists the effects of chemical composition and physical structures of lignocellulosic biomass on enzymatic hydrolysis of biomass. It is evident that to remove these barriers and reduce biomass recalcitrance, efficient pretreatment of biomass needs to be carried out. The role of pretreatment should be to lower lignin content and crystallinity and to make the cellulose surface more accessible to hydrolytic enzymes. Thus, a thorough understanding of the limiting factors of hydrolysis helps in devising suitable pretreatment strategies (Zhao et al., 2012).

Table 1.4: Effects of chemical composition and physical structures on enzymatic digestibility of lignocellulosic biomass.

Factors	Effect on enzymatic digestibility	References
Chemical Composition (CC) – Lignin	Lignin restricts cellulase accessibility to cellulose by acting as a physical barrier. Lignin is also found to adsorb cellulases non – specifically. Also, it reduces enzymatic efficiency by irreversible binding to cellulases.	Mooney et al., 1998; Laureano-Perez et al., 2005
CC – Hemicellulose	Hemicelluloses also reduce enzymatic hydrolysis by acting as physical barriers that restrict access of cellulase to cellulose. Hemicellulose removal increases substrate porosity. Also, C5 sugars are found to inhibit cellulolytic enzymes.	Yang and Wyman, 2004; Mussatto et al., 2008
CC – Acetyl group	Acetyl groups in lignocellulosic biomass prevent the formation of bonds between cellulose and catalytic domains of cellulase. Suitable pretreatment strategies can efficiently remove acetyl groups.	Zhao and Liu, 2011; Zhao et al., 2008
CC – Cell wall protein	Cell wall proteins like expansions and swollenins have positive effect on biomass hydrolysis.	Legaert et al., 2009; Han and Chen, 2007
Physical structure (PS) – Accessible surface area	This is one of the most important factors determining efficiency of enzymatic hydrolysis. Increasing accessible surface area increases the cellulase binding to cellulose, thus increasing sugar yields. Major objective of all pretreatments is increasing accessible surface area.	Rollin et al., 2010; Zhang and Lynd 2004
PS – Specific surface area, particle size, pore size and volume	Specific surface area (SSA) is also important for cellulase accessibility to biomass. Higher SSA implies higher hydrolysis. SSA is a function of particle size, pore volume and size. SSA also takes into account the interior surface area not accessible to enzymes.	Zhu et al., 2009; Zhang and Lynd 2004;
PS – Crystallinity	Crystallinity of cellulose lowers its degradability. Rate of cellulose breakdown in amorphous regions is 3-30 times faster than in crystalline regions. Crystallinity depends on presence of lignin and hemicelluloses. Decrease in crystallinity also implies a higher accessible surface area and lower particle size.	Zhang and Lynd 2004; Zhu et al., 2008
PS – Degree of polymerization (DP)	Lower degree of polymerization of cellulose chains results in higher efficiency of hydrolysis. Lower DP results in larger number of binding sites for enzymes.	Gupta and Lee, 2009; Chandra et al., 2007

1.6.2.1. Role of pretreatment of lignocellulosic biomass in enhancing enzymatic hydrolysis efficiency by improving substrate characteristics

Pretreatment is a crucial step in biomass conversion to bioethanol. In order to efficiently hydrolyze hemicellulose and cellulose to fermentable monomeric sugars, some form of pretreatment is necessary. The chemical, physical and morphological characteristics of lignocellulose are important to the digestibility of the substrate. Pretreatment changes these characteristics and in particular makes the material more accessible for the saccharifying enzymes. The efficiency of pretreatment determines the efficiency of hydrolysis of lignocellulosic substrates as enzymatic hydrolysis of untreated lignocellulosic biomass produces less than 20% glucose from the cellulose fraction (Zhang and Lynd, 2004). Hence, even though pretreatment is costly, it is an integral part of biomass conversion leading to biofuels or other bioproducts (Eggeman and Elander, 2005). A lot of research is being focused on developing highly efficient and cost effective pretreatment strategies (Yang and Wyman, 2008). The major effects of pretreatment on lignocellulosic biomass are:

- Removal of some or all of the lignin that increases porosity of biomass (Mansfield et al., 1999);
- Disruption of the biomass overall structure by lignin structure disruption;
- Relocation of lignin in biomass (Zhang and Lynd, 2004);
- Removal of all or some of hemicellulose that inhibits enzyme accessibility to cellulose;
- Breakdown of hemicellulose structure;
- Reduction in particle size of biomass (Chundawat et al., 2007).
- Reduction in the degree of polymerization (DP) of cellulose by disrupting microfibril structure;
- Variation in crystallinity of the cellulose;

Lignocellulosic biomass contains a significant percentage of lignin which contributes to the limiting hydrolysis of biomass by hydrolytic enzymes (Dijkerman et al., 1997; Jung et al., 2000; Varnai et al., 2010). Hence, research on pretreatment strategies focus on reducing the lignin content in biomass. Various reasons have been suggested to explain the reduction in hydrolytic efficiency of enzymes due to presence of lignin. Some of them are as given below:

- Lignin provides a physical barrier which limits accessibility of cellulases or hemicellulases to biomass (Jung et al., 2000, Palonen, 2004, Varnai et al., 2010).
- Cellulases become non-specifically adsorbed to the lignin (Tu et al., 2009a; Qi et al., 2011).

- Direct inhibition of hydrolytic enzymes by lignin (Berlin et al., 2006; Jing et al., 2009; Morrison et al., 2011)
- Residual lignin in biomass may block the movement of cellulase down cellulose (Zhang and Lynd, 2004).

Research indicates that removal of lignin leads to higher enzymatic saccharification efficiencies. Removal of lignin is achieved by pretreatment of lignocellulosic biomass.

1.6.2.1.1. Different types of pretreatment

There are several methods of pretreatment. The various methods, their modes of action, advantages and disadvantages are as given in Table 1.5. The most commonly used methods for pretreatment of lignocellulosic biomass are acid and alkali pretreatment. Both these are classified as chemical pretreatment methods.

1.6.2.1.1.1. Acid pretreatment

Concentrated HCl and H_2SO_4 are the most commonly used acids to pretreat lignocellulosic biomass. At high operation temperatures, dilute sulphuric acid pretreatment shows high reaction rates and significantly improves cellulose hydrolysis, whereas saccharification efficiency of cellulose is lower at dilute acid pretreatments with moderate temperature (Esteghlalian et al., 1997). An advantage of dilute acid pretreatment is the separation of C5 and C6 sugar streams. This method is efficient in both long retention time – low temperature and short retention time – high temperature operation (Emmel et al., 2003).

1.6.2.1.1.2. Alkali pretreatment

Alkali pretreatment is now the most preferred mode as the focus is now shifted from getting separate hexose and pentose streams to getting higher sugar yields in order to enhance overall efficiency of lignocellulose to ethanol process. This type of pretreatment results in removal of crosslinks of intermolecular ester bonds between hemicelluloses and other components, and removes lignin. Thus the porosity of the biomass increases resulting in higher accessible surface area for cellulases (McMillan, 1994). Pretreatment efficiency depends on lignin content of biomass. Commonly used alkalis are sodium, potassium, calcium, and ammonium-hydroxide. Pretreatment with dilute sodium hydroxide causes biomass swelling, decrease in the cellulose degree of polymerization (DP) and disruption of the lignin

structure. Pre-treatment with alkali can result in a sharp increase in saccharification, with manifold improvement in yields.

Table 1.5: Main principle(s) behind the action of various pretreatment techniques

Pretreatment Method	Main Principle	References	Advantages	Disadvantages
Dilute acid	Partial hydrolysis and solubilisation of hemicellulose; disruption of lignin; fiber fractionation	Chang and Holtzapple, 2000; Wyman et al., 2005	High glucose yield; solubilises hemicellulose	High costs of acids and need for recovery; high costs of corrosive resistant equipment; formation of inhibitors
Steam Explosion (Auto hydrolysis)	Partial hydrolysis and solubilization of hemicellulose; alteration of lignin	Ballesteros et al., 2006	Cost effective; lignin transformation and hemicellulose solubilisation; high yield of glucose and hemicellulose;	Partial hemicellulose degradation; acid catalyst needed to make process efficient with high lignin content material; toxic compound generation
Hot water flow through	Removal of hemicelluloses and some lignin	Jorgensen et al., 2007b	Separation of nearly pure hemicellulose from rest of feedstock; no need for catalyst; hydrolysis of hemicellulose	High energy/water input; long residence time; lower lignin removal
Wet oxidation/ Wet explosion	Removal and partial degradation of lignin; oxidation of some hemicelluloses	Idi and Mohamad, 2011; Menon and Rao, 2012	High sugar yield; No inhibitor formation; low by product generation	High equipment cost
AFEX	Removal of lignin; partial depolymerization of hemicellulose and cellulose	Anwar et al., 2014	High effectiveness for herbaceous material and low lignin content biomass; cellulose becomes more accessible; causes inactivity between lignin and enzymes; low formation of inhibitors	Recycling of ammonia is needed; less effective process with increasing lignin content; alters lignin structure; high cost of ammonia

Table 1.5 continued

Pretreatment Method	Main Principle	References	Advantages	Disadvantages
Organosolvent Alkali	Removal of lignin; small amounts of hemicellulose removal	Cheng et al., 2010	Efficient removal of lignin; low inhibitor formation	Formation of C5 and C6 sugar mixture after hydrolysis; alteration of lignin structure
Supercritical fluid	Hemicellulose removal; cellulose de-crystallization	Anwar et al., 2014	Low degradation of sugars; cost effective; increases cellulose accessible area	High pressure requirements; lignin and hemicelluloses unaffected
Ionic liquids	Solubilisation of cellulose	Menon and Rao, 2012	Lignin and hemicellulose hydrolysis; ability to dissolve high loadings of different biomass types; Mild processing conditions (low temperatures)	High solvent costs; need for solvent recovery and recycle
Biological pretreatment	Lignin removal by lignin peroxidase, laccase etc.	Iqbal et al., 2013	Cost effective; no toxic compound formation; eco friendly; efficient	Number of days required for pretreatment is very large

The selection of a pretreatment method to enhance the hydrolytic efficiency of biomass depends on various considerations:

- reduced cost of the pretreatment which is based on energy and chemical input
- higher efficiency of lignin removal; Varnai et al. (2010) suggest that complete delignification did not seem essential to achieve hydrolysis. Some pretreatments simply change the location of the lignin which can enhance the hydrolysis without the removal of the lignin (Chandra et al., 2007; Varnai et al., 2010).
- lower release of sugars during pretreatment. For higher sugar yields, maximum polysaccharides should be retained in solid fraction even after pretreatment.
- lower sugar degradation products and inhibitor generation.
- maximum recovery of lignin to produce high value products (Romani et al., 2010).

1.6.3. Enzyme factors affecting hydrolysis of lignocellulosic biomass

The various enzyme factors that contribute to the efficiency of enzymatic hydrolysis are source of enzyme, product inhibition, thermal inactivation, activity balance for synergism, specific activity, nonspecific binding, enzyme processibility, enzyme adsorption on biomass and enzyme compatibility (Yang et al., 2011). Hence a detailed study on the various enzymes involved in hydrolysis and their mode of action is necessary to devise strategies to improve enzymatic hydrolysis of lignocelluloses.

1.6.3.1. Enzymes in hydrolysis of lignocellulosic biomass

Enzymatic hydrolysis of lignocelluloses is a complex process involving a multitude of enzymes. Table 1.6 gives a brief overview of the various enzymes catalyzing hydrolysis of lignocellulose. Apart from the classical hemicellulases, cellulases, ligninases and pectinases, several other enzymes like expansions, swollenins etc. contribute to the biomass degradation (Merino and Cherry, 2007; Banerjee et al., 2010a; Harris et al., 2010).

Table 1.6: Major enzymes involved in lignocellulose hydrolysis

Substrate	Enzyme responsible for degradation
Cellulose	Cellobiohydrolase, endoglucanase, β-glucosidase
Hemicellulose	Endo-xylanase, acetyl xylan esterase, β-xylosidase, endomannanase, β-mannosidase, α-L-arabinofuranosidase, α- glucuronidase, ferulic acid esterase, α-galactosidase, p-coumaric acid esterase
Lignin	Laccase, Manganese peroxidase, Lignin peroxidase
Pectin	Pectin methyl esterase, pectate lyase, polygalacturonase, rhamnogalacturonan lyase
	Swollenin, Expansin
	GH61 cellulase enhancing protein
	Cellulase induced proteins (CIP1, CIP2)

1.6.3.1.1. Cellulases

Cellulase is a complex of three types of enzymes namely exo-1,4-β-glucanases (cellobiohydrolase), endo-1,4-β-glucanases (EG) and β-glucosidases (BGL) (Demain et al., 2005). The mechanism of cellulase action is presented in Figure 1.9. Endo-glucanases (EG) cleave cellulose chains from within to liberate reducing and non-reducing ends in the polymer and reduce the degree of polymerization. Cellobiohydrolases (CBH) attacks the ends of glucose chains liberated by endoglucanase action. Cellobiohydrolaes may have a preference for attacking the reducing or non reducing ends of cellulose chains and release cellobioses or cellotrioses (Teeri, 1997). β-Glucosidase (BGL) cleaves the cellobiose to yield glucose monomers.

Figure 1.9: Mechanism of action of cellulases

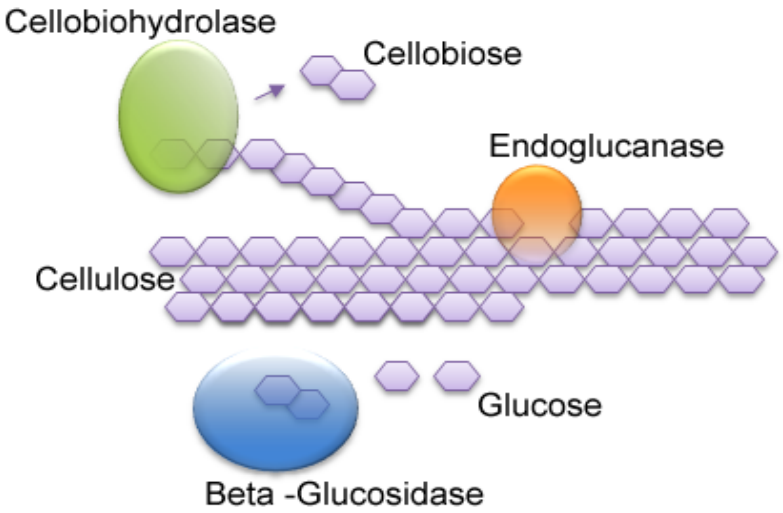

Cellulases are different from other classes of enzymes in that they hydrolyze an insoluble substrate. Sufficient contact of the catalytic domain (CD) of enzyme and the substrate is facilitated by the cellulose binding domain (CBD) of CBH and EG. The CBD is connected to the CD with a flexible linker (Suurnakki et al., 2000). CBDs of cellobiohydrolases are able to move laterally along the cellulose chain while the CD cleaves off cellobiose units (Jervis et al., 1997). Due to the insoluble nature of native cellulose and anchoring of CBDs, cellulases primarily work in a two-dimensional environment involving the unidirectional movement of cellobiohydrolases along the cellulose chain. Also, cellulases do not follow the classical Michaelis – Menten kinetics due to insoluble substrates and limited enzyme diffusion.

1.6.3.1.2. Hemicellulases

The composition of hemicellulose is more varied compared to celluloses and hence larger number of enzymes is needed for hemicellulose degradation. Enzymes degrading hemicellulose can be divided into depolymerising enzymes which cleave the backbone and enzymes that remove substituent which may pose stearic hindrances to the depolymerising enzymes. The mode of action of major hemicellulases is as given in Figure 1.10.

Figure 1.10: Mechanism of action of major hemicellulases

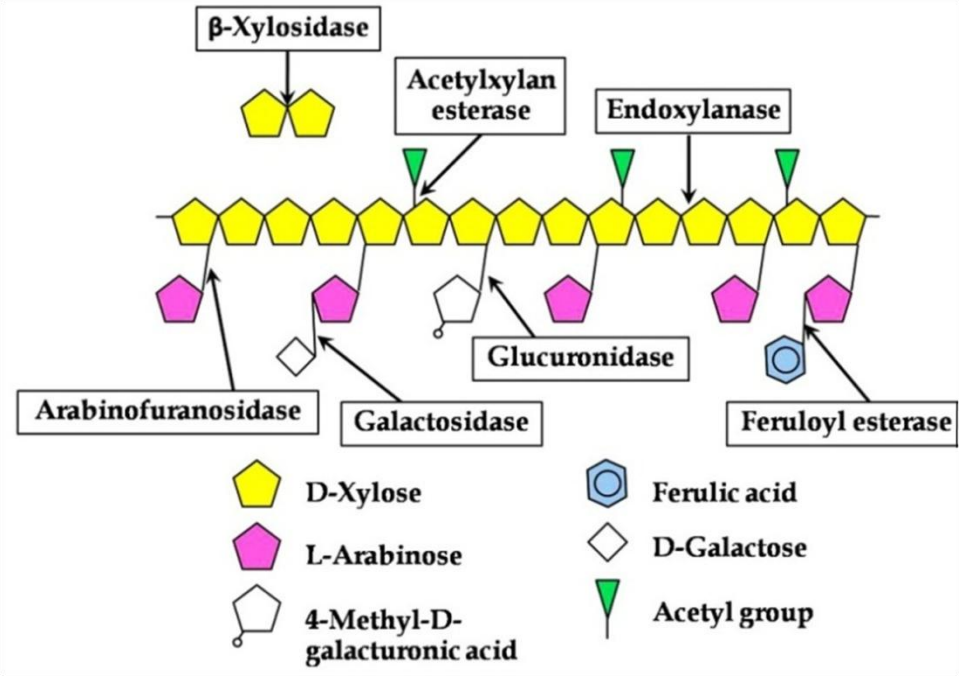

(Source- Ratanakhanokchai et al., 2013)

The major enzyme involved in degradation of xylan chains is endoxylanases, which cleave the xylan backbone of hemicelluloses into xylo – oligomers; and β-xylosidase, which cleaves the xylo oligomers into xylose. Similarly, the enzymes for degradation of mannan are the endomannanase and β-mannosidase. But, xylan chains and mannans are highly branched and several substituents are linked to the backbone like arabinose, acetyl, galactose and glucose which in turn requires several other enzymatic activities to remove these components from the backbone so that the depolymerising enzymes have better access to the main chains. Some of these ancillary enzymes are α-L-arabinofuranosidases, α-glucuronidase, ferulic acid esterase, α-galactosidase, feruroyl esterase, acetyl xylan esterase and acetyl

mannan esterase. Ferulic acid esterases specifically cleave the linkages between hemicellulose and lignin. α-L-arabinofuranosidases also have different specificities with some cleaving 1,2 linkages or 1,3 linkages, while others are able to cleave doubly substituted arabinose residues from arabinoxylan (Meyer et al., 2009).

1.6.3.1.3. Ligninases

Lignin degradation is significant in enhancing the accessibility of cellulases to cellulose. Lignin peroxidase and manganese peroxidase are extracellular fungal heme peroxidases (belonging to LO2 family) with high potency to oxidatively degrade lignin. Upon interaction with H_2O_2, these enzymes form highly reactive Fe(V) or Fe(IV)-oxo species, which abstract electrons from lignin (to cause oxidation or radicalization) either directly or via Mn(III) species. Laccase is a multi-copper oxidase (belonging to LO1 family) that can directly oxidize phenolic parts of lignin, or indirectly oxidize non-phenolic lignin parts with the aid of suitable redox-active mediator. Aryl-alcohol oxidase, glyoxal oxidase and various carbohydrate oxidases are also involved in natural lignocellulose degradation (Bendl et al., 2008; Xu et al., 2009; Sweeney and Xu, 2012).

1.6.3.1.4. Pectinases

The pectin methyl esterases remove methyl groups from pectin to give access to depolymerising enzymes such as polygalacturonase, pectin lyase or pectate lyase (Jayani et al., 2005). Additional rhamno galacturonases and rhamno galacturonan lyases are responsible for degradation of the “hairy regions” in the pectin (Michaud et al., 2003), while pectin acetylesterases remove acetyl groups from acetylated homogalacturonan and rhamno galacturonan (Bonnin et al., 2008).

1.6.3.1.5. Swollenin and Expansin

Expansins are a class of plant proteins which interact with and modify cell walls and/or cell wall components by an unknown activity, thought to result in expansion, slippage or lengthening of cell wall structures (Sampedro and Cosgrove, 2005). Swollenins have weak hydrolytic activity on carboxy methyl cellulose and results in cellulose particle size reduction (Jager et al., 2011; Chen et al., 2010).

1.6.3.1.6. GH61 Cellulase Enhancing Protein

GH61 class of proteins requires a redox active factor for activity. They have weak activity on cellulose and major function is enhancing the activity of cellulases when these are supplemented in the enzyme mixture for cellulose hydrolysis (Harris et al., 2010)

1.6.3.1.7. Cellulose Induced Protein

Cellulose Induced Protein (CIP) also has ancillary activities in lignocellulose degradation which are co-regulated with cellulases. CIP1 is found to have weak activity on *p*-nitrophenyl β-D-cellobioside and some synergistic activity with both GH61 and swollenin (Sweeney and Xu, 2012). CIP2 is an esterase involved in cleaving the methyl ester of 4-*O*-methyl-D-glucuronic acid (Li et al., 2007b).

1.6.3.1.8. Cellulosomes

Microorganisms produce two types of enzyme systems for lignocellulose degradation, namely free and complexed systems. Free enzyme systems occur in many aerobic bacteria and fungi (Zhang and Lynd, 2004). The complexed systems exist as multienzyme complexes named cellulosomes which are mostly found in anaerobic bacteria such as clostridia. The cellulosome has been proposed as the paradigm for synergistic enzyme action with potentially greater activity against lignocellulose than free enzymes (Van Dyk and Pletschke, 2012).

1.6.3.2. Strategies to overcome enzyme factors affecting hydrolysis of lignocellulosic biomass

Various techniques are employed to overcome the limitations caused by enzyme related factors in efficient saccharification of lignocellulosic biomass. Some of the strategies are listed below.

1.6.3.2.1. Glycosyl hydrolases from different microbes

To enhance the hydrolysis efficiency and to reduce the cost of enzyme, research is being undertaken to find more robust enzymes and to understand the mechanism of enzyme interaction with biomass. Complete and efficient hydrolysis of lignocelluloses requires a multitude of enzymes such as cellulases, hemicellulases, pectinases, ligninases etc. (Himmel et al., 1997). Complete hydrolysis of lignocellulosic biomass is observed in hindgut of termite, the rumen of cows, various lignocellulosic biomass composts

and the extreme environmental niches by a mixture of glycosyl hydrolases from different microbial communities (Wei et al., 2009). Many such microbes are being studied for potential application in hydrolysis.

Research is also being conducted to find out more sources of cellulosomes which have efficient enzyme complexes to degrade lignocelluloses, molecular integration of cellulases and hemicellulases into cellulosomal multienzyme complexes resulting from high-affinity interaction between type I dockerin domains of the modular enzymes and type I cohesion modules of a noncatalytic scaffoldin, and a scaffoldin-borne carbohydrate binding module (CBM) to attach to plant cell walls (Fontes and Gilbert, 2010).

1.6.3.2.2. End product inhibition of enzyme

End product inhibition is a major factor that limits enzymatic hydrolysis. When the BGL in the enzyme mixture is less, cellobiose accumulates, thereby inhibiting EGs and CBHs. Hence BGL supplementation improves hydrolysis. If glucose concentration in the hydrolysate becomes high, it inhibits BGL activity. If glucose tolerant BGL is used, high glucose concentrations can be attained as inhibition by glucose could be overcome. Also, higher BGL loadings would reduce BGL inhibition by glucose. Increasing cellulase loading, removing glucose from hydrolysate as it is produced and simultaneous saccharification and fermentation are other methods to overcome product inhibition (Gan et al., 2005).

1.6.3.2.3. Thermal inactivation of enzyme

Studies are being undertaken to find thermostable enzymes. Usually organisms isolated from difficult environmental niches secrete enzymes that are thermo tolerant, halo tolerant or acid tolerant. Other strategies used are site directed mutagenesis and directed evolution to improve the temperature sensitivity of enzymes which would prevent the enzymes from getting deactivated during hydrolysis (Yang et al., 2011).

1.6.3.2.4. Enzyme synergy for biomass digestion

The degree of synergy is defined as “the ratio of the rate or yield of product released by enzymes when used together to the sum of the rate or yield of these products when the enzymes are used separately in the same amounts as they were employed in the mixture” (Kumar and Wyman, 2009a). Synergy depends on the ratio of the enzymes involved (Nidetzky et al., 1994), characteristics of enzymes and on the substrate

features. Higher synergy is observed during hydrolysis of crystalline cellulose in comparison with hydrolysis of amorphous cellulose (El-Naggar et al., 2014). Synergy studies are used to understand the mechanism of action of enzymes and interaction between various enzymes.

Synergy between cellulases have been identified between different cellobiohydrolases (with specificity for reducing and non-reducing ends); between endo and exo-glucanases; between endo-glucanases; between cellobiohydrolases, endo-glucanases and β-glucosidases (Zhang and Lynd, 2004; Qi et al., 2007; Van Dyk and Pletschke, 2012). The complexity of lignocellulose substrates requires numerous enzymes working in synergy, for its hydrolysis. The variation in structure between substrates from different sources and the effect of different types of pretreatments further increase the complexity. To improve the synergy between enzymes, enzyme combinations from various sources are being tested. Also combinations are made from individual enzymes and from commercial enzymes.

1.6.3.2.5. Non Specific binding of enzyme on biomass

Lignin has been reported to bind non-specifically the cellulose hydrolyzing enzymes. This problem could be overcome by using enzymes modified to contain more number of cellulose binding domains in cellulases so that affinity to cellulose is increased. Another strategy to overcome non specific binding is addition of surfactants to hydrolysis mixtures. Sun and Cheng (2002) suggest that non – ionic surfactants are most suitable for improving cellulose hydrolysis. This improvement could be due to hydrophobic interaction of surfactant with lignin, which causes release of non-productively adsorbed enzymes. The hydrophilic portions of the bound surfactant protrude into the aqueous solution and stearically hinder the non-productive adsorption of cellulases and in this way helps to increase cellulose conversion (Eriksson et al., 2002). CBDs of cellulases contribute to the non specific adsorption on lignin. Tween 80 showed competitive binding with cellulases on lignin, which in turn reduces cellulase adsorption on lignin (Tu et al., 2009a). This could also lead to requirement of lower enzyme dosages. The effectiveness of different surfactants varied with the type of pretreatment used, with surfactant having greater effect on acid and steam pretreated straw rather than ammonia or hydrogen peroxide treated straw (Kristensen et al., 2007). Desorption of enzymes for recycling after a hydrolysis cycle can be accomplished using surfactants (Qi et al., 2011).

1.6.4. Challenges in enzymatic hydrolysis of lignocellulose

There are several factors that limit the development of an economic process for enzymatic hydrolysis. Some factors are listed below:

- High cost of the enzyme preparations
- Low cellulase yield from cellulase producers
- Feedback inhibition of beta-glucosidase by its own product glucose
- Temperature and storage stability of the enzyme
- Developing best cocktails of enzymes for a given biomass
- Problems in enzyme reuse due to deactivation and difficulty in recovery of enzyme from hydrolysate
- High enzyme loadings required to attain optimum enzymatic hydrolysis
- Lack of information on enzyme adsorption and desorption kinetics and dynamics of enzymatic hydrolysis
- Low saccharification efficiencies at higher biomass loadings
- Lack of suitable reactor configuration for high solid loading biomass hydrolysis

The various strategies adopted to address these challenges are detailed in the sections below.

1.6.4.1. Strategies to reduce enzyme cost

Enzyme cost is the major contributor to the overall cost of enzymatic hydrolysis. Even though studies are being conducted worldwide to reduce enzyme costs, this is one critical factor that still limits the commercialization of lignocellulose to ethanol production. The following strategies can be used to reduce the enzyme cost:

- Strain improvement of enzyme secreting organisms by mutagenesis, protoplast fusion or recombinant DNA technology
- Screening for overproducing enzymes with novel properties
- Enhancing cellulase activity by using mixed or co culture
- Using cheap and easily available cellulosic sources as substrates for enzyme production

- Production using solid state fermentation which yields a highly concentrated enzyme solution that circumvents the need for enzyme concentration for application in hydrolysis (El-Naggar et al., 2014).

1.6.4.2. Improving cellulase yield from cellulase producers

Lower enzyme production is addressed by gene transfer technology that leads to higher enzyme production in both homologous and heterologous organisms. Mutagenesis (physical or chemical) is also used to enhance enzyme production. But now focus is on gene deletion or over expression to enhance enzyme secretion. For example, deletion of the glucose repressor gene *Cre1* from *T. reesei* improved cellulase production (Kubicek et al., 2009).

1.6.4.3. Reducing feedback inhibition of BGL by glucose

Section 1.6.3.2.2. details the various approaches to mitigate the end product inhibition of BGL by glucose and cellobiohydrolases and endoglucanases by cellobiose.

1.6.4.4. Improving temperature and storage stability of enzyme

Methods to improve thermo stability of enzymes are detailed in section 1.6.3.2.3. Storage stability is enhanced by the addition of various stabilizing agents like sorbitol, mannitol, glycerol, sucrose, polyethelene glycol etc.

1.6.4.5. Development of enzyme cocktails for higher hydrolytic efficiencies

To enhance the efficiency of cellulases for enzymatic hydrolysis of biomass, it is blended with various other ancillary enzymes. These ancillary enzymes act synergistically with cellulases to yield higher amount of sugars. Enzyme synergy studies are carried out to determine the optimal ratio of different enzymes for action on lignocelluloses. More than high cellulase loadings, lower cellulase loadings supplemented with ancillary enzymes optimize hydrolysis and also limit the cost of enzymes (Merino and Cherry, 2007).

Designing of enzyme cocktails tailored for feedstock is essential to optimize degradation of that feedstock. Due to the diverse nature of lignocellulosic biomass, various cocktails need to be developed based on type of feedstock and type of pretreatment. Sills and Gossett (2011) observed that designing tailor made cocktails for different feed stocks is not practical commercially as the lignocellulosic plant

should be capable of operating with different seasonal energy crops. They point out that a tailor made cocktail may be necessary only for substrates with large differences.

Different enzyme ratios for cocktail are reported in literature. This might be due to the use of pure or crude enzymes in the different studies. Application of commercial enzymes in hydrolysis leads to limitations in designing optimized cocktails as commercial enzymes have a multitude of proteins present in them and defining any one activity is challenging (Gao et al., 2011). Duncan and Schilling (2010) reported that apart from concentration of lignin, cellulose and hemicellulose, cell wall anatomy and structure also affect the enzyme ratio optimization. The relationship between an enzyme's turn over and its substrate abundance is not a linear one. Thus, enzyme loading need not correlate with abundance of the substrate targeted by the enzyme (Banerjee et al., 2010b). Enzymes represent a significant cost in bioconversion and therefore the total amount of protein used in saccharification is important (Kumar and Wyman, 2009a).

Composition of biomass also determines the enzyme composition required for hydrolysis. Substrates with higher lignin concentration require higher enzyme loadings to compensate for the non productive adsorption of enzymes on lignin. For example, Boussaid and Saddler (1999) measured the minimum enzyme required to degrade a substrate to completion. Complete hydrolysis of Avicel® (Microcrystalline cellulose) could be attained with 40 FPU/g cellulose. On the other hand, 60 FPU/g cellulose was required to hydrolyze delignified kraft pulp. In contrast to this, even cellulase loadings of 750 FPU/g cellulose could not completely hydrolyze kraft pulp that contained 28% lignin. Enzyme composition also depends upon substrate features. Lower cellulase loadings are required in presence of xylanase. Mixtures with commercial enzymes require higher loadings due to lower specific activity of enzymes.

Pretreatments used on substrates may also have an impact on the enzyme loadings (Kumar and Wyman, 2009a). For example, Wyman et al. (2011) found that higher protein loadings were required for alkaline pretreated substrates, whereas dilute acid, SO_2 and liquid hot water pretreated substrates required lower enzyme loadings for the same levels of hydrolysis. This was related to the hemicellulose content remaining after pretreatment which required additional enzymes such as xylanases (Wyman et al., 2011). Cellulase loadings can be reduced if xylanase is added which improves overall cellulose digestion (Kumar and Wyman, 2009a). In the same manner, supplementation with β-glucosidase can reduce cellulase loadings by removing cellobiose which would inhibit cellulases (Wyman et al., 2011).

According to Sun and Cheng (2002), cellulase loadings of 7–33 FPU/g substrate is generally used, depending on the specific substrate. Cellulase to β-glucosidase ratios are generally used at a 1:2 ratio with loadings of- for example, 15 FPU: 30 CBU (cellobiose/BGL units) per gram of glucan (Samayan and Schall, 2010); 7.5 FPU: 13 CBU/g dry mass (Rosgaard et al., 2007). This ratio is not

always maintained and Pryor and Nahar (2010) used 25 FPU: 31.3 CBU/g cellulose. An optimum ratio of FPU/CMCase/β-glucosidase/xylanase=4.4:1:75:829 was found for hydrolysis of corn stover (Lin et al., 2011). The β-glucosidase is often just added in excess quantities without regard to optimal ratios. Gao et al. (2010) indicated that ratios were also dependent on enzyme loadings, as endoglucanases were more important at low enzyme loadings.

The hydrolytic efficiency of a multi-enzyme mixture in the process of lignocellulose saccharification depends both on properties of individual enzymes and their ratio in the multi enzyme cocktail (Zhou et al., 2009; Berlin et al., 2007). Lin et al., (2011) had used a mixture designed experimental approach to fix the enzyme ratios. This method is a powerful tool for optimization and analysis of the effects of each component as well as interactions between components in a mixture. In a mixture design, the factors are components or ingredients of a mixture and the sum of proportions of mixture components should be equal. In mixture experiments, the measured response is assumed to only depend on the relative proportions of the components in the mixture, but not on the amount of the mixture.

Arantes and Saddler (2011) used a statistical design approach to determine the minimum protein loadings (cellulase and BGL) required to attain optimum sugar yields upon biomass hydrolysis. A 2^4 full factorial design with centered face and 3 replication of middle values was used. High throughput digestion platform GENPLAT was used to optimize enzyme loadings. This technique combines robotic liquid handling, statistical experimental design and automated glucose and xylose assays. Proportions of six enzymes (CBH1, CBH2, EG1, β -glucosidase, GH10 endo- β 1,4-xylanase, and β-xylosidase) were optimized at a fixed enzyme loading of 15 mg/g glucan for release of glucose and xylose from all combinations of five different biomass feedstocks (Banerjee et al., 2010a). A high-throughput microassay, in combination with response surface methodology was used to optimize cellulase, BGL, xylanase and pectinase compositions to enable production of an optimally supplemented enzyme mixture (Berlin et al., 2007).

Several studies have used mathematical models to study the effect of enzyme mixtures in various compositions to optimize hydrolysis of biomass (den Haan et al., 2013). Billard et al., (2012) developed a mathematical quadratic model based on statistical design (response surface design) to optimize enzyme composition in cocktail. Rivera et al., (2010) have used artificial neural network (ANN) modeling to optimize and predict the enzyme composition for better design of enzyme cocktails. They have optimized BGL and cellulase loadings for saccharification of sugarcane bagasse. ANN has the advantage of being able to solve complex biotechnological problems to achieve high operational performance. Gurunathan and Sahadevan (2011) have used ANN followed by genetic algorithm to optimize media components for asparaginase production. ANN has not yet been used in a wide spread manner for optimization of enzyme

cocktails. But this provides several advantages like lesser number of experiments for designing cocktails, faster and robust method particularly in optimization problems etc.

1.6.4.6. Strategies for enzyme reuse

Several strategies have been reported in literature to recycle enzymes used in hydrolysis and economize this unit operation. The enzymes adsorbed on the insoluble solids during hydrolysis could be recycled by adding this residual substrate with fresh substrate. In another strategy, a continuous addition of fresh substrate can be done in the hydrolysis reactor. This would again lead to reduced enzyme loading. Temperature, pH and surfactant concentration were determined to be the major factors affecting enzyme desorption from residue substrate. Increase in enzymatic hydrolysis by 25% could be achieved after three rounds of recycling (Tu et al., 2009b).

Weiss et al., (2013) could recover a significant amount of cellulase activity upon recycling the residual unhydrolyzed biomass left after hydrolysis. They could reduce enzyme dosages by 30% to achieve same glucose yields in subsequent hydrolysis cycles. They could also increase the enzyme productivity by about 50% upon enzyme recycling. This method suffered from a disadvantage that increasing residual solid loading also increases total biomass loading in the reaction mix and lignin content in the system.

Another strategy being increasingly used to recycle enzymes is use of ultra filtration membranes of narrow molecular weight cut off (<50 kDa) that can sieve sugars and retain the enzymes. This could also lead to removal of end product inhibition due to continuous removal of glucose from the hydrolysate. This could increase the hydrolysis efficiency by up to 200% as against batch operations (Yang et al., 2009). It was proposed that if 75% of the enzyme recycled by ultra filtration maintains its active form, the cost benefit of this process could be 18 cents/gal of ethanol produced (Mores et al., 2001).

Chromatographic techniques were also tried to adsorb cellulases from hydrolysate and reuse them. But its applicability is limited due to high cost. Immobilization of enzymes is a promising strategy to recycle enzymes. The main advantages of immobilization are

- Easiness of enzyme handling
- Ease of enzyme separation from hydrolysate
- Higher purity of product due to lower protein contamination
- Possibility of enzyme reuse
- Better storage stability (Sheldon, 2007).

The different methods of immobilization are support binding (carrier), entrapment, encapsulation and cross-linking. Adsorption, ionic binding and covalent binding are various types of carrier based immobilization strategies. Entrapment leads to inclusion of enzymes in a polymer matrix. Here, the immobilization efficiencies are very low. In encapsulation, enzyme is enclosed in a membrane. But this method offers resistance to the substrate diffusion. Cross-linking results in the formation of enzyme aggregates by using bifunctional reagents like glutaraldehyde, able to bind enzymes to each other without resorting to any support.

Immobilization of cellulases is challenging because of insoluble substrate and many immobilization techniques limit the enzyme – substrate interaction. Immobilization of cellulases via covalent bonds appears to be the most suitable technique. Covalent immobilization stabilizes the enzyme and also allows the use of immobilized enzymes for several hydrolysis cycles (Dourado et al., 2002; Li et al., 2007a; Mateo et al., 2007). Cellulases from *T. reesei* were immobilized on Eudragit L-100 by Dourado et al., (2002). This type of immobilization improved the stability of enzymes without loss in its activity. Li et al., (2007) immobilized cellulases on liposomes by means of glutaraldehyde based cross linking of cellulases and liposomes. The immobilized enzyme showed higher hydrolytic efficiency (10%) compared to enzyme immobilized in chitosan gel.

Magnetic nanoparticle (MNP) based immobilization of enzymes is a recent strategy developed to recycle the enzymes. One main advantage of this immobilization strategy is the ease of recovery by application of a strong magnetic field. Since immobilization is done on nanoparticles, a large surface area is available for immobilization. Hence large number of enzyme molecules can be bound to a single particle. As a cellulase component, immobilization of BGL is more suitable since this enzyme does not have to slide along the cellulose fibers for hydrolysis. Another advantage of MNP immobilization is the enhanced storage stability. Since the attachment is usually done by covalent binding, enzyme leaching is prevented, thus enhancing the stability and overall hydrolytic efficiency (Lee et al., 2010; Verma et al., 2013).

1.6.4.7. Reducing enzyme loadings needed to maximize hydrolytic efficiency

Enzyme loadings needed to attain high saccharification efficiency depend upon type of substrate, substrate composition and type of pretreatment. Higher lignin content in biomass leads to a higher requirement of enzyme due to the non specific absorption of enzyme on the biomass. Wyman et al. (2011) reported the requirement of higher enzyme loadings for alkaline pretreated substrates, whereas dilute acid, SO_2 and liquid hot water pretreated substrates required lower enzyme loadings for the same levels of hydrolysis. This was due to high concentration of the hemicellulose content remaining in biomass after

pretreatment with alkali which requires additional enzymes such as xylanases for efficient hydrolysis (Wyman et al., 2011). Enzyme loading also depends on whether the enzyme combination is optimal for the substrate, for example, cellulase loadings will be lower in the presence of xylanase. Higher loadings are required when commercial enzymes are used as they have lower specific activities (Kumar and Wyman, 2009a). The various methods adapted to reduce enzyme loadings are:

- Washing substrate before hydrolysis to remove inhibitors to enzyme
- Addition of surfactants, BSA, PEG 6000 etc., which reduces non specific adsorption of enzyme on lignin
- Addition of xylanase improves overall hydrolysis efficiency without need for higher dose of cellulases
- Supplementation with BGL reduces need for higher cellulase loading as BGL limits end product inhibition
- Inhibition of BGL can be prevented by operating in simultaneous saccharification and fermentation mode and by using glucose tolerant BGL that reduces need for high BGL doses
- Use of enzymes with higher specific activities reduces required enzyme dosage
- Recycling enzyme over repeated batches of hydrolysis
- Lower substrate loadings yields higher hydrolysis efficiency at lower enzyme loadings (Wyman et al., 2011; Kumar and Wyman, 2009a)

1.6.4.8. Understanding enzyme adsorption on biomass during hydrolysis

Adsorption of enzymes on biomass during hydrolysis is always in a dynamic state. Adsorption, desorption, re-adsorption all take place simultaneously with the enzymes shuttling between solid and liquid fraction (Boussaid and Saddler, 1999). Several studies have indicated that the extent of adsorption determines the rate and efficiency of hydrolysis. Also, the first step in hydrolysis of substrate is adsorption of enzymes on biomass (Kim et al., 1992; Boussaid and Saddler, 1999; Arantes and saddler, 2011).

The major parameters affecting enzyme adsorption are substrate characteristics such as the presence of lignin, the method of pretreatment, as well as accessible surface area and pore volume in the substrate. Pretreatment with ionic liquids is found to remove maximum lignin followed by acid and AFEX pretreatments. Substrate factors and surface area are significant as enzymatic hydrolysis of biomass is a surface dominated process and direct physical contact between enzymes and substrate is essential. Many enzyme related factors are also reported to play a significant role in enzyme adsorption

on biomass. Biomass with higher lignin content adsorbs more enzymes due to non specific adsorption of enzyme on lignin. But rate and extent of hydrolysis in this case is lower (Boussaid and Saddler, 1999; Arantes and Saddler, 2011).

Apart from solids effect, enzyme factors are also involved in adsorption of enzymes on biomass. A linear correlation between adsorption of cellobiohydrolases and hydrolysis was observed by Kotiranta et al., (1999). However, they reported that this linear correlation is not observed in case of adsorption of endoglucanases. This might be due to the fact that adsorption capabilities of various enzymes are different and cellobiohydrolases have higher binding affinity for substrate than endoglucanase (Boussaid and Saddler, 1999). This may be affected by the type of carbohydrate binding domain in the enzyme. If the affinity and specificity of CBD is higher, it binds to substrate with higher efficiency leading to higher hydrolysis rates. Kumar and Wyman (2009b) also observed that cellulase adsorption and cellulose hydrolysis was clearly linked, but they found no correlation between xylanase adsorption and hemicellulose hydrolysis.

Higher enzyme adsorption on biomass was found with acid pretreated biomass compared to alkali pretreated substrate (Qi et al., 2011). Kristensen et al. (2009a) observed a decline in adsorption of enzymes when high solid loading was used for hydrolysis. This might be due to inhibition of enzyme by high amounts of product at high solid loading. Due to lower free water in the reaction system and mass transfer limitations, the products formed near the site of enzyme adsorption are not diffused into other parts of reactor and stay near the biomass. This high concentration of products near substrate inhibit the enzyme and reduce further enzyme adsorption thus lowering hydrolysis efficiencies at high solids loading.

Higher adsorption need not translate to higher hydrolysis efficiencies during hydrolysis of lignocellulosic biomass (Boussaid and Saddler, 1999). A severe decrease in enzymatic hydrolysis of biomass was observed due to non productive binding of cellulases on lignin. To overcome this reduction in hydrolytic efficiencies, higher enzyme dosages are needed, but this can lead to higher cost of hydrolysis. Also, higher enzyme loadings can only hydrolyze biomass to a certain extent. Beyond this threshold limit, increasing enzyme loadings does not increase hydrolysis efficiency. Recalcitrance of biomass and lack of accessibility of substrate determines the extent to which hydrolysis takes place (Arantes and Saddler, 2011). Non-productive adsorption of cellulases to lignin depends on the type and affinity of CBD in the cellulases (Palonen et al., 2004).

It has been shown that, unless hydrolysis of the substrate is complete, enzymes remain adsorbed to the recalcitrant, unhydrolysed part of the substrate and this could affect the reuse of enzymes in subsequent batches (Boussaid and Saddler, 1999). Addition of surfactants can help in desorption of

enzymes from residual biomass. This may in turn lead to efficient harvesting of enzymes and their reuse in subsequent hydrolysis batches.

Various methods have been used to study enzyme adsorption on biomass. Bound protein was estimated as the difference between total protein loading and free protein (Arantes and saddler, 2011). The difference between free and total BGL activity was found to estimate bound BGL on biomass (Haven and Jorgensen, 2013). Nitrogen analysis was used to determine the adsorbed proteins by Kumar and Wyman, 2009. The liquid fraction after hydrolysis was removed and the solid fraction was dried and used for nitrogen analysis of the solids by the Elantech nitrogen analyzer and the amount of protein adsorbed onto the pretreated solids was estimated by multiplying the percentage nitrogen by a nitrogen factor (NF - 8.40, 8.27 and 3.25 for Spezyme1 CP, Multifect1 Xylanase, and Novozyme 188, respectively).

Flow ellipsometry was used to quantify the adsorption and surface reactivity of cellulase on a model cellulose film. Adsorption – desorption kinetics of enzyme was studied independent to the reaction kinetics. They suggest that adsorption reaches equilibrium after 1 h of incubation on cellulose. Apart from cellulose hydrolysis kinetics, cellulase activity on cellulose must study in detail enzyme adsorption, adsorption reversibility, adsorption – desorption equilibrium, surface enzyme denaturation and changes in substrate surface area during hydrolysis (Maurer et al., 2012).

Cellulose accessibilities were evaluated using solute exclusion and protein adsorption methods. UV – Visible spectroscopic technique was used to directly measure the adsorbed cellulase on cellulose. Total substrate accessibility to cellulase was measured based on substrate's adsorption capacity for a non hydrolytic fusion protein called TGC which contains a green fluorescent protein tagged carbohydrate binding domain. After allowing sufficient incubation time for adsorption, the non adsorbed protein fraction was measured using a microplate reader. The difference between total protein and free protein gives the amount of bound protein (Wang et al., 2012). Adsorption of cellulases on amorphous regions of cellulose was determined by using a mono cherry fluorescent protein tagged to protein from carbohydrate binding module -family 17 (Gao et al., 2014).

1.6.4.9. Strategies to improve saccharification efficiency at high biomass loadings

One major advantage of high solids hydrolysis is the production of hydrolysate with high sugar concentration. This in turn increases the final ethanol concentration which reduces the processing steps and costs. Lower water content in a high solids system allows for larger system capacity, less energy demand for heating and cooling of the slurry as well as less waste water (Jorgensen et al., 2007a). High substrate loadings lead to lower reaction rates and lesser efficiency of hydrolysis (Kumar and Wyman, 2009a). Concentrations of end products and of inhibitors will increase, causing enzymes and the

fermenting organism to function less optimally. High-solids loadings can also cause insufficient mixing or excessive energy consumption in conventional stirred-tank reactors as the viscosity of slurries increases abruptly at increased solids loadings. Major reasons for this observation is lower enzyme binding and difficulty of enzymes to diffuse through the medium containing low liquid levels (Wang et al., 2011a). Kristensen et al., (2009b) identified factors such as composition of substrate, product inhibition, water concentration and enzyme binding that contributes to lower hydrolysis yields at higher solids loading. As hydrolysis progresses, the liquid medium becomes more viscous which reduces the ability to mix sufficiently and hence reduces enzyme mobility leading to lower productivity (Rosgaard et al., 2007). Various strategies employed to increase biomass loading during hydrolysis are:

1) *Alternate feeding strategies* – Fed batch feeding strategies are used to attain higher final biomass concentrations and these include intermittent substrate feeding or intermittent substrate and enzyme feeding. As intermittent solid loading leads to lower initial viscosity, diffusion and mixing limitations can be minimized or altogether avoided. A fed-batch feeding regime also allows time for the slurry to liquefy before adding additional solids. This in turn helps in maintaining a level of free water that is available for reaction to proceed smoothly. Availability of free water is important as it diffuses inhibitors and products away from enzyme (Modenbach and Nokes, 2013). Also, addition of fresh enzyme with substrate during each feeding interval maintains a constant enzyme – substrate ratio as against a decreasing ratio when all enzymes are added at beginning and substrate is added intermittently.
2) *Addition of auxiliary enzymes* - Enzyme synergy contributes to higher conversion efficiencies at higher loadings. Xylanase addition results in breakdown of hemicelluloses at a higher rate. This in turn leads to improved enzyme accessibility on cellulose resulting in improved hydrolysis efficiency. Hence addition of ancillary enzymes during high solid hydrolysis helps in improving hydrolysis efficiencies.
3) *Reactor designs for high solid loading hydrolysis* – Conventional stirred tank reactors are not suitable for high solid mixing. Hence, alternate reactor configurations are investigated. Majority of researchers use horizontal configurations and gravitational mixing (Dasari et al., 2009; Roche et al., 2009b). The horizontal orientation has several advantages over vertical stirred vessels. They minimize particle settling and local accumulation of reaction products within the reactor, as well as ensuring better enzyme distribution. These types of reactors are also easily scalable from bench-scale to pilot-scale and larger. Power requirements are lower for horizontal reactors equipped with paddles over vertical stirred tank reactors that provide the same level of effective mixing (Dasari et al.,

2009). Roche et al. (2009b) used free-fall mixing in their design for bench-scale reactors for enzymatic hydrolysis. They could achieve up to 80% conversion efficiency at 20% solids loading.

Jorgensen et al., (2007a) used horizontal reactors for enzymatic hydrolysis. This configuration takes advantage of free fall mixing, hence eliminating the need for mechanical agitation. Studies with various mixing speeds in the range 3.3 – 11.5 rpm resulted in no major difference in mixing efficiency. So, energy required for mixing can be significantly lower. The rotating paddles present in the reactor give additional mixing and also provides a scraping action to remove lignocelluloses from reactor walls. Peg mixers are also used in high solid enzymatic hydrolysis.

1.6.4.10. Modeling studies and reactor configurations for enzymatic hydrolysis with high biomass loading

For high-solid saccharification and fermentation, the reaction rate and bioreactor configuration are of critical importance to the economic feasibility of a larger scale industrial process, since this unit operation requires the longest residence time relative to the other major biomass conversion reactions of enzyme hydrolysis and fermentation. These longer residence times during saccharification translate into higher operating and capital costs per unit of product output. Also, high solid hydrolysis translates to high glucose concentration in reactor that implies higher product inhibition of hydrolytic enzymes. Alleviation of this product inhibition, notably the inhibition by the hydrolysis end-product glucose, is therefore a key prerequisite for achieving cost-efficient conversion of lignocellulosic biomass to biofuels.

The conventional stirred tank reactor (STR) is the most commonly used mixing system for enzymatic hydrolysis of lignocelluloses. The major problem associated with STR is inefficient mixing, settling of biomass and the high energy demand for mixing. Several alternate reactor models like plug flow reactor (Thompson and Grethlein, 1979), Percolation reactor (Lee et al., 2000) etc were studied to minimize the problems associated with high solid mixing and product inhibition. Enzymatic hydrolysis is challenging under existing configurations due to the following limitations:

- The reaction system is a dynamically changing heterogeneous system that consists of a solid substrate, i.e. the lignocellulose and a liquid phase of soluble intermediate and final products.
- The product inhibition on the enzymatic reactions.
- The current complicated kinetic models of the reactions only partially describe the hydrolysis events (Andrić et al., 2010).

Several researches are being carried out to study various reactor designs for enzymatic hydrolysis of lignocellulose. Using the stirred tank reactor with Rushton turbine and marine propeller, hydrolysis studies on SolkaFloc® (powdered cellulose) were carried out to evaluate hydrolysis at high solids loading. High solid enzymatic saccharification with up to 20% solids was performed using a reactor with 2 L working volume and various configurations. It was found that at 120 rpm, the reactors with Rushton impellers achieved higher saccharification efficiency and hence higher concentrations of glucose than the reactors with marine impellers. Baffles were found to increase the biomass hydrolysis in reactor with Rushton turbine. Effect of baffles was negligible in mixing efficiency with marine impellers. Baffled reactor always required higher power. Power requirement for mixing with Rushton turbine impeller was higher in comparison to marine propeller. Therefore, a baffled Rushton bioreactor was recommended for a high-solid bioconversion process due to better mixing compared to bioreactor with marine impeller (Um and Hanley, 2008). The reported high solid loadings were obtained here by fed batch approach. This feeding strategy might be the reason for achieving high mixing in stirred tank reactors with Rushton impeller even at high solids loading.

NREL uses an empty tower with slurry entering at top and flowing down due to gravity as the first stage of hydrolysis. The slurry is then pumped into a series of batch reactors where they are hydrolysed to yield sugars. Another reactor system in use is a horizontal reactor with paddle impellers. An advantage of such a system is proposed to be the lower residence time compared to the tower model. Zhang et al., (2012) investigated the application of helical impeller in high solid mixing with up to 30% biomass loading instead of the Rushton turbine. Helical impeller was found to perform better mixing in the reactor.

The geometry of the impeller can play a significant role in effectively mixing biomass slurries. Other geometries tested for high solid hydrolysis by Wang et al. (2011) include a plate-and-frame impeller and a double-curved-blade impeller. The impellers were tested at various speeds and 100 rpm resulted in the best conversion efficiencies for both geometries. However, the plate-and-frame impeller achieved a higher conversion than the double-curved-blade impeller by nearly 18%, indicating that the geometry of the impeller can have an effect on the hydrolysis. This might be due to the fact that plate and frame impeller provides a better consistent mixing regime at all points in the reactor, whereas double curved blade impeller has an axial mixing regime and mixing efficiency would depend on distance from impeller blades. .

Peg mixers were also studied in the hydrolysis of high solids loading. At 20% biomass loading, time required for hydrolysis of unbleached hardwood pulp decreased from 40 h to 1 h in comparison to mixing in shake flasks. This mixer has been proven to be effective in lignocellulose hydrolysis (Zhang et al., 2009a).

Computational fluid dynamics (CFD) is the modern technique which is used to study mixing efficiency of multiphase flows in conventional stirred reactors with either radial or axial type of impellers. The technology evolved as a branch of fluid dynamics with the application of mathematics to forecast various parameters like fluid flow, heat, momentum and mass transfer, chemical reactions and related phenomena. Since it is done without manual interventions and purely through the system, it is free from errors. Extensive use of CFD in fluid modeling also helps in accurate prediction of rheological properties of biomass slurries during hydrolysis which will help in suitable reactor configuration design.

Carvajal et al., (2012) used an anchor impeller for enzymatic hydrolysis of lignocellulose. High solids loading up to 27.5% were used in the reactor with varying impeller rotation speeds. CFD studies were used to identify the significant rheological parameters in hydrolysis. A shear thickening behavior was observed during initial hydrolysis stages. The three-parameter Herschel-Bulkley model was used for CFD modeling of the hydrolysis of Arundo biomass slurries. The model was found to be able to predict the nonlinear rheological behavior of and transition from shear-thickening to a Newtonian behavior during the course of hydrolysis. The estimation of the Herschel-Bulkley parameters shows that the yield stress decreases with time, as a consequence of the reduction in the solid content.

Enzymatic hydrolysis of lignocellulosic biomass in a high shear environment mixed in a torque rheometer was examined. Such a mixing produced shear flows similar to those found in twin screw extruders. In addition, there is a synergistic effect of mixing and enzymatic hydrolysis; mixing increases the rate of cellulose conversion while the increased conversion facilitates mixing. The synergy appears to result in part from particle size reduction, which is more significant when hydrolysis occurs during intense mixing (Samaniuk et al., 2010).

CFD studies were carried out in horizontal scraped surface reactor which was used for pretreatment of high solid corn stover slurries. The uniform suspension speed and other rheological parameters for hydrolysis were estimated by CFD modeling. With 25% biomass loading, 10% higher sugar yields were obtained with this reactor configuration when compared to hydrolysis in shake flask (Dasari et al., 2007a).

Membrane reactors are increasingly being used as a means to circumvent the product inhibition due to high solids loading. Such a reactor enables simultaneous product removal as saccharification proceeds. Other advantages include retention of enzymes in reactor, higher conversion due to reduced product inhibition, hydrolysate with constant product concentration etc. (Yang et al., 2006).

It is evident from literature survey that studies in high solid loading reactors for enzymatic hydrolysis are very limited if not nonexistent. Experimental determination of optimum reactor configuration is not economical and is also time consuming. CFD is an economical alternative to

determine the optimum impeller designs for high solid processing. Hence, studies need to be proceeded in this direction to attain better reactor configurations to maximize the hydrolytic efficiency.

1.7. Conclusion

Even though biofuel research is being carried out for several decades, there is a lacuna of information in various aspects that is probably the reason for second generation bioethanol not becoming a commercial reality. Efforts need to be directed to mitigate several problems which include

- Studies taking into account process integration, increase of fermentation yields and integration of unit operations are still needed in order to make hydrolysis a competitive technology.
- Enzymes must be tailored to the feedstock. Identifying an optimal enzyme combination is of extreme importance in obtaining a high glucose yield for the overall economy of the process.
- Successful optimization of the enzymatic hydrolysis step can only be achieved by incorporating methodologies for rapid development of reliable mathematical models.
- A deeper understanding needs to be developed regarding the dynamics of hydrolysis i.e., the changes to substrate size, composition, porosity, enzyme adsorption, sugar release etc. This would facilitate in designing optimum enzyme loadings required for hydrolysis and also help in better understanding of the overall process.
- Another major challenge in improving overall efficiency of the process is to increase the biomass loading in the hydrolysis reactor.
- High enzyme dosages contribute significantly to the cost of ethanol. Thus strategies need to be devised to recycle the enzymes used in hydrolysis.
- Residence time of the biomass during hydrolysis needs to be reduced to enhance the process efficiency and economics.
- Concerted efforts are required to develop reactor models capable of handling high solid loadings.

1.8. Objectives

With a view to address at least some of the problems mentioned above, the present study was undertaken with the overall objective to improve the enzymatic hydrolysis of lignocellulosic biomass by improving the enzyme blends as well as by fine tuning the parameters that affect hydrolysis. This includes the specific objectives as stated below:

- Blending of different enzymes to create efficient cocktails, their performance evaluation and development of models (eg. ANN) to describe and predict the hydrolysis performance of blends.

- Strategies to improve sugar concentration of hydrolysates by increasing biomass loading; and development of methods to overcome barriers caused by increased solids loading.

- Developing strategies to recycle enzyme through use of immobilized enzymes.

- Developing a better understanding of the dynamics of enzyme adsorption in relation to changes in biomass particle size and properties during hydrolysis, so as to design better methods for enzyme use and formulations of enzymes to overcome limitations of the system.

- Computational Fluid Dynamics studies to understand the limitations of the conventional Rushton turbine impeller in biomass mixing during hydrolysis and to help subsequent design of suitable impellers that are capable of operation with high solids loading.

Chapter 2
Materials and Methods

2.1. Pretreatment of Biomass

Rice straw was milled in a knife mill to reduce the particle size. The milled materials were stored in an air tight container. Pretreatment was carried out at 15% (w/v) biomass concentration and 2% (w/v) sodium hydroxide at 121 °C for 1 h. The pH of pretreated biomass was adjusted to 6.0 using 10 N H_2SO_4. Biomass was later air dried and stored in air tight containers. The compositional analysis of native and pre-treated rice straw was then carried out by two stage acid hydrolysis protocol developed by National Renewable Energy Laboratory (Ruiz and Ehrman, 1996).

2.2. Composition Analysis of hydrolysed biomass

Composition analysis of biomass was carried out as per the NREL protocols (Ehrman, 1994). Three hundred milligram of biomass was dissolved in 10 mL of 64% (v/v) sulfuric acid in a stoppered conical flask and left to hydrolyze at 30 °C in a shaking water bath at 200 rpm for 2 h. Distilled water (90 mL) was then added and the mixture was kept at 121 °C for 1 h in a laboratory autoclave. Small amount of the solution was filtered through 0.2 µm filters for HPLC analysis. The remaining solution and residue were retained for lignin estimation. Carbohydrate concentrations in the hydrolysates were determined using Shimadzu HPLC unit equipped with Phenomenex Rezex RNM column (300 x 7.8 mm) using RI detector. This analysis was performed at 75 °C column temperature and 40 °C detector cell temperature with a flow rate of 0.6 mL/min using degassed Milli Q water as mobile phase. Glucose, xylose, galactose, mannose and arabinose (Sigma Aldrich, USA) were used as standards for HPLC analysis. Acid soluble lignin was measured by UV spectroscopy at 205 nm (Ehrman, 1996). The acid insoluble lignin and ash was estimated by oxidation method in which the sample was heated up to 575 ˚C in a muffle furnace for 3 h (Templeton and Ehrman, 1995).

2.3. Enzymatic hydrolysis

Enzymatic saccharification of pre-treated rice straw was carried out using commercial cellulase from Zytex (Zytex India Private Limited, Mumbai, India), β-glucosidase (BGL) produced using NIIST strain of *Aspergillus niger* NII 08121 (Section 2.7) and xylanase gifted by MAPS enzymes Pvt. Ltd., Gujarat, India. Hydrolysis was carried out at 10% biomass loading (unless specified otherwise), pH 4.8, 50 °C and

200 rpm for 48 h. The sugar stream obtained from hydrolyzed rice straw was analyzed for sugars using HPLC.

2.4. Enzyme Assays

2.4.1. Filter Paper Units (FPU) Assay

FPU activity was determined by modified protocol of Ghosh, 1987. For this, 0.5 mL of appropriately diluted enzyme was incubated with 50 mg of Whatman's No. 1 filter paper (approximately 1x 6 cm strips) in a total reaction volume of 1.5 mL at 50 °C for 1 h. DNS reagent (3.0 mL) was added to terminate the reaction. The reaction mix was then boiled for 5 minutes and the color developed was read at 540 nm after cooling the reaction mix (Miller et al., 1959). The amount of glucose released was then calculated using glucose as standard. One unit of FPU was defined as the amount of enzyme that releases one micromole of glucose per minute under the assay conditions and was expressed as FPU/mL. The calculation was based on the fact that 0.37 FPU releases 2 mg glucose.

2.4.2. Endoglucanase Activity

Endoglucanase activity was determined similar to that for filter paper assay but using Carboxy Methyl Cellulose as substrate (0.5 mL of a 2% Na-CMC solution in citrate buffer [0.05 M, pH 4.8]) instead of filter paper (Ghosh, 1987). The concentration of glucose released was determined by comparing against a standard curve of glucose. CMCase activity was calculated following the concept that 0.185 U of enzyme will liberate 0.5 mg of glucose under the assay conditions and was expressed as U/mL.

2.4.3. Xylanase Activity

Xylanase activity was measured using the modified Bailey et al., (1992) protocol. 500 µl of appropriately diluted enzyme was mixed with 500 µl 1% Beechwood xylan (Sigma Aldrich, USA) prepared in 50 mM sodium citrate buffer, pH 4.8 and incubated for 30 min at 50 °C. After incubation, the reaction was terminated by adding 3.0 mL DNS reagent and boiling the contents for 5 minutes. After cooling, the color developed was read at 540 nm (Miller et al., 1959). The amount of xylose released was calculated using xylose as standard. One unit of xylanase activity was defined as the amount of enzyme that liberates one micromole of xylose per minute under the assay conditions and was expressed as U/mL.

2.4.4. β- Glucosidase activity

β- Glucosidase activity was assayed using p-nitro phenyl-β-D glucopyranoside (pNPG) (Sigma Aldrich, USA) as substrate. The reaction mixture which consisted of 1 mL of citrate buffer (0.05 M, pH 4.8), 0.5 mL of appropriately diluted enzyme sample and 0.5 mL of 5 mM pNPG was incubated at 50 °C for 10 min. Reaction was terminated by adding 2.0 mL of 1 M Na_2CO_3. The absorbance of p-nitro phenol (pNP) released was measured at 400 nm. One unit enzyme activity was defined as the amount of enzyme required for releasing 1 µM of pNP per minute and was expressed as IU/mL (Ghosh and Bisaria, 1987).

2.5. Protein assay

Protein assay was done using the Coomassie brilliant blue reagent according to Bradford's protein assay method (Bradford, 1976) and protein concentration was expressed as mg/mL.

2.6. Estimation of sugars in hydrolysates

Total reducing sugars (TRS) in hydrolysates were measured using the DNS method. Hydrolysate samples were withdrawn and centrifuged at 10,000 rpm for 5min. Supernatant was used for sugar estimation using DNS reagent (Miller et al, 1959) with glucose as standard.

Individual sugars in the hydrolysates were determined by HPLC method using a Shimadzu HPLC unit equipped with Phenomenex Rezex RNM column (300 x 7.8 mm) using RI detector. This analysis was performed at 75 °C column temperature and 40 °C detector cell temperature with a flow rate of 0.6 mL/min using degassed Milli Q water as mobile phase as described in section 2.2 above. Glucose, xylose, arabinose, galactose and mannose were used as standards.

2.7. BGL extraction and concentration by acetone precipitation

BGL enzyme produced from *Aspergillus niger* NII 08121 through solid state fermentation at NIIST (Singhania et al., 2011) and available as dry power was extracted using 10 volumes of 0.05 M citrate buffer (pH 4.8), to obtain the crude enzyme solution. For obtaining a concentrated enzyme preparation of *Aspergillus niger* BGL, 4 volume of chilled acetone (-20 °C) was slowly added to cooled enzyme extract with constant stirring. The mixture was kept for 12 h at -20 °C, followed by centrifugation at 8000 rpm for 15 minutes at 4 °C. The pellet was allowed to dry at room temperature to remove residual acetone. The pellet was then dissolved in 10.0 mL of 50 mM citrate buffer (pH 4.8) and was used for hydrolysis studies.

Chapter 3

Optimization of hydrolysis parameters using Artificial Neural Network models

3.1 Introduction

The most expensive unit operation in the conversion of lignocellulosic biomass to bioethanol is the hydrolysis step. Hydrolysis can be done either by enzymatic or chemical method. Enzymatic route is highly preferred due to lesser environmental impact and lower production of inhibitors. Although major efforts have been directed towards making this unit operation a cost effective one, hydrolysis still accounts for majority of the expenses incurred in the overall process. Critical parameters like enzyme dosage, use of accessory enzymes, cost of enzymes, type of pretreatment, substrate loading, substrate size, substrate and product inhibition, substrate feeding strategy etc. needs to be optimized for development of an economically feasible process. Thus, a lot of focus is given on developing models to optimize hydrolysis and other unit operations involved in second generation bioethanol production process.

Cellulases are a group of enzymes comprising endo and exo glucanases and β glucosidases. Cellulases together with xylanases, β xylosidases and accessory enzymes like arabinofuranosidases, feruloyl esterases etc. work synergistically to hydrolyze cellulose by creating accessible sites for each other to remove obstacles and to relieve product inhibition (Zhou et al., 2009). Cellulases from a single organism have been shown to contain lower activity as against a mixture of cellulases from different sources. Such a multi – component enzyme mixture exhibits a synergistic effect with the resultant hydrolytic activity of cocktail higher than the sum of activities of individual enzymes (Nidetzky et al., 1995; Zhang et al., 2007). Efficiency of hydrolytic enzyme cocktail depends not only on the properties of individual enzymes, but also on the ratio of component enzymes in the mixture (Berlin et al., 2007; Lin et al., 2011). Thus, development of a suitable enzyme cocktail tailored to saccharify lignocellulose is essential to enhance sugar release efficiency.

Majority of the commercial cellulase preparations are *Trichoderma reesei* cellulases which contain high activities of endo and exoglucanases, but very low titers of beta glucosidases that leads to increased accumulation of cellobiose on use in hydrolysis (Duff and Murray, 1996; Nieves et al., 1998). This limitation is overcome by addition of extraneous beta glucosidases to cellulases. A significant correlation between β-glucosidase activity and biomass hydrolysis is reported in the literature.

The hemicellulose which is generally present in higher concentrations on the sheath that covers cellulose micro fibrils forms a barrier that blocks accessibility of cellulase to underlying cellulose. Also, xylans and xylo oligomers more strongly inhibit cellulase competitively, than does glucose or cellobiose (Qing et al., 2010). Removal of hemicelluloses or elimination of their negative effects can therefore

become especially pivotal in achieving higher cellulose conversion with lower enzyme doses. Also, digestion of hemicelluloses with the current commercially available cellulase enzymes is inefficient due to low xylanase activity, leading to further lowering of hydrolysis efficiency (Qing and Wyman, 2011). Xylanase supplementation breaks down hemicelluloses and increases cellulase accessibility to cellulose. Hence, addition of xylanases to the hydrolytic enzyme cocktail is critical in optimizing saccharification yields (Ohgren et al., 2007; Kumar and Wyman, 2009d).

To realize an economically feasible conversion process, the dry matter during hydrolysis should at least be about 20%. To achieve this loading, various strategies are being tried like design of new reactor configurations (Ludwig et al., 2014), enzyme cocktail development (Rivera et al., 2010), fed batch operations etc. (Liu et al., 2010). Higher biomass loading leads to reduced free water content in the reaction mixture. This increases the viscosity leading to inefficient mixing and mass transfer. Eventually, even with higher loadings, the sugar yields decrease. So an optimum biomass loading has to be chosen to minimize the negative effects of higher dry matter and improve the overall economics of the bioconversion.

Apart from enzyme cocktail and substrate loading, particle size reduction of the substrate is a significant factor affecting transportation logistics and the conversion process to bioethanol. Reduction in particle size has been shown to increase the affinity of enzyme to substrate (Gan et al., 2003). It also leads to reduced viscosities which in turn improves mixing in the reactors. But, the size reduction of substrate is an energy intensive process and adds to the cost of the overall production. Thus, particle size of the substrate needs to be optimized to improve the process efficiency of the hydrolysis process.

Artificial intelligence techniques like genetic algorithms (GA) and artificial neural networks (ANN) which are generally used for modeling and optimization of complex phenomena involving various process variables has been used increasingly in recent past for complex biotechnological problems to attain high operational performances (Rivera et al.,2010). It is more suitable for analyzing data which involves interplay of different process parameters in a nonlinear way or when it is too difficult to form deterministic equations. The basic advantage of ANN is that it can offer adaptive solutions and re-estimation of model parameters in relatively simpler forms when compared to other modeling approaches. ANN is a good alternative to conventional empirical modeling which is based on polynomial and linear regressions and statistical approaches (Kose, 2008).

Recently, ANN's are being increasingly used in applications like pattern recognition in chromatographic spectra, functional analyses of genomic and proteomic sequences and optimizing industrial processes (Manohar and Divakar, 2005). It is a highly simplified data processing system that works on the model of biological neuronal simulation (Mandal et al., 2009). A typical ANN structure is represented in Figure 3.1. The basic processing element of ANN is a neuron. The artificial neuron in this

case, receives inputs from other sources, combines them, performs a nonlinear transfer function operation on the input, and then gives the final result in terms of weights and biases (Bas and Boyaci, 2007). The most significant model parameters are the weights and biases.

Figure 3.1: A typical ANN structure

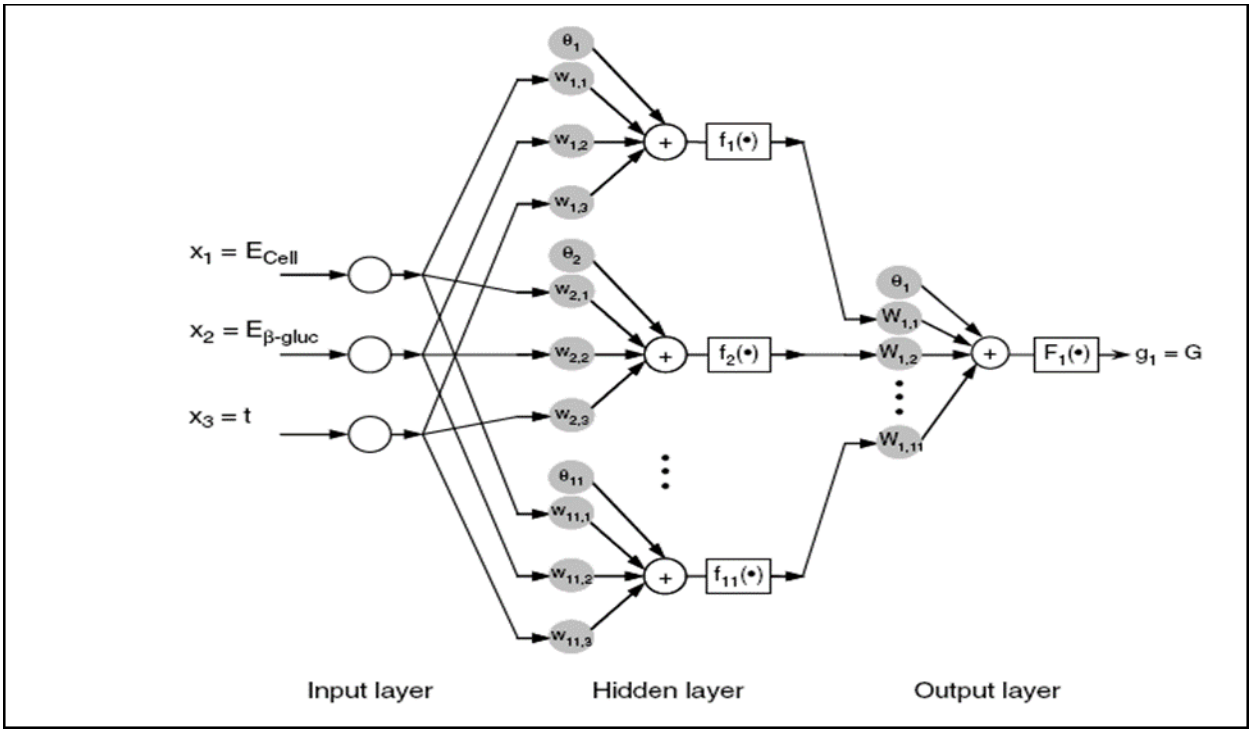

(Adapted from Rivera et al., 2010)

In this chapter, an ANN model was developed which can predict the optimum enzyme cocktail for the hydrolysis process. This model was further extended to study the effect of biomass loading, substrate particle size and reaction time on glucose and xylose concentrations during enzymatic hydrolysis of rice straw.

3.2 Materials and Methods

3.2.1. Pretreatment of Biomass

Pretreatment of rice straw was carried out as explained in section 2.1. Pretreated biomass was then air dried and stored in air tight containers till it is used further. To determine the efficiency of pretreatment and hydrolysis process, composition analysis of native and pretreated biomass was carried out as per the protocol detailed in section 2.2.

3.2.2. Enzymatic hydrolysis with varying cellulase and β-glucosidase loadings

Enzymatic saccharification of pretreated rice straw was carried out using a commercial cellulase (Zytex India Pvt. Ltd., Mumbai, India) and β-glucosidase (BGL) from *Aspergillus niger*. To optimize the cellulase and BGL loading, a full factorial design was used where the cellulase loading was varied from 0–45 FPU/g and BGL loading was varied from 0–0.3 IU/g biomass. Hydrolysis was carried out with 30 mL working volume and 10% solids loading as detailed in section 2.3. Enzymatic assays to determine cellulase and BGL activities were carried out as given in sections 2.4.1 & 2.4.4. Samples were collected after 48 hours of incubation and sugars in the supernatant were analyzed using Phenomenex Rezex RNM HPLC column using RI detector.

3.2.3. Optimisation of cellulase, β-glucosidase and xylanase loadings in enzyme cocktail development for hydrolysis

Enzymatic saccharification was carried out as detailed above including xylanase in the cocktail. Xylanase activity was determined as explained in section 2.4.3. A full factorial 3^3 design as shown in Table 3.1 was used in the optimisation. Cellulase loadings chosen were 5, 10 and 20 FPU/g; BGL loadings chosen were 0.5, 5 and 10 IU/g; and xylanase loadings taken were 2500, 5000 and 7500 U/g. Unblended Zytex cellulase and the commercial cellulase SaccharCEB C6 (SCEB6) from Advanced Enzymes Pvt. Ltd were used as control. Biomass loading was kept constant at 10%. Samples were withdrawn at 0, 2, 4, 6, 8, 10, 12, 24, 28, 32, 36 and 48 h and analyzed for sugars using HPLC.

Table 3.1: Full factorial design to determine optimum enzyme loadings for biomass hydrolysis

Run Number	Cellulase (FPU/g)	Beta-glucosidase (IU/g)	Xylanase (U/g)
1	5	0.5	2500
2	5	0.5	5000
3	5	0.5	7500
4	5	5.0	2500
5	5	5.0	5000
6	5	5.0	7500
7	5	10	2500
8	5	10	5000
9	5	10	7500
10	10	0.5	2500

11	10	0.5	5000
12	10	0.5	7500
13	10	5.0	2500
14	10	5.0	5000
15	10	5.0	7500
16	10	10	2500
17	10	10	5000
18	10	10	7500
19	20	0.5	2500
20	20	0.5	5000
21	20	0.5	7500
22	20	5.0	2500
23	20	5.0	5000
24	20	5.0	7500
25	20	10	2500
26	20	10	5000
27	20	10	7500
Control (Zytex)	20	0.0	0.0
Control (SCEB6)	20	0.0	0.0

3.2.4. Optimisation of biomass loading and particle size for hydrolysis

Pretreated biomass was sieved to separate particles of varying size range. The various size ranges chosen for hydrolysis were < 0.5 mm, 0.5-1.0 mm and >1 mm. Varying biomass loadings chosen were 10%, 15% and 18%. Various combinations of particle size and biomass loadings were taken for hydrolysis to determine the optimum substrate size and substrate loading. The optimum value was achieved by a full factorial design of experiments with varying particle sizes and biomass loadings as shown in Table 3.2. Mixed particle size biomass was taken as control and hydrolysis was carried out as mentioned above with the enzyme cocktail optimized in section 3.2.3.

Table 3.2: Full factorial design to determine optimum biomass loading and particle size for biomass hydrolysis

Run Number	Cellulase (FPU/g)	BGL (IU/g)	Xylanase (U/g)	Biomass Loading (%)	Particle Size (mm)
1	10	5	7500	10	<0.5
2	10	5	7500	10	0.5 – 1.0
3	10	5	7500	10	>1.0

4	10	5	7500	15	<0.5
5	10	5	7500	15	0.5 – 1.0
6	10	5	7500	15	>1.0
7	10	5	7500	18	<0.5
8	10	5	7500	18	0.5 – 1.0
9	10	5	7500	18	>1.0
10	10	5	7500	10	Mixed
11	10	5	7500	15	Mixed
12	10	5	7500	18	Mixed

3.2.5. ANN model development

A Multi-Layer Perceptron (MLP) based feed forward Neural Network Model with Levenberg – Marquardt back propagation algorithm was used in this study to predict the glucose and xylose yields during enzymatic hydrolysis of biomass for varying particle sizes and biomass loadings. This is the most widely used ANN model for optimization studies because of its easy architecture and mathematical form. (Cheng et al., 2008a; Jorjaniet al., 2008).

The ANN model has a multiple layer perceptron neural network (MLP) with interconnected neurons arranged in layers that are input, hidden and output layers. This model represents an input/output model where each layer is interconnected by weights $'w'$ and biases $'b'$, which are adjustable enabling it to model nonlinear functions. Hidden layers are employed to perform complex and non-linear functions on the network (Jorjani et al., 2008). The number of hidden layers can vary and is fixed to get the optimum R^2 value for the model (Ghaffari et al., 2006). Number of neurons in hidden layers is very critical. A higher number of neurons in a particular hidden layer can lead to over fitting of the model where instead of generalization of patterns in the training data set, the network memorizes the pattern. If the number of neurons is lesser, it leads to under fitting of model and hence more training time is needed to find optimum number of neurons (Hussain et al., 1992).

Assuming that an MLP layer consists of an input layer of N neurons, a hidden layer of M neurons and an output layer of K neurons, the relationship between different layers can be described by equation 1.

$$g_k = F\left[\sum_{j=1}^{M} W_{kj}\ f\left(\sum_{i=1}^{N} w_{ji}\, x_i + \theta_j\right) +\ b_k\right] \quad (1)$$

where, j = 1, 2…M; i = 1,2….M and k = 1,2…K. In equation 1, w_{ji} is the weight connecting i^{th} neuron in the input layer to the j^{th} neuron in the hidden layer, θ_j is the bias of the j^{th} neuron in the hidden layer. Similarly, W_{kj} is the weight connecting the j^{th} neuron in the hidden layer to the k^{th} neuron in the output layer and b_k is the bias of the k^{th} neuron in the output layer.

Each neuron in a layer consists of an activation function of the form $f(\cdot) and F(\cdot)$. Output from a neuron is determined by transforming its input using this activation function (Razavi et al., 2003; Moghaddam et al., 2010). In the present formulation $f(\cdot) and F(\cdot)$ are the activation functions of j^{th} neuron in the hidden layer and k^{th} neuron in output layer respectively which are assumed as log sigmoid function and pureline function as given by equation 2 and 3 respectively. The neural network toolbox available in MATLAB (Mathworks, Natick, MA, USA) is used for fitting of the experimental data. Feed-forward back propagation learning algorithm (Levenberg-Marquardt), *trainlm* was used for ANN training. Transfer functions, *logsig*, and *purelin* (pure linear function in the output layer) were used for activation functions.

$$\boldsymbol{f(x) = \frac{1}{(1+e^{-x})}} \tag{2}$$

$$\boldsymbol{F(x) = x} \tag{3}$$

The data set used for training the ANN model must contain at least 100 input/output patterns for better training of the model. Out of the dataset, 70% was taken up for training, 15% for testing and 15% for validating the ANN model.

The mean square error MSE (given by equation 4) was minimized by making adjustments to the network parameters namely error goal, maximum number of epochs (iterations), validation checks etc.

$$\boldsymbol{MSE = \left[\sum_{k=1}^{K}(d_k - g_k)2\right]} \tag{4}$$

In equation 4, g_k is the predicted output of neural network and d_k is the experimental output. Training was fixed at 1000 epochs to avoid overtraining and validation check was done 6 times. Training sequences were executed by varying the number of neurons in the hidden layer. Numbers of hidden neurons were varied from 3 to 10. The networks with varying number of hidden neurons in one hidden layer are trained and the performance of the network is evaluated on the basis of the mean squared error MSE. Lower values of MSE indicate better suitability of the model. After correct simulation on test points based on MSE and correlation coefficient (R^2), training was then performed on all data. After training the ANN using the training data set, validation data was used to evaluate the performance of the training data set based on the ability to correctly predict/ simulate the validation data.

Learning rates and momentum coefficients are two parameters of the model that are used to optimize the ANN parameters. The purpose of developing such a model is to obtain the optimum sugar yields upon varying input parameters.

3.2.5.1. ANN model for optimization of cellulase and BGL levels during hydrolysis

The ANN model for optimization of BGL and cellulase loadings (section 3.2.2) has cellulase and BGL loading as 2 neurons in the input layer and total reducing sugar yield as 1 neuron in the output layer. The corresponding ANN model is schematically shown in Figure 3.2. Of the various architectures investigated, 1 hidden layer with 3 neurons was considered as optimum configuration which is based upon the regression values obtained. The dataset contained 130 input/output patterns for optimization of BGL and cellulase loading.

Figure 3.2: Neural Network diagram used for determining the optimum cellulase and BGL loadings

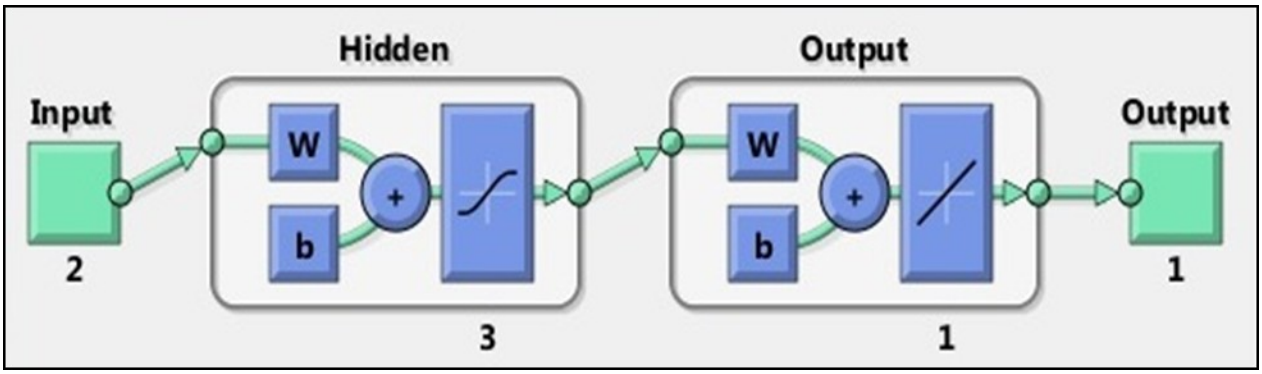

3.2.5.2. ANN model for Optimisation of cellulase, β-glucosidase and xylanase loadings in enzymatic hydrolysis cocktail development

For this optimization study, the input layer of ANN model consists of 4 neurons which correspond to cellulase, BGL and xylanase loading and reaction time (Figure 3.3). Output layer of the ANN model has 2 neurons which correspond to that of glucose and xylose yields. There is one hidden layer with 8 neurons which is chosen after repeated trials to avoid over or under fitting. The data set contained 324 input/output patterns. Followed by ANN model training, a validation check was performed to determine the efficacy of model in predicting the final glucose and xylose yields when different input values are assigned to the input layer of the ANN model. For this purpose, the hydrolysis process was carried out with different

enzyme loadings than used in the factorial design. This dataset was then validated with the model developed above.

Figure 3.3: Schematic view of the ANN model for optimum enzyme cocktail for hydrolysis of rice straw

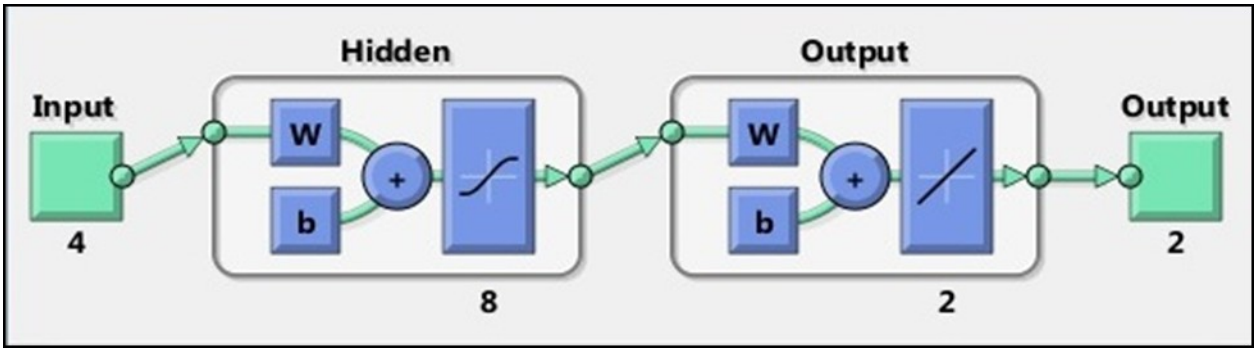

3.2.5.3. ANN model for optimisation of biomass loading and particle size for hydrolysis

Particle size of biomass, biomass loading and time were the three input neurons and glucose and xylose yields were considered as 2 neurons in the output layer for this ANN model (Figure 3.4).This model also contained 1 hidden layer with 8 neurons. 120 input/output data were there in the dataset to optimize biomass loading and particle size.

Figure 3.4: Neural Network diagram used for determining the optimum biomass loading and particle size

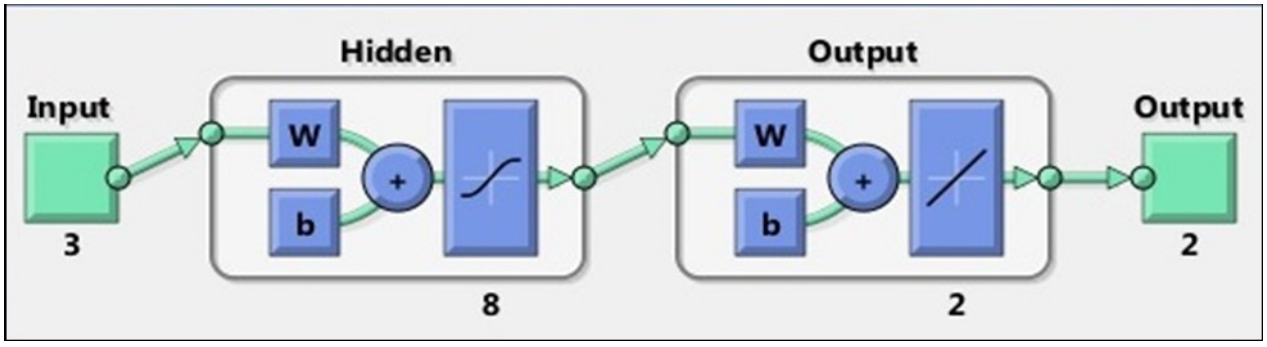

3.3. Results and Discussion

3.3.1. Composition analysis of native and pretreated biomass.

The composition of native and alkali pretreated biomass is shown in Table 3.3. It can be observed that there is a difference in the composition of native and alkali pretreated rice straw. It has been reported that alkali treatment dissolves lignin and hemicelluloses. The primary role of NaOH pretreatment is the disruption of ester bonds between lignin and carbohydrates in the biomass that results in solubility of lignin (Kumar et al. 2009). Maximum amount of glucose that can be obtained is 682 mg per gram of biomass hydrolyzed and maximum xylose yield possible is 211 mg per gram of biomass based on the cellulose and hemicelluloses content of pretreated biomass.

Table 3.3: Chemical Composition of native and 2% alkali pretreated rice straw

Components	Native Biomass (%)	Pretreated Biomass (%)
Cellulose	37.6	61.44
Hemicellulose	14.21	18.59
Lignin	39.8	20.42
Ash	6.37	5.99

3.3.2. Development of ANN model to optimize cellulase and BGL loadings for hydrolysis

3.3.2.1. Full factorial design to predict the effect of BGL supplementation to cellulase

Cellulase was supplemented with BGL in an incremental manner to investigate the effect of supplementation during the hydrolysis process. It may be observed from Figure 3.5, that supplementing BGL to cellulase increases the total reducing sugar yields during biomass hydrolysis. When 0.025 IU/g BGL is added as a supplement to cellulase, there was a rapid increase in rate of reaction and sugar release efficiency. Further increase in BGL loadings from 0.05 IU/g to 0.3 IU/g gave almost similar sugar yields. Also, the hydrolysis efficiencies were very low. Unblended cellulase yielded 40% saccharification efficiency. Blending could only increase it to 47.8%. Maximum sugar yield of 427 mg sugars /g biomass hydrolyzed was obtained with 45 FPU/g cellulase and 0.025 IU/g BGL. At cellulase loadings of 20 to 30 FPU/g and BGL loadings of 0.025 to 0.150 IU/g, 350 to 390 mg/g sugars could be obtained which can be considered an optimum operation range for hydrolysis.

Figure 3.5: Total Reducing Sugar yields for different BGL loadings

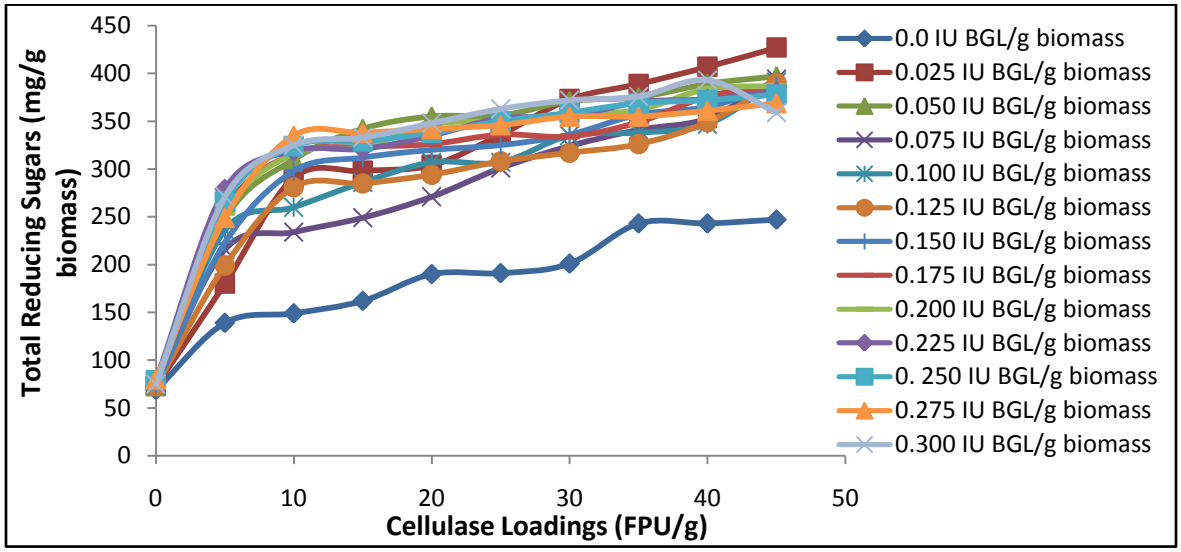

Kumar and Wyman, (2009c) reported that a combined loading of cellulase and BGL of 16.1 mg/g glucan i.e., about 7.5 FPU/g led to a glucose release of 50 to 70% of the theoretical maximum. The β-glucosidase from *Aspergillus niger* is most commonly used in supplementation studies to complement the cellulases from *T. reseei*. Boosting the cellulases with β-glucosidases (BGL) or using microbes with high proportion of β-glucosidase in their cellulases will increase sugar yields during hydrolysis (Del Pozo et al., 2012). The fungi *Tolypocladium cylindrosporum* syzx4, isolated from rotten corn stover was found to be an avid producer of BGL upon growth on agro residues. This thermo acidophilic enzyme when supplemented with the commercial cellulase, Celluclast was found to enhance hydrolysis efficiency by 88.4% (Zhang et al., 2011). BGL from *Acremonium thermophilum* and *Thermoascus aurantiacus*, was found to be more efficient in cellobiose hydrolysis than BGL from Novozyme. A major drawback of these enzymes was their sensitivity to glucose. Sensitivity to glucose implies higher specificity constant for cellobiose which in turn indicates that an optimum mixture of BGL has to be selected based on high activity and glucose inhibition (Teugjas and Valjamae, 2013). Arantes and Saddler (2011) reported that impact of BGL loadings is higher than cellulase loadings for hydrolysis of biomass.

Most researches claim that BGL has a synergistic effect on biomass hydrolysis. Further it is also reported that increasing the BGL loadings beyond a certain limit does not correspond to increase in glucose levels. This is because addition of BGL decreases the cellobiose concentration, but it is susceptible to inhibition and activity loss by cellooligomers and cellodextrins with high degree of polymerization (Kumar and Wyman, 2009a). Certain β-glucosidases are also inactivated by lignin containing substrates like lignocelluloses (Xu et al., 2008; Yang and Wyman, 2006). Effectiveness of a

BGL may also depend upon the type of pretreatment, source of enzyme, substrate type, time of hydrolysis etc. (Tengborget, 2001).

3.3.2.2 ANN training and validation

The ANN model explained in section 3.2.5.1 was used for optimization study. The range of inputs and outputs selected for model development are given in Table 3.4.

Table 3.4: Input and output vectors used for ANN training, testing and validation

Run No.	Input Vectors		Output Vectors
	BGL Loading (IU/g)	Cellulase Loading (FPU/g)	Total Reducing Sugar (mg/g biomass)
1-10	0.0	0, 5, 10, 15, 20, 25, 30, 35, 40, 45	69-247
11-20	0.025	0, 5, 10, 15, 20, 25, 30, 35, 40, 45	73-427
21-30	0.050	0, 5, 10, 15, 20, 25, 30, 35, 40, 45	73-397
31-40	0.075	0, 5, 10, 15, 20, 25, 30, 35, 40, 45	74-394
41-50	0.100	0, 5, 10, 15, 20, 25, 30, 35, 40, 45	74-391
51-60	0.125	0, 5, 10, 15, 20, 25, 30, 35, 40, 45	73-390
61-70	0.150	0, 5, 10, 15, 20, 25, 30, 35, 40, 45	74-387
71-80	0.175	0, 5, 10, 15, 20, 25, 30, 35, 40, 45	79-387
81-90	0.200	0, 5, 10, 15, 20, 25, 30, 35, 40, 45	77-387
191-100	0.225	0, 5, 10, 15, 20, 25, 30, 35, 40, 45	79-381
101-110	0.250	0, 5, 10, 15, 20, 25, 30, 35, 40, 45	79-378
111-120	0.275	0, 5, 10, 15, 20, 25, 30, 35, 40, 45	80-369
121-130	0.300	0, 5, 10, 15, 20, 25, 30, 35, 40, 45	75-359

Out of the 130 data points, 90 data points were used to train the network and 20 data points were chosen for network validation. For the validation process also, optimal number of hidden neurons were determined by varying the number of neurons from 1 to 10. The optimum number was found to be 3 neurons in the hidden layer depending upon the lowest MSE value and highest regression values for the validation dataset. The regression values of training, testing and validation datasets are presented in Table 3.5.

Table 3.5: Regression values of the predicted model

	Samples	R^2
Training	90	0.972
Validation	20	0.984
Testing	20	0.985

The R^2 values of testing and validation data sets is found to approach unity which confirms the dependability of the ANN model in predicting the sugar yields during hydrolysis. Figure 3.6 shows the regression plot for the ANN model. The overall R^2 value of the model was 0.98.

Figure 3.6: Regression diagram of the proposed ANN model

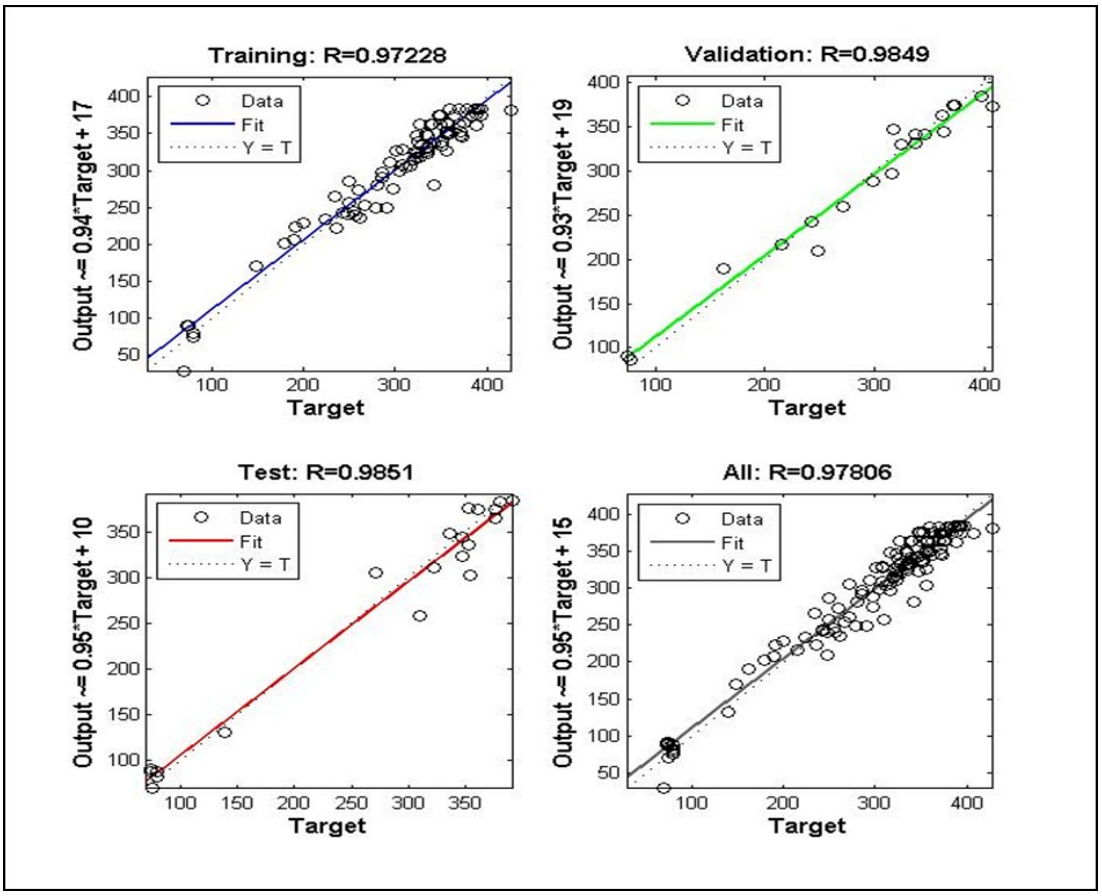

Error histogram of the developed ANN model is shown in Figure 3.7. The blue bars represent training data, the green bars represent validation data, and the red bars represent testing data. This histogram shows clearly the data points where the fit is significantly worse than the majority of data. From this plot, it may be concluded that this ANN model can be used in predicting sugar yields during hydrolysis of biomass when BGL is supplemented with cellulase.

Figure 3.7: Error histogram of the neural network model

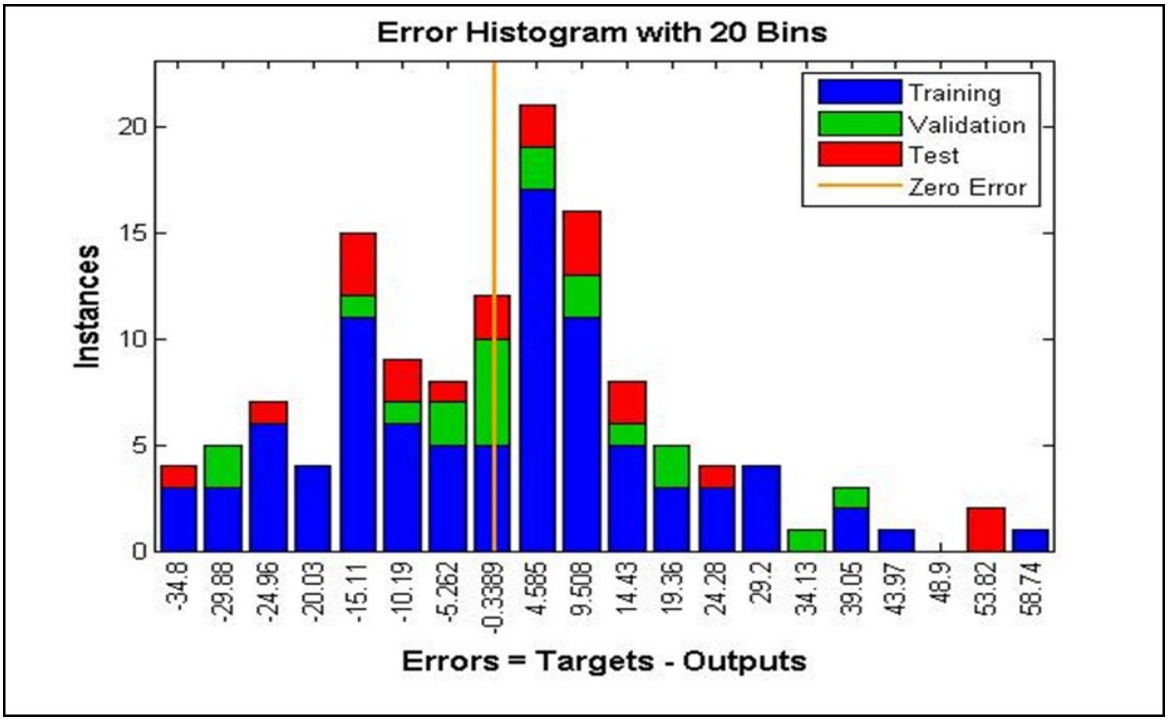

Using the optimized weights and bias given in Table 3.6 and input parameters, the total reducing sugar concentrations can be obtained for different enzyme loadings.

Table 3.6: Optimized parameters (weights and bias) of the ANN model

	Parameters connecting the input and hidden neurons			Parameters connecting the hidden and output neurons	
	w_{j1}	w_{j2}	Θ_j	W_{1j}	$b_1 = -3.058$
j = 1	-1.536	4.347	-0.447	0.032	
j = 2	1.585	0.0024	1.847	1.964	
j = 3	-0.22	3.7504	4.47	1.769	

The developed model is efficient in predicting sugar yields with high accuracy. Alkali pretreated biomass leaves most of the xylan and other pentose sugars in the solids, with the result that xylanase as well as possibly other accessory enzymes are needed in addition to cellulase and BGL to realize high sugar yields. Also, as the efficiency of hydrolysis is very low with only BGL supplementation, optimization studies were carried out with combined supplementation of BGL and xylanase to maximize saccharification yield.

3.3.3 Development of ANN model to optimize enzyme cocktail

3.3.3.1. Results of full factorial design to determine optimum enzyme loadings for biomass hydrolysis

The most significant results of the effect of enzyme cocktail on the hydrolysis runs are presented in Table 3.7. It can be seen that very high efficiencies were obtained when BGL loading is increased. Also higher xylanase supplementation resulted in higher saccharification efficiency. Even with 5 FPU/g cellulase, 75% sugar release efficiency could be attained when the accessory enzymes loading was enhanced.

Table 3.7: Significant results of hydrolysis of biomass upon varying enzyme loading and time

Cellulase (FPU/g)	BGL (IU/g)	Xylanase (U/g)	Time (h)	Glucose (mg/g)	Xylose (mg/g)	% efficiency of glucose production	% efficiency of xylose production
5	5	7500	24	457	158	75.242	94.259
5	10	7500	24	477	176	78.503	104.746*
10	5	7500	12	473	149	77.971	88.436
10	5	7500	24	487	147	80.256	87.338
10	5	7500	28	515	156	84.855	92.936
10	10	7500	8	459	151	75.663	89.877
10	10	7500	10	472	163	77.747	97.111
10	10	7500	12	476	166	78.345	98.607
10	10	7500	24	498	175	81.997	103.992*
10	10	7500	28	501	170	82.499	101.159*
10	10	7500	32	522	184	86.050	109.787*
20	5	7500	8	456	157	75.065	93.176
20	5	7500	10	456	160	75.089	95.469
20	5	7500	12	463	159	76.239	94.462
20	5	7500	24	491	167	80.835	99.481
20	5	7500	28	503	171	82.846	101.929*
20	10	7500	4	464	176	76.465	104.713*
20	10	7500	6	472	175	77.728	103.933*
20	10	7500	8	486	181	80.013	108.025*
20	10	7500	10	491	173	80.906	103.208*
20	10	7500	12	492	168	81.115	100.207*
20	10	7500	24	505	190	83.169	103.251*
20	10	7500	28	514	190	84.670	103.139*

20	10	7500	32	521	192	85.762	104.130*
20	10	7500	36	528	194	86.998	105.761*

** Efficiencies higher than 100% observed as use of RNM column sometimes leads to over estimation of xylose due to closely placed retention times of pentose sugars.*

It was also observed that the initial rate of reaction for xylose production was very high compared to glucose production rate which picked up only gradually. This further substantiates the claim that xylanase removes the xylan residues from the biomass, thus making cellulose more accessible to cellulase. Thus, once the inhibitory xylans are removed, glucose release was enhanced and the final efficiencies were much higher than the hydrolysis efficiency with cellulase alone. Another significant advantage of xylanase and higher BGL supplementation is that the hydrolysis time reduces considerably. Close to 70 – 75% sugar release efficiency was obtained after 12-28 h of reaction. This is significant as lower reaction times imply lower operation costs.

Upon variation of xylanase, a profound increase in hydrolysis yield was observed for the same cellulase and BGL loadings indicating the synergistic effect xylanase has on the hydrolysis efficiency (Figure 3.8A). Increase in xylanase loading not only increased the rate of xylose production, but also gave higher glucose yields. Xylanase loading of 7500 U/g yielded 512 mg glucose/g biomass after 48 h of hydrolysis which is 16 % higher yield as compared to hydrolysis with 2500 U/g. Maximum sugar release takes place by 24 h after which sugar release stagnates

BGL loadings were observed to have a positive effect on glucose yield. Maximum glucose yield was obtained with 10 IU/g BGL even though initial glucose production rates were similar for both 5 and 10 IU/g BGL loading as shown in Figure 3.8B. However, 5 IU/g BGL also gave almost similar glucose yields towards the completion of hydrolysis. It is observed that 7500 U/g xylanase and 10 IU/g BGL loading resulted in 512 mg glucose/ g biomass with just 5 FPU/g cellulase. This substantiates the earlier findings that a multi component enzyme mixture results in synergistic action of the component enzymes and type and source of enzyme is as significant as enzyme dosage in an efficient cocktail development.

When varying cellulase loadings were used, higher loadings led to an initial faster rate of glucose production or cellulose hydrolysis. But as the reaction progressed, the yields were similar (Figure 3.8C). The difference in glucose yield between 10 and 20 FPU/g loading was only around 7 mg. Consequently, it can be asserted that high loadings of cellulase are not needed for attaining high saccharification. It is the ratio of component enzymes in the cocktail that is critical to hydrolysis of biomass.

Figure 3.8: Glucose yield under varying concentrations of supplementary enzymes/cellulase

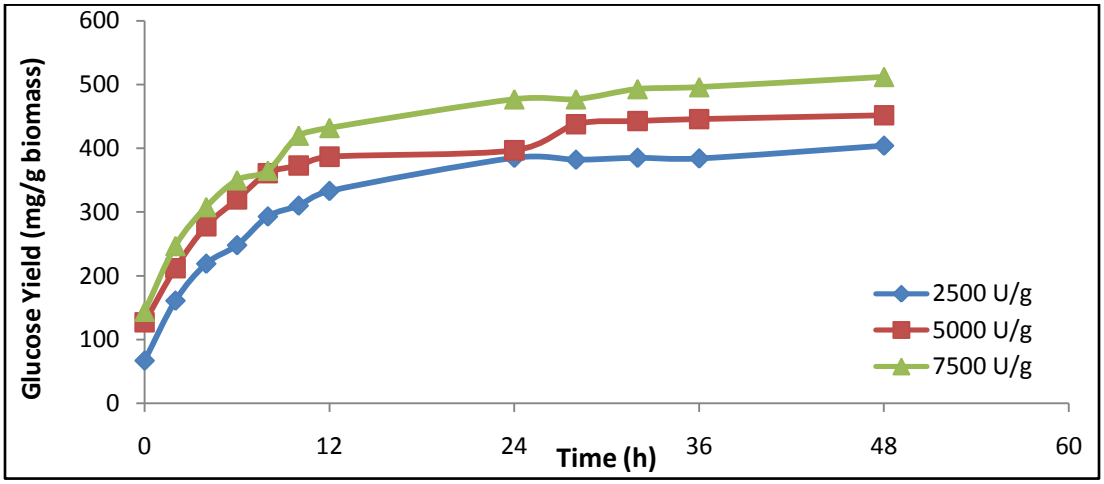

A) Xylanase supplementation at 5FPU /g cellulase and 10 IU/g BGL concentrations

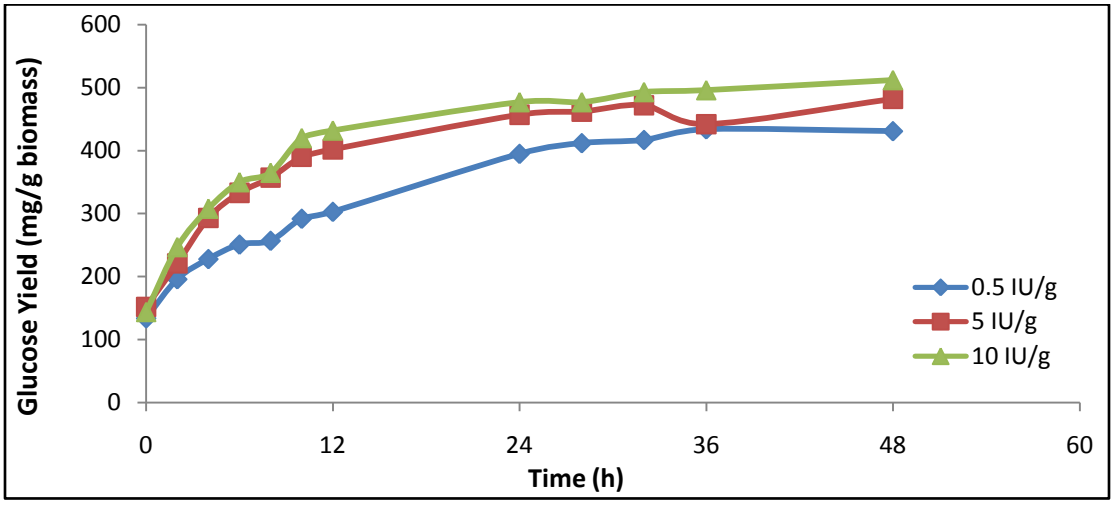

B) BGL supplementation at 5FPU /g cellulase and 7500 U/g xylanase concentrations

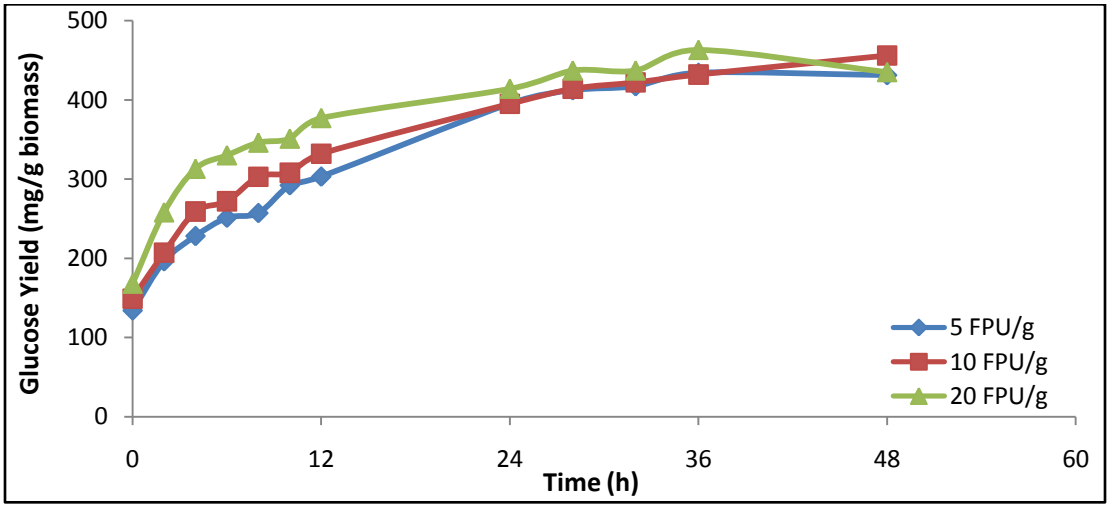

C) Varying cellulase concentration at 0.5 IU /g BGL and 7500 U/g xylanase concentration

From the kinetics studies, it was found that, maximum efficiency achieved was 87% with 20 FPU/g Cellulase, 10 IU/g BGL and 7500 U/g Xylanase upon 48 hours of incubation which yielded 528 mg glucose/g biomass. The enzyme cocktail predicted for optimum hydrolysis was-10 FPU/g cellulase, 5 IU/g BGL and 7500 U/g xylanase with a projected efficiency of 80% in 24 h.

The efficacy of this cocktail for lignocellulose hydrolysis was tested against commercial biomass hydrolyzing enzymes like SaccharicEB C6, Cellic CTec 2 and the individual Novozymes® enzymes blended in the same ratio as with the optimized cocktail. The cocktail developed, performed much better than the commercial enzymes. The maximum efficiency for Zytex was 40% after 48 h. SaccharicEB C6 being a biomass hydrolyzing enzyme gave an efficiency of 54%. Cellic CTec 2 gave slightly higher hydrolysis efficiency than the optimized cocktail. Total reducing sugar yields with Cellic CTec 2 were 79.6% of theoretical yield after 48 h incubation as compared with 73.3% efficiency for optimized cocktail. The efficiency for Novozymes® individual components blended in the ratio as our cocktail had almost similar yields as evident from Figure 3.9. Hence the cocktail developed may be considered as good as commercial enzymes for biomass hydrolysis.

Figure 3.9: Comparative yields among different enzymes

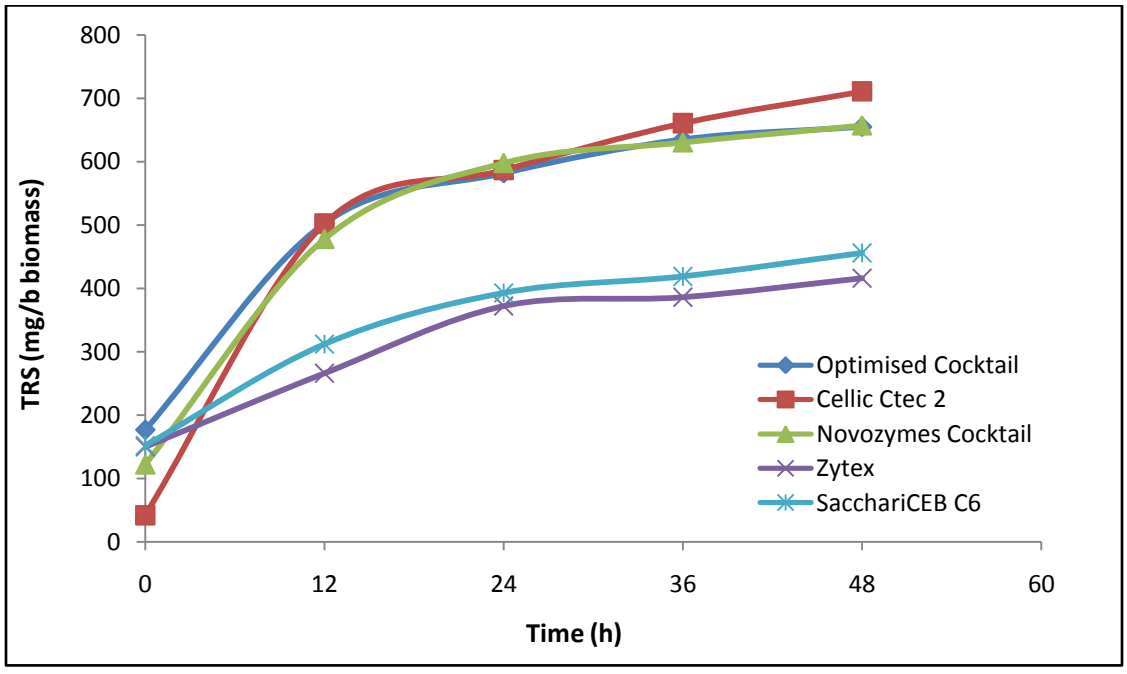

Several studies have reported the confirmative effect of addition of BGL and xylanases on overall hydrolysis efficiency enhancement. Upon hydrolysis of steam pretreated corn stover in the presence of xylanase at 60 mg/g cellulase, it was found that glucose release efficiency increased from 45% to more

than 80%. Xylan hydrolysis also increased from 56% to 95%. Addition of xylanase without cellulase reduced xylan hydrolysis (Hu et al., 2011). A xylanase loading of 100 IU/ g cellulose could enhance glucose and xylose yields by 19.5% and 18.6% respectively after 72 h of hydrolysis (Alvira et al., 2011). On the other hand, Qing and Wyman (2011) reported that addition of extra xylanase or xylosidase to cellulose beyond the optimum concentration, reduced cellulose conversions. Addition of 7.5 FPU/g glucan resulted in glucose release with 81% efficiency. But addition of xylanase reduced glucose yield by 7%. They postulated that this might be due to hemi-cellulases hindering cellulases or occupation of cellulose catalytic sites non-productively. Also some reports suggested that there exists synergism between xylanase and cellulase enzymes that decreases at high enzyme loadings above saturation limit (Kim et al., 1998).

One of the reasons for the synergistic action of xylanase with cellulase on enzymatic hydrolysis of biomass is the removal of xylan coat from the pretreated biomass that improves cellulose accessibility to cellulases (Bura et al., 2009; Kumar and Wyman, 2009d). Ryu and Kim (1998) suggest that xylanases increase the available cellulose for cellulase interaction due to their binding on to lignin. Xylanases also contribute to enhanced cellulose degradation by increasing fiber porosity and fiber disintegration that leads to increase in surface area of cellulose for cellulase binding (Arantes and saddler, 2010).

3.3.3.2 ANN model training and validation

The ANN model to develop an optimum enzyme cocktail for hydrolysis consisted of 4 input parameters namely cellulase, BGL and xylanase loadings and hydrolysis time. The two output parameters were glucose and xylose yield. Here, the ANN structure was optimized to contain 8 hidden neurons in 1 hidden layer. The range of inputs and outputs selected for model development are given in Table 3.8.

Table 3.8: Input and output vectors used for ANN training, testing and validation

Run Number	Input Vectors				Output Vectors	
	Cellulase (FPU/g)	BGL (IU/g)	Xylanase (U/g)	Time (h)	Glucose (mg/g)	Xylose (mg/g)
1	5	0.5	2500	0 - 48	68 - 362	78 - 132
2	5	0.5	5000	0 - 48	103 - 454	63 - 145
3	5	0.5	7500	0 - 48	134 - 431	71 – 139
4	5	5	2500	0 - 48	77 - 408	74 – 146
5	5	5	5000	0 - 48	95-451	63 – 181
6	5	5	7500	0 - 48	152 - 482	67 – 177
7	5	10	2500	0 - 48	67 - 404	82 – 181

8	5	10	5000	0 - 48	127 - 452	92 – 185
9	5	10	7500	0 - 48	144 - 512	96 - 174
10	10	0.5	2500	0 - 48	64 - 349	71 – 130
11	10	0.5	5000	0 - 48	107 - 417	85 – 172
12	10	0.5	7500	0 - 48	149 - 456	71 – 168
13	10	5	2500	0 - 48	90 - 414	84 – 161
14	10	5	5000	0 - 48	80 - 420	43 – 155
15	10	5	7500	0 - 48	148 - 489	57 – 153
16	10	10	2500	0 - 48	77 - 432	88 – 162
17	10	10	5000	0 - 48	119 - 445	95 – 180
18	10	10	7500	0 - 48	193 – 492	87 – 181
19	20	0.5	2500	0 - 48	76 - 397	86 – 165
20	20	0.5	5000	0 - 48	108 - 390	114 – 142
21	20	0.5	7500	0 - 48	168 - 435	86 – 144
22	20	5	2500	0 - 48	96 - 405	105 – 173
23	20	5	5000	0 - 48	128 - 426	91 – 169
24	20	5	7500	0 - 48	288 - 489	134 – 180
25	20	10	2500	0 - 48	88 - 414	83 – 185
26	20	10	5000	0 - 48	124 - 472	91 – 166
27	20	10	7500	0 - 48	174 - 501	91 - 195

For the optimization of number of hidden neurons and hidden layers, the number of neurons was varied from 1 to 10 and the optimum number was found to be 8. The optimum number was chosen based on the lowest MSE value and highest regression values for the validation dataset. Out of the 324 data points, 226 data points were chosen for validation of the network. The MSE and regression values of training, testing and validation datasets are as given in Table 3.9.

Table 3.9: Error and regression values of the predicted model

	Samples	MSE	R^2
Training	226	1.60728e-4	0.995
Validation	49	2.3044e-4	0.992
Testing	49	2.86434e-4	0.993

The R^2 values of testing and validation data sets was found to be close to unity which confirms the reliability of the ANN model in predicting the sugar yields during hydrolysis. The overall R^2 value of the model was 0.99. Figure 3.10 shows the regression plot of the proposed ANN model.

Figure 3.10: Regression diagram of the ANN model

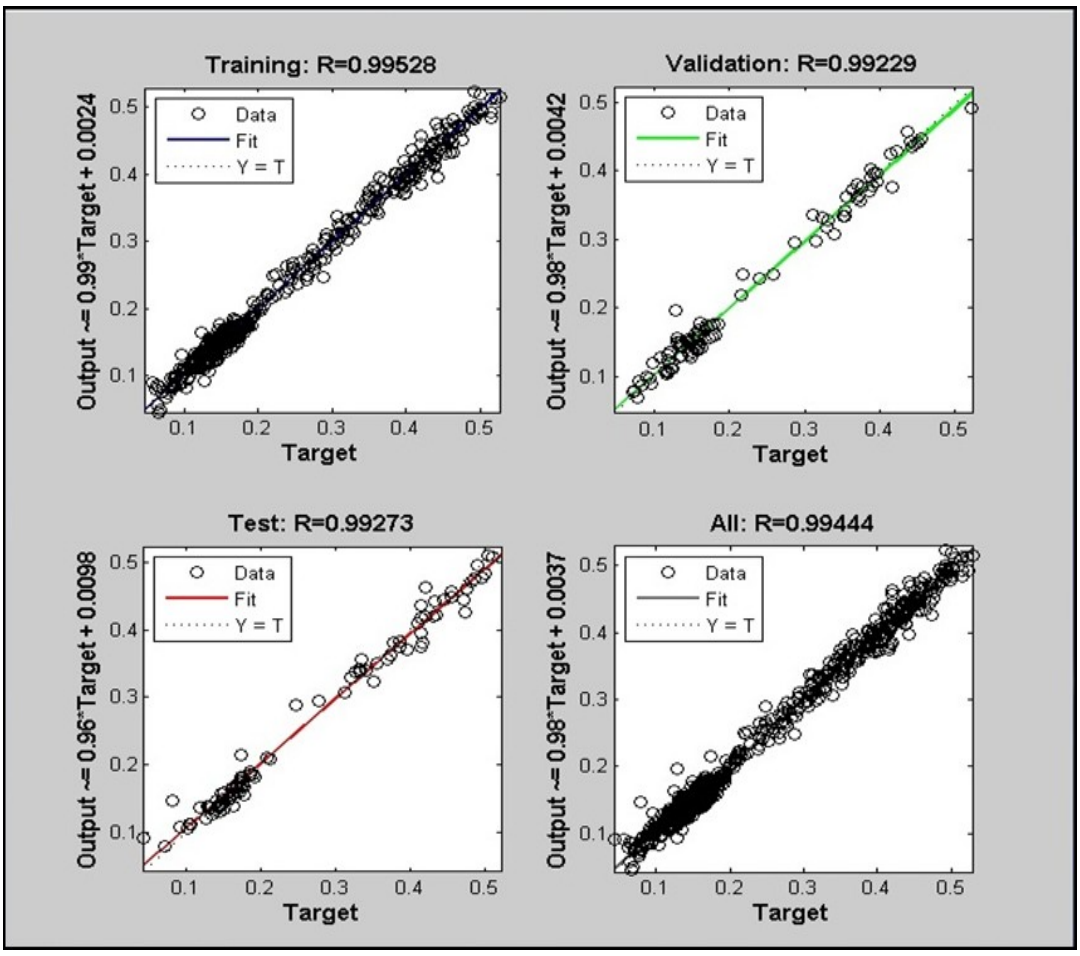

The corresponding error histogram of the proposed ANN model is shown in Figure 3.11.This histogram shows clearly, which are the data points where the fit is significantly worse than the majority of data. Hence it can be concluded that the model is quite efficient in predicting the glucose and xylose yields when cellulase, BGL, xylanase loadings and reaction times are given.

Figure 3.11: Error histogram of the proposed ANN model

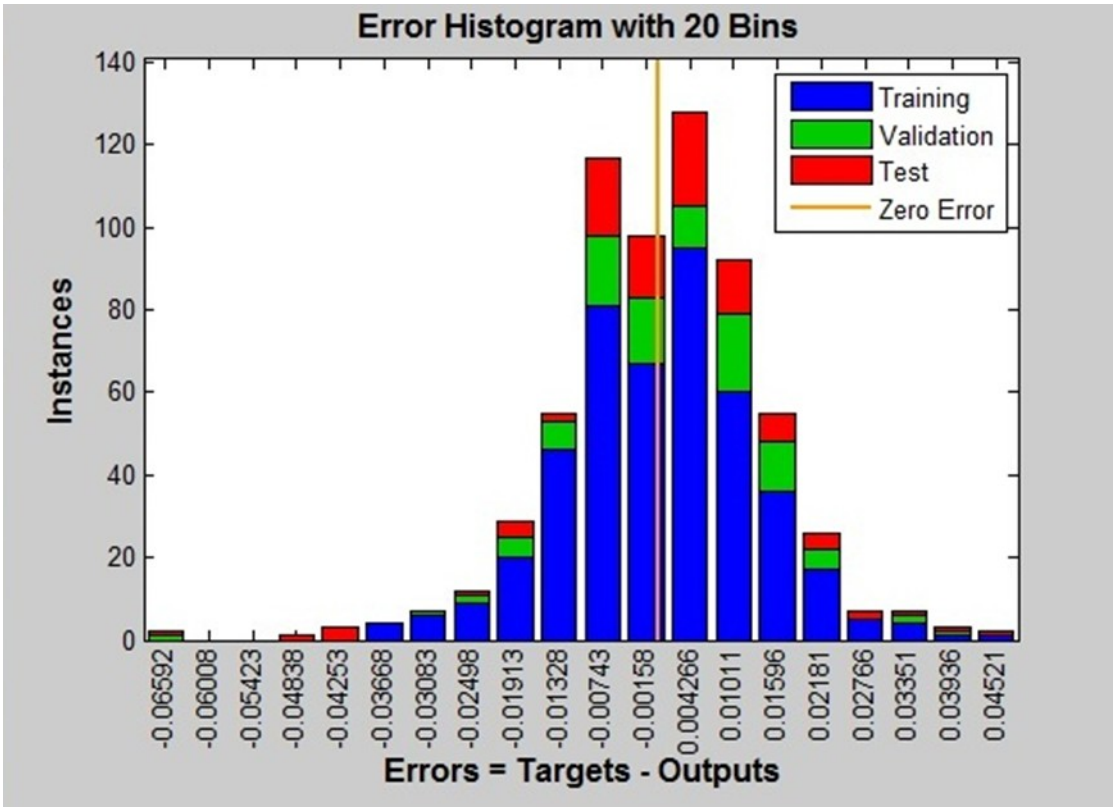

Figure 3.12: Experimental validation of ANN predicted sugar yields.

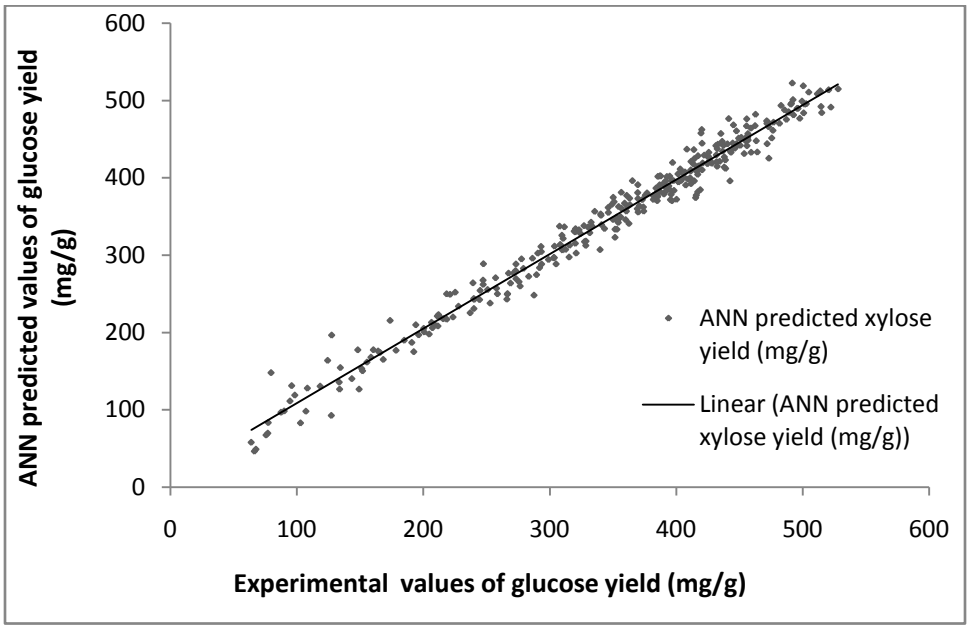

A) Comparison of ANN simulated and experimental glucose yields (mg/g).

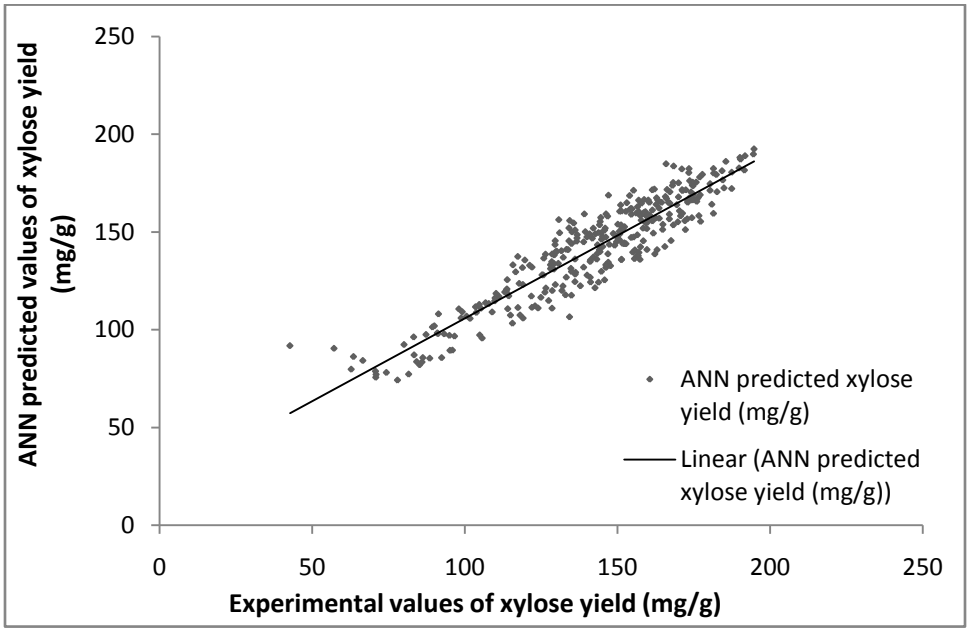

B) Comparison of ANN simulated and experimental xylose yields (mg/g)

Table 3.10: Optimized parameters (weights and bias) of the ANN model

	Parameters connecting the input and hidden neurons					Parameters connecting the hidden and output neurons		
	w_{j1} (i=1)	w_{j2} (i=2)	w_{j3} (i=3)	w_{j4} (i=4)	Θ_j	W_{1j} (k=1)	W_{2j} (k=2)	b_k (k=1,2)
j=1	2.4887	-0.0673	-1.3936	0.725	-1.8163	-0.0869	-0.0002	-1.918
j=2	0.1943	0.5989	0.1554	0.1016	-0.4787	0.8207	0.7828	-1.2856
j=3	-0.0687	-0.1935	0.0115	5.2242	6.0092	2.2804	1.8453	
j=4	1.2549	1.146	3.0778	0.0166	-0.3342	-0.033	-0.0897	
j=5	0.1544	4.391	0.221	1.0304	-1.2018	-0.2381	-0.1403	
j=6	-0.5012	-0.6515	-0.0812	-1.3748	-1.4412	-0.455	-0.2399	
j=7	-1.0939	-1.1221	2.6758	1.3117	-2.8269	0.0947	0.0306	
j=8	0.6932	-0.4358	3.9022	1.0756	2.0482	0.0586	0.0206	

Performance of ANN model in describing the correlation between experimental and predicted glucose and xylose yields (mg/g) at various time intervals are shown in Figures 3.12A and Figure 3.12B. The overall R^2 values for these data sets are 0.98 and 0.86 for the predicted glucose and xylose concentrations which proves the capability of proposed ANN model in predicting accurately the glucose and xylose yields during hydrolysis.

It may be concluded that the model effectively tracks the trajectory of the experimental observations. Using the optimized weights and bias of the ANN model as given in Table 3.10, and the input parameters of enzyme loadings and different time intervals, the glucose and xylose concentrations upon rice straw hydrolysis can be predicted.

3.3.3.3 Validation of ANN model

To validate the model obtained, hydrolysis was carried out with varying loadings of cellulase, BGL and xylanase other than those used for performing the initial experiments and glucose and xylose yields quantified. The experimentally obtained data was fit with the model. The validation runs performed are given in Table 3.11.

Table 3.11: Validation data set for ANN model

Sample #.	Cellulase (FPU/g)	BGL (IU/g)	Xylanase (U/g)	Time (h)	Glucose (mg/mL)	Xylose (mg/mL)	TRS (g/g)
1	8	1.5	3500	4	0.205	0.200	0.446
2	8	1.5	3500	8	0.206	0.206	0.459
3	8	1.5	3500	12	0.245	0.208	0.501
4	8	1.5	3500	24	0.259	0.295	0.586
5	8	1.5	3500	36	0.272	0.304	0.585
6	8	1.5	3500	48	0.230	0.355	0.598
7	15	4	6000	4	0.262	0.219	0.527
8	15	4	6000	8	0.275	0.221	0.542
9	15	4	6000	12	0.285	0.254	0.584
10	15	4	6000	24	0.325	0.351	0.690
11	15	4	6000	36	0.352	0.362	0.728
12	15	4	6000	48	0.366	0.393	0.771

13	18	8	3000	4	0.231	0.200	0.455
14	18	8	3000	8	0.240	0.218	0.485
15	18	8	3000	12	0.245	0.232	0.510
16	18	8	3000	24	0.269	0.339	0.617
17	18	8	3000	36	0.296	0.368	0.674
18	18	8	3000	48	0.320	0.383	0.712

The regression coefficient was found to be 84% even with a different set of pretreated biomass (Figure 3.13). Hence, the model developed could be used for predicting the response upon hydrolysis with different enzyme loadings and different time points.

Figure 3.13: Regression plot of ANN validation

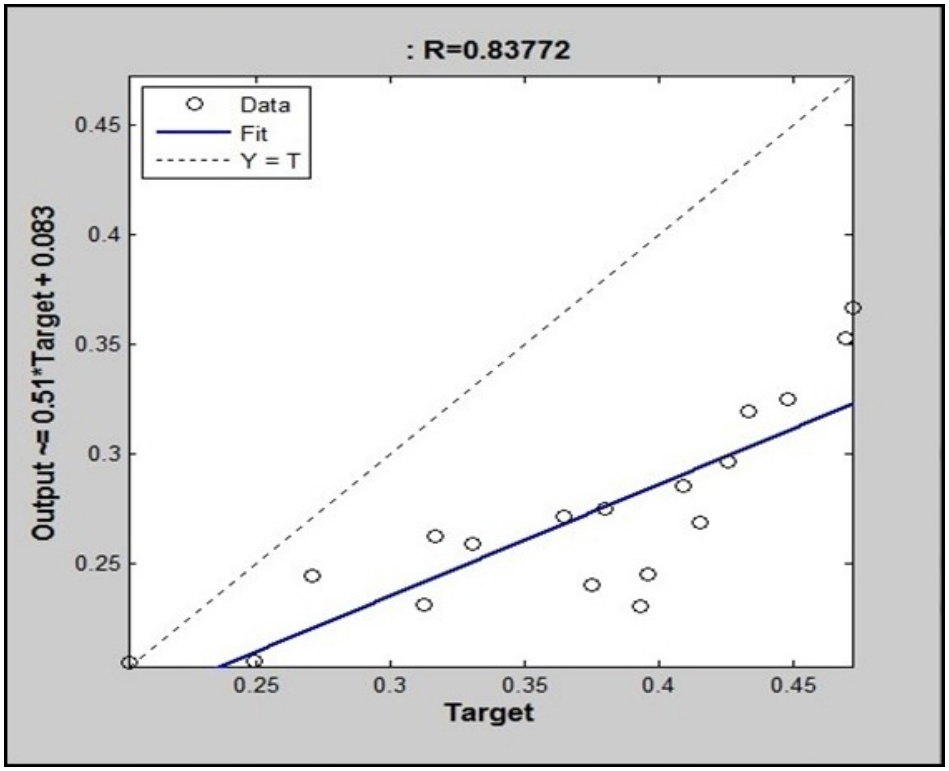

3.3.4. Development of ANN model to optimize biomass loading and particle size

3.3.4.1. Results of full factorial design to determine optimum biomass loading and particle size for biomass hydrolysis

The most significant results of the hydrolysis runs for various solids loading and particle sizes are shown in Table 3.12. It can be seen that very high efficiencies are obtained when the loading is low. More than 80% efficiency can be attained if the substrate loading is kept at around 10%. It is evident from Figure 3.14A, the efficiency of glucose production decreases as the biomass loading increases. But, as the loading increases, sugar concentration in the hydrolysate increases. Biomass loading of 18% yielded a hydrolysate with ~ 133 mg/mL total reducing sugars, of which 78 mg was glucose. This hydrolysate needs to be concentrated only twice to yield enough sugars for alcohol fermentation which will give adequate alcohol to allow separation by distillation. Hence, the energy required for concentration is decreased, which in turn leads to improved economics of bioethanol production.

Table 3.12: Hydrolysis of biomass at various biomass loadings and particle sizes

Sample No.	Biomass Loading (%)	Particle Size (mm)	Time (Hr)	Glucose (mg/mL)	TRS* (mg/mL)	% efficiency of glucose production
1	10	< 0.5	24	45.12	63.29	66.16
1	10	< 0.5	28	49.55	73.88	72.66
1	10	< 0.5	32	53.22	80.49	78.04
2	10	0.5 – 1.0	24	42.48	59.78	62.29
2	10	0.5 – 1.0	28	47.47	73.99	69.60
2	10	0.5 – 1.0	32	55.56	83.61	81.47
3	10	> 1.0	24	41.28	65.62	60.53
3	10	> 1.0	28	51.64	80.34	75.72
3	10	> 1.0	32	51.99	81.93	76.24
4	15	< 0.5	24	54.12	81.37	52.90
4	15	< 0.5	28	63.59	103.14	62.16
4	15	< 0.5	32	67.19	109.41	65.67
5	15	0.5 – 1.0	24	56.58	85.49	55.31
5	15	0.5 – 1.0	28	66.94	108.28	65.43
6	15	> 1.0	24	60.31	95.00	58.95
6	15	> 1.0	28	70.01	114.44	68.43
7	18	< 0.5	24	69.73	104.85	56.80

7	18	< 0.5	28	76.15	126.28	62.03
8	18	0.5 – 1.0	24	69.34	123.48	56.48
8	18	0.5 – 1.0	28	78.04	140.26	63.57
9	18	> 1.0	24	69.25	121.06	56.41
9	18	> 1.0	28	78.51	140.95	63.95
10	10	Mixed	12	41.02	64.13	60.14
10	10	Mixed	24	47.93	77.18	70.28
10	10	Mixed	28	59.04	90.69	86.57
11	15	Mixed	24	60.34	109.32	58.98
11	15	Mixed	28	69.41	118.78	67.85
12	18	Mixed	24	70.59	128.68	57.50
12	18	Mixed	28	76.34	133.66	62.18

* TRS –Total reducing sugar

Figure 3.14: Glucose yield with varying biomass loading and particle sizes

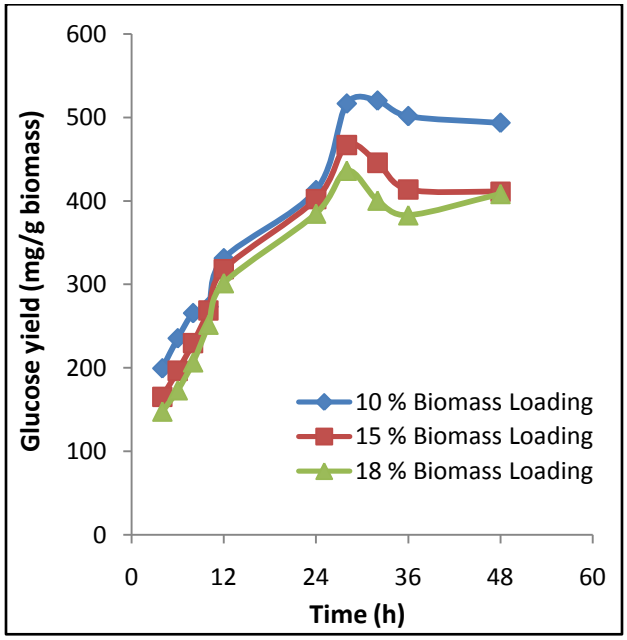

A) Varying biomass loading and particle size at >1mm

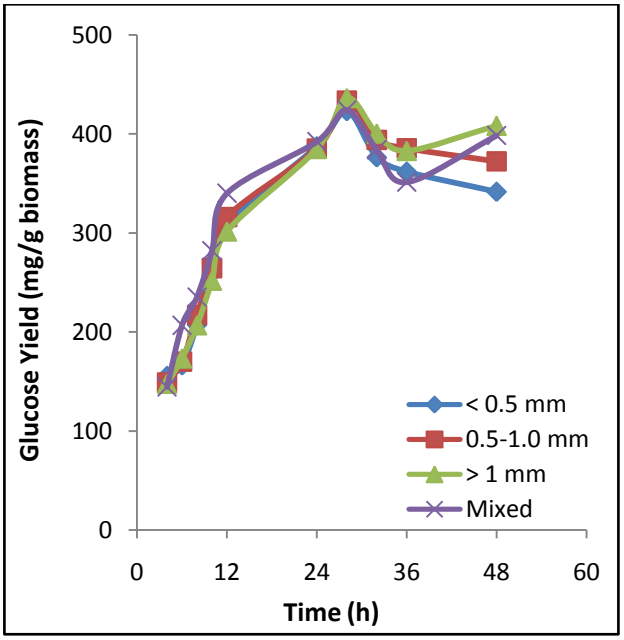

B) Varying particle size and 18% biomass loading

Particle size has been reported as a major parameter affecting enzymatic hydrolysis. In the present study, it was observed that there was no major effect of particle size on the sugar yields as shown in Figure 3.14B. Hence it can be concluded that, it is better to use a mixed particle size as it does not require an additional unit operation to sieve the pre-treated biomass. Also, if a mixed particle size is used, biomass

wastage is reduced. Hence, based on the findings of this study, it is concluded that 18% biomass loading with a mixed particle size is an optimum condition for carrying out further hydrolysis reactions.

Hodge et al., (2008) used acid pretreated maize straw for bioethanol production. They observed that upon 48 h of incubation, the yield of hydrolysis was about 60% with 15% biomass loading. Results are comparable with that obtained in the present study where, after 28 h of incubation, the efficiency of hydrolysis was 67%. They also conducted studies at higher loadings up to the range of 30%. However, in this case, the yields were only about 45%.

Free water is very important for efficient enzymatic hydrolysis. At higher biomass loadings, available free water in the reaction system decreases which seriously inhibits hydrolysis. Free water is essential for mass transfer and also reduces shear stress on particles which in turn reduces power required for mixing (Hodge et al. 2009). As free water in the hydrolysis mixture decreases, viscosity of the mixture increases and hence limits mass transfer and increases power required to mix the contents. Relation between yield of sugars and biomass loading is not linear. This might be due to substrate inhibition, product inhibition, lower water content, lower adsorbed enzyme on substrate etc. (Kristensen et al., 2009a). To offset these disadvantages, longer hydrolysis times and higher enzyme dosages are required which may again lead to increased cost of the overall process.

Even with all the above mentioned disadvantages, it is observed that increasing substrate loading in hydrolysis in turn increases product concentration. Higher sugar concentrations in hydrolysate can offset the need for concentration step which could reduce energy use and costs associated with the various unit operations (Kristensen et al., 2009b). To make the process economical, biomass loading should be at least 20% during hydrolysis to get 8% sugar which can be fermented to attain 5% (v/v) alcohol that can be distilled from the broth without forming an azeotrope (Modenbach and Nokes, 2013). With higher biomass loadings, smaller scale reactors would be sufficient to attain equivalent hydrolysate. Thus energy requirement for heating, cooling, mixing etc. would be greatly reduced (Roche et al. 2009a).

Particle size has been reported as a major parameter affecting enzymatic hydrolysis. There are many reports which suggest the positive effect of reducing particle size on hydrolysis. Vidal et al., (2011) reported that physical size reduction of biomass can itself improve hydrolysis efficiencies by 50%. An increase in glucose yield up to 60% within 10 h of hydrolysis was observed by Yeh et al., (2010) when particle size of microcrystalline cellulose was reduced to 25.5 μm. Dasari and Berson (2007b) suggested that improvement in hydrolysis could be due to lower viscosities of smaller size particles. This would in turn mean more available free water and hence lesser mass transfer limitations. Also, increase in yield could be due to increased surface area of biomass which implies higher area for enzyme adsorption and also better mass and heat transfer. Another reason for higher conversion could be higher porosity of lower size particles (Khullar et al., 2013).

On the contrary, a number of studies have also reported that there is no correlation between particle size and hydrolysis (Mansfield et al., 1999). Chang and Holtzapple (2000) reported that below mesh size 40 (0.040 mm), particle size does not affect hydrolysis. Rivers and Emert (1988) reported that rice straw hydrolysis is not dependent on average particle size of biomass or percentage of fines.

3.3.4.2. ANN Training and validation

The potential of different ANN structures with 3 input parameters namely particle size, biomass loading and incubation time, 8 hidden neurons in 1 hidden layer and 2 output parameters – glucose and xylose concentration was assessed to determine the optimized condition for hydrolysis of alkali pretreated rice straw. The range of inputs and outputs selected are given in Table 3.13.

Table 3.13: Input and output vectors used for ANN training, testing and validation

Run No.	Input Vectors			Output Vectors	
	Biomass Loading (%)	Particle Size	Time (h)	Glucose (mg/mL)	Xylose (mg/mL)
1	10	<0.5 mm	4-48	21.1-41.7	7.2-15.9
2	10	0.5 – 1.0 mm	4-48	21.4-43.4	7.5-15.5
3	10	>1.0 mm	4-48	19.9-49.3	7.06-15.3
4	15	<0.5 mm	4-48	26.4-55.3	12.6-21.05
5	15	0.5 – 1.0 mm	4-48	23.4-60.1	11.6-22.3
6	15	>1.0 mm	4-48	24.7-61.6	13.15-22.8
7	18	<0.5 mm	4-48	27.9-61.4	12.3-24.2
8	18	0.5 – 1.0 mm	4-48	26.6-67.0	14.7-25.01
9	18	>1.0 mm	4-48	26.5-73.4	14.2-24.9
10	10	Mixed	4-48	20.3-44.7	7.1-12.9
11	15	Mixed	4-48	25.4-60.1	12.9-21.8
12	18	Mixed	4-48	26.0-71.6	15.01-24.3

Out of the 120 data points, 18 data points were chosen for validation of the network. For the validation process also, optimal number of hidden neurons were determined by varying the number of neurons from 1 to 10. The optimum number was found to be 8 depending upon the lowest MSE value and highest regression values for the validation dataset. The MSE and regression values of training, testing and validation datasets are as given in Table 3.14.

Table 3.14: Error and regression values of the predicted model

	Samples	MSE	R^2
Training	84	5.6789e-0	0.99
Validation	18	9.491e-0	0.98
Testing	18	15.554e-0	0.97

The R^2 values of testing and validation data sets were found to approach unity which confirms the reliability of the ANN model in predicting the sugar yields during hydrolysis. Figure 3.15 shows the regression plot for the ANN model. The overall R^2 value of the model was 0.98.

Figure 3.15: Regression diagram of the ANN model

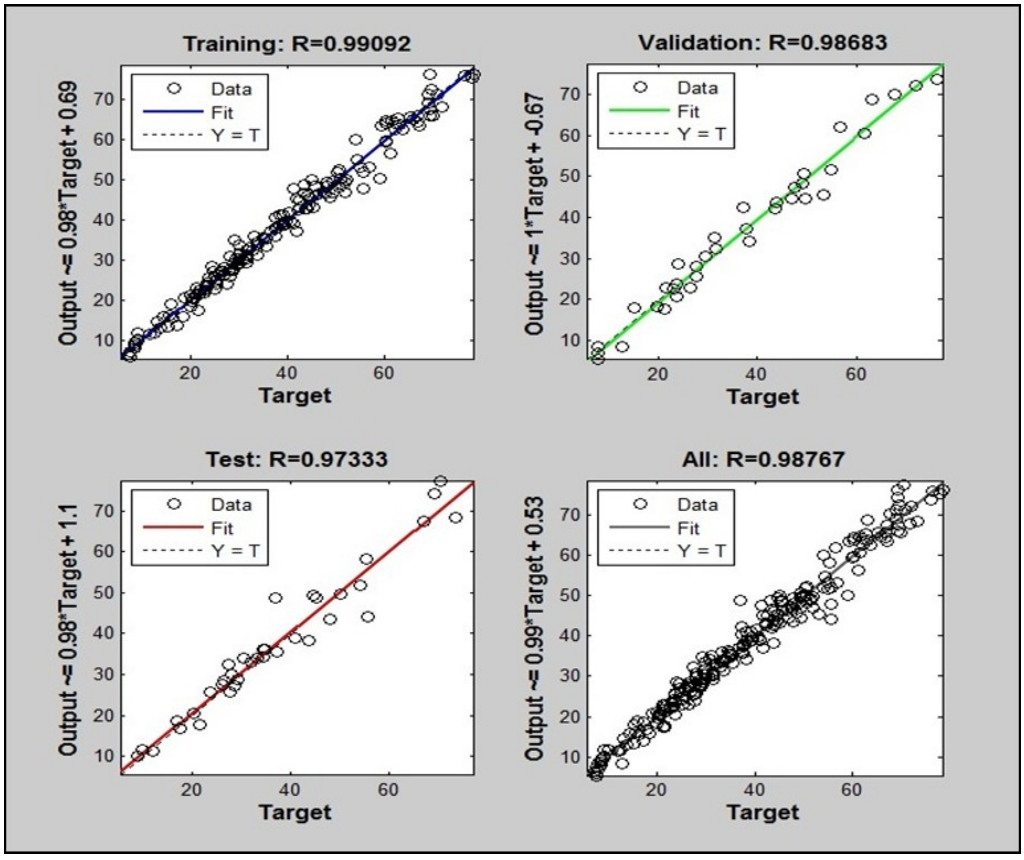

The corresponding error histogram of the model is shown in Figure 3.16. The histogram shows clearly, the data points where the fit is significantly worse than the majority of data. It is evident from the error histogram also that the relative error between experimentally observed and model predicted values was very less.

Figure 3.16: Error histogram of the neural network model

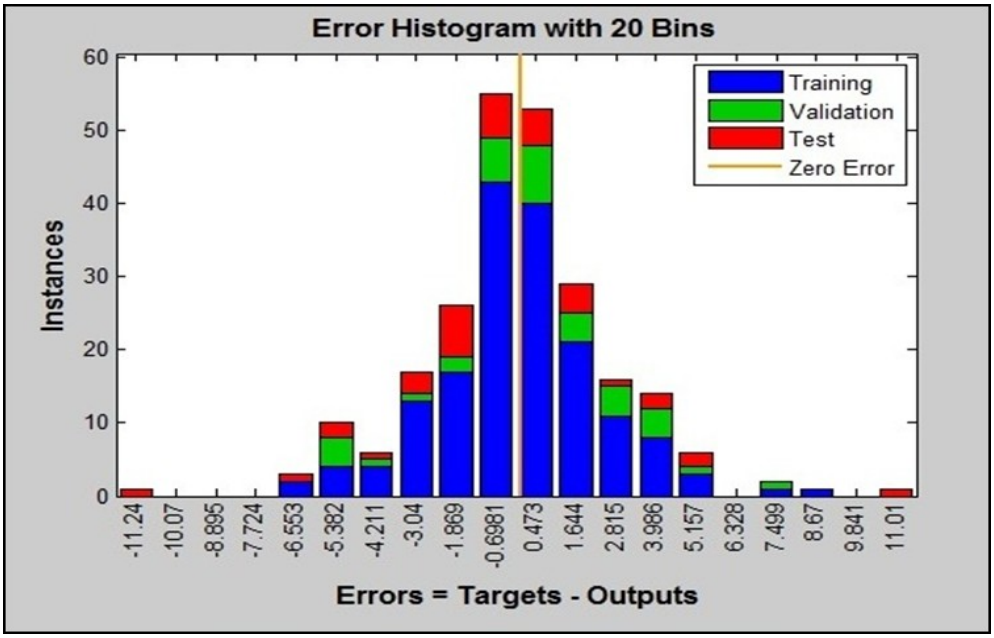

Fig 3.17: Experimental Validation of ANN predicted sugar yields

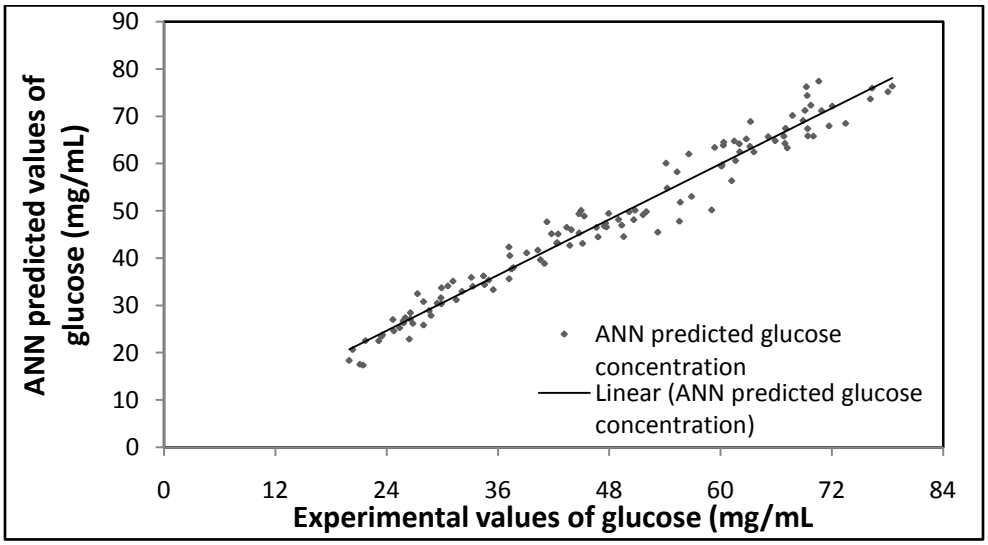

A) Comparison of ANN simulated and experimental glucose yields (mg/mL).

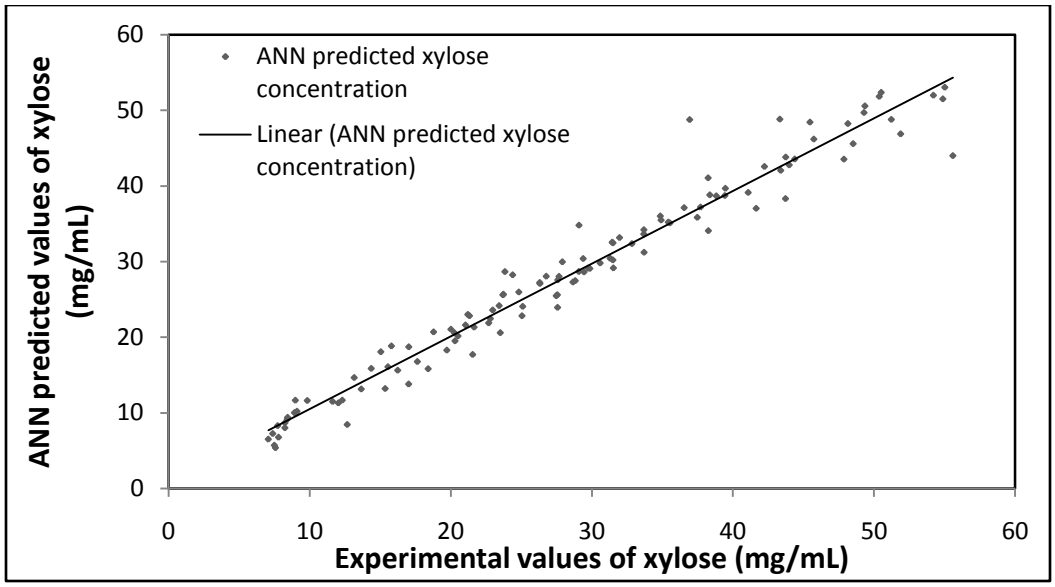

B) Comparison of ANN simulated and experimental xylose yields (mg/mL)

Table 3.15: Optimized parameters (weights and bias) of the ANN model

	Parameters connecting the input and hidden neurons				Parameters connecting the hidden and output neurons		
	w_{j1} (i=1)	w_{j2} (i=2)	w_{j3} (i=3)	Θ_j	W_{1j} (k=1)	W_{2j} (k=2)	b_k (k=1,2)
j=1	7.7228	-0.2718	-4.2862	-6.8043	0.3242	-0.2842	-4.7031
j=2	4.2549	3.9993	4.3758	-5.7108	0.0131	-0.1858	-1.522
j=3	-6.0963	-3.2922	1.1356	4.1719	0.0007	-0.2592	
j=4	6.2427	0.3837	3.3900	-2.9653	-0.1333	0.3942	
j=5	0.1177	0.8301	0.4129	0.3196	0.2427	-0.0018	
j=6	-1.6662	-0.6530	-1.3187	-1.928	-0.1607	-0.3640	
j=7	-0.5098	0.1261	0.3268	-0.8075	-1.2047	-0.0426	
j=8	-0.1826	-0.0217	1.0434	1.7844	4.6052	1.2868	

Performance of ANN model in describing the correlation between experimental and predicted glucose and xylose concentrations (mg/mL) at various time intervals are shown in Figures 3.17A and Figure 3.17B. The overall R^2 values for these data sets are 0.97 and 0.96 for the predicted glucose and xylose concentrations which proves the capability of proposed ANN model.

Table 3.15 gives the optimized weights and bias of the proposed ANN model. Using these parameters as inputs, the glucose and xylose concentrations can be obtained for different biomass particle sizes, biomass loading and at different time intervals.

There are not many reports on the application of ANN models in the area of conversion of lignocellulosic biomass to bioethanol. Redding et al., (2011) developed an ANN model to simulate the dilute acid pretreatment of Bermuda grass. Rivera et al., (2010) developed an ANN model to predict the optimum enzyme loadings for hydrolysis of sugarcane bagasse. The authors have used an MLP with back propagation algorithm and one hidden layer. Their study was focused on comparing the results predicted by the classical design of experiments (DOE) with ANN technique for sugar yields and they showed that the R^2 value for ANN model was much higher than the DOE model. Pramanik (2004) had used ANN model to predict the ethanol and cell mass yield during batch fermentation of grape waste using yeast. The model used contained 2 hidden layers with 15 and 16 neurons. The number of neurons in the input layer was 5. The network was trained at any given time to give only one output, either ethanol concentration or cell mass. O'Dwyer et al., (2008) verified the potential of neural network methodology to predict biomass digestibility based upon various structural features like lignin content, cellulose crystallinity, acetyl content etc. Zhang et al., (2009b) also reported better predictability of sugar yields during hydrolysis by ANN model when compared to quadratic models. Except for problems related to generalization of model, ANN offers a very attractive alternative to complex stochastic and kinetic models as proved in this study.

3.4. Conclusions

Prediction of the optimal glucose and xylose yields is one of the main aims of this study. It was observed that effectiveness of hydrolysis strongly depends upon cellulase and beta-glucosidase loadings. In the initial studies, the overall reducing sugar yields were found to be lower than optimum efficiencies previously reported. Hence studies were carried out with higher loadings of BGL and other accessory enzymes to maximize hydrolysis efficiencies. In the kinetics experiments with both xylanase and BGL, maximum efficiency achieved was 87% with 20 FPU/g Cellulase, 10 IU/g BGL and 7500 U/g Xylanase upon 48 h of incubation. It was observed that majority of the reaction was over by 12 h of incubation. Of the three enzymes, xylanase had the most profound effect on sugar yield. The cocktail studied performed much better than the commercial enzymes. The maximum efficiency for Zytex cellulase was 40% after 48h. SaccharicEB C6 being a biomass hydrolyzing enzyme gave an efficiency of 54%. Cellic CTec 2 gave slightly higher hydrolysis efficiency than the optimized cocktail. The combination of enzymes chosen for further studies is: 10 FPU/g cellulase, 5 IU/g BGL and 7500 U/g Xylanase.

It was found that particle size did not have a significant impact on sugar yield and hence mixed particle size is recommended for hydrolysis. The variation in sugar yield upon increase in biomass loading was profound. Higher biomass loading led to decrease in yield and hence brought down the efficiency of hydrolysis. Eighteen percent biomass loading yielded a hydrolysate with ~133 mg/mL total sugars off which 78 mg was glucose. This hydrolysate would require only 2 fold concentration to yield enough sugars to be fermented to produce adequate alcohol that can be separated by distillation. The high regression values close to unity indicate the adequacy of the ANN models developed in all cases to predict the reducing sugar yields upon different enzyme loadings, biomass loadings and particle sizes. The model can not only predict the reducing sugar yield profiles, but can also determine the optimum range of enzyme loadings and biomass loadings to obtain optimum reducing sugar yields.

The optimum conditions obtained using the model is specific for the raw material type and pretreatment conditions. Variation in these parameters may lead to the requirement of further training / fine-tuning the network.

The lack of mathematical models to predict the efficiency of various unit operations and concerted efforts to optimize them is one reason for such high costs of bioethanol production. Hence model development is significant in realizing economical bioethanol production. In the present study artificial neural networks models were developed to optimize the various factors that affect the biomass hydrolysis. High regression values close to unity indicates the adequacy of the ANN model developed to predict the sugar yields upon different biomass loadings and substrate sizes while keeping other hydrolysis parameters constant. The major enzyme that contributes more to enzymatic hydrolysis was found to be xylanase. It was found that effectiveness of hydrolysis strongly depends upon biomass loadings, whereas particle size did not have a significant impact on sugar yield. Higher loadings decrease the sugar yield but concentration of sugars in the hydrolysate increases. Optimum hydrolysis condition for rice straw is 10 FPU/g Cellulase, 5 IU/g BGL, 7500 U/g Xylanase, 18% biomass loading and a mixed particle size with reaction time between 12-28 h.

Chapter 4

Dynamics of enzyme adsorption, variation in biomass particle size and composition during hydrolysis

4.1. Introduction

Enzymatic hydrolysis of biomass is considered as the unit operation that contributes most to the cost of lignocellulosic ethanol and this is largely due to the high enzyme loadings required for higher sugar yields and the long reaction times typically ranging from 48 – 96 h. There are not many reports that have studied whether such a long duration is required for optimum hydrolysis. On the other hand, extensive work has happened on the optimization of enzyme loadings and determination of the factors influencing efficient hydrolysis of biomass. The major factors affecting enzymatic hydrolysis can be divided into direct factors like cellulase accessibility to cellulose, non specific binding of cellulases to lignin, enzyme efficiency and substrate/product inhibitions etc. and indirect factors like cellulose pore size, hemicelluloses and inhibitors, temperature, pH, ionic strength, substrate loadings etc. (Ooshima et al., 1983; Kim and Hong, 2000; Kumar, 2008; Kumar and Wyman, 2008, 2009d). These factors contribute to the requirement of high protein loadings and extended reaction times for efficient lignocellulose hydrolysis (Zhang and Lynd, 2004, 2006).

Increasing enzyme loading might increase the sugar released, but only till a plateau corresponding to the maximum adsorption density of cellulase is reached. Enzyme loading required to achieve efficient hydrolysis of biomass depends on the accessibility of cellulosic portion of biomass to the enzyme (Karlsson et al., 1999; Kotiranta et al., 1999; Jeoh et al., 2007). In spite of the variability in source, structure, chemical composition and difference in pretreatment strategy used, cellulose-rich substrates with highly accessible cellulose, require a lower enzyme loading per gram of cellulose to obtain higher and faster hydrolysis compared with substrates containing less accessible cellulose. So, it may be assumed that limited accessibility of enzymes to cellulose fibers is the rate limiting factor in enzymatic hydrolysis of biomass (Arantes and Saddler, 2011). Attaining quick and complete conversion of lignocellulosic biomass at low enzyme loadings is a major technical challenge to be overcome that is preventing commercialization of second generation bioethanol production.

There are mainly three phases during enzyme catalyzed hydrolysis of lignocellulosic biomass. First phase is characterized by an initial high glucose release due to higher reaction rates as a result of speedy adsorption of enzymes on to biomass. Second phase starts when the rate of reaction slows down and glucose release is almost at a constant rate. During this time the cellulose conversion would have reached around 50 – 70%. The last phase is when there is a steady decrease in reaction rate and rate of

glucose production is very slow. This is the phase of conversion of recalcitrant or inaccessible cellulose (Arantes and Saddler, 2011; Gao et al., 2014).

To attain complete conversion of lignocelluloses including that of the inaccessible cellulose, very high reaction times and high enzyme loadings are essential. In many cases, even upon very high protein loadings of commercial cellulases and carrying out the reaction for very long periods, complete hydrolysis cannot be achieved (Hogan et al., 1990; Mooney et al., 1998). Gregg and Saddler (1996) have proven that long hydrolysis duration in order to attain complete cellulose saccharification increases the operating cost of hydrolysis unit operation and hence makes lignocellulose to bioethanol production process uneconomical. Effect of hydrolysis time and protein loading on the hydrolysis of recycled paper sludge and cotton gin waste was studied by Shen and Agblevor (2008). It was found that higher enzyme loadings to attain >90% cellulose hydrolysis was non economical due to the high cost of enzymes which adds on to the overall hydrolysis cost.

In order to maximize enzymatic hydrolysis efficiencies, different strategies like usage of accessory enzymes and lower reaction times are employed. Also, in certain reports, higher loadings of enzymes for shorter reaction periods are used, and these are then recycled after hydrolysis to economize the overall process. In such cases, it is essential that these accessory enzymes and cellulases be recovered after hydrolysis and reused. It was observed that cellulases can remain adsorbed on to the biomass or remain in free form in the supernatant after hydrolysis (Tu et al., 2009b; Yang et al., 2010; Pribowo et al., 2012; Lindedam et al., 2013). Extensive studies on the cellulase adsorption kinetics on biomass, desorption kinetics, adsorption reversibility, surface enzyme denaturation, changes in surface area of cellulose during digestion and re-adsorption are important to enhance knowledge regarding the potential of cellulase recycling and reuse. To understand the detailed mechanism of cellulose hydrolysis by cellulase, surface behaviors needs to be thoroughly understood (Maurer et al., 2012). This study also aids in quantifying cellulose deconstruction. Re-adsorption on fresh substrate is an efficient strategy to recover cellulases from supernatant after hydrolysis (Lee et al., 1995; Qi et al., 2011; Lindedam et al., 2013).

The present chapter deals with the study of enzyme adsorption dynamics during biomass hydrolysis. The time required to attain high sugar yields (> 75% cellulose conversion) was optimized so as to economize the overall hydrolysis process. Studies were also carried out to analyze the particle characteristics and composition during the course of hydrolysis to build a stronger understanding of the changes to biomass during the process of hydrolysis.

4.2. Materials and Methods

4.2.1. Enzymatic hydrolysis of alkali pretreated rice straw

Rice straw was pretreated using dilute alkali as per the protocol in section 2.1 and stored in air tight containers until further use. Enzymatic saccharification of pretreated rice straw was carried out using commercial cellulase from Zytex (Zytex India Private Limited, Mumbai, India), BGL from *Aspergillus niger* and Xylanase gifted by MAPS enzymes Pvt. Ltd., Gujarat, India. Hydrolysis was carried out as detailed in section 2.3 in a 20 L bioreactor (BBraun/Sartorius, Germany) with 15 L working volume. Biomass loading was 10% and optimized enzyme cocktail containing 10 FPU/g cellulase, 5 IU/g BGL and 7500 U/g xylanase was used for hydrolysis. Samples were withdrawn at 2 h interval till 12 h and later at 24, 30, 36 and 48 h. Samples were centrifuged and supernatant was recovered. Pelleted biomass was washed thrice with buffer containing 0.01% Tween 80 to remove adsorbed enzymes and sugar and the wash was collected. Sugars in the supernatant and adsorbed onto biomass were analyzed by HPLC using a Phenomenex Rezex RNM column and RI detector. Protein content was estimated by Bradford's method (Bradford, 1976). Enzyme assays were done as per the protocol detailed in section 2.4. Composition analysis of native, pretreated and solid fraction left after hydrolysis was carried out as per the NREL protocols explained in section 2.2.

4.2.2. Immunochemical determination of enzyme adsorption on biomass

Samples of 1 mL volume from the hydrolysis reaction at each interval were centrifuged (5000 rpm for 5 min at 4 °C) and the supernatant was discarded. To the pellet, blocking buffer containing 3% Bovine serum albumin (BSA) was added and incubated for 3 h at 37 °C with continuous slow mixing. Pellet was washed thrice with dilution buffer (phosphate buffered saline) containing 1% BSA. Antibody solution containing rabbit anti-endoglucanase IgG labeled with fluorescein isothiocyanate (FITC) (BIOSS Antibodies, USA) at 1:250 dilution in dilution buffer was added to the sample and incubated in dark at 37 °C with continuous mixing for 2 h. Samples were then centrifuged and the supernatant discarded. The pellet was washed thrice with dilution buffer. Dilution buffer was then added to the pellet and fluorescence intensity of the samples were read with excitation and emission wavelengths 495 nm and 520 nm respectively using Multimode reader (Tecan Infinite Pro, Switzerland). Appropriate positive control with pure cellulose and negative control without antibody were also treated the same way as the samples and fluorescence intensities were measured. Enzyme binding was also visualized using BD pathway 855 Confocal microscope (BD Biosciences, USA) and images were acquired.

4.2.3. SDS PAGE of adsorbed proteins (before and after wash)

The proteins adsorbed on the biomass, present in wash and retained on biomass after successive washes were determined by Sodium Dodecyl Sulphate PAGE (SDS PAGE) by the method of Laemmli (1970). The gels (1.5 mm thickness) with 12% strength of acrylamide were prepared using a slab gel apparatus (Protean Xi, Biorad, USA). The gels were loaded with 50 µL samples and were subjected to electrophoresis at 200 volts until the dye front reached 1.0 mm above the bottom of separating gel. Molecular mass standards from PageRuler© Prestained protein ladder (Thermofisher Scientific) were loaded on each gel.

4.2.4. Particle Size Analysis

Particle size analysis was carried out to determine the change in particle size during hydrolysis. The measurement was done using dynamic light scattering in a particle size analyzer (Microtrac-S3500, Bluewave, USA) and analysed using Flex® software.

4.2.5. Porosity Measurement

Nitrogen adsorption/desorption isotherm measurements of the air dried (at room temperature) samples were performed with a Micromeritics Gemini 2375 instrument. All the samples were degassed at 200 °C for 2 h before adsorption measurements. Desorption isotherm was used to determine pore – size distribution using Barret – Joyner – Halender (BJH) model. Adsorption isotherm was determined by BET isotherm.

4.2.6. Characterization of native and pretreated biomass

4.2.6.1. X-Ray Diffractogram Analysis of biomass

The X-ray diffractogram which indicates the crystallinity of rice straw during the course of hydrolysis was analyzed in a XEUSS SAXS/WAXS system using a Genixmicro source from Xenocs, operated at 50 KV, 0.6 mA; radiation was Cu Kα (λ= 1.54 Å) and grade range between 10 to 30° with a step size of 0.03°. 2D patterns were recorded on a Mar345 image plate and processed using Fit2D software. Measurements were made in transmission mode.

4.2.6.2. Fourier Transform Infrared Spectroscopic analysis of biomass

Fourier Transform Infrared (FT-IR) spectroscopic analysis was carried out to detect changes in functional groups present on the biomass due to hydrolysis. FT-IR spectrum was recorded between 4000 - 400 cm^{-1} using a Shimadzu Spectrometer with detector at 4 cm^{-1} resolution and 25 scans per sample. Discs were prepared by mixing 3 mg of dried sample with 300 mg of KBr (Spectroscopic grade) in an agate mortar. The resulting mixture was pressed at 10 MPa for 3 minutes and this sample was used for IR spectrum recording.

4.2.6.3. Scanning Electron Microscopic analysis

Physical changes in the native and hydrolysed rice straw were observed by scanning electron microscopy (SEM). Images were taken at magnification of 500 X using a ZEISS EVO 17 Special edition, scanning electron microscope. The specimens to be coated were mounted on a conductive tape and coated with gold palladium and observed using a voltage of 10 to 15 KV.

4.3. Results and Discussion

Thorough and efficient contact between enzyme and cellulose is the prerequisite for efficient enzymatic hydrolysis (Meng and Ragauskas, 2014). Enzyme (Cellulase)-Substrate (Cellulose) interactions occur at a liquid–solid interface, which requires physical adsorption of enzyme to cellulose for the hydrolysis reaction to occur. Hence, the degree to which cellulase adsorbs to cellulose in lignocellulosic biomass provides some indication of digestibility (Van Dyk and Pletschke, 2012).

4.3.1. Dynamics of enzyme adsorption on biomass

Adsorption of cellulase on biomass was determined using fluorescently labeled anti-endoglucanase antibody (α-EG Ab) to specifically bind the enzyme. Fluorescent intensity spectra were studied to determine the λ_{max} of antibody, biomass samples labeled with the FITC conjugated antibody, as well as negative and positive controls. The spectra obtained were as given in Figure 4.1.

Figure 4.1: Fluorescent intensity spectra of FITC labeled antibody – alone or bound to biomass

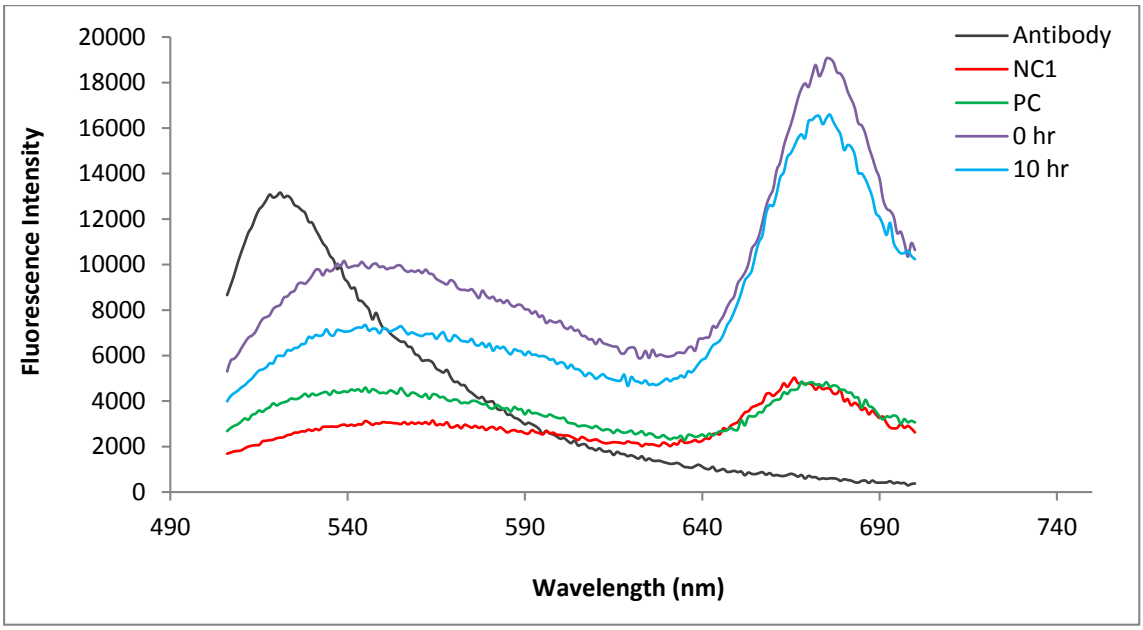

NC- Negative control, PC –Positive control, 0h and 10h –Biomass samples withdrawn at 0h and 10h and labelled with FITC conjugated anti-EG antibody

From the spectrum, λ_{max} value for FITC labeled antibody was ascertained as 521 nm. Hence emission was checked at 520 nm. Table 4.1 gives the λ_{max} of the antibody, enzyme loaded biomass samples with fluorescently labeled antibody and biomass. Though the biomass had auto fluorescence at 675 nm, this does not affect the quantification of antibody labeled biomass since the absorption maxima were at different wavelengths. There was a shift in λ_{max} value upon conjugation of antibody with enzyme, which normally indicates that the antibody to enzyme binding has been successful.

Table 4.1: λ_{max} of antibody, antibody bound to enzyme on biomass and biomass

	Antibody	Antibody bound to enzyme on biomass	Biomass
λ_{max} (nm)	521	545	675

Since the antibody was tagged with FITC, a green fluorescence was visible in the biomass to which enzyme was adsorbed. Fluorescence was more in the biomass samples during initial period of hydrolysis (Figure 4.2). Pure cellulose incubated with enzyme and probed using FITC labelled αEG Ab (FITC-αEG Ab) was taken as positive control. Biomass incubated with enzyme alone (No FITC-αEG Ab) was taken as negative control.

Figure 4.2: Endoglucanase adsorption on biomass during hydorlysis

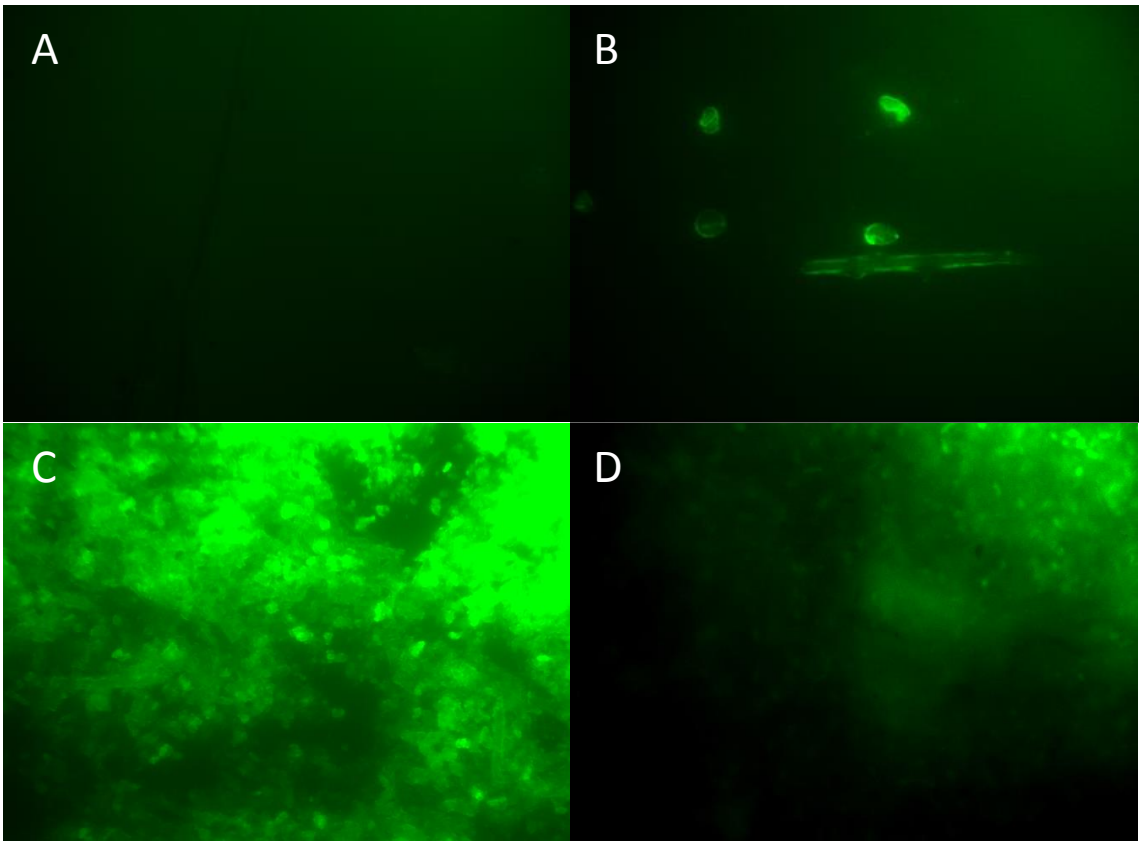

A) Negative control – Biomass with enzyme, unlabelled | B) Positive control – Pure cellulose with enzyme and antibody | C) Biomass with enzyme conjugated antibody at 12h D) Biomass with enzyme conjugated antibody at 48 h | All images captured at same magnification.

Fluorescent microscopy (Figure 4.2) as well as the fluorescent intensity measurements using spectrofluorometry (Figure 4.3) indicated that enzyme adsorption on biomass was highest during the initial phase of hydrolysis (Till~12h). Maximum enzyme was adsorbed within the first 15 minutes of hydrolysis (Figure 4.3). Concentration of bound enzyme (fluorescent intensity) decreased rapidly till 2h and remained at a relatively constant and high level from 2-12 h of reaction, which also corresponded to the rapid rate of sugar release. Endoglucanase is the enzyme which starts the breakdown of cellulose polymer by nicking the β 1-4 linkages paving way for attack of exoglucanases and in a way can act as a representative protein to monitor overall cellulase activity. Both endoglucanases as well as cellobiohydrolases (exoglucanases) require the enzyme to be bound to cellulose for their activity and hence the level of enzyme adsorption on cellulose is important and indicative of the efficiency of hydrolysis. Close to 90% conversion of cellulose (589 mg/g glucose release) was attained in the first 12 h of hydrolysis, but further increase in the reaction times resulted in a gradual decrease of sugar concentration possibly due to transglycosylation activity of beta glucosidase whereby cellobiose or cello-

oligomers are formed. This could also be due to non specific adsorption of sugars on lignin and unhydrolysed biomass.

Figure 4.3: Enzyme adsorption on biomass during hydrolysis

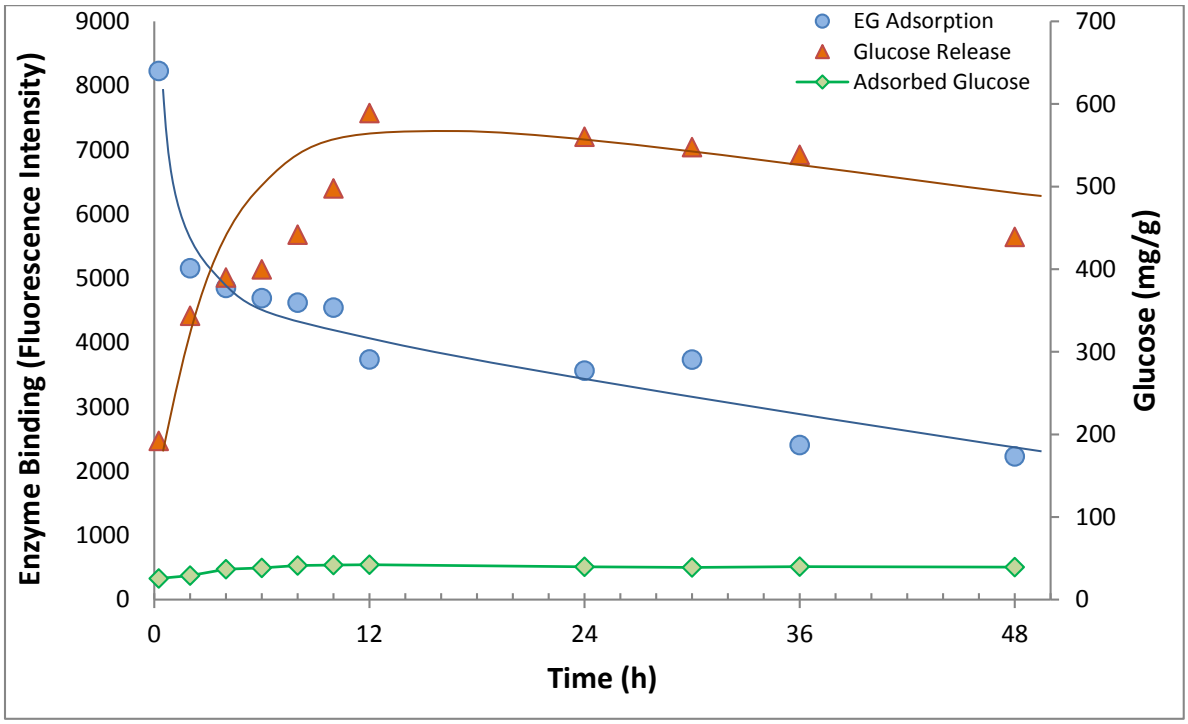

Further investigation is required to understand the actual reasons for this reducion in sugar concentration. It may be assumed that after 12 h there is no more hydrolysis of cellulose, possibly due to the difficulty to access crystalline regions of cellulose which constitute the major fraction in the residual biomass after the easily hydrolyzable amorphous regions have been digested. Apparently, it seems that hydrolysis beyond 12 h does not make any difference in final sugar yields and it is prudent to terminate the reaction after 12 h. This could be a significant observation that would help to reduce the overall cost of biomass conversion since it translates to plant operation for significantly lesser duration saving on energy and operational costs.

In the present study, considerable amount of small particles were visible toward the end of rapid hydrolysis phase and afterwards as compared to the solid biomass fiber at 0-2 h (Figure 4.4). A similar phenomenon was observed by Luterbacher et al., (2015). They found that at longer hydrolysis durations, small particles that bind enzyme but show no auto fluorescence appeared. These particles were crystalline cellulose, majorly cellulose nanocrystals, which are highly recalcitrant and resistant to degradation and detach from the main biomass as hydrolysis proceeds.

Figure 4.4: Changes in biomass particle morphology during hydrolysis

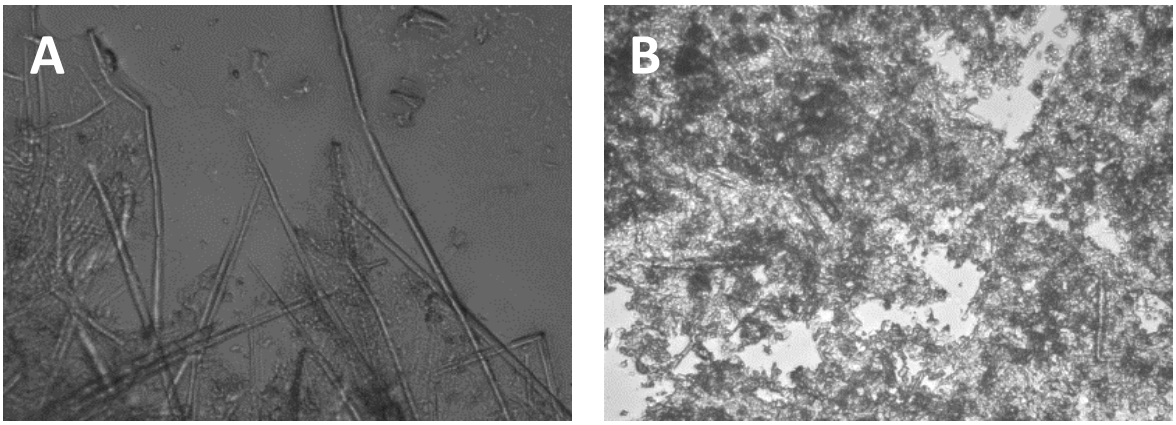

Phase constrast images of biomass particles A) 15 minutes into hydrolysis B) 12h into hydorlysis

Enzyme adsorption on biomass and their efficiency have a major effect on enzymatic hydrolysis of lignocellulosic biomass (Chang and Holtzapple, 2000; Zhang and Lynd, 2004; Kumar, 2008). Many studies have reported direct correlation of enzyme adsorption on biomass and hydrolysis rate (Lee and Fan, 1981; Kumar and Wyman, 2009b). In a study to identify barriers to accessibility of cellulose by enzyme using *T. reesei* Cel7A (cellobiohydrolase), it was observed that higher conversion of cellulose was obtained when *T. reesei* Cel7A bound cellulose in higher concentrations (Pellergrini et al., 2014). Substrate related factors like pretreatment severity, drying after pretreatment and cellulose crystallinity directly affect the enzyme accessibility to biomass. It was postulated that removing xylans during pretreatment enhanced cellulase accessibility to cellulose, and lead to higher conversion of cellulose to glucose (Jeoh et al., 2007).

In the present study, it was found that enzyme adsorption on biomass and the hydrolysis efficiencies decreased with time, which may be due to both substrate and enzyme features (Desai and Converse, 1997; Mansfield et al., 1999) and physical parameters such as product inhibition of enzymes by sugars and oligomers (Kumar and Wyman, 2009d).

Adsorption of enzymes on biomass is the first step in the enzymatic hydrolysis of biomass. Many investigations have been carried out that determine the dynamics of enzyme adsorption and desorption on pure cellulose and biomass. Pellegrini et al., (2014) studied the reversibility of adsorption of Cel7A, Cel6A, (cellobiohydrolase) and Cel7B (endoglucanase) from *Hyrpocrea jerorina* on pure cellulose. They found that these cellulase components bind reversibly to cellulose. Hence, the adsorbed and free enzymes are in dynamic equilibrium. A similar observation was found in the present study where, bound and free enzyme concentration stabilizes after initial hours of hydrolysis (Figure 4.5). Many reports have

suggested that the adsorption of cellulase on cellulose is irreversible or partially irreversible. Hence, simple equilibrium adsorption models cannot explain the hydrolysis process.

Figure 4.5: Free and adsorbed enzyme activities during hydrolysis of biomass

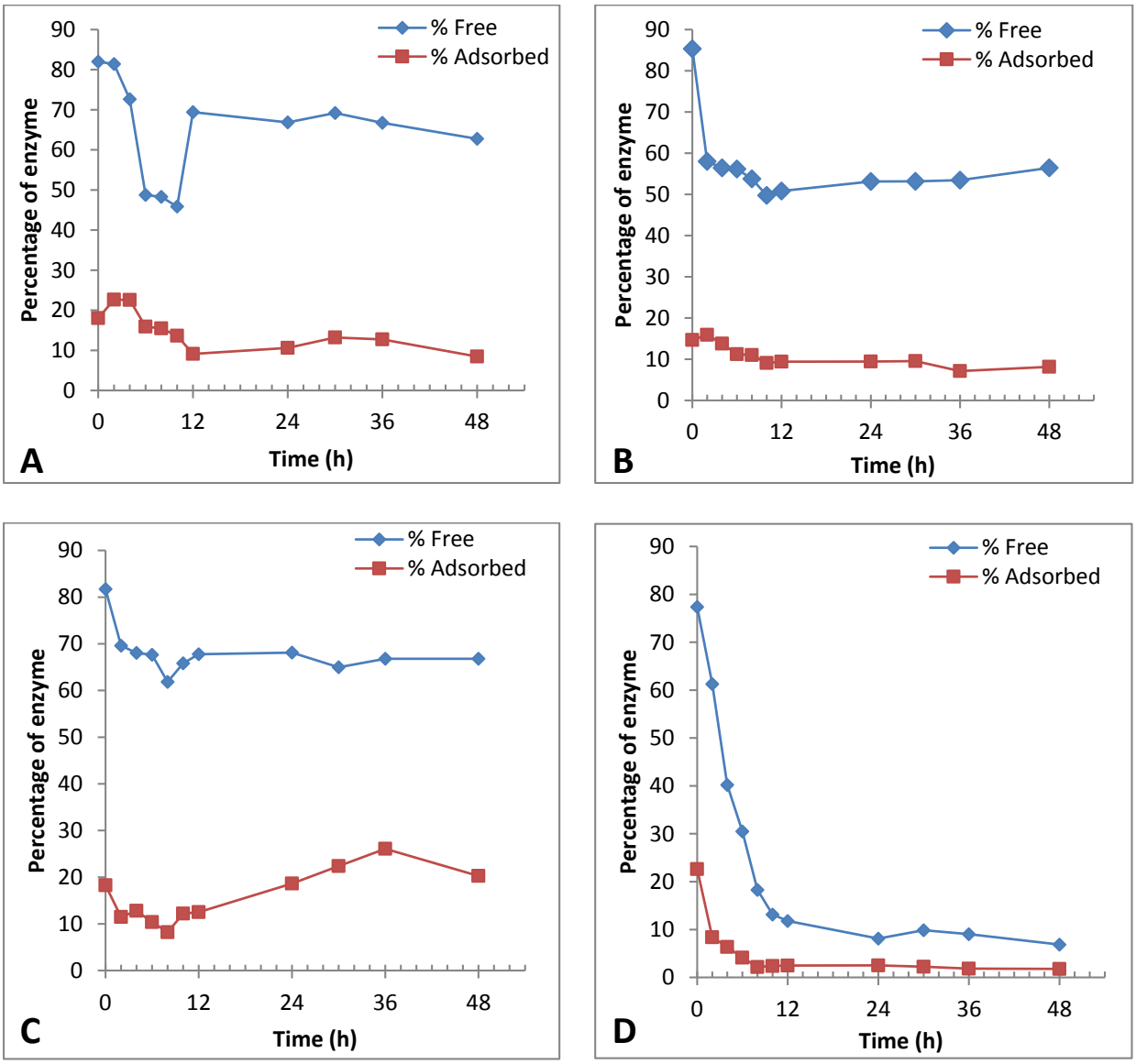

A) Cellulase (FPU) activity B) Endoglucanase activity C) BGL activity D) Xylanase activity

The total cellulase activity (FPUs) in the reaction mixture was determined and it was found that the bound enzyme activity was higher till 10 h of hydrolysis (Figure 4.5A). After this, the adsorbed activity decreased. Corresponding to the higher adsorbed activity, there was a decrease in free enzyme activity till

about 8 h which then increased and become constant from ~12 h. This can be correlated with the glucose release graph in Figure 4.3 where maximum glucose release was observed till 12 h of hydrolysis. Apparently, when the bound enzyme activity was high, glucose release was also higher. As free and adsorbed enzyme activity becomes constant after 12 h, the rate of hydrolysis also decreased.

Similarly, the adsorbed endoglucanase activity decreased slightly after 2 h and became more or less constant after 12 h of hydrolysis (Figure 4.5B). The free enzyme activity also declined rapidly till 2 h and then stabilized after 12 h. The rapid decrease in free enzyme might be due to loss in activity or denaturation of enzyme. It can also be due to non specific binding of enzyme on phenolics. Free endoglucanase activity also reduced as hydrolysis proceeded and became relatively constant after 10 h. The glucose release correlated with the changes in adsorbed endoglucanase activity and decreased after 12 h when adsorbed endoglucanase activity was less

The bound and free activities of β-glucosidase (BGL) was also measured and similar to endoglucanase, the activity declined with time until 8 h, but later increased marginally as is evident from Figure 4.5C. This might be due to decreased cellulose in biomass and increased cellobiose accumulation or non specific adsorption. The free BGL decreased initially due to higher adsorbed enzyme, but later after 8 hours became more or less constant. This might be due to constant rates of glucose release and hence equilibrium might have attained between bound and adsorbed enzymes.

The availability of accessory enzyme, xylanase was found out and is shown in Figure 4.5D. The bound xylanase was continuously decreasing. This might be because the rate of hemicellulose digestion is much higher during initial stages of hydrolysis. After the interlinking xylan sheets have been hydrolysed, cellulase gets more accessibile surface on cellulose and cellulose digestion becomes faster. Also, as hydrolysis proceeds, hemicelluloses are broken down to pentoses and released to the liquid medium. So specific adsorption of xylanases on biomass reduces considerably. As with endoglucanase, the free enzyme reduces rapidly till 10 hours and later becomes constant. The rapid reduction may be due to deactivation of enzyme or denaturation of protein.

It was observed that total protein in free liquid was higher than protein adsorbed on to the biomass (Figure 4.6). Free protein content increased till 12 h and then declined and became stable around 24 h. On the other hand, adsorbed proteins increased till 36 h and decreased after that.

In all the above cases, it was found that free enzyme activities were much higher than the bound. This implies the high protein loadings used for hydrolysis. In majority of the cases, over 75% of the protein given is present in supernatant during the initial periods. Hence, the enzyme loading need to be optimised to attain efficient hydrolysis rates at lower final protein concentrations and in lesser time. Use of lower reaction times would also imply that enzymes used in reaction may be recovered atleast partially before they are deactivated due to harsh hydrolysis conditions.

Figure 4.6: Changes in protein binding profile during biomass hydorlysis

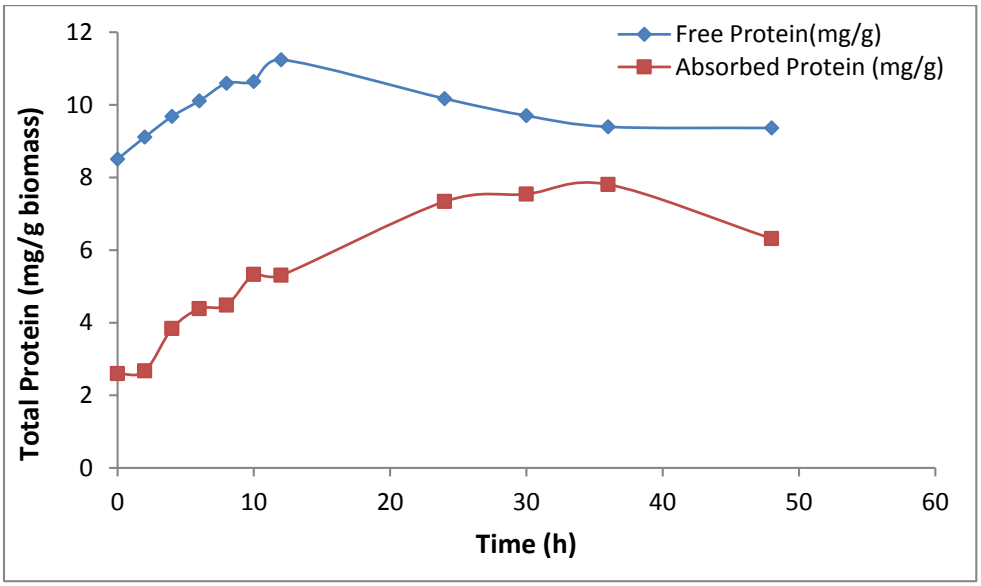

A significant amount of active enzymes remaining in supernatant could be recovered by recycling the liquid phase. During early hydrolysis time, enzyme adsorbs to biomass and then progressively returns to the solution as hydrolysis proceeds. At 50 °C, which is the usual operation temperature for enzymatic saccharification, enzymes undergo thermal deactivation, deactivation by shear forces or contact with air – liquid interphase. To enhance the stability of the enzymes, hydrolysis may be carried out at moderate temperatures. Also, Cel7A and Cel7B were found to be less stable than β-glucosidase, as reduction in their activity was more profound compared to that of BGL (Rodrigues et al., 2012; Rodrigues et al., 2014).

Alasepp et al., (2014) also reported reduction in cellulase activities as the hydrolysis proceeds. This reduction is observed with cellulase cocktails also and in reactions with pure celluloses or lignocelluloses. This effect significantly hampers the industrial use of cellulases for biomass hydrolysis as the rate of hydrolysis may fall significantly before the conversion of cellulose have reached to an optimum value. Cellulase activity may be reduced in the later stages of hydrolysis by accumulated products and the depletion of substrate with good reactivity.

Thus, thermal deactivation, product accumulation and substrate depletion might be the reason for decreasing enzymatic activities observed here as hydrolysis proceeds. In the present study also, reduction in BGL activity was found to be lesser than total FPU and endoglucanase activity reductions.

Many studies have reported that the adsorption of Cel7A, Cel7B and other cellulolytic enzymes were higher during the initial phase of hydrolysis (Tu et al., 2009b; Yang et al., 2010; Qi et al., 2011; Pribowo et al., 2012). These studies had also reported that during peak hydrolysis time window (~24 h),

more enzyme activity was in adsorbed form, especially when a lower enzyme loading was used. It was also demonstrated that increasing cellulase loading (from 20 FPU to 40 FPU) actually resulted in lower enzyme adsorption on biomass. This was speculated to be due to the higher cellulose conversion and saturation of biomass surface (Rodrigues et al., 2014).

Studies using low protein loadings might observe only the hydrolysis of accessible cellulose, overlooking the factors that control the saccharification of cellulose at high hydrolysis efficiencies. On the other hand, studies using high enzyme loadings would possibly mask the factors limiting efficient hydrolysis, by saturating the substrate with enzyme. It was suggested that increasing the hydrolysis time from 24 h to 48 or 72 h does not significantly increase the glucose yields for hydrolysis of steam pretreated corn fiber and indicated that the 'plateau phase' for conversion of cellulose was reached within the first 24 h of hydrolysis (Arantes and Saddler, 2011).

Gao et al., (2014) suggested that most of the amorphous cellulose inside Avicel® (microcrystalline cellulose) particles is not accessed by cellulases and the easily accessible amorphous cellulose on the surface of Avicel® is hydrolyzed at the beginning of hydrolysis itself with high rates of conversion. Further hydrolysis process was proposed to occur in a layer – by – layer process with amorphous and crystalline regions hydrolyzed simultaneously. Hemicellulase binding to substrate is also essential for hemicellulose hydrolysis (Sun et al., 1998; Zilliox and Debeire, 1998). But the complexities of the hemicellulose structure and multitude of enzymes involved in its hydrolysis have resulted in limited studies of hemicellulolytic enzymes–substrate interactions for real biomass.

The efficiency of enzyme detachment from biomass was determined by SDS PAGE analysis of the slurry after repeated washes to remove adsorbed proteins. It was observed that even after three washes with buffer containing Tween 80, considerable amount of protein/enzyme was still bound to the biomass (Figure 4.7). This could be due to an irreversible adsorption onto lignin present in the biomass. It is also possible that the irreversible binding may be to cellulose itself. This irreversible adsorption might be a reason for lower activities observed in the adsorbed fraction of enzymes on biomass, during enzymatic saccharification.

Figure 4.7: SDS PAGE analysis of adsorbed and free proteins on biomass

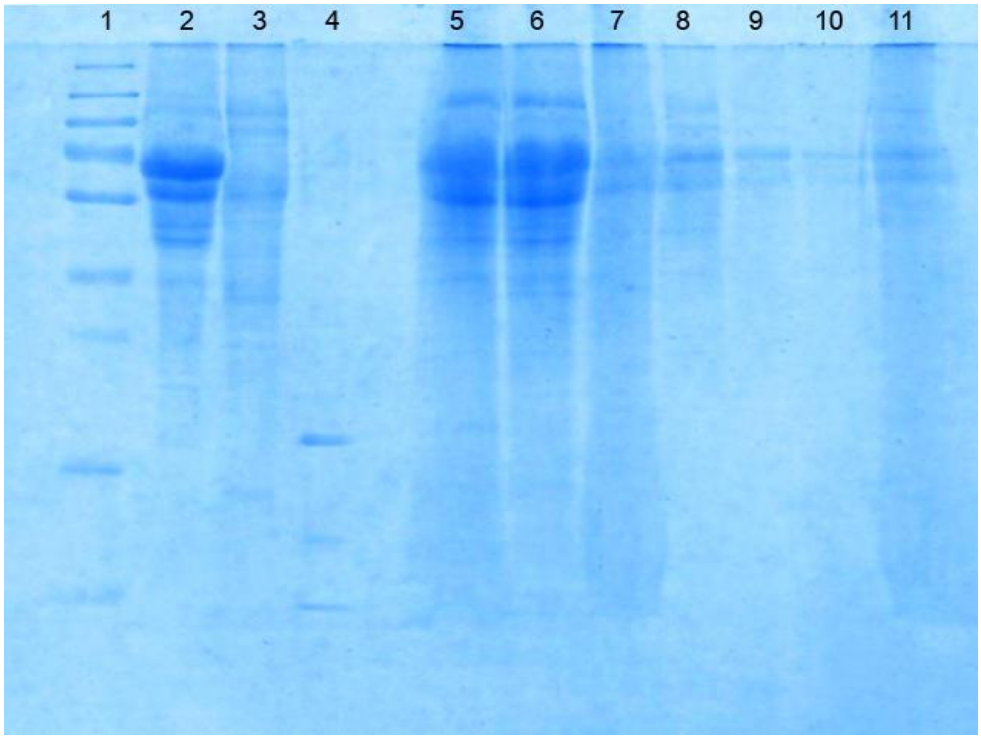

Lanes: 1 – Protein marker | 2 – Zytex cellulase | 3 – *A. niger* BGL| 4 - Xylanase from palkoxylanase
5 – Biomass slurry | 6 – Biomass pellet after supernatant removal| 7 – Supernatant after hydrolysis|
8 – First wash buffer of biomass| 9 – Second wash buffer of biomass
10 – Third wash buffer of biomass 11 – Biomass after 3 washes

4.3.2. Composition analysis of hydrolysed biomass

To understand the reaction dynamics, composition analysis of the residual biomass was carried out and data is presented in Figure 4.8. It was observed that, as the hydrolysis proceeds, the composition undergoes a major change. Biomass that was 58.78% cellulose and 27% lignin becomes 11% cellulose and 47% lignin at the end of 48 hours. This is in agreement with the glucose yield data which gives a maximum conversion of cellulose at 90.09%. Hence around 10% of the biomass remains unhydrolysed. Also, after 12 h, the reduction in cellulose content is very slow. This implies that majority of reaction has been completed within 12 h. Lignin and ash content also becomes more or less constant after 12 h. Acid soluble lignin was almost constant from the beginning till the end of hydrolysis. Ash content increased from 6% to 28% after 48 h of hydrolysis. Hemicellulose content also decreased as the hydrolysis progressed since xylanase supplementation results in xylose release during the hydrolysis.

Figure 4.8: Compositional analysis of biomass during hydrolysis

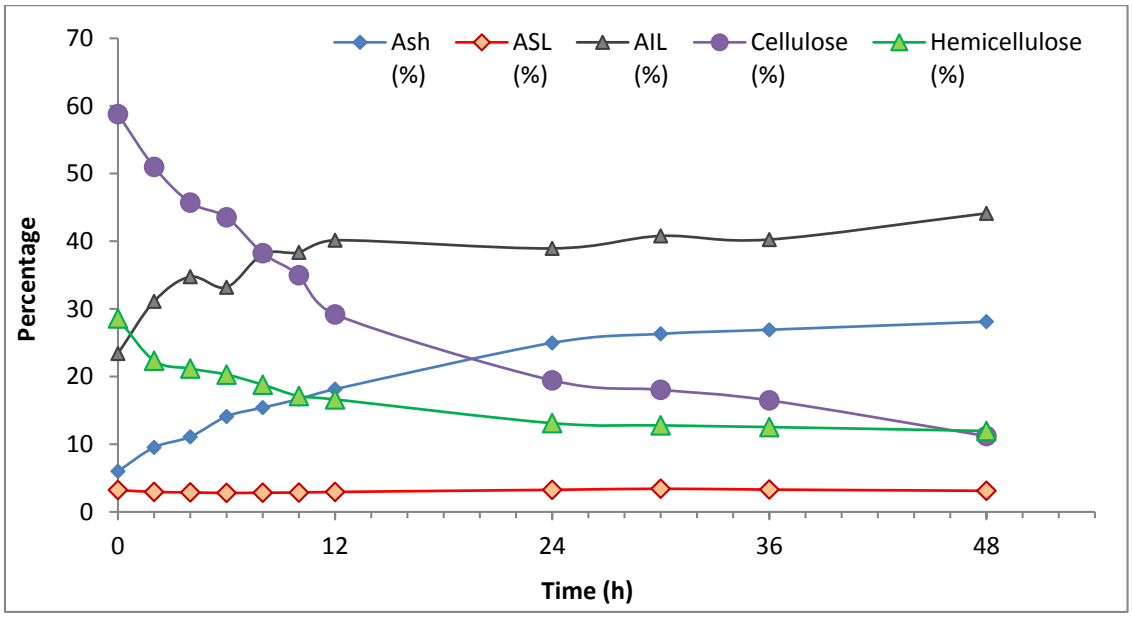

These observeations provide a clue to why adsorbed enzyme concentration decreased till 12 h. A comparsion of Figures 4.3, 4.5 and 4.8 would clearly indicate the correlation between cellulose content in the biomass and enzyme adsorption. The reduction in cellulase adsorption on biomass can safetly be attributed to the reduction in cellulose content of the biomass during 0-12 h. Enyme adsorption appeared to stabilize as cellulose content in biomass become almost constant after 12 h of hydrolysis. By this time, the biomass was more of lignin and ash and interestingly the non specific adsorption was far less than the specific adsorption on cellulose. Also, it has been reported previously that presence of lignin in the lignocellulosic biomass hinders enzyme access/adsorption to cellulose chains by its protective sheathing and reduces cellulase effectiveness and hence overall hydrolysis efficiency due to non specific and unproductive binding and stearic hindrance (Mansfield et al., 1999; Chang and Holtzapple, 2000). Hence, lignin removal by various pretreatment strategies have shown to improve cellulose digestibility by improving cellulose accessibility, higher adsorption of enzyme on substrate and increased cellulase efficiency due to removal of cross linkages to carbohydrates (Chang and Holtzapple, 2000; Yang and Wyman, 2004; Pan et al., 2005; Ohgren et al., 2007).

The intrinsic characteristics of lignin in biomass and its recalcitrance due to pretreatment reduce the enzymatic conversion of cellulose to sugars. As a result, higher protein loadings and longer hydrolysis times are required for efficient enzymatic hydrolysis of lignocellulose. It was also reported that cellulases are bound not only to cellulose, but also to phenolics that are left behind after hydrolysis (Lu et al., 2002a). Kumar and Wyman (2009b) reported that delignification enhanced enzyme effectiveness but did not have significant impact on cellulose accessibility. Delignification was found to enhance xylose release

more than glucose release and hence did not control cellulose accessibility directly. They observed that it indirectly controls cellulose accessibility by allowing rapid hydrolysis of hemicellulose. Deacetylation was also reported to improve cellulose accessibility and enzyme effectiveness and hence biomass digestibility (Jeoh et al., 2007).

4.3.3. Particle size variation during hydrolysis

Particle size plays a major role in determining the efficiency of hydrolysis. It has been observed that during the course of hydrolysis, the initially thick and semi solid reaction mixture becomes a newtonian liquid at the end of reaction. A reduction in particle size is obvious and the relevance of this property change in hydrolysis was also investigated. The morphology of particles during hydrolysis is shown in Figure 4.9. It is clearly visible from this figure that particle size reduces as hydrolysis proceeds.

The particle size distribution was measured during the course of hydrolysis and is as shown in Figure 4.10. At the beginning of hydrolysis, majority of the biomass particles were in the range 500 – 2000 µm. By 12 h, this distribution had already shifted to < 400 µm. At the end of hydrolysis, majority of the particles were of size less than 100 µm. The variation in average particle size during hydrolysis is as represented in Figure 4.11. The decrease in particle size was primarily due to hydrolysis of cellulose to glucose which causes erosion. Hydorlysis process also leads to cellulose fiber rupture which again results in particle size reduction

Figure 4.9: Morphology changes of biomass particles during hydrolysis

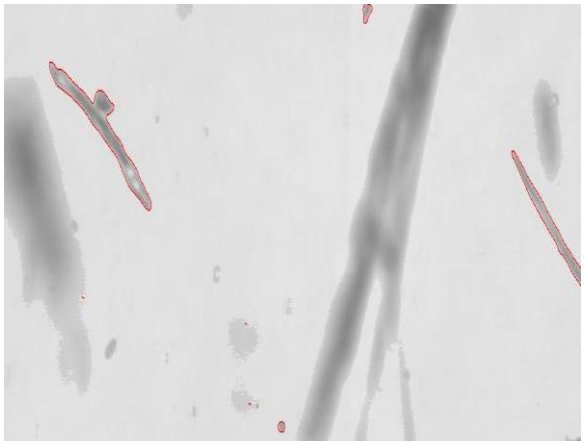

Biomass particles at the start of hydorlysis showing original size distribution

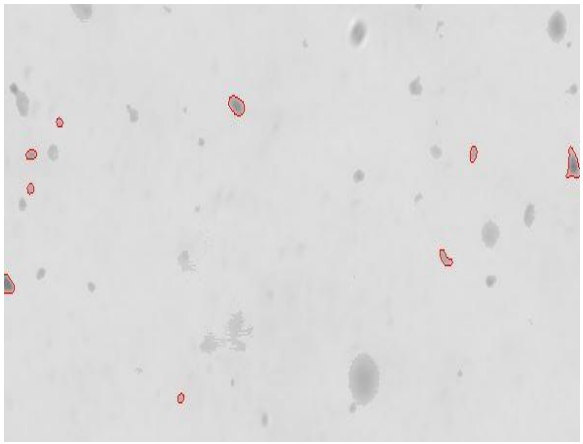

Biomass particle size distribution at 12h into hydrolysis

Figure 4.10: Particle size distribution during hydrolysis of biomass

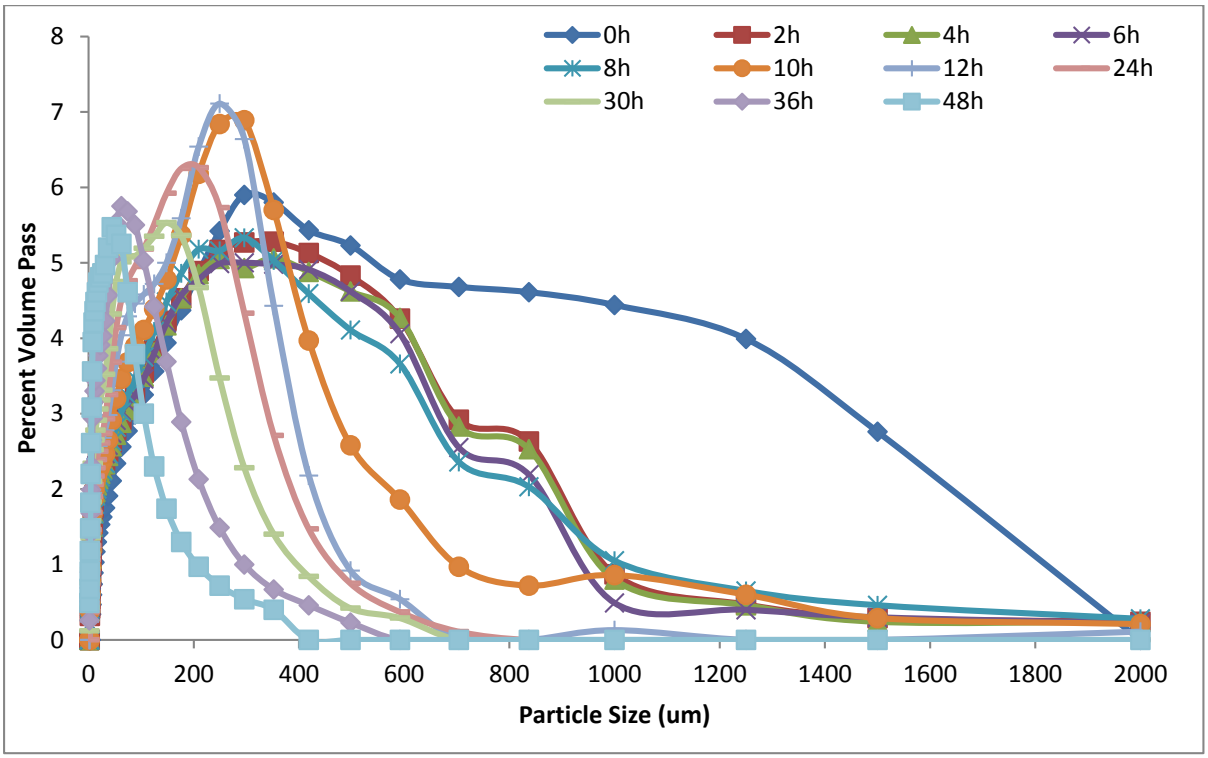

Figure 4.11: Average particle size of biomass at various time points during hydrolysis

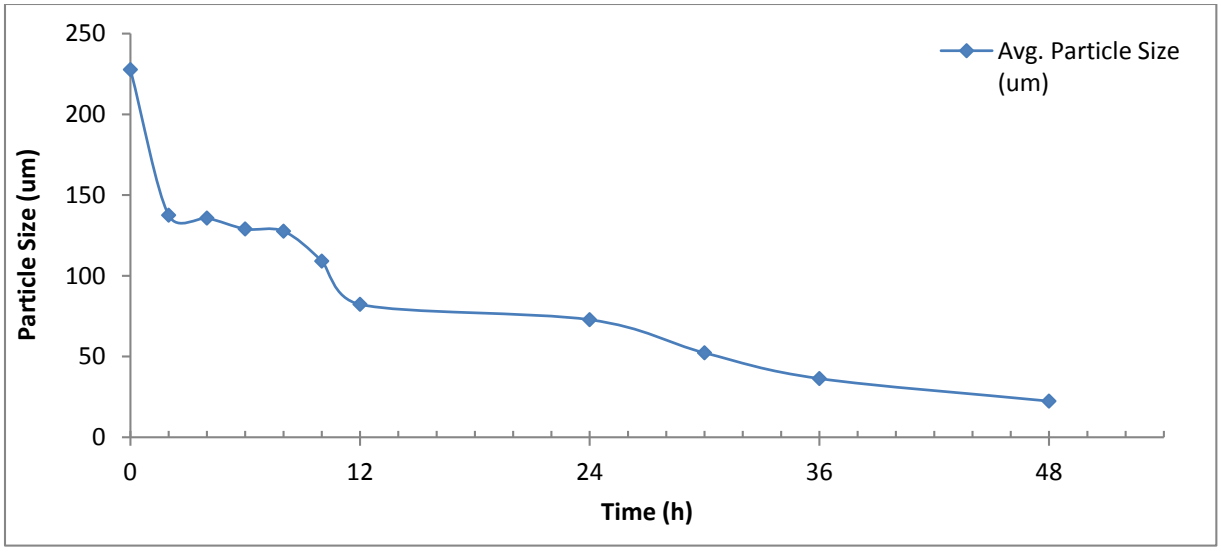

The average particle size was 227.7 µm at the start of hydrolysis. It reduced to 82.3 µm during 12th hour and further down to 22.39 µm after 48 h. The reduction in size also was much rapid during the initial 12 h whereafter the rate of size reduction was much lower. The obvious reason for reduction in size would be

release of glucose and pentoses from the particles resulting in the particles becoming smaller and compositionally more of lignin and ash and less of sugars.

4.3.4. Physico Chemical Characterization of hydrolysed biomass

4.3.4.1. XRD studies on biomass during hydrolysis

X-Ray Diffraction studies revealed increased amorphous and decreased crystalline regions in the biomass as hydrolyisis proceeds (Figure 4.12). This once again proves the loss of cellulose from biomass and the increase in lignin content. Cellulose is the component that imparts crystallinity to biomass and lignin imparts amorphous nature. Hence the reduction in crystallinity can be correlated to cellulose hydrolysis and therefore enhanced lignin concentration.

Figure 4.12: XRD studies on the biomass

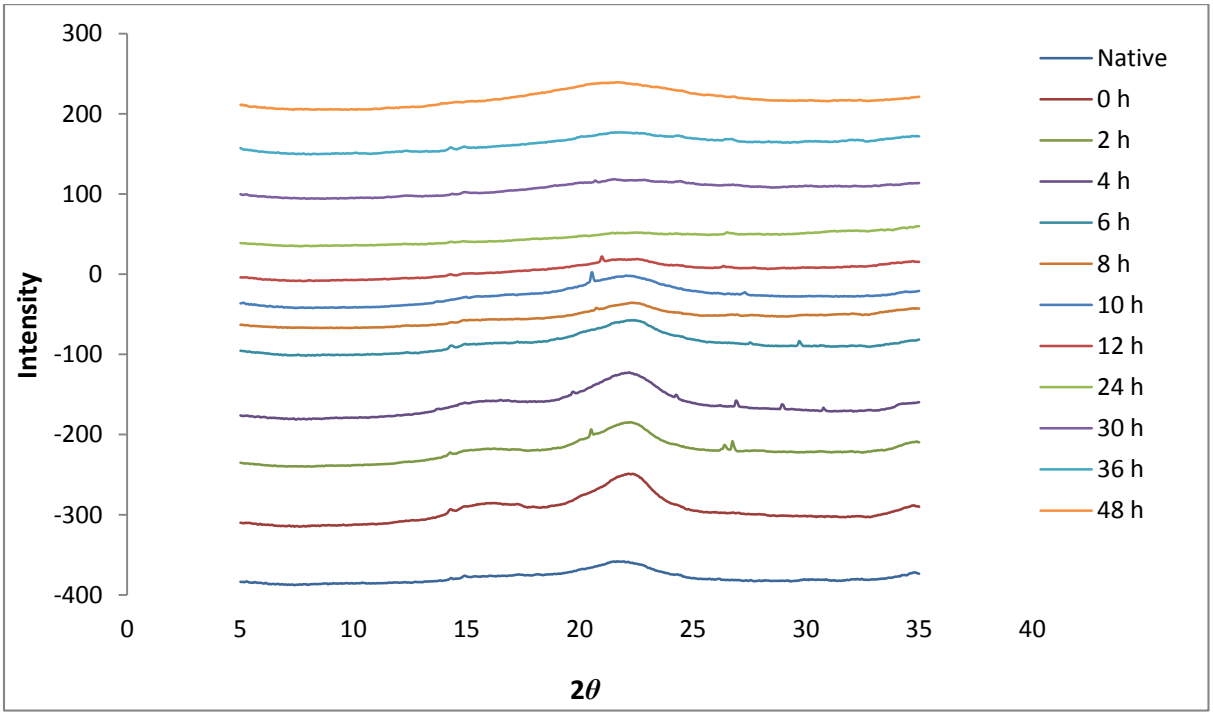

4.3.4.2. FT-IR Spectrum of biomass

FT-IR spectrum (Figure 4.13) revealed major changes in the chemical composition of biomass with time during hydrolysis. The changes observed through FTIR spectra were in agreement with the composition data.

Figure 4.13: FT-IR spectrum of biomass during hydrolysis

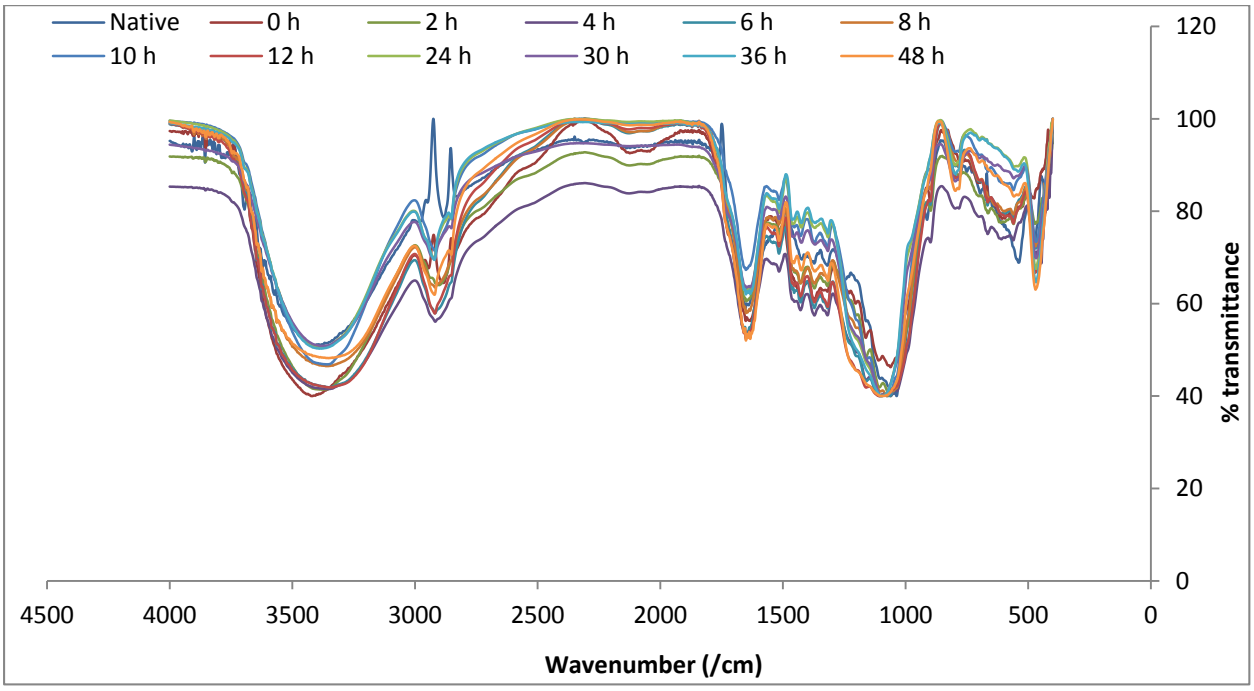

The decreased transmittance at wavelnumber 1605/cm, 1501/cm, 1328/cm and 1239/cm indicated higher amount of lignin as hydrolysis proceeds. These wavelenghths correspond to aromatic skeletal vibrations and C=O stretch; aromatic C=C stretching from aromatic ring of lignin; phenolic hydroxyl group; and syringyl ring breathing and C-O stretching out of lignin respectively. Similarly, increase in transmittance with time at wave numbers 2924, 1740, 1643 and 1374/cm indicated loss of hemicelluloses and celluloses. Transmittance at these wavenumbers correspond to –CH stretching of methyl groups; C=O stretching of unconjugated ketones, carbonyls, ester groups and in xylan acetates; absorbed O-H and conjugated C-O; and aliphatic C-H deformation vibrations in cellulose and hemicellulose respectively.

4.3.4.3. SEM Analyses of biomass

SEM images also showed a progressive breakdown in structure of biomass with time (Figure 4.14). After about 12 – 24 hours, biomass was no longer visible as strand and were just fine particles clumped together. Cellulose breakdown is achieved by surface shaving or planing of biomass. Arantes and Saddler (2010) had proposed that to attain optimum enzymatic hydrolysis, cellulose chains in the highly ordered and tightly packed regions of lignocellulosic structure should be delaminated, disrupted or loosened so that the effective biomass surface area increases. This leads to higher cellulase accessibility to cellulose. They also observed cellulose fiber swelling and disintegration to smaller fibers during hydrolysis before-

Figure 4.14: SEM images of biomass at varying time points of hydrolysis

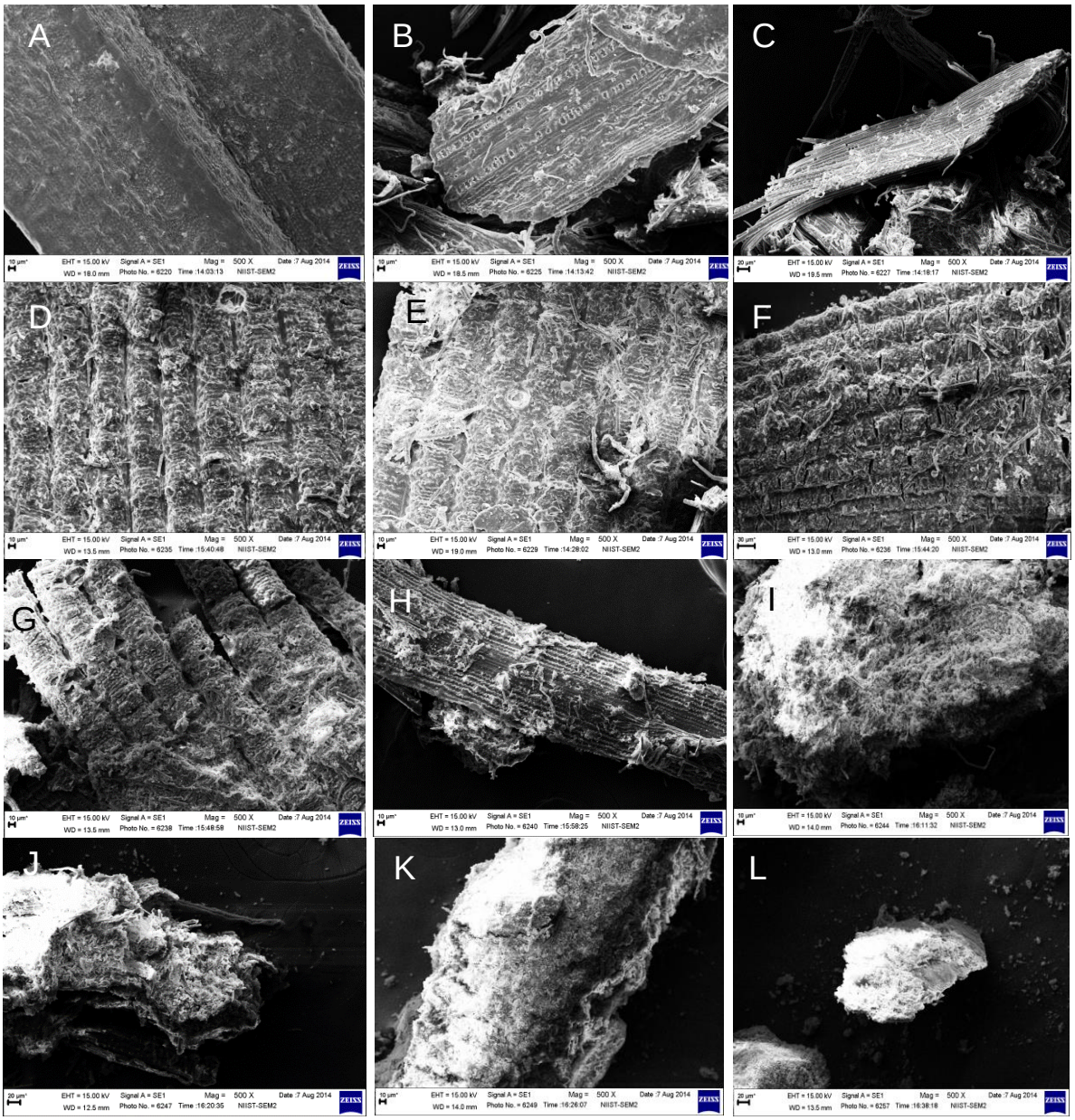

A) Native biomass B-K) Biomass samples taken at 0 h, 2 h, 4 h, 6 h, 8 h, 10 h,12 h, 24 h, 30 h, 36 h and 48 h

-higher reaction rates of glucose release were observed. It was proposed that cellulases are initially adsorbed onto surfaces where there is a visible deformation in cellulosic microfibrils, which is followed by enzyme penetration to interfibrillar spaces. Presence of the large enzyme molecules within the narrow interfibrillar space causes mechanical pressure on the cavity walls resulting in the swelling of cellulose structure. This leads to broadening of the space which results in the accommodation of more water

molecules between microfibrils. These water molecules penetrates further into the interfibrillar space and breaks the hydrogen bonds between cellulose chains which leads to disassociation of the microfibrils.

A similar phenomenon has been observed in the present study, where the cellulose fibers appear to be disintegrating and breaking up as hydrolysis proceeds. During the latter half of hydrolysis, strands are no longer visible and only cellulose aggregates in the form of small particles are seen. Disintegration of the microfibrillar structure with progress of hydrolysis was evident from the SEM images of biomass particles at different time points. It could be speculated that the disruption of the cellulosic structure enhances the accessibility of cellulase to deeper regions in cellulose contributing to higher efficiency of enzymatic saccharification.

4.3.4.4. Porosity Profile

Porosity of the biomass is important since it could be a determining factor in cellulose accessibility. Figure 4.15 shows the variation in porosity of biomass with progress in hydrolysis. It was found that porosity of biomass decreases till about 24 h into the hydrolysis and thereafter remains unchanged. Size of typical cellulase enzyme is ~5.1 nm (Grethlein, 1985). Since the average pore size at the beginning of hydrolysis is 12 nm, this may not be a rate limiting factor for cellulase penetration. Throughout hydrolysis, the pore size never dropped below 8.3 nm.

Figure 4.15: Porosity profile of biomass during hydrolysis

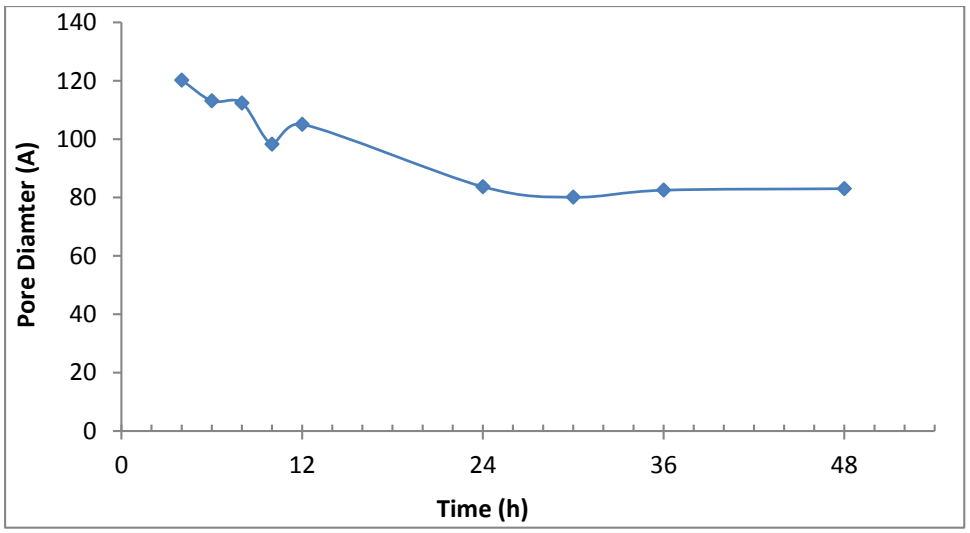

Cellulosic materials are porous substances with heterogeneous surfaces. Their available surface area is classified as exterior and interior surfaces. Interior surfaces generally consist of pores and cracks that arise due to the discontinuous packing of cellulose fibrils. They also contain surface openings, slits, pores, and

voids that are created due to removal of non cellulosic substances during pretreatment or hydrolysis. The external surface area of cellulosic-rich materials is largely determined by the individual overall fiber dimensions (Jeoh et al., 2007). Grethlein (1985) showed that initial hydrolysis rate and pore size accessible for cellulase are directly proportional. SEM analyses of the samples showed several pores, slits and voids during the rapid hydrolysis phase (0-12 h) whereas during the later stages organized structure was absent due to the loss of cellulose (Figure 4.14). Without cellulose to maintain the structure, it can be assumed that the pores would collapse and also the available surface area for enzyme adsorption decreases.

Reports suggest that cellulase penetration into celluloses is the first step in the cellulosic biomass hydrolysis. Cellulase penetration into pores/fissures in the biomass initiates the hydrolysis, after swelling the cellulosic fibers. Hence, porosity was suggested to be an important factor that influences the amount of enzyme adsorbed on the biomass (Esteghlalian et al., 2001; Ishizawa et al., 2007; Gao et al., 2014; Luterbacher et al., 2015). Majority of the previous studies have reported an increase in porosity during the hydrolysis. The converse was observed in the present study. This might be due to the fact that drying of biomass to measure porosity using BET isotherm may lead to collapse of pores and hence faulty measurements. Apparently porosity measurements using alternate non-disruptive methods would be necessary to resolve this issue.

4.4. Conclusions

The major observation from the present study was that enzyme binding to the biomass is most efficient during initial hours of hydrolysis, largely determined by the cellulose content, and most of the enzyme provided in the reaction mix was not actually participating in the hydrolysis (not binding to biomass) and were free in the solution. It could therefore be assumed that high protein loadings may not be necessary to achieve high enzymatic efficiencies and the hydrolysis efficiencies are more related to the efficiency of enzyme binding on cellulose than the quantity of enzyme provided. This provides the hint that pre-treatment of biomass plays a major role since it will influence the cellulose accessibility to a large extent. Another major finding was that the time of hydrolysis (at least in the case of alkali pretreated rice straw) need not be 48 – 96 h as is commonly practiced. Majority of the cellulose conversion takes place during the initial 12 h of hydrolysis. This again is advantageous since it would imply a reduction in the time of reaction. A lower enzyme loading and reduced time of hydrolysis can therefore be attained with a biomass pretreated to achieve maximal cellulase adsorption. Major interventions then would be to improve the thermal stability and half life of enzymes so that they continue to act with maximal efficiencies throughout the initial hours of hydrolysis.

Chapter 5

Impact of various modes of hydrolysis on saccharification efficiency

5.1. Introduction

Recently, the focus in hydrolysis optimization targets high solid loading saccharification of lignocellulosic biomass. Literature defines high solids as concentrations from 12-15% insoluble solids (Hodge et al., 2009). At high solids concentration, the mixture reaches homogeneity. High solid enzymatic hydrolysis applications are limited due to a few factors that affect the conversion efficiencies in this process. One of the major challenges here is the lack of availability of free water in the reactor. Free water is a critical parameter that lowers the mass transfer resistance due to high viscosity of biomass and acts as a lubricant between the coarse biomass particles so as to reduce friction between them. Reduction in viscosity is important to lower the power requirement by impellers (Hodge et al., 2009; Kristensen et al., 2009b). High viscosity and mixing problems also lead to lower heat transfer efficiencies, due to which local temperature variations are observed. Water also helps in the mass transfer of enzymes and products in the reaction system and prevents the building up of inhibitors in any particular zone in the reactor (Gervais et al., 1988).

As biomass loading approaches 20% (w/v), all free water is absorbed by the solids and hence, apparent viscosity increases leading to inefficient mixing. Zhang et al., (2010) reported that increasing biomass loadings from 15 to 30% for hydrolysis of pretreated corn stover increased the energy required for mixing from 79.5 MJ/ tonne slurry to 1009.2 MJ/tonne slurry. They found that more than half the energy produced from the increased concentration of ethanol obtained by high solids loading was consumed in mixing the hydrolysis mixture, compared to 9% energy consumption for mixing in ethanol produced by lower solids loading.

Increasing the solids loading leads to an increase in sugar content, but this increase is not linear and the sugar yield decreases with higher biomass loadings. The reasons for this might be product inhibition, substrate effects, low water content and enzyme adsorption limitations (Kristensen et al., 2009b). Efficient hydrolysis of biomass requires longer reaction times. However, longer hydrolysis times (>72-96 h) translate to higher operation costs (Xu and Ding, 2007; Bommarius et al., 2008). Also, higher biomass loadings necessitate higher enzyme dosages, which again contribute to the high cost of hydrolysis. Hence a balance between the biomass and enzyme dosages and reaction times are required while optimizing biomass hydrolysis for higher glucose yields

In spite of all these limitations, there are several benefits of operations at high solid loadings, the most important of which is attaining high sugar concentration, which facilitates improved downstream

process and product recovery. This reduces the capital cost and operating cost due to reduction in energy required for concentration of the hydrolysate and subsequent distillation of fermented hydrolysate. Besides, it helps to reduce the number of operations required to attain similar ethanol yields compared to batch processes that uses lower biomass loadings. Studies have reported that about 10% overall lignocellulose to bioethanol operation cost may be reduced when the solid level is increased from 20% to 30% (w/v) (Schell, 2005). It is well established that ethanol concentration should at least be about 4% to 5% (w/v) to make the distillation process economically feasible. Zacchi and Axelsson (1989) report that when ethanol concentration in the fermentation broth increased to 5% from 1%, energy consumption reduced by about two – thirds in a single distillation unit for final concentration of 94.5% (w/w) ethanol.

Batch hydrolysis above 15% solids loading faces high viscosity and mixing problems in addition to requirement of high power for mixing (Fan et al., 2003). Hence, fed batch modes of operation are suggested as an alternative mode to attain higher biomass loadings (Rosgaard et al., 2007; Lu et al., 2010; Chandra et al., 2011; Yang et al., 2011). In fed batch mode of operation, initial apparent viscosities are lower. Hence diffusion and mixing limitations can be at least partially overcome by this mode of operation. A fed-batch operation also allows time for the initial reaction mixture to partially hydrolyze the solids so that the slurry liquefies to some extent before the next substrate feeding. Hence, the level of free water is maintained in the reaction mixture every time during the course of reaction. This aids in efficient mixing so that the products formed and inhibitors are distributed throughout the reactor and not found concentrated in certain zones in the reactor. Thus inhibition of hydrolysis is minimized (Modenbach and Nokes, 2013).

Critical parameters to be considered for fed batch operation are the feeding time and strategy of biomass and enzyme addition so that high hydrolysis rates are maintained. Addition of enzymes along with biomass at each feeding interval enhances the overall hydrolytic efficiency. Yang et al., (2011) have reported a higher conversion efficiency of 70.6% at 30% solids loading. They propose that fresh enzyme addition might be increasing sugar yields due to replacement of enzymes non - productively bound to lignin or inactivated due to long reaction times. Constant addition of enzyme with substrate also maintained a constant enzyme – substrate ratio in the mixture.

At fed batch mode with intermittent biomass addition and complete addition of enzymes at the beginning of reaction, Ma et al., (2011) reported a 75% conversion efficiency of celluloses at 25% biomass loading. Batch processes with same loadings yielded efficiencies of 50% whereas intermittent biomass and enzyme feeding strategy gave 84% conversion efficiency. Thus, it can be concluded that under properly designed operation conditions, fed batch mode could lead to higher conversion efficiencies for high solids loading hydrolysis. Rosgaard et al., (2007) also reported that enzyme – substrate ratios are constant in intermittent enzyme and biomass feeding strategy, whereas this ratio decreases when all the

enzymes are added at the beginning itself. In the fed batch modes with full initial enzyme addition, rates of reactions are higher at the beginning due to higher enzyme availability. But the final yields in both schemes were same.

Thus, in the present study, hydrolysis to attain higher biomass loadings was studied. As batch mode is not suitable for loadings above 10%, semi batch mode was used to attain higher loadings and higher conversion efficiencies. The efficacy of the three semi batch modes – intermittent biomass addition, intermittent enzyme addition and intermittent biomass and enzyme addition were studied to determine the best mode of operation to achieve high sugar yields.

5.2. Materials and Methods

5.2.1. Enzymatic hydrolysis of biomass with varying modes of operation

Alkali pretreatment of rice straw was carried out as in section 2.1. Pretreated biomass was air dried at room temperature and stored in airtight containers. To determine the efficiency of pretreatment and hydrolysis, composition analysis of native and pretreated biomass was done as per the protocol in section 2.2. Enzymatic saccharification of pretreated rice straw (moisture content 17.5%) was carried out using cellulase from Zytex India Ltd., β-glucosidase (BGL) from *Aspergillus niger* and xylanase from MAPS India Pvt. Ltd. The optimum conditions used were: Cellulase -10 FPU/g, BGL-5 IU/g, Xylanase-7500 U/g, reaction temperature -50 °C and 200 rpm agitation. Total reaction volume was 30mL that contained 15 mL sodium citrate buffer (0.05 M, pH 4.8), 0.15 mL of Tween 80, 0.45mL of antibiotic solution (Penicillin-streptomycin mix, Himedia, India) and enzymes as per the reaction design was added into the reaction mix. Distilled water was added to make up the reaction volume. Batch (B) and semi batch (SB) reaction modes were performed and three strategies were tried in semi batch mode – intermittent biomass addition (SB1), intermittent enzyme addition (SB2) and intermittent biomass and enzyme addition (SB3). Biomass or enzyme was added intermittently at 0, 2, 4, 6, 8, 10 and 12 h into hydrolysis. The different sample runs under various modes were done as given in Tables 5.1, 5.2, 5.3 and 5.4. Samples were collected after 12, 24, 36 and 48 h of incubation and sugars in the supernatant were analyzed by HPLC using Phenomenex Rezex RNM HPLC column and RI detector.

Table 5.1: Experiment design for batch mode of hydrolysis (B)

Biomass Loading (%)	Biomass Loading (g)	Cellulase (FPU)	BGL (IU)	Xylanase (U)	Cellulase (mL)	BGL (mL)	Xylanase (mL)	Moisture corrected Biomass (g)
5	1.50	15.0	7.50	11250	0.18	0.09	1.66	1.76
8	2.25	22.5	11.25	16875	0.26	0.14	2.49	2.64
10	3.00	30.0	15.00	22500	0.35	0.18	3.32	3.53
13	3.75	37.5	18.75	28125	0.44	0.23	4.15	4.41
15	4.50	45.0	22.50	33750	0.53	0.27	4.97	5.29
18	5.25	52.5	26.25	39375	0.62	0.32	5.80	6.17
20	6.00	60.0	30.00	45000	0.71	0.36	6.63	7.05
23	6.75	67.5	33.75	50625	0.79	0.41	7.46	7.93
25	7.50	75.0	37.50	56250	0.88	0.45	8.29	8.81
28	8.25	82.5	41.25	61875	0.97	0.50	9.12	9.69
30	9.00	90.0	45.00	67500	1.06	0.54	9.95	10.58

Table 5.2: Experiment design for semi batch mode of hydrolysis with intermittent biomass loading (SB1)

Biomass Loading (%)	Biomass Loading (g)	Cellulase (FPU)	BGL (IU)	Xylanase (U)	Moisture corrected Biomass (g)	Biomass to be added at each 2h interval till 12 h (g)	% Increase in Biomass Loading in each interval
5	1.50	15.0	7.50	11250	1.76	0.252	0.71
8	2.25	22.5	11.25	16875	2.64	0.378	1.07
10	3.00	30.0	15.00	22500	3.53	0.504	1.43
13	3.75	37.5	18.75	28125	4.41	0.629	1.79
15	4.50	45.0	22.50	33750	5.29	0.755	2.14
18	5.25	52.5	26.25	39375	6.17	0.881	2.50
20	6.00	60.0	30.00	45000	7.05	1.007	2.86
23	6.75	67.5	33.75	50625	7.93	1.133	3.21
25	7.50	75.0	37.50	56250	8.81	1.259	3.57
28	8.25	82.5	41.25	61875	9.69	1.385	3.93
30	9.00	90.0	45.00	67500	10.58	1.511	4.29

Table 5.3: Experiment design for semi batch mode of hydrolysis with intermittent enzyme addition (SB2)

Biomass Loading (%)	Biomass Loading (g)	Enzyme Loading (Units) Total						Enzyme Loading (Units) Quantity added at each time interval					
		Cellulase (FPU)	BGL (IU)	Xylanase (U)	Cellulase (mL)	BGL (mL)	Xylanase (mL)	Cellulase (FPU)	BGL (IU)	Xylanase (U)	Cellulase (mL)	BGL (mL)	Xylanase (mL)
5.0	1.5	15.0	7.50	11250	0.18	0.09	1.66	2.14	1.07	1607	0.03	0.01	0.24
7.5	2.3	22.5	11.25	16875	0.26	0.14	2.49	3.21	1.61	2411	0.04	0.02	0.36
10.0	3.0	30.0	15.00	22500	0.35	0.18	3.32	4.29	2.14	3214	0.05	0.03	0.47
12.5	3.8	37.5	18.75	28125	0.44	0.23	4.15	5.36	2.68	4018	0.06	0.03	0.59
15.0	4.5	45.0	22.50	33750	0.53	0.27	4.97	6.43	3.21	4821	0.08	0.04	0.71
17.5	5.3	52.5	26.25	39375	0.62	0.32	5.80	7.50	3.75	5625	0.09	0.05	0.83
20.0	6.0	60.0	30.00	45000	0.71	0.36	6.63	8.57	4.29	6429	0.10	0.05	0.95
22.5	6.8	67.5	33.75	50625	0.79	0.41	7.46	9.64	4.82	7232	0.11	0.06	1.07
25.0	7.5	75.0	37.50	56250	0.88	0.45	8.29	10.71	5.36	8036	0.13	0.06	1.18
27.5	8.3	82.5	41.25	61875	0.97	0.50	9.12	11.79	5.89	8839	0.14	0.07	1.30
30.0	9.0	90.0	45.00	67500	1.06	0.54	9.95	12.86	6.43	9643	0.15	0.08	1.42

Table 5.4: Experiment sheet for semi batch mode of hydrolysis with intermittent biomass and enzyme loading (SB3)

Biomass Loading (%)	Biomass Loading (g)	Total Enzyme Loading (Units)			Moisture corrected Biomass (g)	Biomass to be added each 2h interval till 12h (g)	% Increase in Biomass Loading in each interval	Enzyme Loading (Units) Quantity added at each time interval					
		Cellulase (FPU)	BGL (IU)	Xylanase (U)				Cellulase (FPU)	BGL (IU)	Xylanase (U)	Cellulase (mL)	BGL (mL)	Xylanase (mL)
5.0	1.50	15.0	7.50	11250	1.76	0.25	0.71	2.14	1.07	1607.14	0.03	0.01	0.24
7.5	2.25	22.5	11.25	16875	2.64	0.38	1.07	3.21	1.61	2410.71	0.04	0.02	0.36
10.0	3.00	30.0	15.00	22500	3.53	0.50	1.43	4.29	2.14	3214.29	0.05	0.03	0.47
12.5	3.75	37.5	18.75	28125	4.41	0.63	1.79	5.36	2.68	4017.86	0.06	0.03	0.59
15.0	4.50	45.0	22.50	33750	5.29	0.76	2.14	6.43	3.21	4821.43	0.08	0.04	0.71
17.5	5.25	52.5	26.25	39375	6.17	0.88	2.50	7.50	3.75	5625.00	0.09	0.05	0.83
20.0	6.00	60.0	30.00	45000	7.05	1.01	2.86	8.57	4.29	6428.57	0.10	0.05	0.95
22.5	6.75	67.5	33.75	50625	7.93	1.13	3.21	9.64	4.82	7232.14	0.11	0.06	1.07
25.0	7.50	75.0	37.50	56250	8.81	1.26	3.57	10.71	5.36	8035.71	0.13	0.06	1.18
27.5	8.25	82.5	41.25	61875	9.69	1.38	3.93	11.79	5.89	8839.29	0.14	0.07	1.30
30.0	9.00	90.0	45.00	67500	10.58	1.51	4.29	12.86	6.43	9642.86	0.15	0.08	1.42

5.3. Results and Discussion

5.3.1. Composition Analysis of native and alkali pretreated rice straw

Alkali pretreatment increased cellulose content from 38.65% to 59.87% and hemicellulose content from 18.46% to 20.95% in rice straw. Based on the cellulose and hemicellulose content, the theoretical maximum sugars that could be released from this biomass was calculated as 664 mg of glucose and 180 mg of pentose (C5) sugars per gram of pretreated biomass. Table 5.5 shows the complete composition analysis of native and alkali pretreated rice straw

.

Table 5.5: Composition Analysis of native and pretreated rice straw

Sample	Cellulose (%)	Hemicellulose (%)	Acid Soluble Lignin (%)	Acid Insoluble Lignin (%)	Ash (%)
Native rice straw	38.65	18.46	4.69	31.57	6.37
Alkali Pretreated rice straw	59.87	15.95	3.22	13.41	5.99

5.3.2. Hydrolysis of rice straw upon varying biomass loading and modes of operation

Table 5.6 gives the most significant results for hydrolysis with high biomass loadings and batch and semi batch mode of hydrolysis operation. It was observed that beyond 15% biomass loading, in semi batch mode with intermittent biomass and enzyme addition, hydrolysate with more than 8% (w/v) sugar yield could be obtained. Glucose concentration should be at least 80 g/L (Larsen et al., 2008) to yield 4% (w/w) ethanol that can be distilled out from fermentation broth economically (Zacchi and Axelsson, 1989). Hence, the hydrolysate produced through semi batch operation could be directly used for fermentation without concentration, which reduces the overall cost of hydrolysis operation. Glucose concentrations of 136 mg/mL could be obtained with 30% biomass loading. Among the different modes of hydrolysis operation tried, batch mode was least efficient and gave lowest amount of sugars. In majority of the conditions experimented, semi batch mode with intermittent biomass and enzyme loading gave highest sugar concentrations.

Table 5.6: Biomass hydrolysis efficiencies at varying biomass loadings and modes of operation

	Glucose Release (mg/mL)			
Sample	B	SB1	SB2	SB3
15%-24 h	79.30	71.03	61.25	87.19
15%-36 h	71.70	78.35	71.12	85.34
15%-48 h	82.29	85.32	78.39	89.39
17.5%-12 h	61.11	63.03	59.13	67.91
17.5%-24 h	72.40	76.93	66.38	75.03
17.5%-36 h	75.10	80.29	73.54	83.43
17.5%-48 h	74.99	73.28	71.16	89.37
20%-12 h	63.67	72.11	59.36	73.36
20%-24 h	77.09	83.44	81.67	90.49
20%-36 h	87.67	94.41	91.34	95.62
20%-48 h	81.60	81.12	78.98	90.69
22.5%-12 h	58.75	86.02	68.88	91.13
22.5%-24 h	63.73	92.99	83.38	98.43
22.5%-36 h	66.15	101.86	94.66	105.11
22.5%-48 h	86.89	114.12	109.71	111.54
25%-12 h	64.55	85.12	74.94	94.25
25%-24 h	80.13	104.80	99.98	109.81
25%-36 h	82.14	106.35	101.49	117.57
25%-48 h	89.62	111.91	106.64	107.37
27.5%-12 h	50.08	86.91	80.23	98.05
27.5%-24 h	52.67	103.63	98.95	112.96
27.5%-36 h	62.88	115.29	108.21	115.59
27.5%-48 h	61.72	120.21	113.28	125.27
30%-12 h	52.15	97.37	90.32	98.48
30%-24 h	58.06	108.36	97.55	110.81
30%-36 h	68.79	115.41	107.15	115.68
30%-48 h	78.38	130.52	116.10	135.86

5.3.2.1. Glucose and Xylose yields during hydrolysis with varying biomass loadings

Upon varying biomass loadings and modes of operation, significant difference was observed in the sugar yields. Higher loadings gave hydrolysate with higher sugar concentrations. But in those cases, efficiency of hydrolysis was lower. Therefore, to optimize the concentration of hydrolysate, a balance needs to be struck between optimum biomass loading and mode of hydrolysis operation.

5.3.2.1.1. Glucose and xylose yields with 5% biomass loading

With 5% loading, it was observed that free water availability in the hydrolysis mixture was very high. In all the different modes of hydrolysis, glucose yields were almost similar. Around 29 – 31 mg/mL glucose was formed in every reaction mode. Xylose production was higher in hydrolysis using intermittent biomass and enzyme loading. Around 7.9 mg/mL xylose was formed with SB3 mode after 48 h. The glucose and xylose yield profiles are as given in Figure 5.1A and 5.1B.

Figure 5.1: Sugar release at 5% biomass loading and under different modes of operation

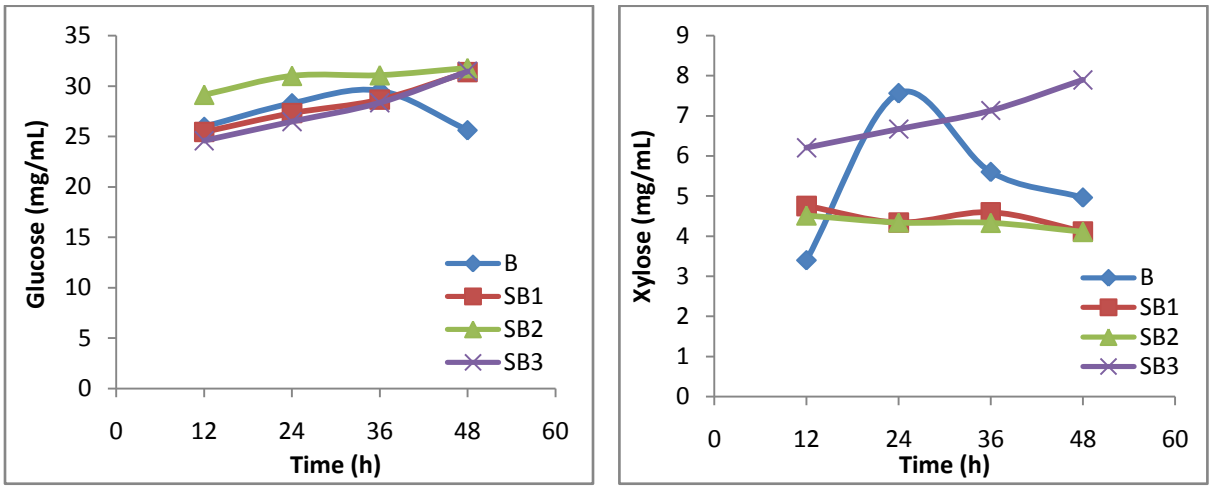

A) Glucose Release

B) Xylose Release

5.3.2.1.2. Glucose and xylose yields with 7.5% biomass loading

For biomass loading at 7.5%, the reaction mixture was not viscous and was uniform slurry with easiness of mixing. In this case also, high hydrolysis efficiencies for cellulose were observed in all the modes of operation. Among the different modes of hydrolysis, glucose yields were higher for SB2 and SB3. 72 – 95% conversion efficiencies were observed. Hemicellulose conversion to xylose was higher in SB3 as in

the previous case. A maximum efficiency of around 52.5% xylose production was observed. The glucose and xylose yield profiles are as given in Figure 5.2A and 5.2B.

Figure 5.2: Sugar release at 7.5% biomass loading and under different modes of operation

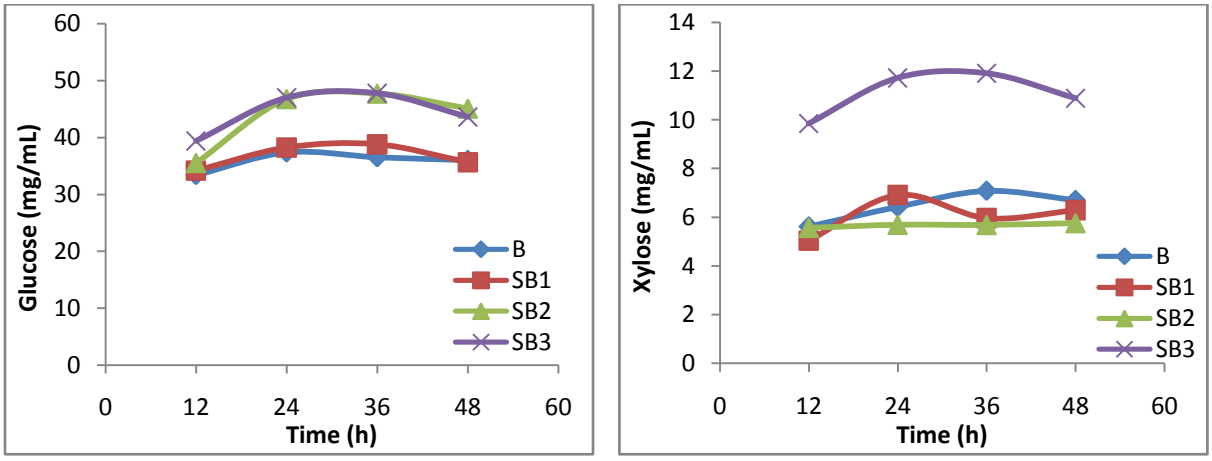

A) Glucose Release B) Xylose Release

5.3.2.1.3. Glucose and xylose yields with 10% biomass loading

Figure 5.3: Sugar release at 10% biomass loading and under different modes of operation

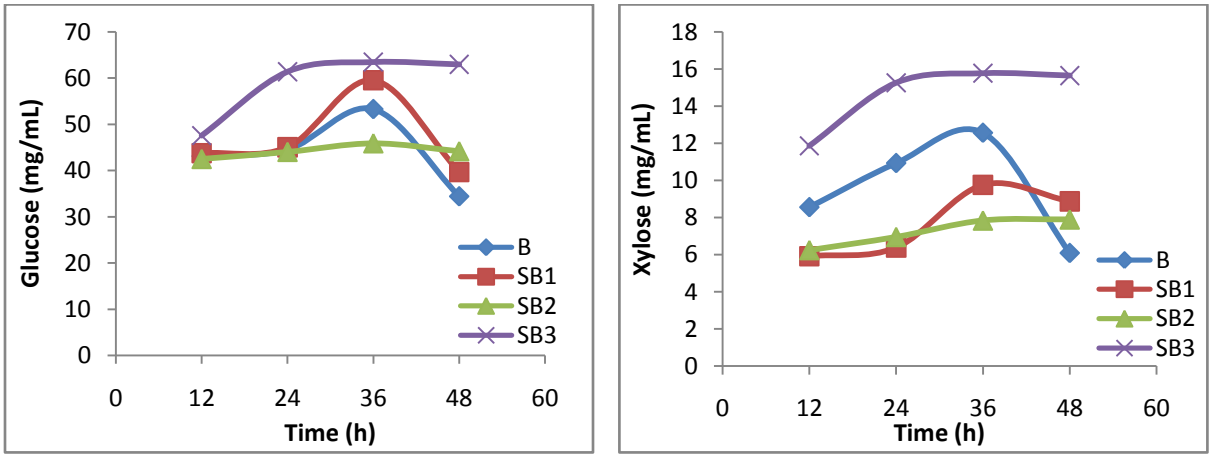

A) Glucose Release B) Xylose Release

Biomass loading of 10% was used throughout the studies as the standard substrate loading. With 10% loading, the reaction mix had a good consistency and viscosity was not high enough to prevent proper mixing. In this case, glucose yields were higher with SB3 mode of operation. Hemicellulose hydrolysis also followed the same trend with higher yields with SB3 mode. For both yields, SB2 mode was found to

produce least amount of sugars. The maximum glucose concentration obtained was 63.4 mg/mL and 15.65 mg/mL was observed for xylose yields as shown in Figure 5.3A and 5.3B respectively.

5.3.2.1.4. Glucose and xylose yields with 12.5% biomass loading

At 12.5% biomass loading, viscosity of the initial reaction mix increased. However, as the reaction progressed, it became less viscous. Even though initial glucose production rates were higher with SB3, at the end of reaction, comparable yields were obtained with SB1. With SB3, hydrolysate with 79 mg/mL glucose could be obtained after 36 h of hydrolysis (Figure 5.4A). This hydrolysate can be taken up for fermentation without any concentration step. As in previous cases, xylose release was higher with SB3. The hydrolysate contained around 19.7 mg/mL xylose when SB3 mode was used for 36 h of hydrolysis (Figure 5.4B).

Figure 5.4: Sugar release at 12.5% biomass loading and under different modes of operation

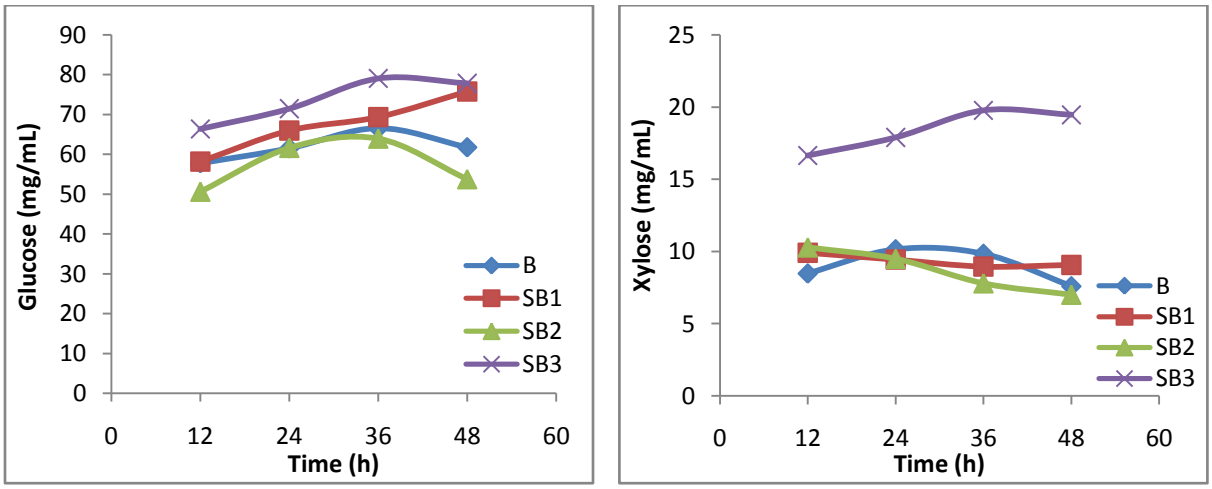

A) Glucose Release

B) Xylose Release

5.3.2.1.5. Glucose and xylose yields with 15% biomass loading

15% biomass loading also yielded homogeneous reaction slurry. In all the modes of operation except SB2, more than 80 mg/mL glucose concentration in the hydrolysate could be obtained. Hence, 15% loading was found to be the minimum requirement to yield hydrolysate that contains 8% sugar for direct fermentation without concentration step. Maximum concentration of 89.3 mg/mL was observed with SB3

mode after 48 h reaction (Figure 5.5A). As with glucose, xylose concentration also improved and a maximum concentration of 22.3 mg/mL was observed with SB3 after 48 h of hydrolysis (Figure 5.5B).

Figure 5.5: Sugar release at 15% biomass loading and under different modes of operation

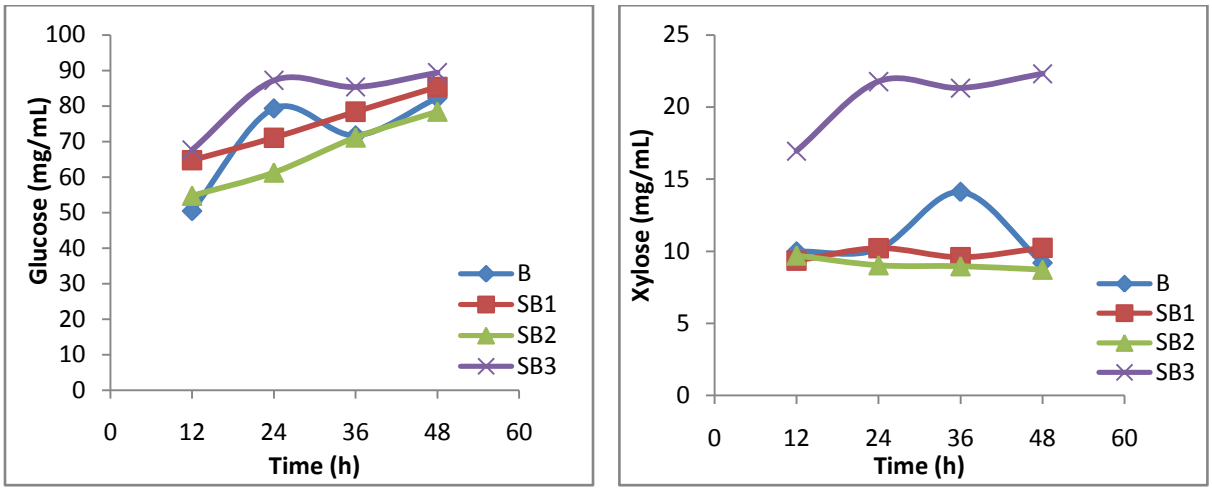

A) Glucose Release B) Xylose Release

5.3.2.1.6. Glucose and xylose yields with 17.5% biomass loading

Figure 5.6: Sugar release at 17.5% biomass loading and under different modes of operation

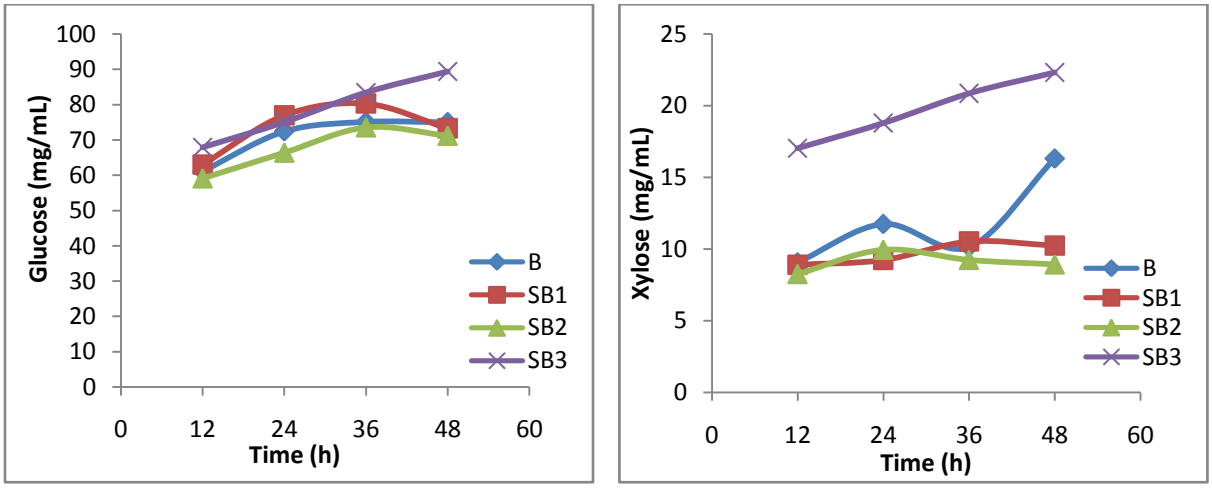

A) Glucose Release B) Xylose Release

Increasing the biomass loading to 17.5% resulted in a viscous slurry. This is particularly so in case of batch mode of operation. In case of SB1 and SB3, the slurry was less viscous. Highest viscosity was obtained for SB2 mode as the available free liquid is lesser at the initial time due to intermittent addition

of enzyme. The initial glucose production rates were similar for all modes, but after the completion of hydrolysis, SB3 yielded hydrolysate with 89.3 mg/mL glucose (Figure 5.6A). Lowest yield of 71.16 mg/mL was obtained with SB2 mode. Xylose production was also least with SB2 mode (Figure 5.6B).

5.3.2.1.7. Glucose and xylose yields with 20% biomass loading

The rate of glucose production was almost similar with 15%, 17.5% and 20% loading. At 20% biomass loading also, maximum glucose concentration obtained was only 95.6 mg/mL for SB3 mode and 94.4 mg/mL with SB1 mode as against a maximum glucose yield of 89.3 mg/mL with 17.5% loading. The glucose production profiles are as shown in Figure 5.7A. Xylose yields were similar for B, SB1 and SB2. Maximum xylose yield was obtained with SB3 mode. As with glucose production rate, xylose production rate was also similar over the loading range 15 – 20%. Maximum xylose obtained was 23.9 mg/mL (Figure 5.7B).

Figure 5.7: Sugar release at 20% biomass loading and under different modes of operation

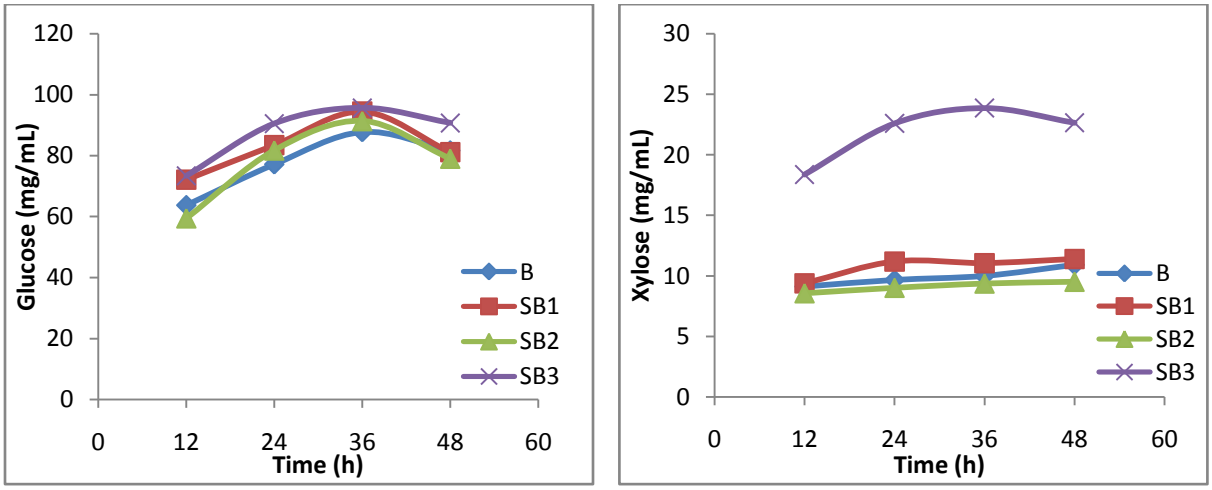

A) Glucose Release

B) Xylose Release

5.3.2.1.8. Glucose and xylose yields with 22.5% biomass loading

For 22.5% biomass loading, mixing efficiency was very low, especially for batch and SB2 mode. As a result, sugar release was also lower for these modes. As against 58.16 % glucose production efficiency in batch mode, 76.8% efficiency was obtained with SB2 mode. Maximum glucose release was 114.12 mg/mL for SB2 mode after 48 h hydrolysis (Figure 5.8A). Xylose release was similar for B, SB1, and

SB2 modes as in previous cases. Among B, SB1 and SB2 modes, maximum xylose yield was 13.29 mg/mL whereas, SB3 yielded 27.9 mg/mL xylose (Figure 5.8B).

Figure 5.8: Sugar release at 22.5% biomass loading and under different modes of operation

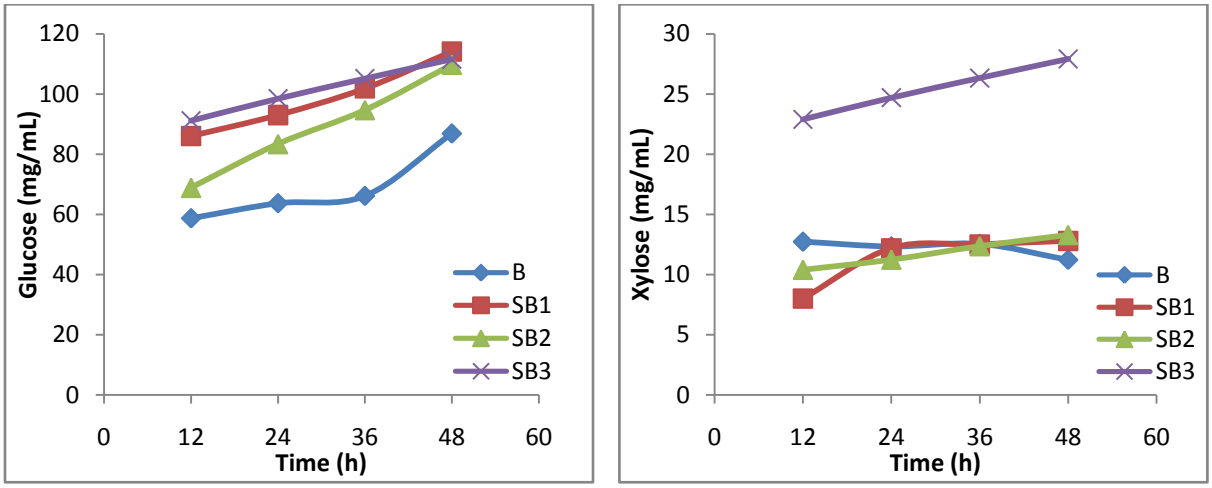

A) Glucose Release B) Xylose Release

5.3.2.1.9. Glucose and xylose yields with 25% biomass loading

Figure 5.9: Sugar release at 25% biomass loading and under different modes of operation

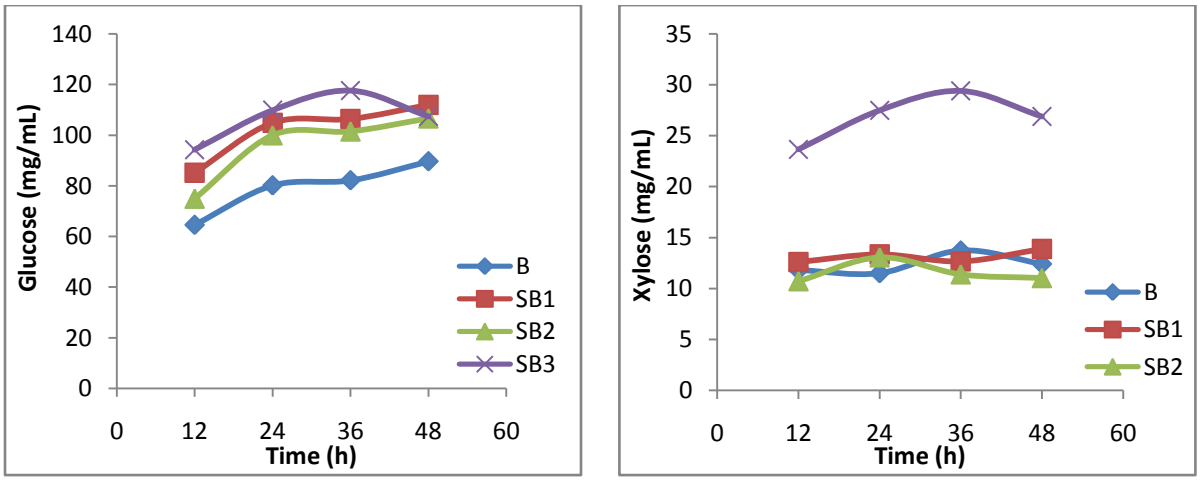

A) Glucose Release B) Xylose Release

Increasing the solids loading to 25% further reduced the efficiency of hydrolysis of batch mode. The 2.5 % increase in biomass loading, reduced glucose production efficiency to 53.9% from 58.16% in batch

mode. Even in SB3, a 4% reduction in efficiency was observed. Initial reaction rates are higher with SB3, and towards the end of hydrolysis a marginal dip in yield was observed for both glucose and xylose (Figure 5.9A and figure 5.9B). Maximum glucose release was 117. 6 mg/mL with SB3 mode after 36 h of hydrolysis. Xylose release was much higher with SB3 mode. Maximum xylose release was 29.4 mg/mL which was more than double of 13.90 mg/mL obtained with SB1 mode.

5.3.2.1.10. Glucose and xylose yields with 27.5% biomass loading

For biomass loading at 27.5%, the reaction mixture was very viscous and in certain cases, even sampling was hard. Free water availability for B and SB2 was very low. The rates of reaction and final yields for all the semi batch modes of operation were same for glucose production (Figure 5.10A). All the semi batch modes also yielded hydrolysate with more than 8% glucose. But due to lower free water, volume of hydrolysate was very low in all modes. Hence, even though concentration of hydrolysate is high, its volume is very low. This might limit the usage of such high loadings. Maximum glucose yield was 125.26 mg/mL with SB3 mode. For xylose yields, SB3 mode was the preferred one with maximum yield of 31.30 mg/mL (Figure 5.10B).

Figure 5.10: Sugar release at 27.5% biomass loading and under different modes of operation

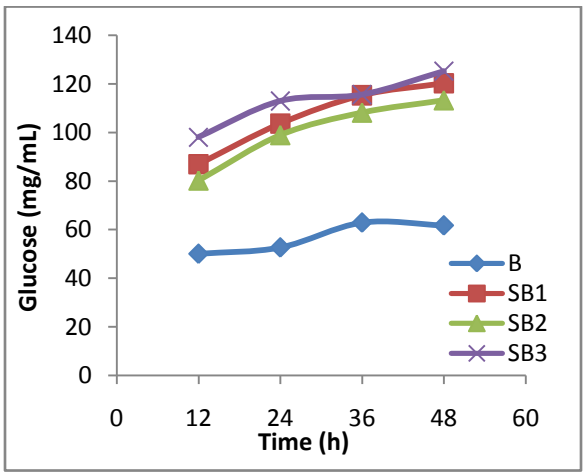

A) Glucose Release

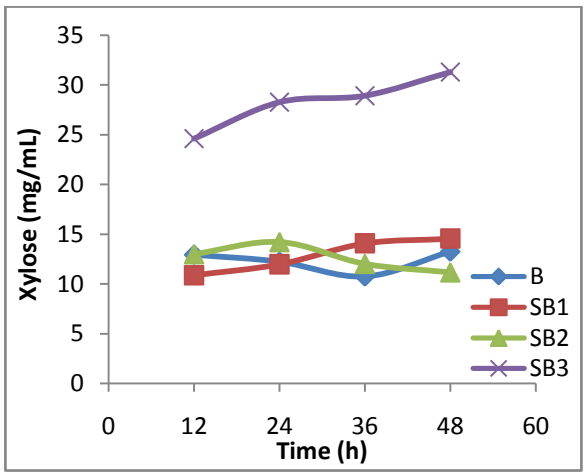

B) Xylose Release

5.3.2.1.11. Glucose and xylose yields with 30% biomass loading

At 30% loading also, free liquid in hydrolysis mixture was very low. This leads to sampling difficulties particularly for batch mode. Off the semi batch modes, SB1 and SB3 were found to yield higher glucose

than SB2. Maximum glucose obtained was 135.86 mg/mL with SB3 mode (Figure 5.11A). But the efficiency of sugar release was as low as 68.07% even with SB3 mode which was found to be the best mode for higher solids loading. Maximum xylose yield was 33.90 mg/mL with SB3 mode (Figure 5.11B).

Figure 5.11: Sugar release at 30% biomass loading and under different modes of operation

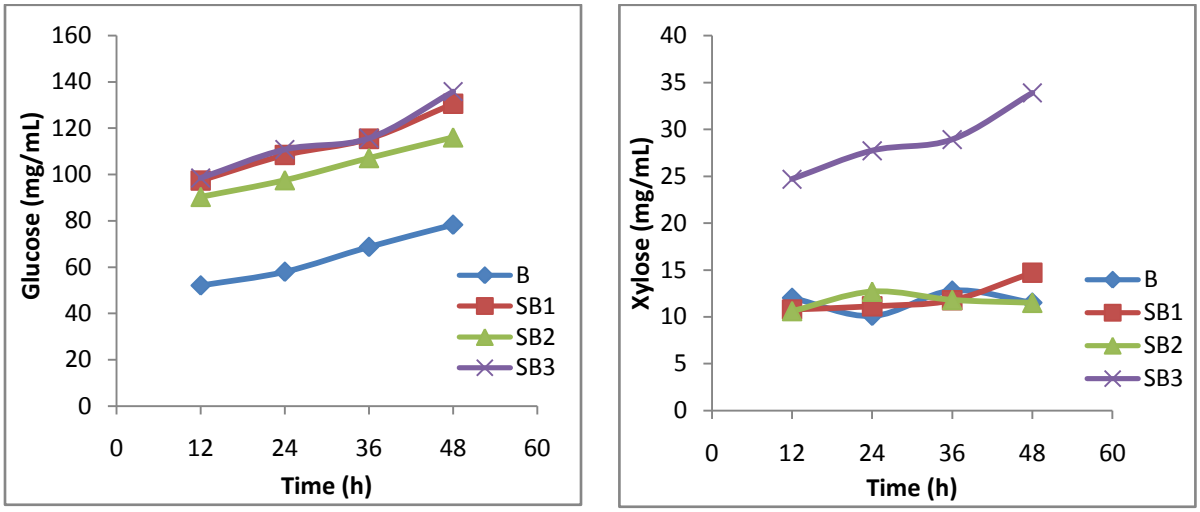

A) Glucose Release

B) Xylose Release

Cui et al., (2014) had developed a newer technology to enhance enzymatic saccharification of corn cob. These substrates were decrystallised using phosphoric acid which was then used for hydrolysis. For the fed batch operation, 2 feeding strategies were employed. One in which intermittent substrate feeding was employed (all enzymes added initially in reaction vessel), and the other in which intermittent addition of enzyme and biomass was followed. They reported that a solids loading of up to 30% could be attained with a glucose yield of 143.5 g/l in 2 h which is comparable with the 135.86 g/l glucose yield obtained under similar feeding strategy in this study. They proposed that intermittent enzyme and substrate feeding strategy could reduce the glucose inhibition and irreversible binding of enzyme to lignin. Hence, enzyme effectiveness increases which in turn increases the hydrolytic efficiency.

Morales-Rodríguez et al., (2010) developed a model for fed batch hydrolysis of pretreated corn stover. They used three control strategies namely, controlling solids loading alone, controlling solids with cellulose degrading enzymes and finally controlling solids loading with cellulose and cellobiose degrading enzymes. They found that the third strategy provided higher cellulose conversion and could also lead to reduced enzyme usage compared to batch process and hence the cost of overall hydrolysis could be improved, which is the main aim of fed batch hydrolysis. They could reduce about 10.7% of the enzymes used.

It has been reported that irrespective of feeding strategy, fed batch SSF significantly improves mixing in the reactor. This would eventually lead to lower energy consumption for mixing, which is one of the most crucial factors for an efficient and economical hydrolysis. Ethanol yield also increased from 9.5 g/L to 40 g/L while shifting from batch to fed batch mode (Koppram and Olsson, 2014). Fed batch strategy is also capable of handling larger solids loading than batch processes with the same reactor volumes. This will result in reduction in capital and operational costs due to reduction of equipment size and energy usage for heating, cooling and mixing (Roche et al., 2009b).

There are several reports which have evaluated the efficacy of feeding strategy on fed batch hydrolysis efficiency. SSF was used for 10% and 14% biomass loadings in both batch and fed batch mode. Mixing was found to be better in fed batch mode. Also, adding enzymes and substrate in intervals, pre mixed or otherwise was found to be superior to batch mode or fed batch operation with substrate feeding intermittently. Pre-mixing was better as hydrolysis would have been initiated before the mixture is introduced into the reactor. Intermittent addition of substrate has the advantage of higher mixing efficiency and lower insoluble load in the reactor at any given time. Intermittent enzyme and substrate addition has the advantage of lower enzyme inhibition due to accumulated products and lower inactivation of enzyme due to longer exposure to harsher conditions of hydrolysis. Batch process with 14% solids loading yielded about 52% (of theoretical yield) ethanol yield in comparison with 59% yield with fed batch strategy involving intermittent biomass and enzyme addition (Hoyer et al., 2010).

Several studies report the efficacy of intermittent substrate and enzyme feeding over substrate feeding alone. By using both substrates and enzyme feeding strategy, xylose conversion in simultaneous saccharification and co fermentation could be increased from 40% to 50% compared to substrate feeding alone. This feeding methodology could also enhance the solids loading to 11% (Olofsson et al., 2010). The maximum sugars reported here with 20% solids loading for batch hydrolysis was 80.78 g/L. Fed batch strategy with intermittent substrate addition enhanced the sugar release to 127 g/L (Gupta et al., 2012).

Batch and fed batch approach was evaluated for high solids loading simultaneous saccharification and fermentation (SSF) of steam pretreated spruce. The fed-batch SSF were initiated with slurry containing 6% solids loading. Batch additions for four times were performed during the first 24 h to reach final solids loading of 10%. It was found that both batch and fed – batch approach gave similar ethanol yields of 40 – 44 g/L except during the first 24 h when SSF yielded higher ethanol due to reduced cell inhibition (Rudolf et al., 2005).

5.3.2.2. Comparative yields of glucose with varying biomass loadings

5.3.2.2.1. Comparative yields of glucose with varying biomass loadings in batch mode of hydrolysis

It was observed that as the solid loading increased, hydrolytic efficiencies reduced (Figure 5.12). With 5% biomass loading, the highest cellulose conversion efficiency of 88.84% was obtained. Maximum glucose produced was 590 mg/g biomass. Consistent with previous results, 10% loading gave 80.12% cellulose conversion efficiency. But the advantage of increasing loading was obtaining a hydrolysate with very high concentrations of glucose so as to facilitate direct fermentation of hydrolysate without the need for a concentration step. But, even after increasing loadings to 30%, sugars above 8% (w/v) could be obtained in only very few loadings. It was found that for loadings above 17.5%, it was difficult to mix the biomass efficiently. For 17.5 – 20% loadings, even though the reaction mixture was initially a non moving solid, it became homogeneous slurry after 12 h of incubation. However, increasing the loadings further was a challenge for sampling as well. Free liquid was not available in 25 – 30% biomass loadings. So even though high amount of sugar is present in them, the volume of hydrolysate is very low. Hence, batch process may not be suitable for use with loadings higher than 17.5%. 20% biomass loading yielded glucose production efficiency of 65.96%. Increasing solids loading to 25% and 27.5% reduced cellulose production efficiency to 53.92% and 34.34% respectively.

Figure 5.12: Glucose yields at varying biomass loadings in batch mode of operation

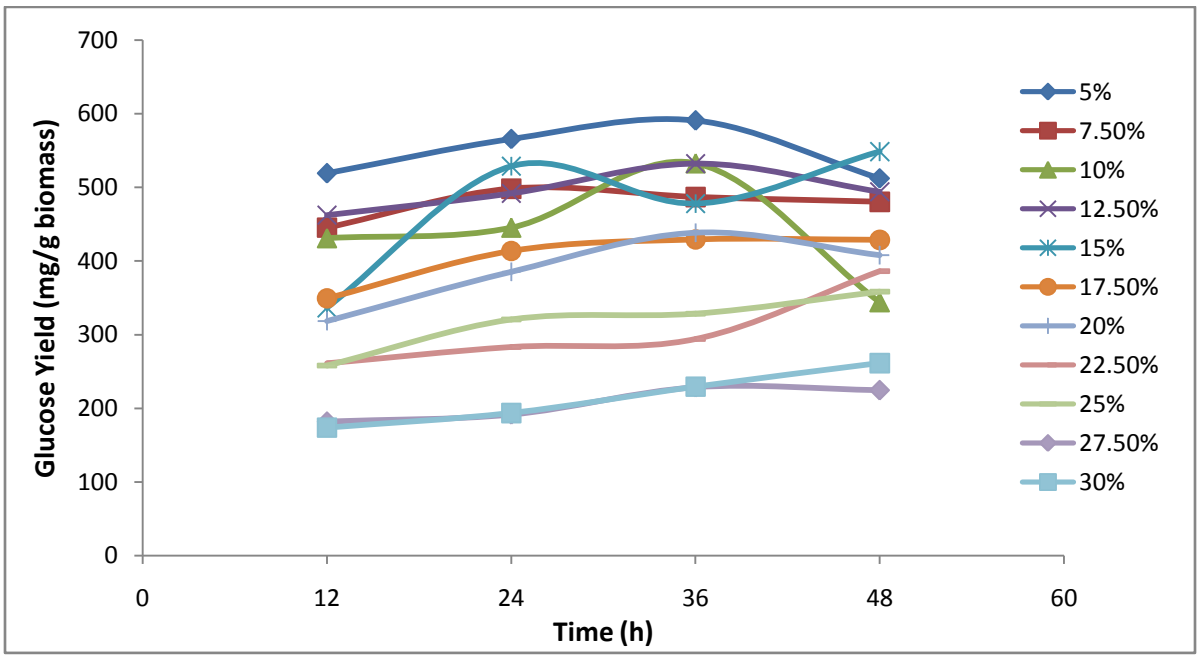

5.3.2.2.2. Comparative yields of glucose with varying biomass loadings in semi batch mode of hydrolysis with intermittent biomass loading

To overcome the deficiencies with batch mode of hydrolysis at higher solids loadings, semi batch modes were carried out. It was found that with intermittent biomass loadings, hydrolysis with higher solid loadings could be achieved. As with the batch mode, increasing the biomass loading resulted in a decreased overall hydrolytic efficiency (Figure 5.13). But on comparison with batch mode, SB1 mode gave higher efficiencies of glucose production for every biomass loading. Efficiency of glucose release with 5% solid loading was 94.42 % and 627 mg glucose was released with this loading. Even with 10% biomass loading, efficiency enhanced to 89.61%. Increasing biomass loadings beyond 15% yielded hydrolysate with sugar content higher than 80 mg/mL. The biggest advantage was that even at higher loadings above 20% and till 25%, mixing was efficient due to initial high free water availability. With each portion of biomass added, it was hydrolyzed to some degree before the next batch solids were loaded. Since, available enzyme in the reaction mixture was in excess, the added biomass was at least partially hydrolyzed before next addition, hence reducing the effective solid load in the mixture and improving overall mixing efficiency even at higher loadings. Even with 25% and 30% biomass loadings, 67.32% and 65.12% efficiency of glucose production could be attained. Hence this mode is suitable for very high solid loading hydrolysis reactions.

Figure 5.13: Glucose yields at varying biomass loadings in semi batch mode of operation with intermittent biomass addition

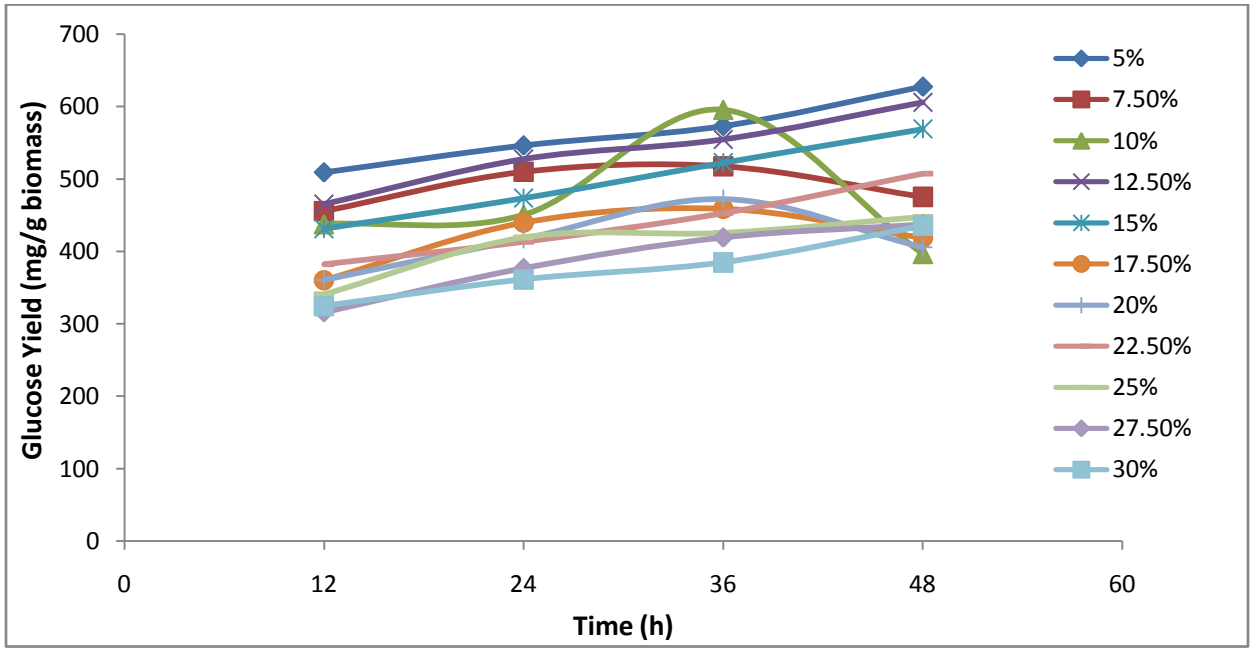

5.3.2.2.3. Comparative yields of glucose with varying biomass loadings in semi batch mode of hydrolysis with intermittent enzyme loading

Another semi batch mode of operation for enzymatic hydrolysis of biomass carried out was intermittent enzyme loading mode. Here, all the biomass was added at the beginning of the reaction and enzyme was added at intervals. This mode was also better in terms of hydrolysis efficiency than the batch mode, but was inferior to SB1 mode of operation. This mode could also be used when high solid loading hydrolysis is to be carried out. As evident from Figure 5.14, as biomass loadings increases, hydrolysis efficiency decreases. Efficiency of glucose release with 10% solid loading was 68.97% which was lower than that observed with batch or SB1 mode. Around 459 mg/g glucose was attained with this loading. In this case, increasing loadings beyond 20% yielded hydrolysate with glucose content higher than 8% (w/v). One disadvantage of SB2 mode was the lack of free water in higher loadings. As all the biomass was added initially and enzymes as batches, reaction mixture contained very low amounts of water and whatever liquid was available was imbibed by the biomass. This lead to an inefficient mixing and the mixture behaved like a solid during the initial duration of hydrolysis. For biomass loadings above 20%, this mode of operation is not feasible due to difficulty in mixing and lowers hydrolysate volumes even though the efficiencies are higher than batch mode. Even with 30% biomass loading, 58.28% efficiency of glucose production could be attained.

Figure 5.14: Glucose yields at varying biomass loadings in semi batch mode of operation with intermittent enzyme addition

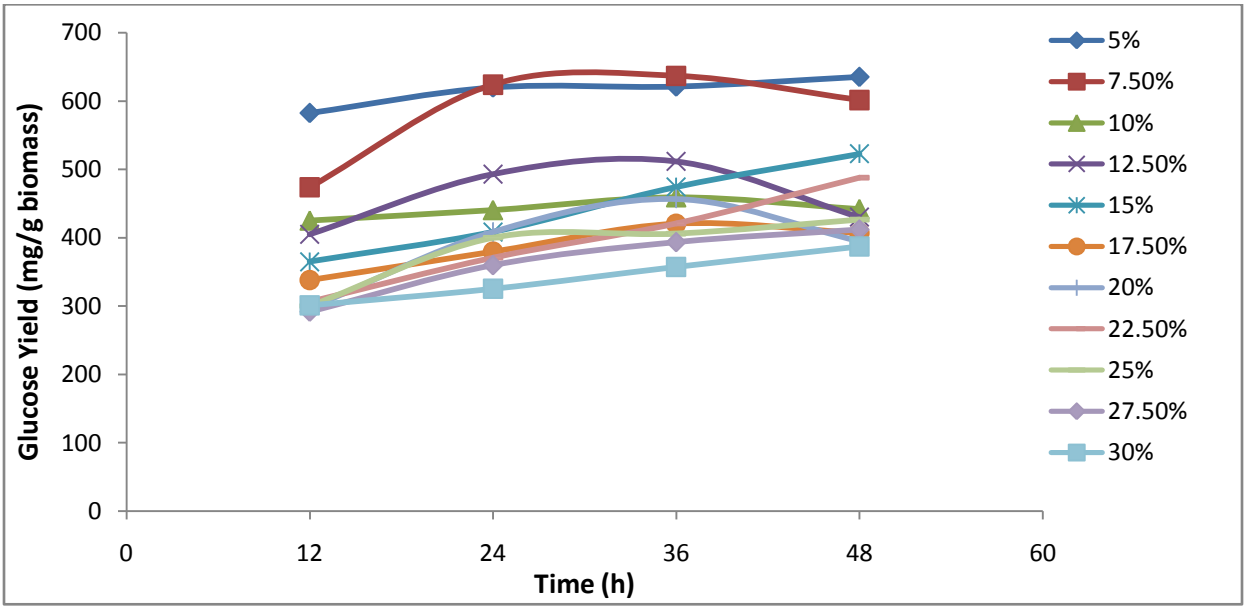

5.3.2.2.4. Comparative yields of glucose with varying biomass loadings in semi batch mode of hydrolysis with intermittent biomass and enzyme loading

Intermittent biomass and enzyme loading was found to be the best mode of hydrolysis operation for high solid loading hydrolysis. In this case, as against 5% loading, 7.5%, 10%, 12.5% and 15% loadings had higher reaction rates for glucose production (Figure 5.15). Conversion efficiency as high as 95.48% could be attained with 10% solids loading. The maximum glucose yield obtained was 637 mg for 7.5% solid loading. Beyond 15% solids loading, all mixtures gave hydrolysate with 80 mg/mL glucose. Even at loadings above 15%, mixing was not a challenge as batch wise addition of biomass and enzyme gave sufficient free liquid in the mixture. For every batch of biomass and enzyme added, biomass was partially hydrolyzed by the enzyme before the next batch of solids and enzyme were added. Hence, the accumulation of non hydrolyzed residue was lowered that could further aid in better mixing and hence better hydrolytic efficiencies. Even with higher loadings like 22.5 – 25%, biomass mixing was efficient and free water availability was not limiting. But for 30% loading, free water in the mixture was low and hence mixing was difficult. But, beyond 36 h of reaction time, mixing improved. Volume of hydrolysate also increased after 36 h of incubation. Hence, SB3 mode was found to be the best mode of operation for hydrolysis of high solid loading reactions.

Figure 5.15: Glucose yields at varying biomass loadings in semi batch mode of operation with intermittent biomass and enzyme addition

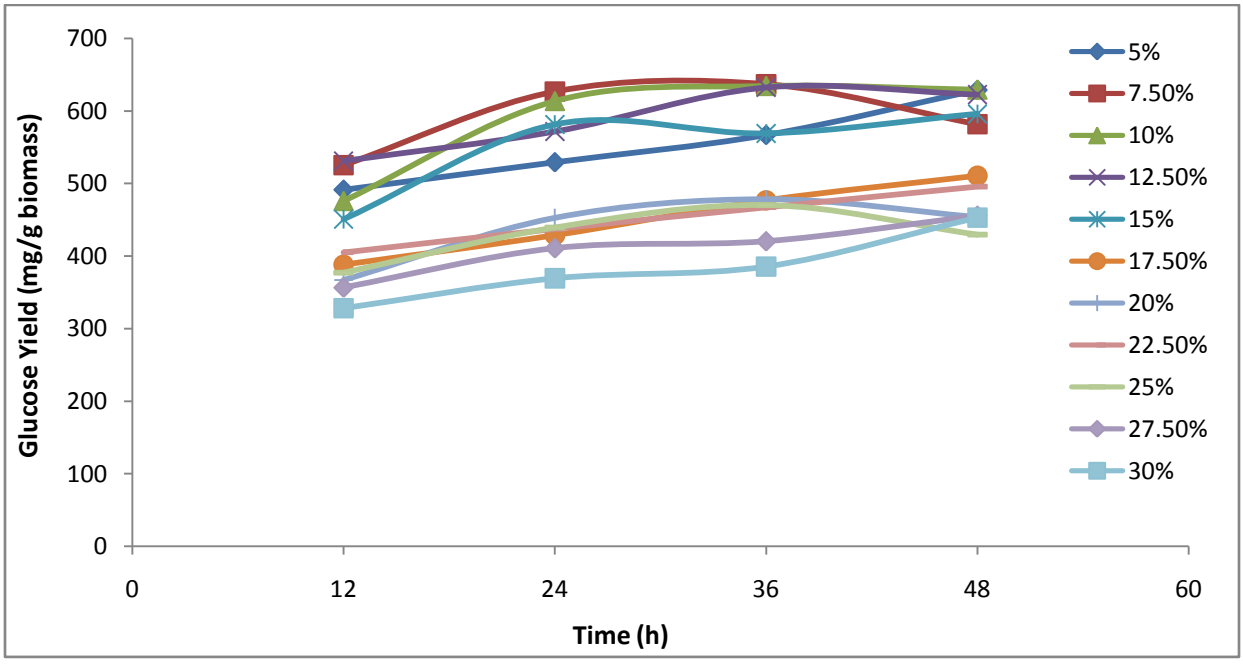

5.3.2.3. Comparative yields of xylose with varying biomass loadings

5.3.2.3.1. Comparative yields of xylose with varying biomass loadings in batch mode of hydrolysis

Xylose production efficiencies were much lower than glucose release efficiencies. Maximum efficiency obtained was 83.29% xylose yield at 5% solid loading (Figure 5.16). At 5% loading, 151 mg/g xylose was produced after 24 h of hydrolysis. A reduction in xylose yields was observed after 24 – 36 h of hydrolysis due to adsorption on residual biomass. As with glucose production in batch mode, xylose production also decreased with increasing biomass loadings. Hydrolytic efficiency was only 23.33% for xylose production at 30% biomass loadings. At 10% solid loading, efficiency of hemicellulose degradation was 69. 44%. Lower yields at higher loadings maybe due to inefficient mixing and mass transfer.

Figure 5.16: Xylose yields at varying biomass loadings in batch mode of operation

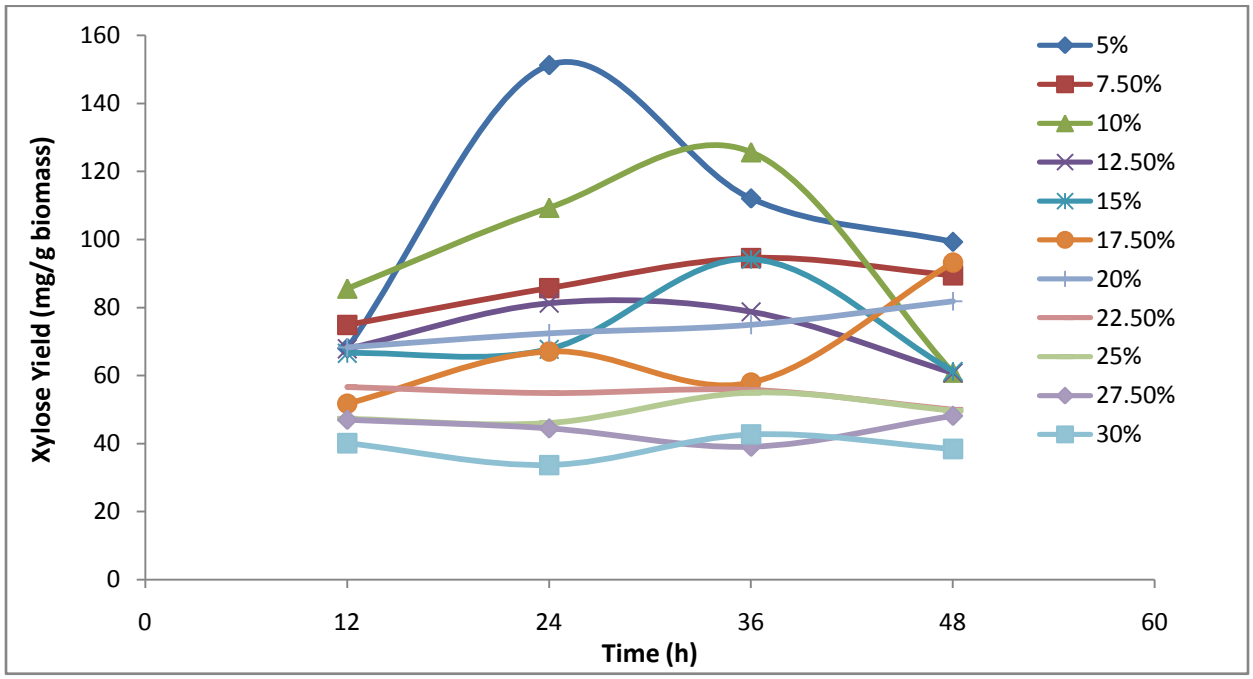

5.3.2.3.2. Comparative yields of xylose with varying biomass loadings in semi batch mode of hydrolysis with intermittent biomass loading

In semi batch mode of hydrolysis with intermittent biomass addition, 10% biomass loading yielded higher xylose than 5 % as against the batch mode. Maximum xylose produced was 97.5 mg/g biomass and the efficiency of production was 54.44 % with 10% loading (Figure 5.17). Batch mode gave higher efficiencies with loadings up to 20%. Beyond this loading SB1 was found to yield higher xylose. Xylose

production was observed to decrease with higher biomass loadings. Hemicellulose hydrolytic efficiency of 27. 22% was observed with 30% biomass loading which was higher than that obtained for the same loading in batch mode. Above 15% solid loading, more than 10 mg/mL xylose production was consistently observed.

Figure 5.17: Xylose yields at varying biomass loadings in semi batch mode of operation with intermittent biomass addition

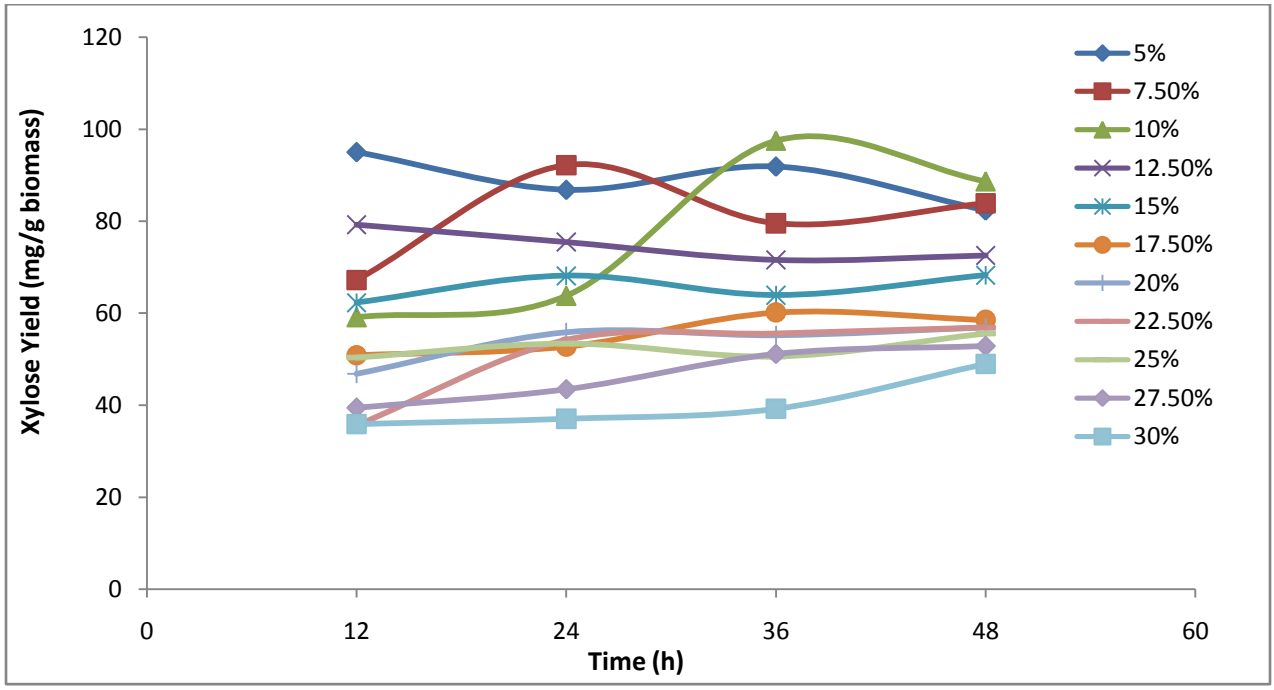

5.3.2.3.3. Comparative yields of xylose with varying biomass loadings in semi batch mode of hydrolysis with intermittent enzyme loading

Hydrolysis with intermittent enzyme loading yielded very low xylose production efficiencies. Maximum xylose yield of 90.3 mg/g biomass was obtained with hydrolysis at 5% loading. Efficiency of hemicellulose hydrolysis here was 50.17% (Figure 5.18). Progressive reductions in efficiencies were observed with increase in biomass loadings. A xylose production efficiency of 23.33% was observed with 30% biomass loading. As in previous cases, increasing biomass loadings gave decreased xylose yields. At 10% solid loading, efficiency of hemicellulose degradation was only 43.89. Loadings above 22.5% resulted in hydrolysate with more than 10 mg/mL xylose.

Figure 5.18: Xylose yields at varying biomass loadings in semi batch mode of operation with intermittent enzyme addition

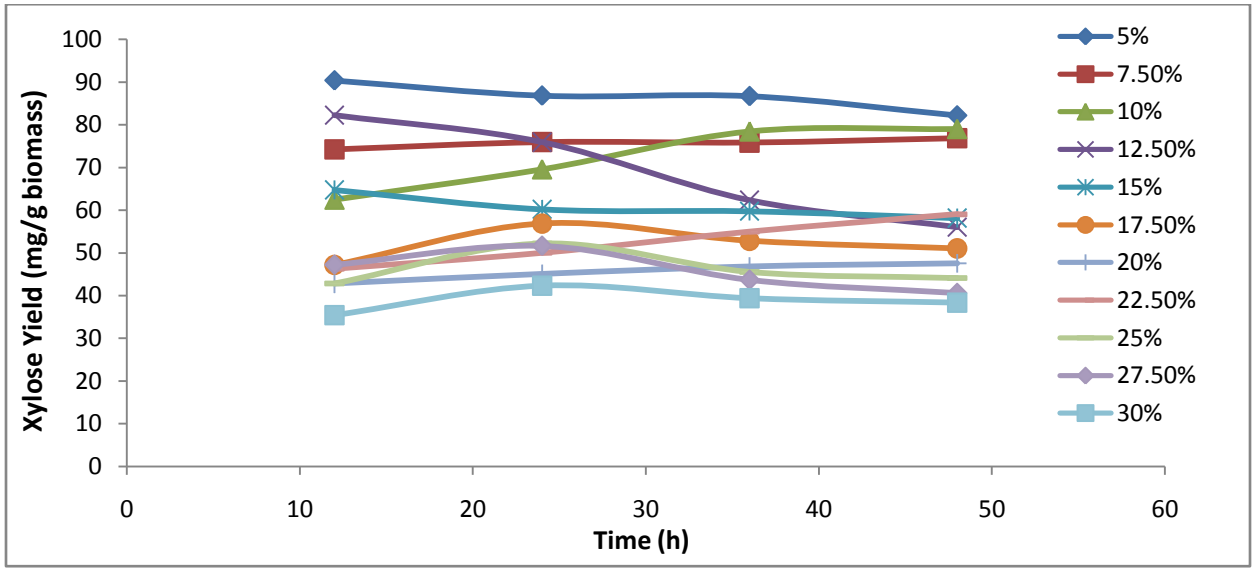

5.3.2.3.4. Comparative yields of xylose with varying biomass loadings in semi batch mode of hydrolysis with intermittent biomass and enzyme loading

Figure 5.19: Xylose yields at varying biomass loadings in semi batch mode of operation with intermittent biomass and enzyme addition

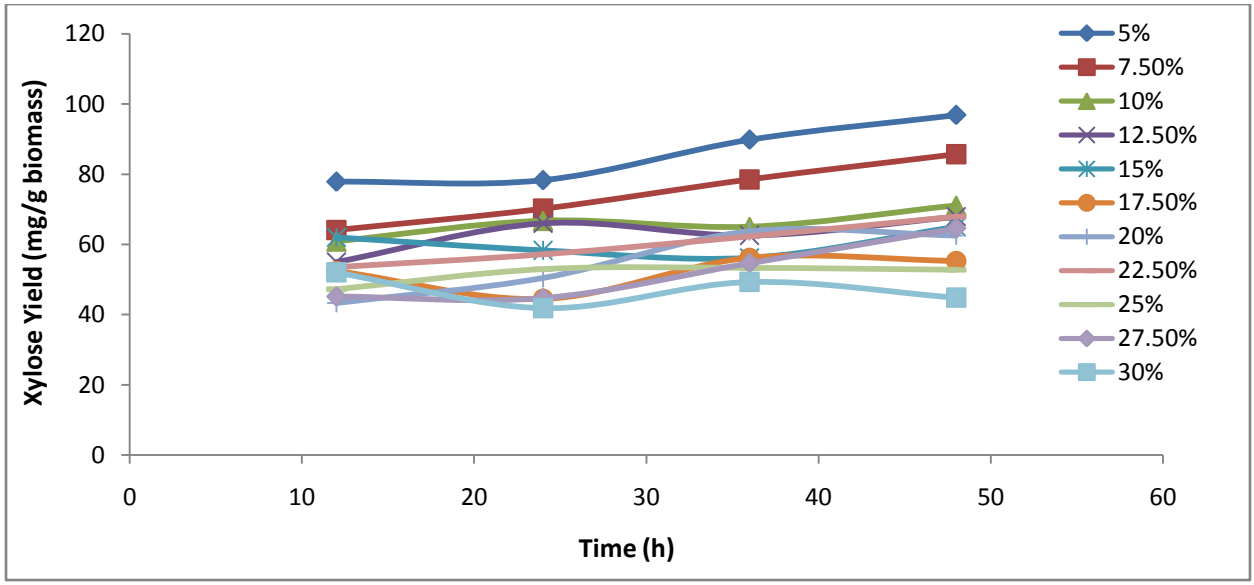

Intermittent biomass and enzyme loading lead to highest xylose concentrations in the hydrolysate. Maximum efficiency of 53.89% for xylose production was observed with 5% biomass loading. Maximum yield was 96 mg xylose/g biomass at 5% biomass loading (Figure 5.19). At 10% loading, maximum

xylose yield was 71 mg/mL after 48 h of reaction. As in previous cases, lower loadings resulted in higher hydrolytic efficiency. Hydrolytic efficiency was only 28.89% for xylose production at 30% biomass loading. In contrast to other modes of operation, solid loadings from 7.5% onwards yielded hydrolysate with over 10 mg/mL xylose. With 30% loading, 33.90 mg/mL xylose was achieved after 48 h of hydrolysis.

Increase in biomass loadings lead to decrease in the efficiencies of enzymatic hydrolysis of lignocellulosic biomass. This might be due to reduced mass transfer of cellulase enzymes due to highly viscous biomass slurry and also due to inhibitory effect of the sugars formed. Inefficient heat transfer is also a result of high biomass loadings that hamper efficiency of saccharification. Another problem encountered with high solid loading enzymatic hydrolysis is the absorption and retention of hydrolysate by non hydrolyzed biomass that reduces the available volume of hydrolysate and hence reduces the productivity of hydrolysis process (Ioelovich and Morag, 2012). A high substrate loading during enzymatic hydrolysis increases the concentration of inhibitory compounds (Kristensen et al., 2009b). Due to these factors, increased substrate loadings during enzymatic hydrolysis lowered the efficiency for conversion of biomass to fermentable sugars (Jorgensen et al., 2007a; Hodge et al., 2008).

Hydrolysis of biomass at higher loadings (10 – 40% loading) results in changes in volume and density. Hence determining hydrolytic efficiencies based on sugar concentration in hydrolysate and using assumed initial reaction volume leads to over estimation of the efficiency. Therefore, estimating amount of insoluble solids in hydrolysate, sugar concentration and specific gravity of hydrolysate can be used to determine the efficiency of conversion accurately (Kristensen et al., 2009b).

Hodge et al., (2006) developed a model to optimize high solids loading of hydrolysis in stirred tank reactor with solid loadings greater than 15%. The model was developed to consider the effect of feeding a stream of pretreated corn stover and enzymes for a fed batch approach. Thus, an open loop control feeding profile that controls the solid loadings and enzymes at a manageable level was devised. This would lead to easily manageable slurries during hydrolysis reactions.

Several studies have been carried out to study the effect of high solids loading on enzymatic hydrolysis of biomass. High solids loading reduced the efficiency of enzymatic hydrolysis of lignocellulosic biomass. Hodge et al., (2008) proposed that mass transfer limitations are not a challenge till 20% solids loading (w/w) which indicates that inhibition at loadings below this level are due to soluble components like inhibitors (HMF, acetic acid, furfurals etc). Haykir and Bakir (2013) observed that glucose release efficiency decreased from 67% to 55% when substrate loading was increased from 3% to 15% (w/v) for alkali pretreated cotton stalk.

A new impeller was designed to fit in a stirred tank reactor to efficiently hydrolyze reaction mixtures containing high solids loading that can yield hydrolysate with > 100 g glucose/kg biomass.

The reactor contained a segmented helical stirrer which could efficiently mix highly viscous mixtures. Hydrolysis in this reactor was more efficient than hydrolysis in shake flasks. Using the reactor, alkali pretreated wheat straw could be hydrolyzed to yield 110 g glucose/kg biomass at conversion efficiency of 76% and biomass loading of 20% after 48 h. Organosolv-pretreated beech wood could be efficiently hydrolyzed even at 30% biomass loading with an efficiency of 72% (Ludwig et al., 2014).

With a baffled rushton impeller, higher hydrolysis efficiencies were reported compared to baffled marine impeller at high solids loadings. The digestibility reduced from 50.7% to 29.4% after 96 h of hydrolysis when solid loading was increased from 10 to 20% (w/v) (Byung – Hwan and Hanley, 2008).

On the other hand, similar cellulose conversion efficiencies for increasing solid loadings were reported by Liu et al., (2012). They reported that after 96 h of incubation, hydrolysis with 10, 15, 20, 25 and 30% solids loading yielded 75.6, 75, 74.2, 73.7 and 72.5% conversion efficiency. Final ethanol concentration increased by 195% when biomass loading was increased from 10 to 30%.

5.4. Conclusions

High solid loading enzymatic hydrolysis is essential to attain efficient saccharification that would yield a concentrated hydrolysate with high glucose content so that this unit operation is made economical. From the results of the present study, it can be concluded that at high biomass loadings (>15- 17.5%), batch hydrolysis is inefficient due to mass transfer constrains. At loadings around 5 – 15%, both batch and semi batch modes of hydrolysis yield relatively similar yields. For loadings greater than 17.5%, semi batch modes are optimum. Off the three semi batch feeding strategies tried, intermittent biomass and enzyme addition strategy was found to be optimum due to the better mixing efficiencies possible and higher glucose concentrations achievable. In this approach, hydrolysate with >8% (w/v) glucose concentration could be achieved above 15% biomass loading, which can be directly used for fermentation. This leads to reduction in energy needed for concentration step which reduces the overall hydrolysis cost. For biomass loadings higher than 25%, mixing is a challenge and hence very low cellulose conversion efficiencies were obtained. Maximum glucose concentration achieved was 136mg/mL with 30% loading and 48 h incubation.

Chapter 6
Enzyme recycling in biomass hydrolysis by use of magnetic nanoparticle immobilized *β*- glucosidase

6.1. Introduction

One of the main obstacles in making the bioprocess for conversion of lignocellulosic biomass to bioethanol economically viable is the cost of the enzymes used for biomass hydrolysis (Alfren and Hobley, 2014). Inhibitory effects of glucose and cellobiose on the biomass hydrolyzing enzymes are the major factors contributing to the high consumption of enzymes which leads to higher ethanol production costs. This is a critical issue when operations with higher substrate loadings are carried out, which leads to higher product inhibition (Lee et al., 2010). Most commercial cellulases are produced by filamentous fungi, especially *Trichoderma reesei* strains that suffer the disadvantage of having very low titers of β-glucosidase (BGL) which is not sufficient for an efficient biomass hydrolysis (Lynd et al., 2002). Hence, for optimizing hydrolysis conditions, these cellulase preparations are often supplemented with extraneous BGL. Cost of adding such accessory enzymes limit the applications of such strategies. A practical approach to this problem would be to immobilize the enzyme so as to facilitate easy recovery and reuse of the enzyme which could compensate the cost of BGL supplementation.

Type of immobilization is the most critical factor affecting enzyme stability. The technique of immobilization may be by binding to a support (carrier), entrapment (encapsulation) and cross linking. The choice of immobilization method depends on the enzyme, support, chemical reagents and reactor (Gargouri et al., 2004). Binding to the support can either be by physical means that include hydrophobic or van der Waals interactions or by ionic or covalent bond formation. Physical means of immobilization enhances the flexibility of the system, but it is not industrially applicable due to the possible detachment of enzymes under change in ionic strength and pH. Covalent binding is a sturdy immobilization technique as it prevents leaching of enzymes and yields a derivative with greater stability. The main drawback of this technique is the increased probability of enzyme deactivation. Entrapment of enzyme in polymer networks or microcapsules is used for industrial purposes – eg. in hollow fiber reactors. Cross linking of enzymes using bifunctional reagents offers highly concentrated enzyme activity, high stability and low production cost owing to exclusion of carriers (Sheldon 2007). Other techniques include formation of enzyme aggregates, affinity binding on ligand etc. Hence, identification of an ideal immobilization system for BGL is important for achieving the desired characteristics for biomass conversion.

During the last decade, the field of nano-biocatalysis has established its potentials and effective enzyme immobilization with high enzyme loading and activity have been achieved using nanostructured materials such as nano porous media, nanofibers, nanotubes and nanoparticles (Kim et al., 2006; Kim et al., 2008). These nanomaterials offers several advantages like high surface area that leads to high enzyme loading and thus, high enzyme activity per unit mass or volume of the carrier. In most of the cases of immobilization on nanomaterials, an increase in enzyme activity due to enhanced enzyme stability was reported (Kim et al., 2007). Nanoparticles are defined as particulate dispersions or solid particles with a size in the range of 10-1000 nm (Mohanraj and Chen, 2006). A number of inorganic carriers can be used for enzyme immobilization like alumina, silica and zeolites. The bottleneck in this technology is to design immobilization of enzyme in such a way so as to facilitate easy separation of immobilized nanoparticle for easy recycling.

Magnetic nanoparticles (MNPs) based immobilization leads to easy recovery of enzymes under strong magnetic fields even from viscous reactants/products and these can be reused in subsequent hydrolysis reactions. When the magnetic field is turned off, these particles behave like non-magnetic particles as they have no magnetic memory. So they re-disperse in the medium and can be used for multiple cycles of separation and re-dispersion (Franzreb et al., 2006). Figure 6.1 gives the schematic representation of hydrolysis of cellulose using immobilized enzyme and its recycling. Magnetic nanoparticles have been synthesized with different compositions and phases, including iron oxides, such as Fe_3O_4 and γ-Fe_2O_3, pure metals, such as Fe and Co, spinel-type ferromagnets such as $MgFe_2O_4$, $MnFe_2O_4$ and $CoFe_2O_4$, as well as alloys such as $CoPt_3$ and FePt. The common methods of synthesis employed include co-precipitation, thermal decomposition and/or reduction, micelle synthesis, hydrothermal synthesis and laser pyrolysis techniques (Lu et al., 2007).

In the present study, an attempt was made to prepare magnetic nanoparticles and to improve its stability by silica coating. Crude β-glucosidase from *Aspergillus niger* was covalently immobilized onto non-porous magnetic nanoparticles. The possibility of using immobilized beta glucosidases for hydrolyzing rice straw, its recovery using magnetic field and reusability was examined.

Figure 6.1: Schematic presentation of hydrolysis of cellulose and enzyme recycling using BGL immobilized on magnetic nanoparticles

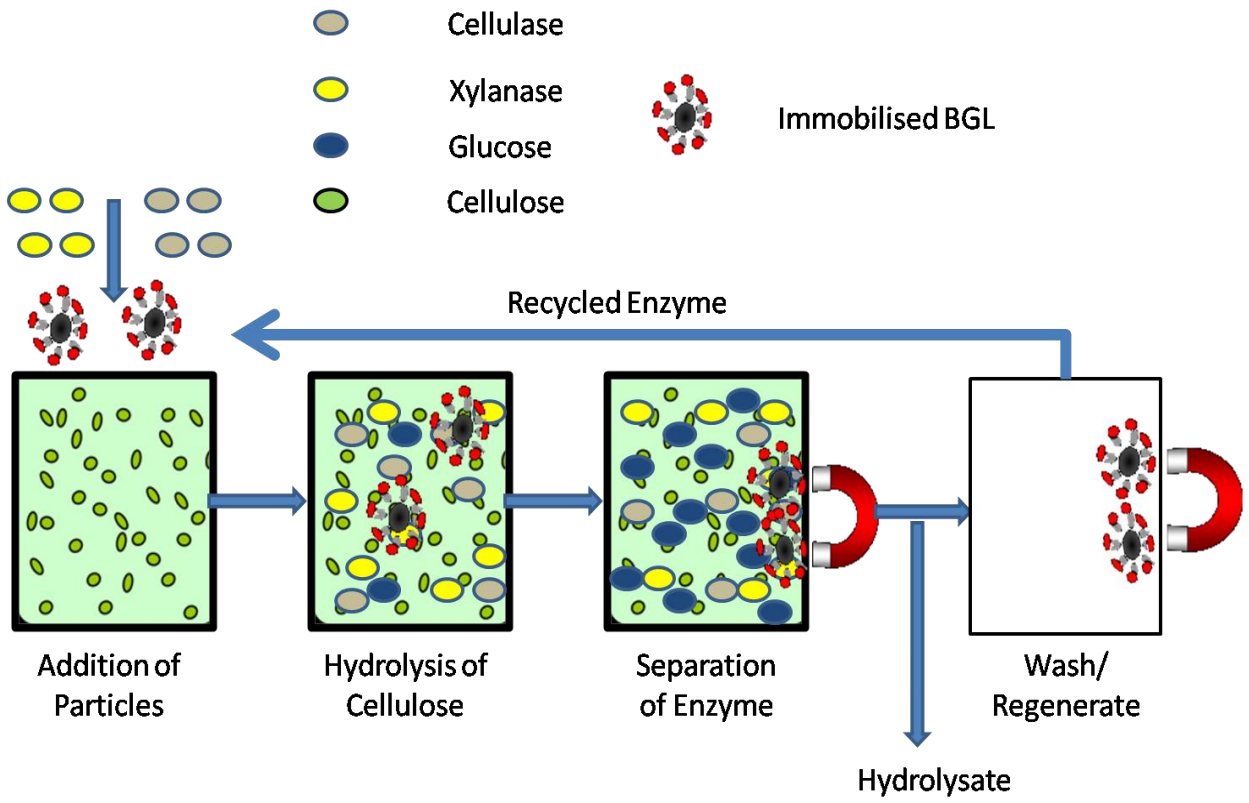

6.2. Materials and Methods

6.2.1. Synthesis of magnetic nanoparticles

Magnetic nanoparticles were synthesized by a modified protocol of Berger et al., (1999). Stock solutions of 2 M $FeCl_2.4H_2O$ and 1 M $FeCl_3.6H_2O$ prepared in 2 M HCl were mixed in the ratio 1:4 respectively and 0.7 M aqueous ammonia solution was added drop wise into the solution with constant stirring in a nitrogen atmosphere. Once a black precipitate of magnetite (Fe_3O_4) was formed, stirring was stopped and the precipitate was allowed to settle. Supernatant was decanted and rest of the suspension was centrifuged at 4000 rpm for 5 minutes. Supernatant was discarded to obtain the dark sludge like magnetite. Magnetite was washed thrice with distilled water and recovered as pellet after centrifugation (2000 rpm, 5 minutes). The pellet was then dried at 50 °C overnight and stored until used.

6.2.2. Silica coating of magnetic nanoparticles

For enhancing the stability of magnetic nanoparticles, silica coating was performed as per modified protocol of Bo et al., (2008). Sodium silicate (10.98 g) was dissolved in deionized water and the pH of the solution was adjusted to 12.5 by addition of 2 M HCl. Magnetic nanoparticles (0.5 g) prepared as outlined in section 6.2.1 were then added to this solution and subjected to ultrasonication for 30 minutes. HCl (2 M) was then added drop wise in to the solution with continuous stirring in a magnetic stirrer at 60 °C under nitrogen atmosphere so as to attain a pH of 6-7 in a time span of 3 h. The precipitate was then washed several times with deionized water and recovered as pellet by centrifugation at 2000 rpm for 5 minutes. The precipitate was then dried at 50 °C overnight.

6.2.3. Functionalisation of magnetic nanoparticles

Functionalisation of magnetic nanoparticles was performed using 3-amino propyl –triethoxysilane (APTES) as per the protocol of Can et al., (2009). Eight hundred and forty five milligrams of silica coated magnetic nanoparticles were sonicated in 50 mL 50% ethanol for 30 minutes using a 10 s on/off cycle. To this suspension, 3.405 mL of APTES was added and the solution was stirred at 40 °C under N_2 atmosphere for 2 h. The suspension was then cooled to room temperature and the APTES modified nanoparticles were collected by centrifugation at 2000 rpm for 5 minutes. The pellet was then washed thrice with deionized water and dried at 50 °C.

6.2.4. Immobilization of β-glucosidase

Immobilization protocol as outlined by Can et al., (2009) was used with minor modifications. 1.53 g of functionalized silica coated nanoparticles was dispersed in 60 mL 5% glutaraldehyde. The suspension was kept overnight with stirring at 4 °C. The nanoparticles were recovered using a magnet and washed thrice with deionized water. To this, β-glucosidase equivalent to 500 IU in citrate buffer (pH 4.8, 0.05 M) was added and incubated at 4 °C for 5 h with mild agitation. After incubation, the nanoparticles were separated by a magnet and washed thrice with citrate buffer (pH 4.8, 0.05 M). The immobilized nanoparticles were stored at 4 °C in citrate buffer (pH 4.8, 0.05 M). The particles were diluted and β-glucosidase activity was determined as outlined in section 2.4.4.

6.2.5. Thermogravimetric analysis of MNPs

Thermogravimetric analysis was carried out on MNPs dried at 70 °C in a differential thermal analyzer, STA6000 (Perkin Elmer, Netherlands) in flowing oxygen using a heating rate of 10 °C/min in the temperature range 33–1000 °C and the corresponding weight loss was determined.

6.2.6. Analysis of magnetic nanoparticles by Scanning Electron Microscopy (SEM)

The nanoparticles were spread on clean cover slips and dried at 50 °C for 16 h. The samples were then coated with gold palladium and observed using a voltage of 10 to 15 KV using scanning electron microscope (JEOL JSM-5600 SEM).

6.2.7. Analysis of magnetic nanoparticles by Atomic Force Microscopy (AFM)

To study the size and surface morphology of nanoparticles, atomic force microscopy was employed using NTEGRA (NT-MDT) operating with a use tapping mode regime. The nanoparticles were filtered through 0.22 µm filter and the filtrate was serially diluted to 10^{-3} dilutions. 100 µl of the 10^{-3} dilution were spread across clean cover slips and were dried at 50 °C for 16 h. The samples were then analyzed using atomic force microscope. Micro-fabricated TiN cantilever tips (NSG10) with a resonance frequency of 299 kHz and a spring constant of 20–80 Nm^{-1} were used.

6.2.8. Analysis of magnetic nanoparticles by Dynamic Light Scattering Spectrophotometry (DLS)

Suspension of MNPs, silica coated MNPs (Si-MNP), Si-APTES-modified MNPs (Si-APTES-MNP), glutaraldehyde linked Si-APTES-MNP and enzyme immobilized MNP in deionized water were filtered through 0.22 µ filter. The size of nanoparticles was analyzed using Zeta Potential Analyzer (Malvern Instruments). The suspension was poured into a plastic cuvette and the light scattering of nanoparticles were measured against distilled water as blank.

6.2.9. Analysis of MNPs by X-ray Diffractometry

The X-ray diffractogram which indicates the composition, lattice structure and crystallinity of MNPs was analysed in a PANalytical (Netherlands), X- pert pro diffractometer system, operated at 40 KV, 30 mA; radiation was Cu Kα (λ= 1.54 Å) and grade range between 10 to 90° with a step size of 0.03°.

Measurements were made in transmission mode. Structure refinement of the XRD data was performed by X'Pert High Score Plus software.

6.2.10. Analysis of MNPs by Fourier Transform Infrared Spectroscopy

Fourier Transform Infrared (FT-IR) spectroscopic analysis was carried out to detect changes in functional groups present on the MNPs due to various modifications. FT-IR spectrum was recorded between 4000 - 400 cm^{-1} using a Shimadzu IR Spectrometer with detector at 4 cm^{-1} resolution and 25 scans per sample. Discs were prepared by mixing 3 mg of dried sample with 300 mg of KBr (Spectroscopic grade) in an agate mortar. The resulting mixture was then pressed at 10 MPa for 3 minutes. And this sample was used for IR spectrum recording.

6.2.11. Lignocellulosic biomass hydrolysis using MNP immobilized BGL

Enzymatic hydrolysis was carried out as mentioned in section 2.3 with 10 FPU/g cellulase, 7500 U/g xylanase and 5 IU/g BGL. Instead of the free BGL, reaction mixture was supplemented with MNP immobilized BGL. Experiments were also conducted with higher units of BGL (30 and 60 IU/g) to determine the effect of high BGL loadings. The immobilized enzyme was recovered using a strong magnet, washed with citrate buffer (pH 4.8, 0.05 M) and reused in subsequent reactions.

6.3. Results and Discussion

6.3.1. Synthesis of magnetic nanoparticles

Magnetic nanoparticles (Magnetite-Fe_3O_4) were synthesized by co-precipitating $FeCl_2$ and $FeCl_3$ in presence of ammonia.

$$2FeCl_3 + FeCl_2 + 8NH_3 + 4H_2O \rightarrow Fe_3O_4 + 8NH_4Cl$$

The nanoparticles which appeared as black precipitate were washed with deionized water, dried at 50 °C and were stored in an air tight container. The magnetic nature of the particles was ascertained by their movement under an external magnetic field (Figure 6.2). Magnetic nanoparticles are very sensitive to presence of oxygen in air. In certain cases, these particles undergo oxidation or phase transition and form maghemite, γ-Fe_2O_3 or hematite which has lesser magnetic properties compared to magnetite. Thus the process was done in nitrogen atmosphere to yield magnetite (Mashhadizadeh and Amoli-Diva, 2012).

Figure 6.2: Spiking effect of magnetic nanoparticles under the influence of an external magnetic field.

Thermogravimetric analyses indicated that the magnetite nanoparticles were stable and the weight loss was only 14.3% after heating up to 999 °C in oxygen atmosphere which indicated that no hydroxides or precursors were left in the reaction. There is a small mass loss up to 200 °C. This might be due to loss of water molecules and CO_2.

Figure 6.3.: Thermogravimetric Analysis of MNP

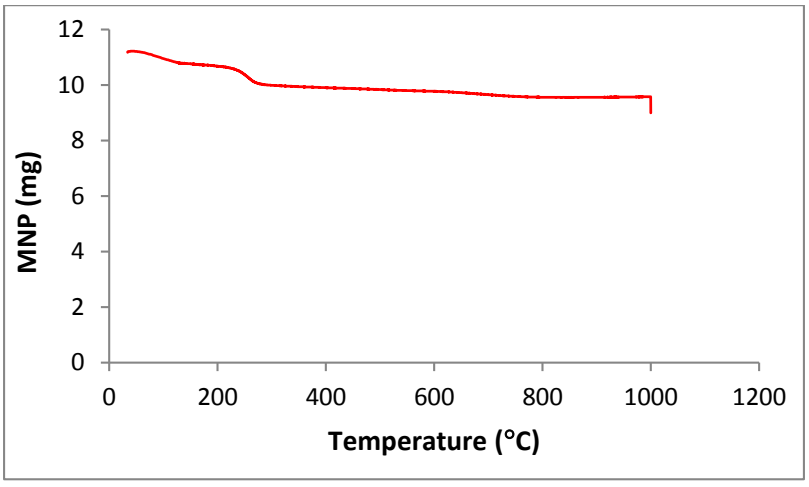

Similar results were obtained by Chen et al., (2012) who found that magnetic nanoparticles show an initial small mass loss at temperatures below 200 °C due to desorption of adsorbed water and CO_2. At temperatures above 200 °C, they observed negligible weight loss for Fe_4O_4-MNP. Heating beyond 999.8 °C leads to a rapid reduction in residual MNP mass. This might be due to disintegration of the compound

(Figure 6.3). On the other hand, Zhang et al., (2014a) observed that Fe_3O_4 was thermally stable, and there was no obvious weight loss over the entire testing temperature range of 0 – 800 °C.

SEM analysis of magnetic nanoparticles revealed that the preparation contained mostly spherical particles. Presence of irregular shaped particles with uneven margins was also observed (Figure 6.4). The size, shape and composition of magnetic nanoparticles depend on the Fe_2^+/Fe_3^+ ratio, type of salt, reaction temperature, pH and ionic strength of the media (Lu et al., 2007).

Figure 6.4: SEM image of magnetic nanoparticles

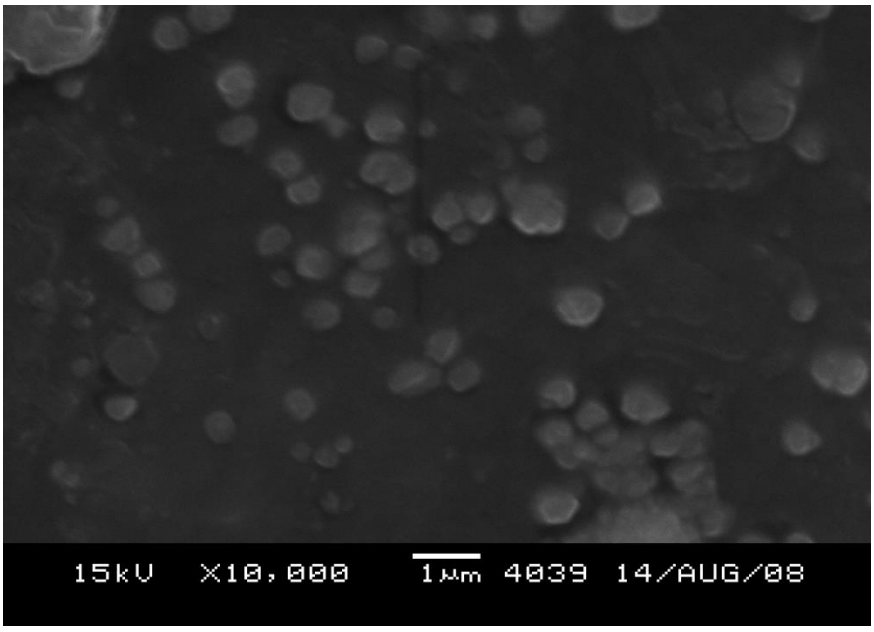

Atomic force microscope is a scanning probe microscope used to image and measure the properties of material, chemical and biological surfaces. AFM is capable of performing spectroscopic analyses and can make measurements of biological samples in physiological conditions (Bustamante et al., 1997). It can probe the sample and make measurements in three dimensions enabling the presentation of 3-dimensional image of the sample surface (Blanchard, 1996). The AFM images of magnetic particles synthesized in the present study confirmed their nanoscale size (Figure 6.5).

Figure 6.5: Surface morphology of magnetic nanoparticles with corresponding 3D size range

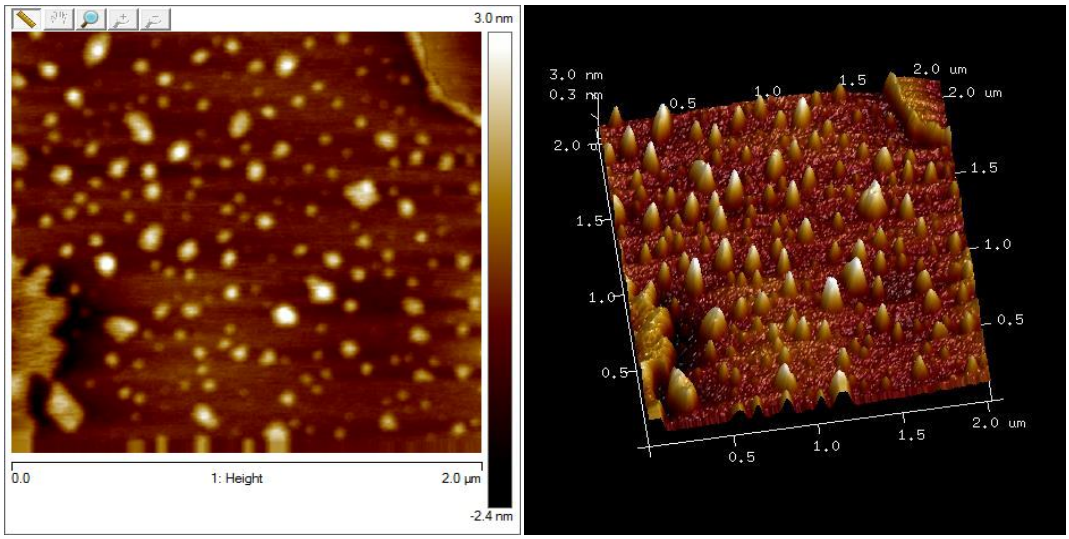

These images are for highly diluted MNP suspensions (10^{-6} dilution). So, there was no significant agglomeration as is evident from the size distribution graph (Figure 6.6). Maximum particles are in the range 53-55 nm. Both irregular and spherical particles were observed.

Figure 6.6: Particle Size (diameter) distribution histogram of magnetic nanoparticles

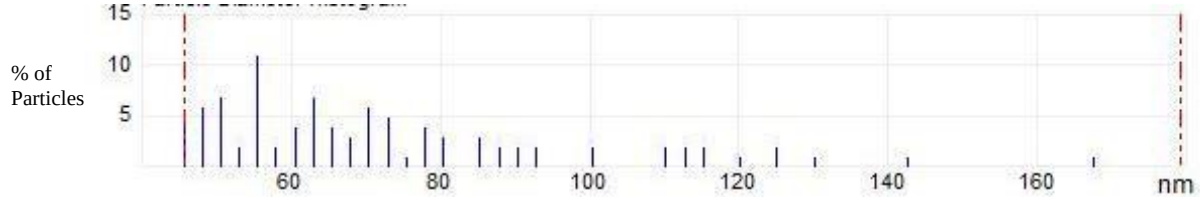

Dynamic light scattering analysis showed two peaks of size corresponding to 152.9 nm and 50.88 nm (Figure 6.7). With AFM, the nanoparticle size was ascertained to be between 53-55 nm. Usually, due to their small size and large surface area nanoparticles tend to agglomerate and are found as large aggregates (Mohanraj and Chen, 2006). This problem is even more profound in case of magnetic nanoparticles which tend to stick together due to their magnetism. This agglomeration might be the reason for observance of a peak corresponding to 152.9 nm.

Figure 6.7: DLS analysis of magnetic nanoparticles

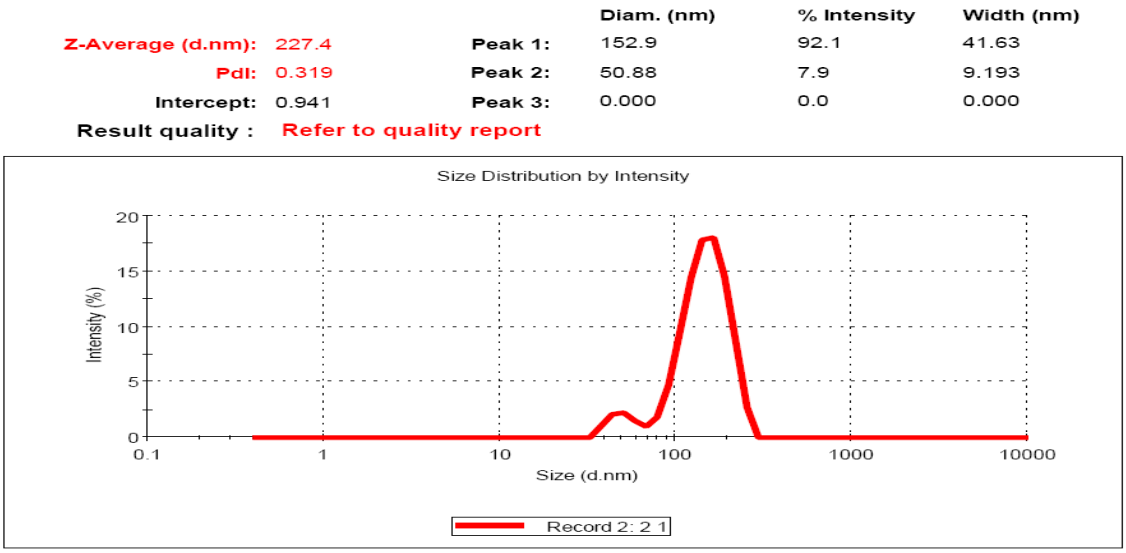

6.3.2. Preparation of silica coated magnetic nanoparticles

The major properties of magnetic nanoparticles that need to be considered while employing them for enzyme immobilization include chemical stability, high dispersibility in liquid media and uniformity in size. Magnetic nanoparticles are very sensitive to oxidation and under ambient conditions may get oxidized leading to deposition of oxide layers on the iron particle. Due to magnetic dipole interactions, they also have a tendency to agglomerate into large clusters which hinders their use in immobilization. To protect magnetic nanoparticles from oxidation and agglomeration, encapsulation using carbon, silica, metal oxides, organic polymers or surfactants is usually carried out (Faraji et al., 2010).

Silica coating of nanoparticles offers several advantages. It prevents agglomeration and also oxidation of the particles, thus enhancing its chemical stability. The mode of action of silica in stabilizing nanoparticles is by sheltering the magnetic dipole interaction through its coating and by bringing negative charges on the surface of the silica shell which in turn enhances coulombic repulsion and hence reduces aggregation (Lu et al., 2002b). Another advantage is that the size of nanoparticles can be controlled from tens of nanometers to several hundred nanometers by changing the ratio of SiO_2 to Fe_3O_4 or by repeated coating of the nanoparticle with silica. Silica chemistry is well known and hence standard procedures can be followed to immobilize enzymes on silica shells. Moreover, silica particles are hydrophilic, biocompatible and stable in most bio-systems (Aissaoui et al., 2014). Silica coating of magnetic nanoparticles also offers ease of surface modifications and creation of abundant silanol groups which can be easily activated by functional groups (Lu et al., 2007; Wang et al., 2011b).

The magnetic properties of nanoparticles were maintained even after silica coating as evident from by their spiking effect under an external magnetic field (Figure 6.8).

Figure 6.8: Spiking effect of silica coated magnetic nanoparticles under the influence of an external magnetic field.

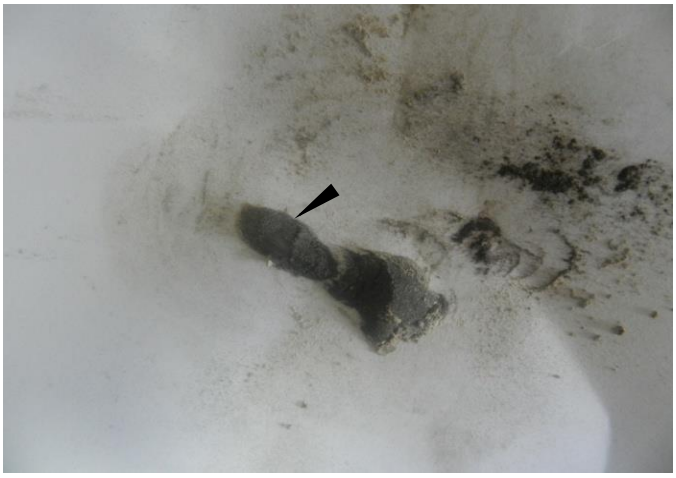

Arrow head shows spiking effect under magnetic field

Silica coating of magnetic nanoparticles caused increase in particle size. DLS analysis revealed two peaks, the major one corresponding to a size of 440 nm and a minor peak corresponding to 73.69 nm. (Figure 6.9).

Figure 6.9: DLS analysis of silica coated magnetic nanoparticles

			Diam. (nm)	% Intensity	Width (nm)
Z-Average (d.nm):	729.8	Peak 1:	440.0	81.9	64.72
PdI:	0.624	Peak 2:	73.69	18.1	9.934
Intercept:	0.968	Peak 3:	0.000	0.0	0.000
Result quality :	Refer to quality report				

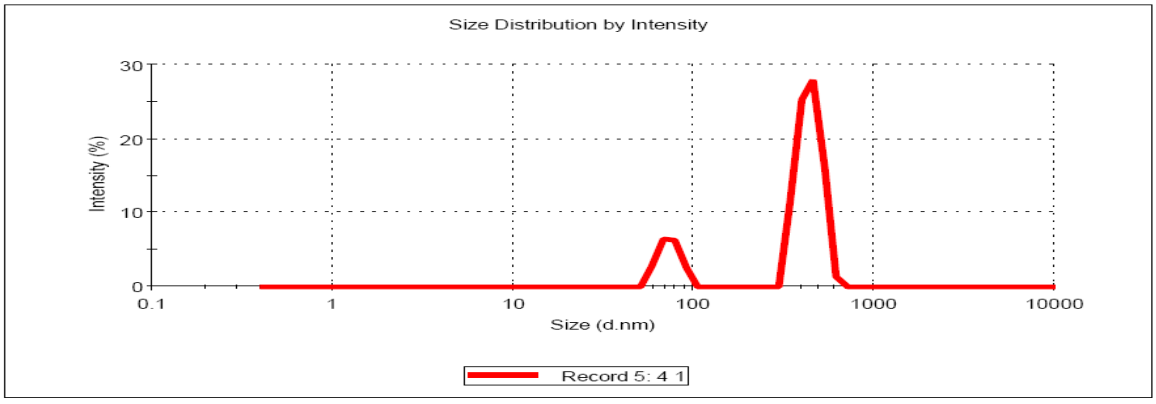

6.3.3. Functionalization of magnetic nanoparticles

Silica coated magnetic nanoparticles were functionalized using APTES (3-aminopropyltriethoxysilane). Upon silica coating of magnetic nanoparticles, their surface is often terminated with a silanol group which can react with various coupling agents that enables them to be attached to specific ligands for targeted actions. Functionalization with APTES provides free amino group which is the preferred functional group for binding to biological compounds. APTES couples to Si-MNP by forming Si—O—Si covalent bonds. APTES hydrolyzes in the presence of water and silanol group's condensate with metal hydroxyl groups on the nanoparticles surface. The modified magnetic nanoparticles with amino-silane shell are biocompatible (Shen et al., 2004).

APTES coupling of silica coated magnetic nanoparticles caused increase in particle size. DLS analysis revealed two peaks, the major one corresponding to a size of 359.7 nm and a minor peak corresponding to 96.75 nm (Figure 6.10). Reduction in size of major fraction could be due to lower aggregation of nanoparticles.

Figure 6.10: DLS analysis of APTES coupled silica coated magnetic nanoparticles

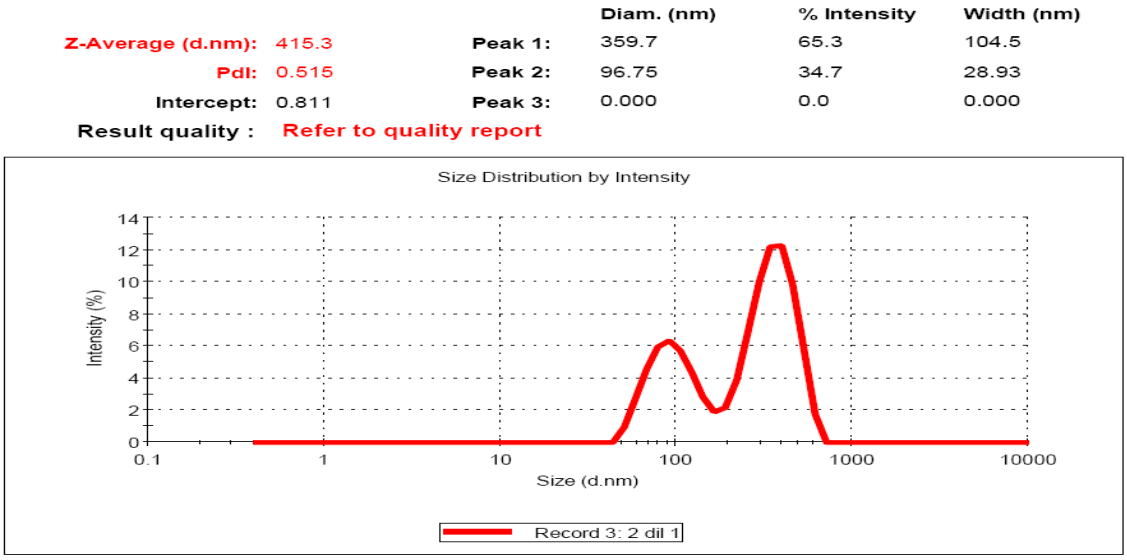

6.3.4. Immobilization of β-glucosidase on to silica coated magnetic nanoparticles

β-glucosidase (BGL) enzyme was immobilized by covalent binding with glutaraldehyde reagent. The enzyme immobilized nanoparticles were separated by a magnet and washed thrice with citrate buffer and stored at 4 °C in citrate buffer (pH 4.8, 0.05 M). An immobilization efficiency of 21.91% could be achieved with the conditions used. Out of 500 IU used for immobilization, only 109.9 IU could be

retained on the MNPs (Table 6.1). To attain better immobilization efficiencies, optimization of immobilization technique, glutaraldehyde concentration, APTES concentration and other significant parameters need to be optimized. The immobilized enzymes showed 100% storage stability at 4 °C for one month. After 3 months of storage, only 11% activity loss was observed.

Table 6.1: Efficiency of immobilization of BGL on MNPs

Enzyme used	Total BGL activity in magnetic nanoparticles (U)	Efficiency of immobilization (% activity retained on MNPs)
Aspergillus niger BGL (crude)	109.56 (0.071 IU/mg MNP)	21.91

Lee et al., (2010) reported that polymer nanofibres with BGL immobilized on them by glutaraldehyde cross linking and aggregate formation retained 91% of the initial activity after 21 days of incubation in shaking conditions. Magnetic nanoparticle immobilized BGL from *Trichoderma reesei* retained 98% activity even after 45 days storage (Valenzuela et al., 2011). Upon immobilization to magnetic aluminum nitride nanoparticles, BGL showed activity retention of 78.4% (Pan et al., 2008). A maximum immobilization efficiency of 93% was obtained by Ahmad and Sardar (2014), when a high amount of cellulase per mg of APTES modified TiO_2 nanoparticles was loaded. Covalent immobilization of the BGL of *Agaricus arvensis* on functionalized silicon oxide nanoparticle by Singh et al., (2011) yielded a high efficiency of 85%. Verma et al., (2013) found 93% enzyme binding using glutaraldehyde mediated covalent binding. DLS analysis of enzyme immobilized nanoparticles revealed a single peak of size 203 nm (Figure 6.11).

Figure 6.11: DLS analysis of enzyme immobilized magnetic nanoparticles

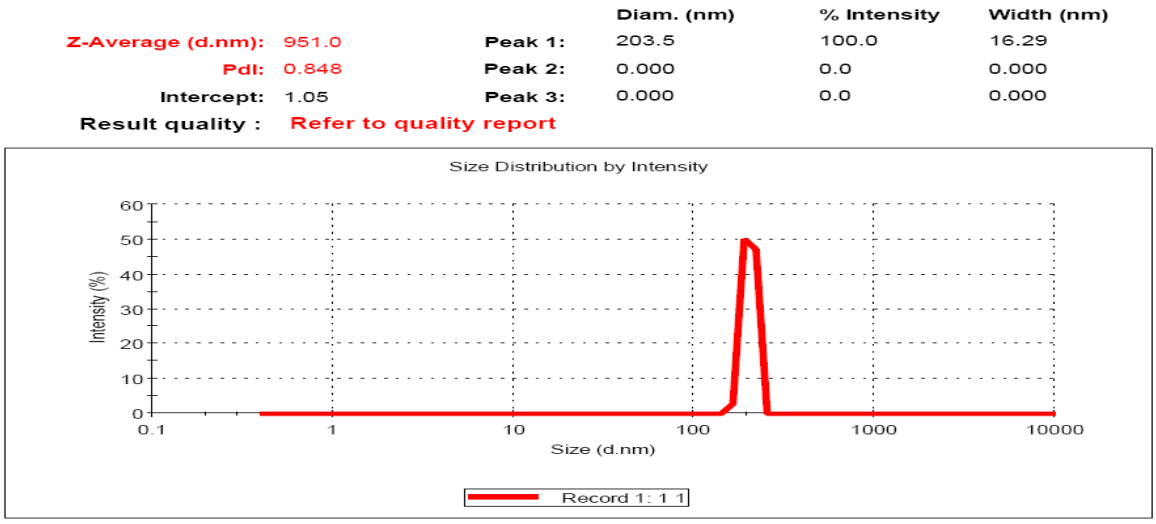

6.3.5. X Ray diffractogram of MNP and modified MNPs

XRD analysis indicated that the MNPs are magnetite with the diffraction peaks (2θ) at 35.6°, 43.3°, 53.8°, 57.3° and 62.8° ascribed to the (311), (400), (422), (511) and (440) planes of Fe_3O_4 matching exactly with the standard data of magnetite (JCPDS no. 19-0629) (Figure 6.12). Furthermore, absence of weak peaks at diffraction angles 15.0°, 18.2°, 18.4° and 26.1° which corresponds to that of maghemite (PDF 39–1346) also confirmed that the synthesized material was indeed magnetite. From the Figure 6.12, it was apparent that the diffraction pattern of magnetic particles coated with silica is close to magnetite. Thus, silica coating does not appear to change the phase of the magnetite particles synthesized. A broadening of the peaks was observed at low diffraction angles. This broad reflection at low 2θ values (20°~30°) is attributed to the amorphous thin layer of silica coating on MNPs (Chen et al., 2012). For both APTES functionalized and glutaraldehyde linked MNPs, peaks at diffraction angles consistent with standard for magnetite were observed. Also, upon immobilizing with BGL, peaks at 2θ = 35.6°, 43.3°, 48.5° and 73.9° were observed which again corresponds to the standard peaks for magnetite. This confirms that functionalization and immobilization does not change phase of magnetic particles.

Figure 6.12: X- ray diffractogram of MNP and modified MNPs

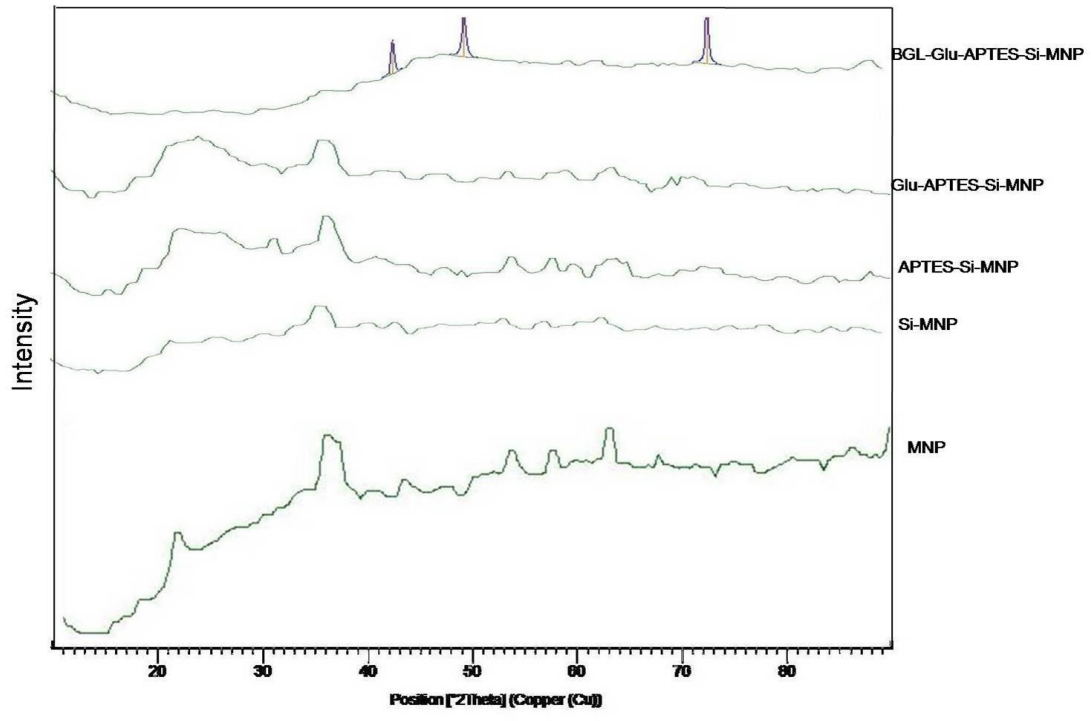

6.3.6. FT-IR spectrum of MNP and modified MNPs

To characterize the nanoparticles synthesized, FT-IR was employed. This is an effective tool to determine the efficiency of surface modification and immobilization on MNPs. Figure 6.13 depicts the FTIR spectra of magnetite and modified MNPs. In the spectrum for MNP, prominent bands were visible in the low frequency region below 800 cm^{-1} due to the iron oxide skeleton. Other regions of the spectrum contain relatively weaker bands. This kind of spectrum is characteristic of magnetite (Fe_3O_4). As in the case of standard magnetite spectrum (Gupta and Gupta, 2005), peaks were observed at 408.9, 576.5 and 584.5 cm^{-1} for the MNPs synthesized. These peaks are due to the vibrations of Fe–O bonds. Appearance of a broad band near 1103 cm^{-1} due to Si-O-Si anti-symmetric stretching vibrations indicates the existence of SiO_2 coating on the nanoparticles (Chang and Tang, 2014). The peak at 1554 cm^{-1} corresponds with the -NH_2 characteristic peak in APTES coated magnetic silica particles (Chen et al., 2012). The adsorption band at 2843 cm^{-1} and 1652 cm^{-1} are due to stretching vibration of -CH_2 and presence of –NH_2 respectively (Bo et al., 2008). The broadened peak around 3200 cm^{-1} was presumably due to the free amino groups which is overlapped by the O–H stretching vibration which is frequently observed in cases of MNP functionalization with amino derivatives. In glutaraldehyde attached MNPs, a peak was observed at 1676 cm^{-1} which is due to –CN bond formation. The weak band at 2947 cm^{-1} was due to aldehyde group (Alex et al., 2014). The absorption peak at 1625 cm^{-1} is characteristic of BGL which is suggestive of C = O stretching (Verma et al., 2013; Abraham et al., 2014).

Figure 6.13: FT-IR spectrum of MNPs and modified MNPs

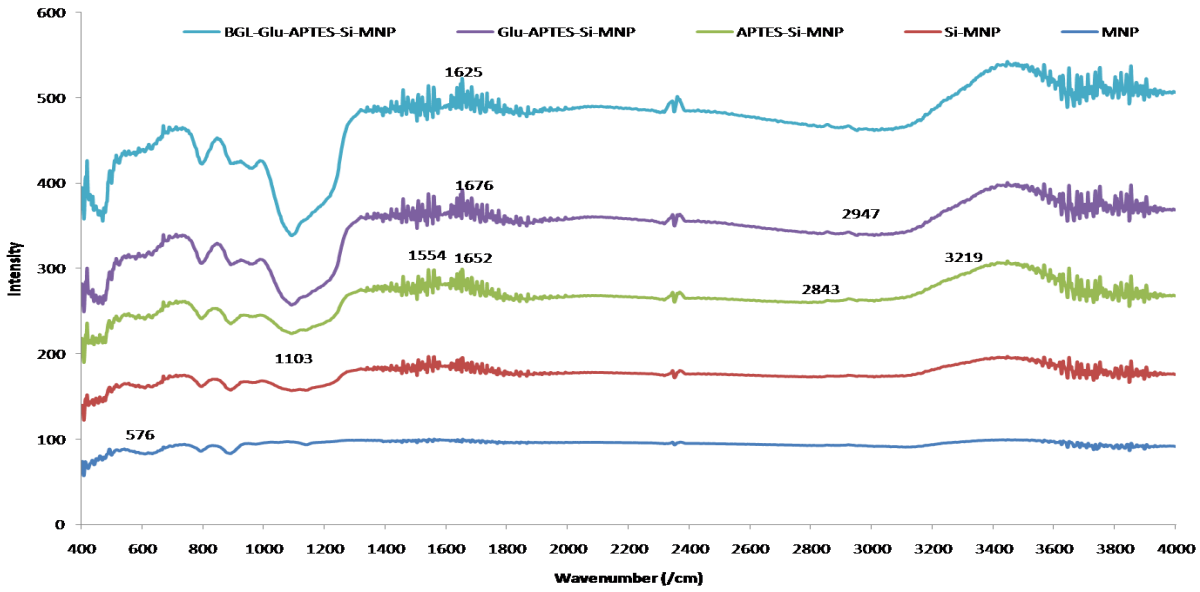

6.3.7. Lignocellulosic biomass hydrolysis using MNP immobilized BGL

Hydrolysis of alkali pre-treated rice straw was done with magnetic nanoparticle immobilized BGL. In the optimised cocktail containing 10 FPU cellulase/g biomass, 7500 U xylanase/g biomass and 5 IU BGL/g biomass, free beta glucosidase was replaced with immobilized BGL and reaction was carried out for 48 h at 50 °C for a mixture containing 10% biomass loading. The reducing sugar yields thus obtained were compared with those obtained for hydrolysis with Cellic CTec 2 and the individual enzymes of Novozymes mixed in the same ratio as in the optimised cocktail used in the present study. Hydrolysis with Cellic CTec 2 gave only marginally higher (4.08%) reducing sugars as compared to that with optimised cocktail supplemented with immobilized BGL. Similar yields were observed for hydrolysis with free and immobilized BGL and with the Novozymes cocktail (Figure 6.14). Total reducing sugar (TRS) yield with free enzyme was 654 mg/mL and that with immobilized enzyme was 681 mg/mL.

Upon loading 5 IU BGL/g cellulose, Tu et al., (2006) observed that Eupergit C immobilized β-glucosidase was as effective at hydrolyzing lignocellulosic substrates like organosolvent and acetic acid pretreated softwood pulps as well as model cellulosic substrates like Avicel® as the free enzyme, when used at the same protein loading. Borges et al., (2014) reported that free BGL could hydrolyse cellobiose with 100% efficiency in 12 h whereas glutaraldehyde cross linked BGL could only hydrolyse cellobiose with 58% efficiency. Free and immobilized BGL yielded 79% and 71% glucose respectively upon hydrolysis of pre-treated microalgal cellulosic residue. The lower activity for immobilized BGL could be due to the inefficient distribution within the reaction mixture as against the soluble free enzyme. Another factor contributing to higher efficiency of free BGL may be the high mass transfer resistance of immobilized BGL (Tan and Lee, 2015).

Figure 6.14: Performance of MNP-BGL in comparison with free BGL hydrolysis

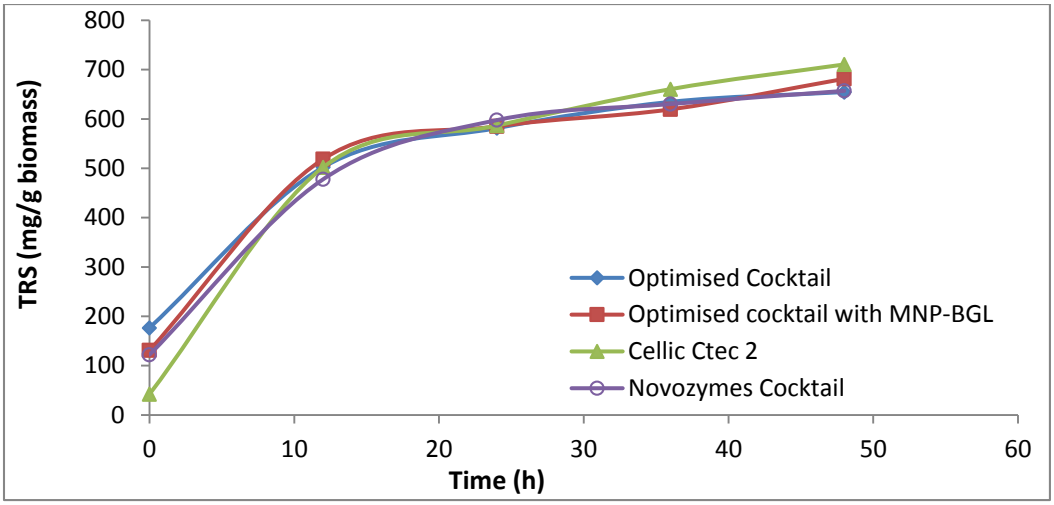

6.3.7.1. Recycling studies with MNP-BGL

For industrial applications, it is essential that immobilized BGL is reusable without significant drop in activity. Hydrolysis was carried out with fresh immobilized BGL in cycle 1. After 48 h of hydrolysis, this MNP-BGL was separated by means of a strong magnet, washed with citrate buffer (pH4.8, 50 mM) and reused for hydrolysis in cycle 2. This process was repeated till 5th cycle of hydrolysis. The efficiency of recycling was based on the reducing sugar yield in each cycle and activity retention after successive hydrolysis reactions.

In the first cycle, yield of reducing sugars was 681 mg/g biomass which got reduced to 626 mg/g sugars in the second cycle as is seen from Figure 6.15A. In each subsequent hydrolysis step, there was a small reduction in final sugar yield. After 5 cycles of hydrolysis, the decrease in sugar yield was only 19.97%. From Figure 16.5B it is evident immobilized BGL retained 69% of its activity even after 5 cycles of hydrolysis of rice straw. In earlier work, Tu et al. (2006) showed that immobilized BGL was stable for up to six cycles of cellulose hydrolysis carried out for 48 h at 45 °C. There are many reports that claim higher cycles of reusability for immobilized BGL. But majority of them use a commercial substrate (either cellobiose or pNPG) for a shorter hydrolysis duration of 10 – 15 min. Verma et al., (2013) report that their enzyme could retain up to 80% activity till 8th recycle and was stable up to 16 cycles of 10 minute hydrolysis at 60 °C. A residual activity of 84.9% after 10 cycles of hydrolysis with each cycle operated for 3 h at 50 °C was obtained by Tan and Lee (2015).

Figure 6.15: Reusability study on immobilized BGL

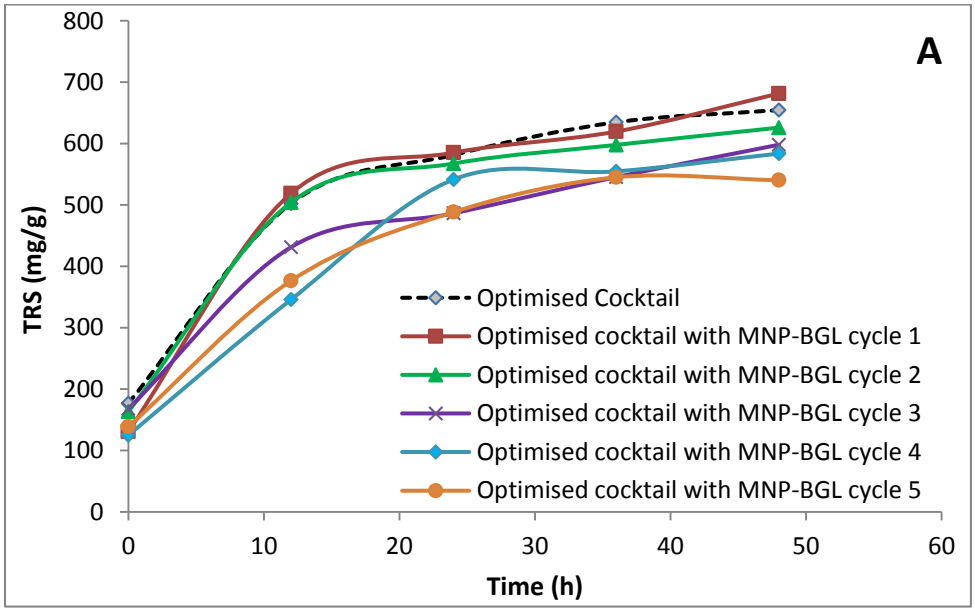

A) Operational stability of immobilized BGL during hydrolysis

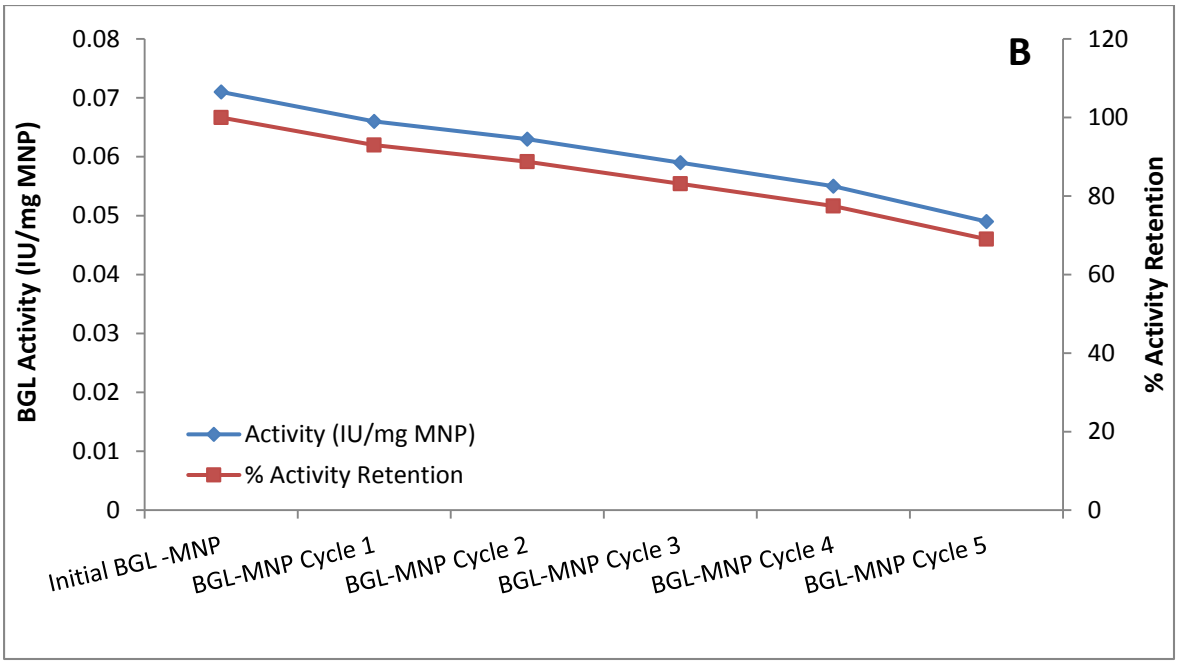

B) Activity retention of immobilized BGL upon reuse in hydrolysis

6.3.7.2. Impact of high BGL loadings on hydrolysis

Higher BGL loadings are effective in overcoming product inhibition due to increased glucose accumulation during the course of hydrolysis. This problem is aggravated in cases where higher substrate concentrations are used to obtain concentrated glucose solutions for fermentation. Lower amounts of BGL in the enzyme used for hydrolysis also lead to increased accumulation of cellobiose which can also inhibit BGL. One of the strategies to overcome product as well as substrate inhibition is to have an enzyme cocktail with high loadings of BGL (Duff and Murray, 1996). Hence, in the present study, high dosages of MNP-BGL (30 and 60 IU/g biomass) were supplemented to the enzyme cocktail. As the BGL is immobilized, the cost of addition can be mitigated due to recycling of the enzyme.

As the BGL loading increased, there was an increase in sugar yields and 726 and 752 mg/g sugar was released when 30 and 60 IU/g was supplemented respectively in the reaction mixture. In comparison, when 5 IU/g BGL was supplemented, the sugar release was only 681 mg/g (Figure 6.16), which implied an increase of 9.44% with increased BGL supplementation. Also, as the BGL loading increased, maximal sugar release was attained in a shorter duration. Upon 60 IU/g BGL loading, peak sugar yield could be achieved after about 12 h of hydrolysis against 48 h required in the case of normal BGL loading. This acceleration in reaction rates can translate to reduction in operation costs. Other reports on usage of higher BGL loadings also support these observations. Hydrolysate with >5% glucose was obtained in the case of municipal solid waste pulp upon increasing BGL loading from 12.5 to 25 mg/g (Puri et al., 2013).

Supplementing 5 and 25 mg/L BGL to cellulose hydrolysis led to a reduced cellobiose accumulation and increased glucose production with increase in BGL loadings during SSF of cellulose to yield ethanol (Lee et al., 2010).

Figure 6.16: Enzymatic hydrolysis with high dosage of MNP-BGL

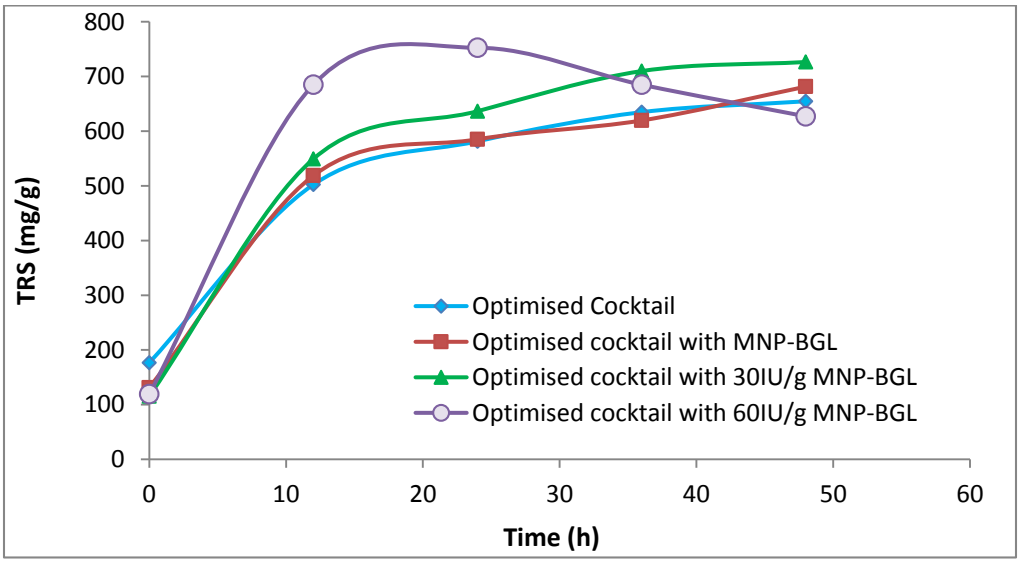

6.4. Conclusions

The current work demonstrated the advantages of using immobilized enzymes by minimizing the consumption of BGL during lignocellulose hydrolysis and making the process of fermentable sugar production and hence bioethanol, economical and feasible. Since the immobilization was done on magnetic nanoparticles, it imparted additional advantages of being cost effective, having high immobilization efficiency, high thermo stability and excellent reusability, longer storage stability and easy recovery. Magnetic nanoparticles synthesized in the present study were coated with silica and BGL was effectively immobilized on them which were confirmed by XRD studies, FTIR spectroscopy and enzyme assays. An immobilization efficiency of 21.91% could be attained. Replacing free BGL with MNP BGL in the optimized enzyme cocktail for hydrolysis produced similar sugar yields. Also, repeated hydrolysis for 5 cycles did not reduce the sugar yields significantly and the MNP BGL retained 69% of activity even after the 5^{th} cycle. Higher loadings of BGL could improve the reaction rates bringing down the time required to attain maximum sugar yield. Hence, high loadings can be used in hydrolysis by MNP BGL without increasing the cost and with the advantages of reduced reaction times and reusability. These properties of immobilized BGL make this nano biocatalytic system of potential interest in bioethanol production process.

Chapter 7

CFD simulation of hydrolysis reactors with different impeller types for high solids loading

7.1. Introduction

To convert second generation bioethanol production process to a cost competitive and economic technology, a high solids loading enzymatic hydrolysis process needs to be devised. Such a process could in turn, reduce the capital investment costs and result in higher ethanol titers, which in turn, would lower the energy demand for distillation step, resulting in significant lowering of final ethanol costs (Galbe and Zacchi, 2002; Jorgensen et al., 2007a; Hodge et al., 2008). The current enzymatic hydrolysis process requires about 90% by weight of water in the reaction zone. Enzymatic saccharification to yield glucose takes about 72 to 144 h and is usually carried out at low solids concentrations of 10 to 12% by weight (Aden et al., 2002). Ideally, a concentration of 30 to 40% by weight of lignocellulosic biomass in reaction mixer is believed to be the optimum loading to make the overall production process cost-competitive (Zimbardi et al., 2002).

At biomass loadings greater than 30% by weight, the reaction mixture behaves as a semi solid in which free water availability is very low. Mixing biomass slurries is challenging under these conditions and this leads to lower efficiencies of heat and mass transfer (Carrasco and Roy, 1992; Hodge et al., 2008, 2009). Cavaco-Paulo and Almeida (1994) observed that mechanical mixing enhanced the rate of enzymatic saccharification of cotton fibers. Ingesson et al., (2001) and Roche et al., (2009b) also supported the finding that the rate of enzymatic hydrolysis increased upon mechanical agitation of biomass. Mechanical agitation has been claimed to render the cellulosic content in biomass to more amorphous form than crystalline cellulose. Hence hydrolysis efficiency increases as amorphous cellulose is more susceptible to enzymatic hydrolysis (Lenting and Warmoeskerken, 2001). On the other hand, Roche et al., (2009b) hypothesized that enhancement in saccharification efficiency was due to uniform distribution of enzymes throughout the reaction mixture.

The appropriate selection of mixing systems needs knowledge on operating conditions such as agitation speeds and fluid rheology and other properties. When the fluid viscosity is low, the rotational speed of impeller is usually maintained high enough to produce turbulent flows. Turbulent flows are essential in mixing operations to impart efficient mass transfer. Most common reactors use Rushton turbines or pitched blade impellers to attain higher rotations and turbulence.

Enzymatic hydrolysis alters the rheological properties of biomass. Biomass viscosity increases rapidly when the solids concentrations increases above 10% by weight in the reaction mixer. At such large concentrations, biomass slurries behave as a non-Newtonian fluid which is generally characterized

by a shear thinning type of fluid, with large apparent viscosity and yield stress that increases with the concentration of biomass (Ehrhardt, 2008; Knutsen and Liberatore, 2009; Roche et al.,2009a; Stickel et al., 2009; Ehrhardt et al., 2010). Ehrhardt (2008) and Ehrhardt et al., (2010) found that resistance to flow of dilute acid hydrolyzed corn stover decreased with time upon addition of enzymes when measured in a torque rheometer. Roche et al. (2009a) observed a decrease in yield stress of acid hydrolyzed corn stover with time during its enzymatic hydrolysis. This decrease could be attributed to a decrease in insoluble solids concentration due to enzymatic degradation of biomass.

The complex rheological behavior of the biomass slurry during enzymatic hydrolysis poses critical challenges to efficient mixing. One vital aspect is the enzyme–substrate contact. With the conventional mixers, process performance is poor due to formation of stagnant zones in the reactor which reduces the enzyme-substrate contact. Another significant point is the thermal deactivation of enzyme due to higher heat generation from the moving parts of the reactor. High levels of shear stress in the reactor also inactivate the enzyme due to damages in its molecular structure (Reese and Ryu, 1980). Hence, conventional stirred tank reactors with typical Rushton and disc impeller configurations are not feasible for hydrolysis of lignocellulosic biomass due to high power requirements from the high stirring speeds needed to mix the slurry and keep the solids suspended.

Different mixer configurations, such as a peg mixer (Zhang et al., 2009a), helical ribbon mixers (Zhang et al., 2010) and a tumbling reactor (Jorgensen et al., 2007a) have been investigated for carrying out enzymatic hydrolysis of lignocellulosic biomass. But energy consumption for mixing is not reported in these studies. Hence it is difficult to assess mixing efficiency and energy requirements for enzymatic saccharification. These systems are generally described with a pseudo-single-phase approach with non-Newtonian models, such as the Power Law expression or the Herschel-Bulkley model (Carvajal et al., 2012).

In recent years, Computational fluid dynamics (CFD) has been used extensively to study the mixing efficiency in conventional stirred reactors with either radial or axial type of impellers. Computational Fluid Dynamics (CFD) is a computer-based tool for simulating the behavior of systems involving fluid flow, heat transfer, and other related physical processes. It works by solving the equations of fluid flow (in a special form) over a region of interest, with specified (known) conditions on the boundary of that region. Since all the calculations and simulations are done by computers, it reduces the total effort required in the experiment design and data acquisition. The various applications of CFD include: mass, momentum and heat transfer in industrial processes (boilers, heat exchangers, combustion equipment, pumps, blowers, piping, etc.), aerodynamics of ground vehicles, aircraft, missiles, film coating, thermoforming in material processing applications, flow and heat transfer in propulsion and

power generation systems, ventilation, heating and cooling flows in buildings, chemical vapor deposition (CVD) for integrated circuit manufacturing, heat transfer for electronics packaging applications etc.

Figure 7.1: Schematic View of the main elements of CFD code

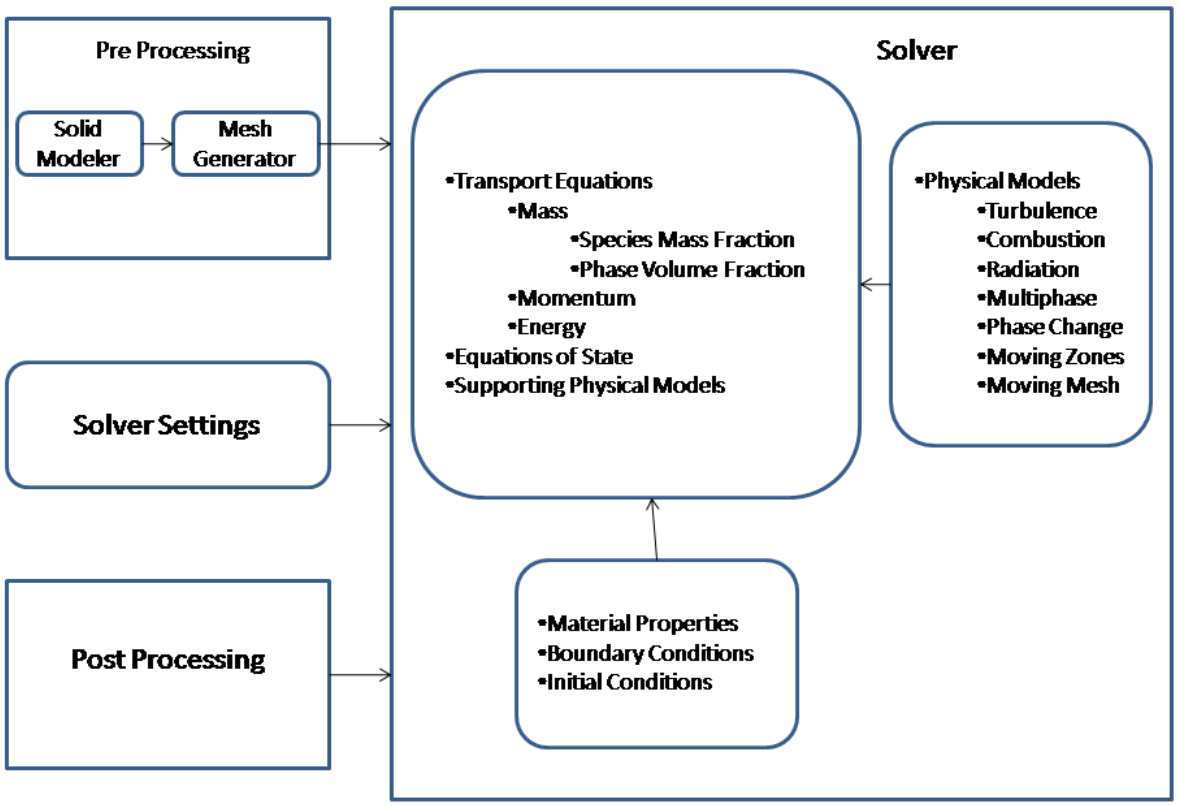

Application of CFD to analyze a fluid problem requires the following steps. First, the mathematical equations describing the fluid flow are written. These are usually a set of partial differential equations. These equations are then discretized to produce a numerical analogue of the equations. The domain is then divided into small grids or elements. Finally, the initial conditions and the boundary conditions of the specific problem are used to solve these equations. The solution method can be direct or iterative. In addition, certain control parameters are used to control the convergence, stability and accuracy of the method. All CFD codes contain three main elements as depicted in Figure 7.1: (1) A pre-processor, which is used to input the problem geometry, generate the grid, define the flow parameter and the boundary conditions to the code; (2) A flow solver, which is used to solve the governing equations of the flow subject to the conditions provided; (3) A post-processor, which is used to manage the data and show the results in graphical and easy to read format.

In the studies described in this chapter, CFD was used to understand the complex hydrodynamics of conventional stirred tank reactors with two types of impellers: Rushton turbine and double helical impeller which is used for enzymatic hydrolysis process with high solids loading. The biomass-enzyme-water reaction mixer is treated as a single continuous fluid with varying viscosity of shear thinning type. Based on CFD predictions, the performance of the both the impellers are compared in terms of mixing.

7.2. Materials and Methods

7.2.1. Design of Stirred tank reactor

The dimensions of the vessel for stirred tank reactor are designed based on the standard calculations as given in Perry's Chemical Engineers Handbook (Perry and Green, 1997). The Rushton turbine and double helical impeller are also designed based on the standard conditions given in the handbook and by the method suggested by Couper at al., (2005). The reactor vessel was designed to process 4 L biomass slurry containing 25% solids loading by weight. The dimensions of the reactor designed are given in Table 7.1. The calculations are carried out by taking biomass density, ρ as 1022 kg/m^3 and viscosity, μ as 0.83 Pa-s (from literature). Figure 7.2 shows the designed stirred tank reactor.

Table 7.1: Design characteristics of stirred tank reactor

Characteristics	Stirred Tank Reactor
Material of Construction	SS316L
Working Volume	4 L
Capacity	6 L
Tank Diameter (D)	0.1563 m
Tank Height (H)	0.3126 m
H/D Ratio	2:1
Working Volume Height	0.2085 m

Figure 7.2: Schematic view of the designed Stirred tank reactor

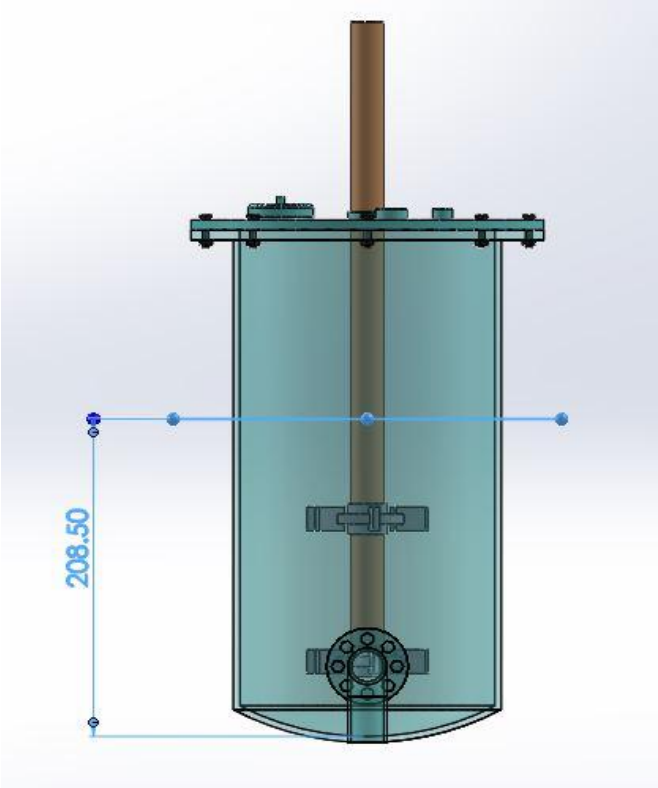

7.2.2. Design of Rushton turbine

Rushton turbine is one of the most commonly used radial impellers in industry. One of the major disadvantages of using Rushton turbine in a stirred tank reactor is its inefficiency in mixing high viscosity samples. But the main advantage of using this type of turbines is that they transmit more power to the mixture than any other impeller type. Turbulent range is often seen at $N_{Re} \geq 10^3$ or 10^4. Rushton turbine is designed as per the standard design criteria and the design parameters obtained are given in Table 7.2. (Fondy and Bates, 1963; Corpstein et al., 1994; Couper et al., 2005). Power number values are estimated from the standard calculation procedure as given in Perry's Chemical Engineers Handbook (Perry and Green, 1997). Figure 7.3A depicts the schematic view of the designed Rushton turbine impeller. To overcome the disadvantage of smaller impeller size, baffles are installed to create more turbulence and two impellers are used as shown in Figure 7.3B.

Table 7.2: Design parameters for Rushton turbine impeller

Impeller Dimensions	Expression for calculation	Rushton Turbine Impeller
Impeller Diameter, Di	0.25 *D	0.039 m
Reynolds Number, N_{Re}	$(D_i^2*N_i*\rho)/\mu$	54
Power Number, N_p	Ref: Perrys HB, Pg 15-25,fig:15-23	7.2 for 1 impeller; 14.4 for 2 impellers
Pitch	$2*D_i$	0.078 m
Number of impellers		2
Blade width	$0.20*D_i$	0.0078 m
Blade Height	$0.20*D_i$	0.0078 m
Blade Thickness		4 mm
Clearance between blades and walls of reactor	0.75*D	0.117 m
Off Bottom Clearance	0.25*D	0.039 m
Width of baffles	D/12	0.013 m
Shaft Diameter	Based on calculations for bending moment	15 mm
Shaft Length from bearing to impeller		0.30 m
Tip speed, N_i	10-12 fps (industry standard)	3.5 m/s (1712 rpm)
Power required by impeller	$N_p* \rho*N_i^3*D_i^5$	0.3 KW (including allowance for service factor, and start up power)
Torque of impeller		1.7 Nm
Blade angle		NIL

Figure 7.3: Schematic view of the designed impeller of Rushton type

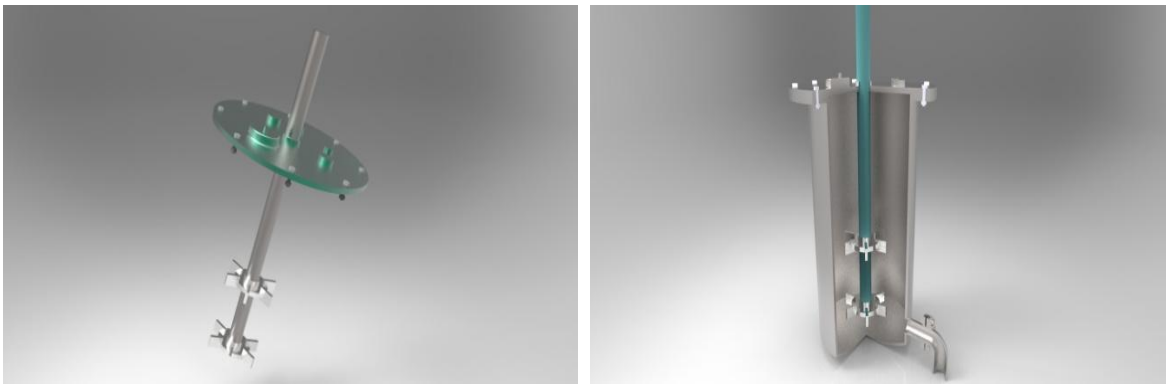

A) Impeller with head plate B) Impeller positioned inside the reactor

7.2.3 Design of double helical impeller

The standard design criteria which were used for designing double helical impeller and the design parameters are given in Table 7.3 (Couper et al., 2005). Power number values were estimated from the standard calculations procedure as given in Chemical Engineers Handbook by Perry and Green (1997). Figure 7.4 shows the schematic view of the designed double helical impeller. This type of impeller is used in applications where highly viscous substances need to be mixed. A 30° turn in the blade angle was provided to give an upward thrust to the slurry. For such turbines, usually laminar flow persists at N_{Re} = 100. As turbulent flow regimes are better suited for higher mixing efficiency, higher Reynolds numbers are favored.

Figure 7.4: Schematic view of the designed helical impeller

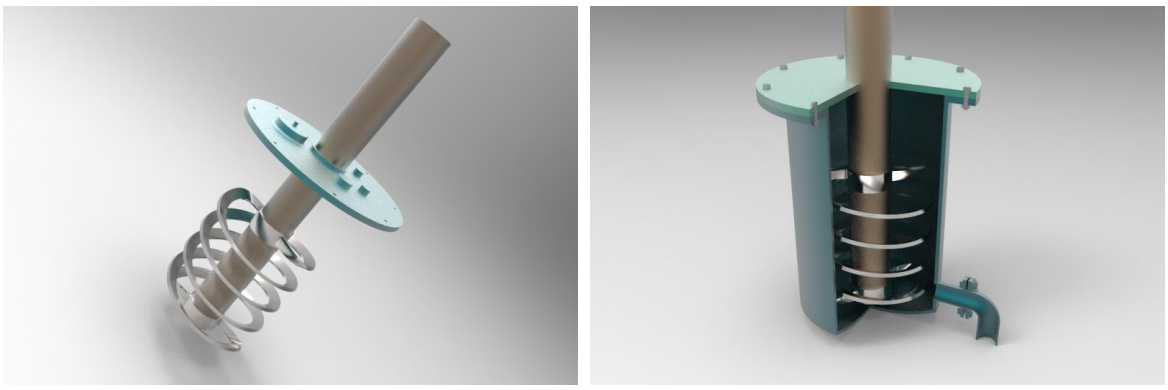

A) Impeller with head plate B) Impeller positioned inside the reactor

Table 7.3: Design parameters for double helical impeller

Impeller Dimensions	Expression for calculation	Double helical Impeller
Impeller Diameter, Di	0.90 *D	0.141 m
Reynolds Number, N_{Re}	$(D_i^2*N_i*\rho)/\mu$	138
Power Number, N_p	Ref: Perrys HB, Pg 15-25,fig:15-23	4
Pitch	D_i	0.141 m
Number of coils		2
Blade width	$0.20*D_i$	0.03 m
Blade Height	D_i	0.141 m
Blade Thickness		4 mm
Clearance between blades and walls of reactor	0.10*D	0.015 m
Off Bottom Clearance	0.05*D	0.0078 m
Shaft Diameter	Based on calculations for bending moment	20 mm
Shaft Length from bearing to impeller		0.30 m
Tip speed, N_i	1.33 – 2.5 m/s (industry standard)	2.5 m/s (340 rpm)
Power required by impeller	$N_p* \rho*N_i^3*D_i^5$	0.4 KW (including allowance for service factor, and start up power)
Torque of impeller		11.3 Nm
Blade angle		30°

7.2.4. CFD modeling of stirred reactors with Rushton turbine and Double helical impeller

During the last two decades, Computational fluid dynamics (CFD) has become an important tool in understanding the flow phenomena, developing new processes and optimizing the existing processes (Ranade, 2002). In recent times, CFD has been used to quite satisfactorily forecast mixing behavior in terms of mixing time, power consumption, flow pattern and velocity profiles. Once a validated solution is obtained through CFD, it can provide valuable information that would not be easy to obtain experimentally.

7.2.4.1 Governing equations

The laminar flow of a fluid in an isothermal mixing tank with a rotating impeller is described by the following continuity and momentum equations (Ranade, 2002):

$$\frac{\partial \rho}{\partial t} = -\nabla . \rho v \quad (1)$$

$$\frac{\partial (\rho v)}{\partial t} = -\nabla(\rho v v) - \nabla \rho + \nabla \tau + \rho g + F \quad (2)$$

where ρ , p , v , g , F and τ respectively are the fluid density, pressure, velocity, gravity, external force, and the stress tensor (shear stress) given by

$$\tau = \mu \left[(\nabla v) + (\nabla v)^T - \frac{2}{3}(\nabla v) I \right] \quad (3)$$

In the above equation, μ is the molecular viscosity, and I is the unit tensor. For incompressible fluids, the stress tensor is given by

$$\tau = \mu \left[(\nabla v) + (\nabla v)^T \right] = \mu D \quad (4)$$

where D is the rate of strain tensor. For multidimensional flow of non-Newtonian fluids, the apparent viscosity (μ) is a function of all three invariants of the rate of deformation tensor. However, the first invariant is zero for incompressible fluids, and the third invariant is negligible for shearing flows (Bird et al., 2002). Thus, for the incompressible non-Newtonian fluids, μ is a function of shear rate, which is given by

$$\gamma = \sqrt{\frac{1}{2}(D:D)} \quad (5)$$

It can be seen that γ (shear stress rate) is related to the second invariant of D.

7.2.4.2. Rheological model

A rheological model is needed for calculation of apparent viscosity of the Non-Newtonian fluids for solving equations 1-5. The non Newtonion model used for describing the system is based on Ostwald's Power Law (equation 6). The power-law model remains the simplest and most widely used to describe the rheological properties of non-Newtonian fluids with yield stress and shear thinning properties (Bird et al., 2002).

$$\tau = K(\partial u/\partial y)^n \quad (6)$$

where, τ is shear stress (N-m), K is the flow consistency index (Pa-s), n is flow behavior index and $\partial u/\partial y$ is the shear rate (s^{-1})

The consistency index constant, K, measures consistency of a fluid's viscosity. The higher a fluid's K, the more viscous is the fluid. The flow behavior index number, n, measures the degree of non-Newtonian behavior. Index numbers less than one describe psuedoplastic fluids (Uhl and Gray, 1966). As n approaches 1, the fluid exhibits Newtonian behavior.

7.2.4.3. Simulation of impeller rotation

Even though there are four methods available for the simulation of impeller rotations, commonly used method is the Multiple Reference Frame (MRF) approach. In this approach, a rotating frame (i.e. co-ordinate system) is used for the region containing the rotating components while a stationary frame is used for stationary regions (Luo et al., 1994). In the rotating frame containing the impeller, the impeller is at rest. In the stationary frame containing the tank walls and baffles, the walls and baffles are also at rest. The momentum equations inside the rotating frame is solved in the frame of the enclosed impeller while those outside are solved in the stationary frame. A steady transfer of information is made at the MRF interface as the solution progresses.

Consider the rotating frame at position r_0 relative to the stationary frame. The rotating frame has the angular velocity ω. Any arbitrary point in the fluid domain is identified by the position vector *r* from the origin of the rotating frame. The fluid velocities can then be transformed from the stationary frame to the rotating frame using

$$v_r = v - u_r \tag{7}$$

where υ_r is the relative velocity viewed from the rotating frame, υ is the absolute velocity viewed from the stationary frame, and u_r is the "whirl" velocity due to the moving frame which is given by

$$u_r = \omega * r \tag{8}$$

When the equation of motion is transferred to the rotating reference frame, the continuity and momentum equations respectively become

$$\frac{\partial \rho}{\partial t} = -\nabla . \rho v_r \tag{9}$$

and

$$\frac{\partial (\rho v_r)}{\partial t} = -\nabla(\rho v_r v_r) - \rho\,(2\omega * v_r + \omega * \omega * r) - \nabla p + \nabla \tau_r + \rho g + F \tag{10}$$

where $2\omega \times v_r$ and $(\omega \times \omega \times \boldsymbol{r})$ respectively are the Coriolis and centripetal accelerations, and τ_r is the stress tensor based on v_r. The momentum equation for the absolute velocity is

$$\frac{\partial(\rho v)}{\partial t} = -\nabla(\rho v_r v) - \rho\,(\omega * v) - \nabla p + \nabla\tau + \rho g + F \quad (11)$$

where $(\omega \times v)$ embodies the Coriolis and centripetal accelerations. The MRF method is recommended for simulations in which impeller-baffle interaction is weak. With this method, the rotating frame section extends radially from the centerline or shaft out to a position that is about midway between the blade's tip and baffles. Axially, that section extends above and below the impeller. In the circumferential direction, the section extends around the entire vessel.

7.2.4.4. CFD model validation

CFD model validation is done by comparing the power numbers calculated against the literature reported values. Also, the various characteristic curves for the impeller (impeller power vs rpm; shear rate vs apparent viscosity etc.) are plotted and compared against the standard literature curves. According to equation 12, higher the viscosity of the fluid due to high solids loading, higher is the power required for mixing. Higher values of torque imply higher power consumption. Operating the reactor at lower agitation speed will reduce power consumption. But low agitation speed does not provide adequate mixing for higher solids loading enzymatic hydrolysis which results in poor heat and mass transfer that affects the saccharification efficiency.

$$P = 2\pi N_i \tau \quad (12)$$

where, P is impeller power (W), N_i is Impeller rotation speed (rps) and τ is Shear stress (N-m)

From the CFD simulations, value of τ is obtained. The value of power required by the impeller for mixing at the given speed is obtained by substituting τ in equation 12. The power number, which is a characteristic value for a specific impeller type is calculated using equation 13 once the value of power is obtained using equation 12.

$$N_p = \left(P \middle| \rho N_i^3 D_i^5\right) \quad (13)$$

where, N_p is Power number for impeller (dimensionless), P is the impeller power (W), ρ is Density of slurry (kg/m^3), N_i is Impeller rotation speed (rps) and D_i is impeller diameter (m).

Reynolds number (N_{Re}) is a dimensionless number which is generally used to characterize the flow pattern in a reactor. The flow is considered to be turbulent when the Reynolds number is above 2000 and the value less than 2000 implies the flow is laminar. The Reynolds number is calculated using

equation 14 and this value is plotted for various values of power number to check whether the pattern is comparable with standard literature pattern.

$$N_{Re} = \left(N_i D_i^2 \rho \middle| K\gamma^{n-1}\right) \quad (14)$$

where, γ is Shear stress rate (s^{-1})

7.2.4.5. Modeling of impeller types using CFX solver

Meshing was done using the grid generation tool, ICEM CFD 14.5 (Ansys Inc., Canonsburg, PA, USA) which was used to generate the three-dimensional grids of the reactor model. The mathematical model was solved in CFX 14.5 (Ansys Inc.). The initial and boundary conditions were specified as: 1) the impeller and shaft regions were stationary relative to the fluid domain; 2) no slip wall; 3) the residual error was set as 1×10^{-4}; and 4) the Eulerian-Eulerian and the k-ε turbulence model were applied. The apparent viscosity of the slurry was set at 0.83 Pa.s. Density was set at 1022 kg/m^3 estimated experimentally for 25% solid containing slurry.

7.3. Results and Discussion

7.3.1. Numerical Methodology

As explained in the previous sections**,** the reactor and the impellers were created in SolidWorks 2013 (Dassault Inc., Vélizy-Villacoublay, France) and imported in the commercial CFD software ANSYS CFX 14.5. This commercial code was then used for the steady state hydrodynamic simulation of Non-Newtonian fluid flow in the stirred reactor. Steady state simulations were performed for two different type of impellers for various rotational speeds. The apparent viscosity of the fluid was taken as 0.83 Pa.s. Density was set at 1022 kg/m^3 which was estimated experimentally for a 25% loading of solids by weight. The computational domain was discretized by using the grid generation tool, ICEM CFD 14.5 (Ansys Inc., Canonsburg, PA, USA). The numerical solutions of the set of equations explained in the earlier sections consists of the following steps: (a) translation of partial differential equations into their discretized form in the form of linear algebraic equations (b) using a suitable algorithm to handle various interactions (3) finally solving the resulting algebraic equations. The second order equivalent to high resolution discretization scheme was applied for obtaining algebraic equations for momentum, turbulent kinetic energy and dissipation rate. Pressure-velocity coupling was achieved by the Rhie-Chow algorithm (1983). No slip boundary conditions were applied on the tank walls and shaft. The free surface of the tank

was considered as degassing boundary condition. The governing equations were solved using the coupled multi grid solver technology of ANSYS CFX 14.5. The criterion for convergence was set as $1\ X\ 10^{-4}$ for the RMS error for all the governing equations. The RMS (Root Mean Square) residual was obtained by taking all of the residuals throughout the domain, squaring them, taking the mean and then taking the square root of the mean for each equation

7.3.2. Flow pattern prediction in a stirred reactor with Rushton turbine

Model parameters used for CFD simulations are shown in Table 7.4. Maximum 10000 iterations were carried out for each simulation. As a first step, water was used as a liquid and the hydrodynamics was simulated using ANSYS-CFX. It can be observed from Figure 7.5A that, there are no stagnant zones and the typical radial flow pattern characteristic of Rushton turbine is visible throughout the reactor at 856 rpm and efficient mixing is obtained. The maximum velocity observed here was 4.2 m/s which is a high velocity. Higher mixing and higher velocities were observed closer to impeller blades. But when the simulation is extended to high solids loading of enzymatic hydrolysis, the mixing with Rushton turbine impeller is inefficient as evident from Figure 7.5B. At the same impeller speeds, no mixing was found for biomass slurry containing 25% solids by weight (Figure 7.5B). Minimum velocity was observed near the impeller blades. All the remaining portion of the tank showed stagnant zones and no radial circulation were observed in those regions. Hence, it can be concluded that at this rotation, efficient mixing and hence efficient hydrolysis is not possible.

Table 7.4: Model parameters used for CFD simulation of STR with Rushton turbine

Parameter	Rushton turbine containing stirred tank reactor
Mode of Simulation	3D
Grid size	226540 nodes (108030 for impeller and 118510 for tank)
Time step	0.001 s^{-1}
Upper S	1000 s^{-1}
'K' value	1565.4 [kg m^{-1} $s^{-1.968}$]
'n' value	0.032

In the second set of simulations, the impeller rotation was increased up to 2000 rpm. Similar observations were found for higher speeds like 1200 rpm (Figure 7.5C) and 2000 rpm (Figure 7.5D).

Figure 7.5: Velocity profiles predicted by CFD for Rushton turbine at different impeller rotation speeds

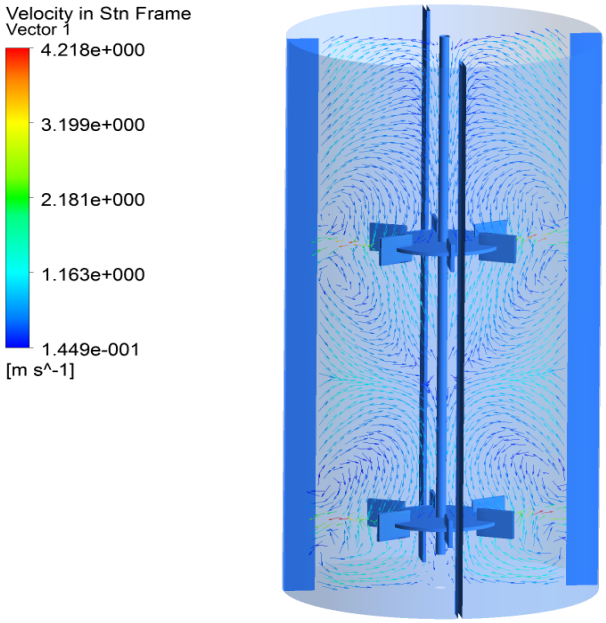

A) Velocity profile of water at 856 rpm

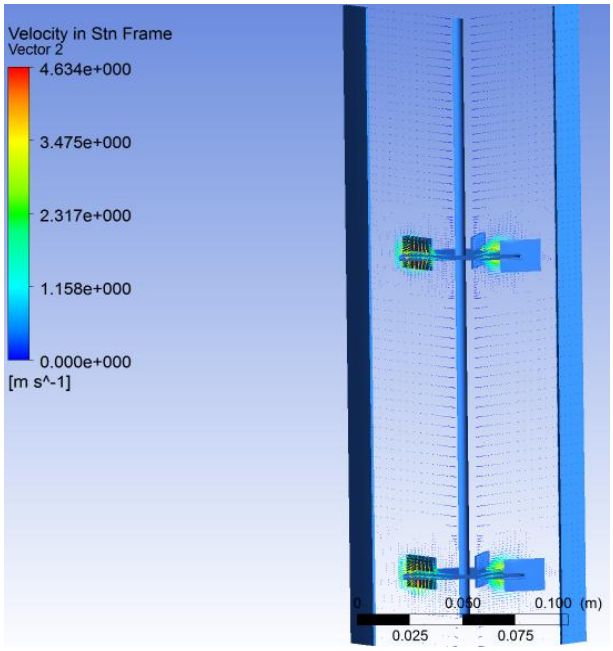

B) Velocity profile of biomass slurry (25%) at 856 rpm;

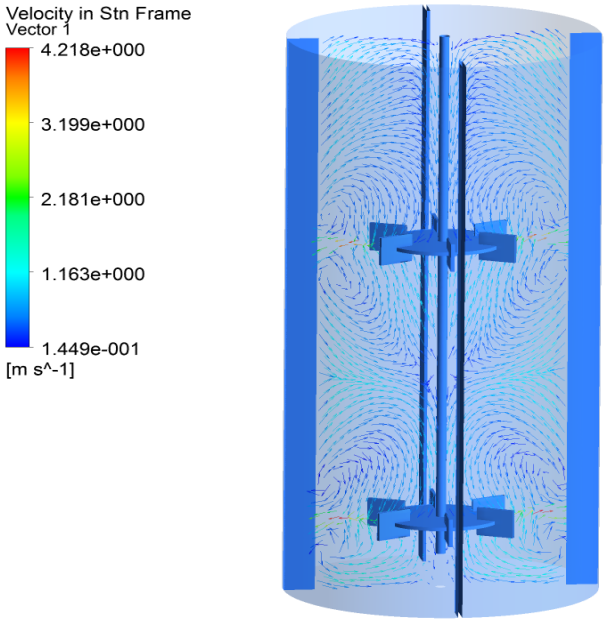

C) Velocity profile of biomass slurry at 1200 rpm

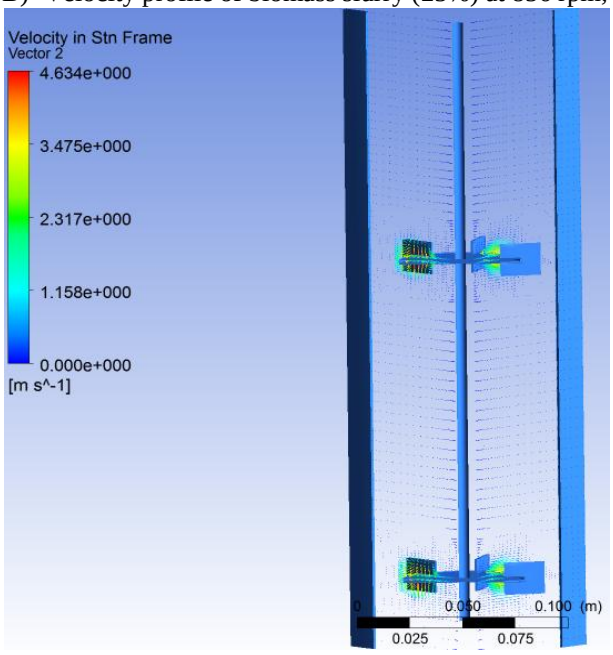

D) Velocity profile of biomass slurry 2000 rpm

In all these cases, except near the impeller, no mixing was observed. Rotation speeds above 2000 rpm were not tried as such high rotations are not feasible industrially due to the high power consumption.

Thus alternative strategies were employed which were to change the values of K and n. K value was varied from 500 to 2000 and the value of n was varied from 0.02 to 0.32. In all these simulations, highly inefficient mixing was observed even though the value of torque was very high. This might be due to the high viscosity of the biomass slurry. Thus, it can be concluded that Rushton turbine cannot be used in high solids reactor for hydrolysis of lignocellulose.

High solid containing biomass slurry behaves like a Non-Newtonian fluid with pseudo plastic characteristics. As the apparent viscosity of these fluids depends on the shear rate, rheology of the hydrolysis mixture also depends on shear rate. Pseudo plastic fluids are shear thinning, i.e. their apparent viscosity decreases with increasing shear. Consequently, in stirred tank reactors, pseudo plastic fluids have relatively low apparent viscosity in the high-shear zone near the impeller, and relatively high apparent viscosity when the fluid is away from the impeller. As a result, stagnant zones are formed in the reactor away from the impellers. In these zones, efficient mass and heat transfer does not take place leading to inefficient mixing. Usually, these negative effects are countered by impeller geometry modification and by employing impellers with larger diameters.

Not many studies have been carried out in mixing operations of high viscous materials with Rushton turbines. Tsui and Hu, (2011) reported that for highly viscous fluids, flow pattern is generally laminar instead of turbulent as power requirement increases with increase in rotation speed. They suggest that using smaller turbine impellers for these cases is inefficient due to formation of stagnant zones in the reactor areas away from impeller. Hence, Rushton turbine is inefficient in high viscosity fluid mixing.

A reactor with a small diameter impeller, generally a Rushton turbine, results in the fluid experiencing the applied power of impeller as shear at high impeller rotation rates. With shear thinning pseudo plastic fluids, Rushton turbines under ungassed conditions formed dead zones up to about 70% in the reactor. This problem was ascribed to the existence of viscosity gradients in the reactor, which are generated by the different shear rates found in the vessel. If mass transfer is also considered along with viscosity gradient, the mixing problem becomes graver (Espinosa-Solares et al., 1997).

7.3.3. Flow pattern prediction in a stirred reactor with double helical impeller

Model parameters used for CFD simulations are shown in Table 7.5. Maximum 10000 iterations were carried out for each simulation. The number of nodes in the mesh was lesser here compared to Rushton impeller.

Table 7.5: Model parameters used for CFD simulation of STR with double helical impeller

Parameter	Double helical impeller containing stirred tank reactor
Mode of Simulation	3D
Grid size	108954 nodes (42757 for impeller and 66197 for tank)
Time step	0.001 s^{-1}
Upper S	1000 s^{-1}
'K' value	1565.4 [kg m^{-1} $s^{-1.968}$]
'n' value	0.032

The numerical meshing used for double helical impeller is shown in Figure 7.6. This type of meshing is called tetrahedral meshing. The efficiency and smoothness of CFD simulation depends on the efficiency of meshing. Higher the number of nodes in a mesh, more accurate the modeling results are. In the present case, the numbers of total nodes in the mesh were 108954. The total numbers of elements were 550274.

Figure 7.6: Typical mesh used for CFD simulation

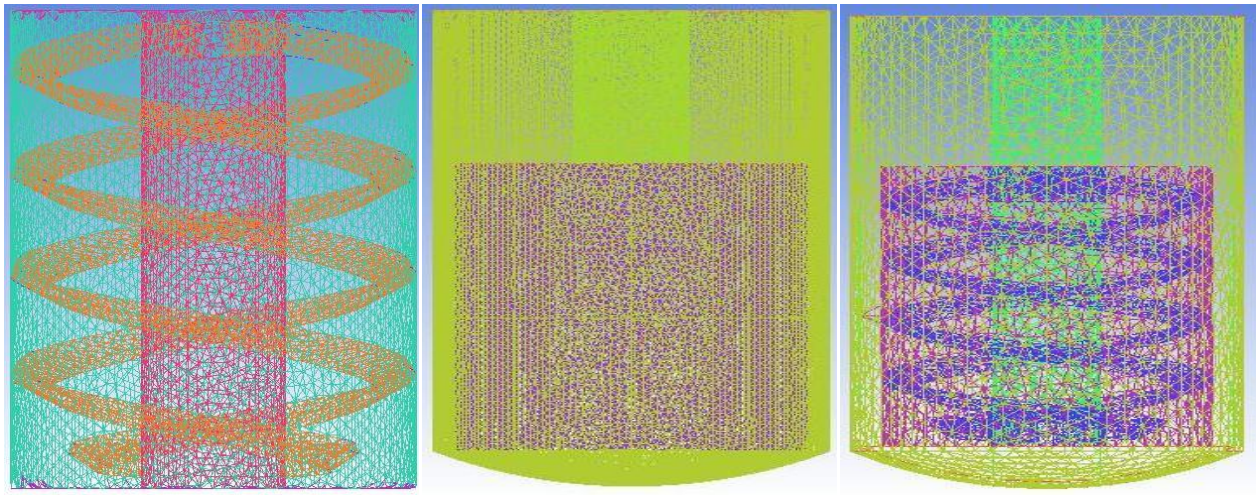

A) Impeller mesh B) Tank mesh C) Full geometry mesh

The velocity profiles predicted by CFD simulation for double helical ribbon impeller are shown in Figure 7.7. Figure 7.7A details the velocity profile of water at 340 rpm. While designing the impeller, the required rpm for efficient mixing was calculated as 340 rpm. Hence, a comparison was made between the velocity profiles of biomass slurry with 25 % solids by weight and water at the same rotational speed. It is evident from Figure 7.7B that this impeller shows higher mixing efficiency for highly viscous biomass slurries. The maximum velocity of 2.56 m/s was obtained for biomass slurry which was higher than the maximum velocity value of 2.46 m/s when water was used as a fluid. This might be due to the fact that

the fluid is still in laminar regime because of the low Reynolds number. Also, this observation is matching with the reported conclusions that the helical impellers are better suited for mixing of high viscous samples and not suitable for low viscous fluid mixing (Robinson and Cleary, 2012).

Figure 7.7: Velocity profiles predicted by CFD for double helical impeller at different rotation speeds

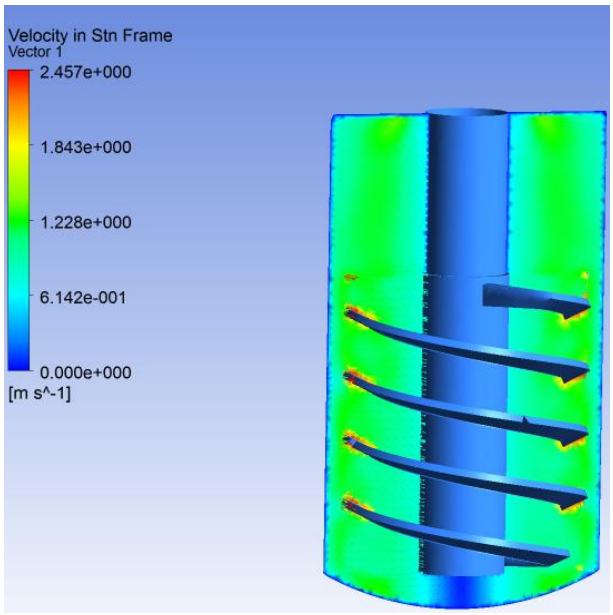

A) Velocity profile of water at 340 rpm

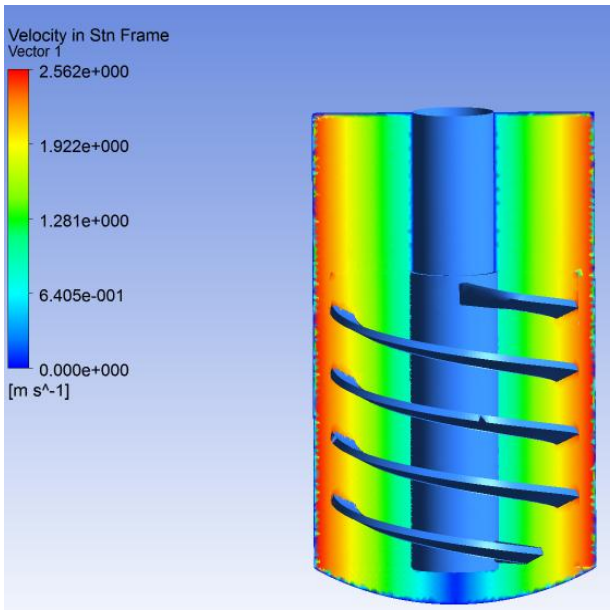

B) Velocity profile of biomass slurry (25%) at 340 rpm

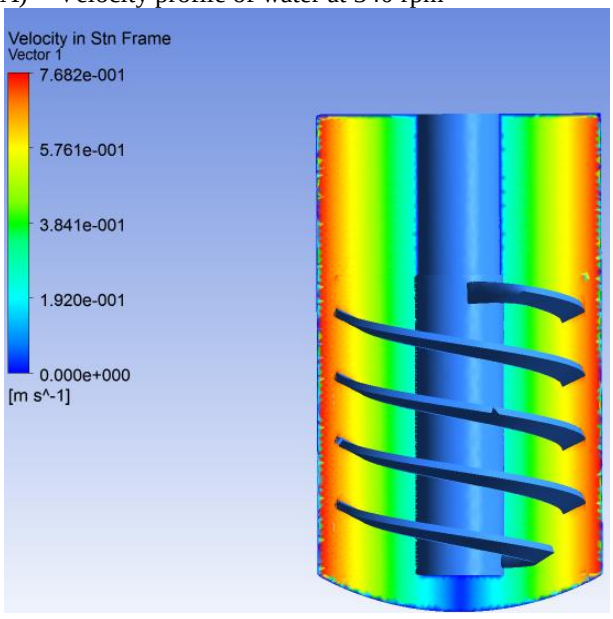

C) Velocity profile of biomass slurry at 100rpm

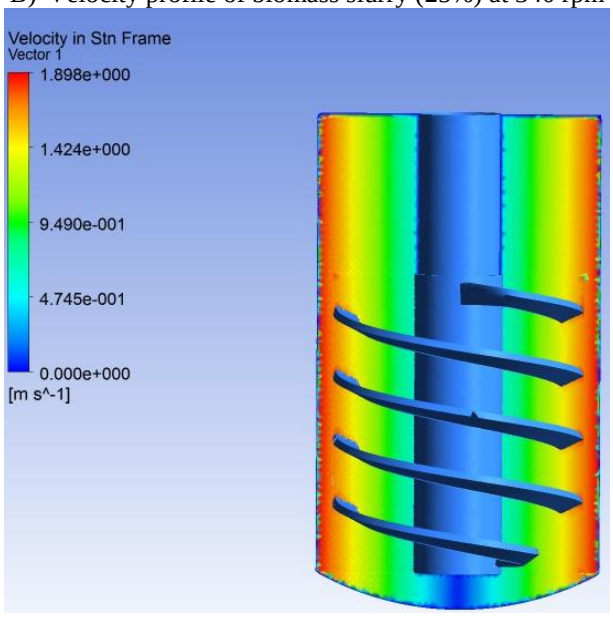

D) Velocity profile of biomass slurry 250 rpm

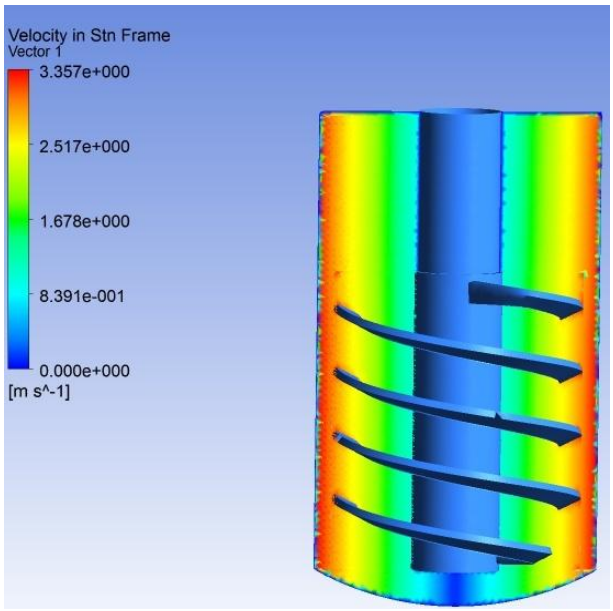

E) Velocity profile of biomass slurry at 450 rpm

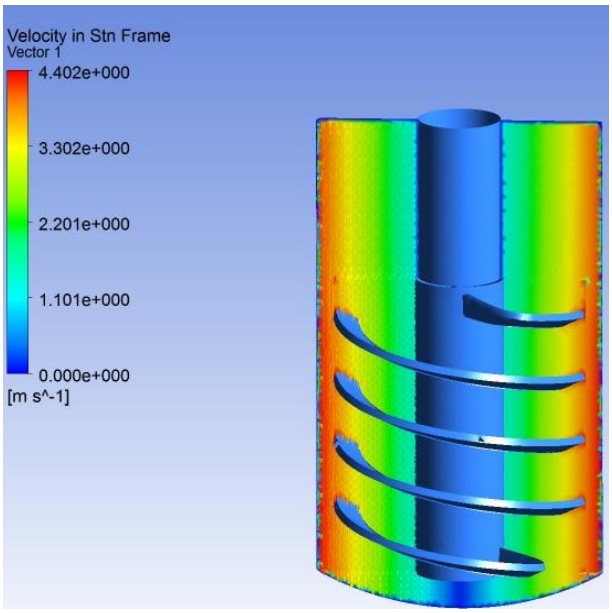

F) Velocity profile of biomass slurry at 600 rpm

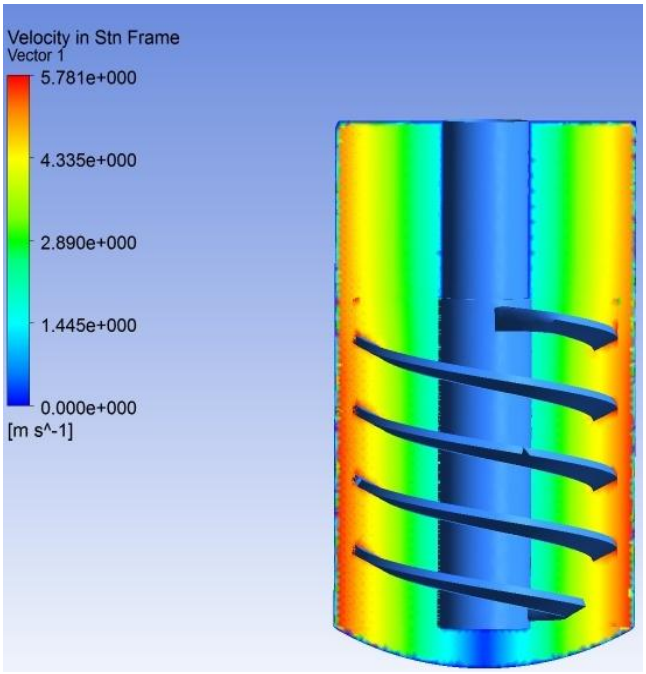

G) Velocity profile of biomass slurry at 800 rpm

When the rotation speed was reduced to a lower value of 100 rpm (Figure 7.7C), it was observed that efficient mixing is present closer to walls of the reactor. The maximum velocity was around 0.768 m/s for biomass slurry, but the mixing was more or less uniform throughout the reactor. As the rotation speed is

increased the maximum fluid velocity also increases. Also, in all the cases, velocity values were higher near the walls of the reactor than the edges of the impeller. Closer to shaft, mixing was lesser. At 250 rpm (Figure 7.7D), maximum liquid velocity increased to 1.896 m/s. For 400 rpm the maximum velocity increased to 3.357 m/ (Figure 7.7E) and the maximum velocity was around 4.402 m/s when the rotational speed of the impeller was increased to 600 rpm (Figure 7.7F).When the rotational speed was further increased to 800 rpm, the maximum velocity of the biomass slurry was found to be around 5.781 m/s (Figure 7.7G).

Thus, in comparison to Rushton turbine impeller, double helical impeller gives higher mixing efficiency and higher uniform velocity distribution. Also, this impeller has the advantage of attaining higher velocities at relatively lower rotation speeds and maintaining a laminar flow throughout the reactor region. From the mixing profiles, it could be observed that there was no stagnant zone formation and hence, a relatively efficient mixing could be attained.

Hence, it could be conclusively stated from the CFD simulation results that helical impellers are better suited for high solid loading enzymatic hydrolysis of lignocellulosic biomass in comparison with the conventional Rushton turbines.

The various characteristic curves for the results obtained from CFD simulations were plotted. Torque was obtained from the simulation results and was substituted in equation 12 to calculate the power imparted by impeller. This value was then used in equation 13 to calculate the power number. Reynolds number was then calculated using equation 14. Shear rate was also obtained from the simulation result which was substituted in the viscosity equation to calculate the value of apparent viscosity.

Figure 7.8A shows the variation of power number with respect to Reynolds number. Power number decreases as Reynolds number increases. A similar observation was reported by Ameur et al., (2013). The possible reason for such a rapid decrease in power number could be due to a rapid reduction in apparent viscosity with increase in impeller rotation speed (Ameur et al., 2013). Figure 7.8B shows the logarithmic power number variation with logarithmic Reynolds number. Zhang et al., (2014b) also reported a similar trend and he observed that increase in impeller speed leads to increased viscous dissipation, thus resulting in lower power numbers.

Figure 7.8: Power number as a function of Reynolds number

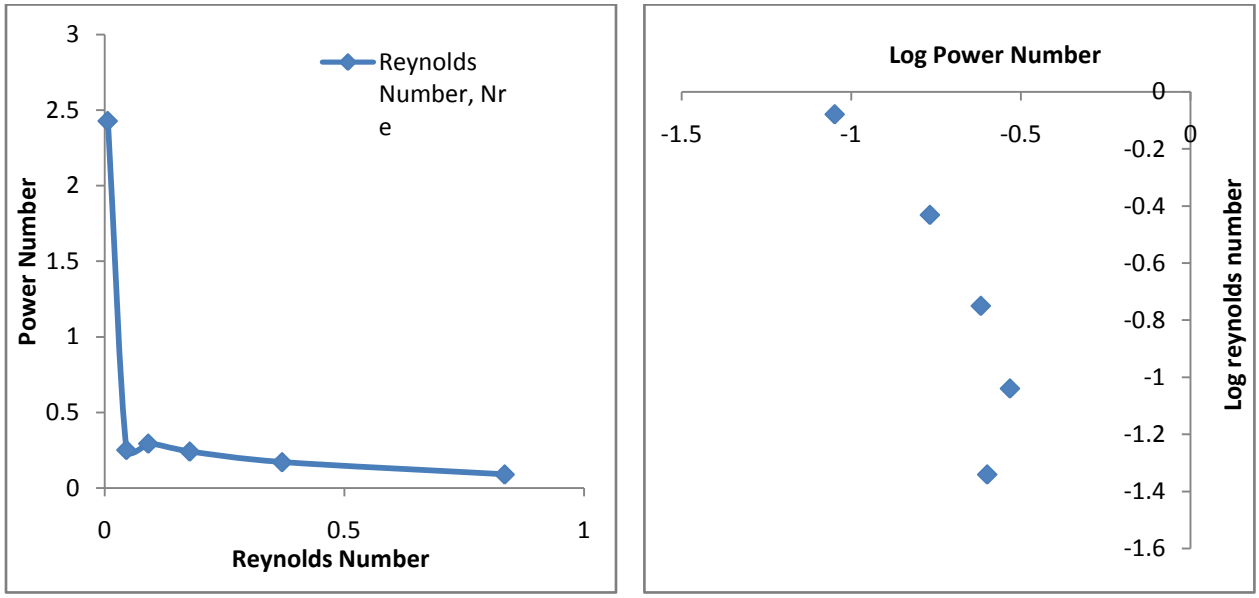

A) On a normal scale

B) On logarithmic scale

Figure 7.9: Shear rate and apparent viscosity as a function of impeller speed

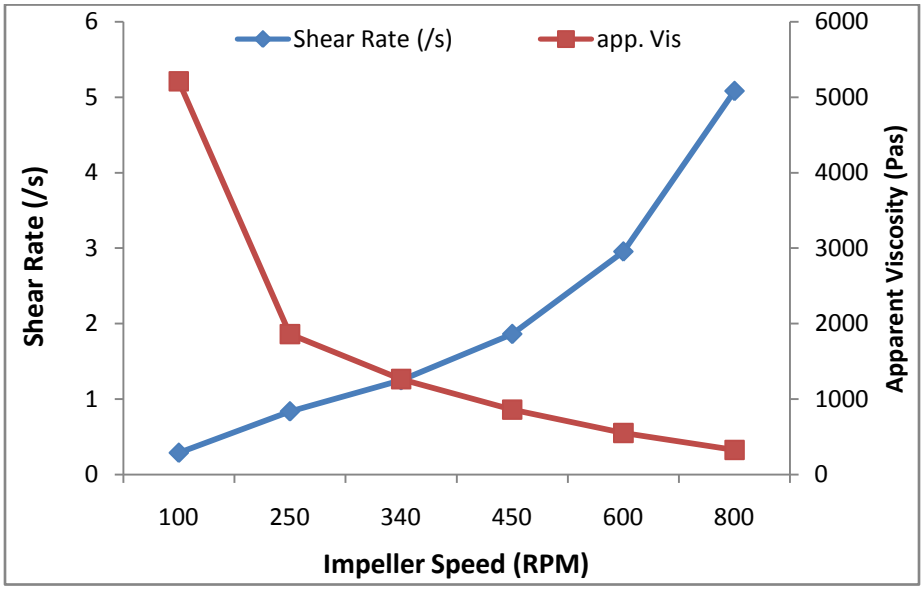

The values of shear rate and apparent viscosity as obtained from CFD simulations were plotted as a function of rotational speed in Figures 7.9 to 7.11 on different scales. From Figure 7.9, it can be observed that the increase in impeller speed results in increase in the shear rate and hence the apparent viscosity of the biomass slurry decreases. When the shear rate and apparent viscosity are plotted on the logarithmic

scale, it shows a linear variation with a negative slope (Figure 7.19). A similar trend was reported by Zhang et al., (2014b).

Figure 7.10: Logarithm of apparent viscosity as a function of logarithm of shear rate.

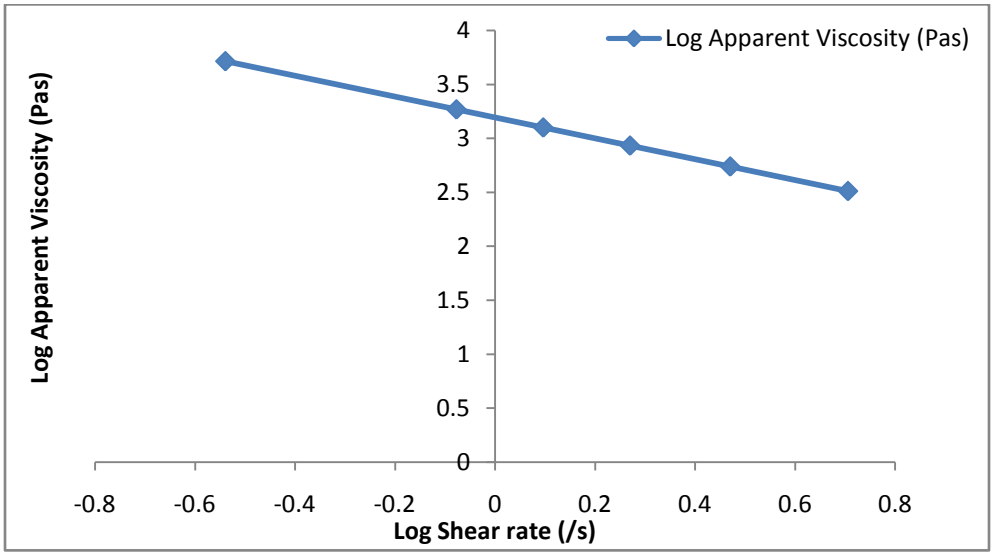

Figure 7.11: Shear rate and torque as a function of impeller speed

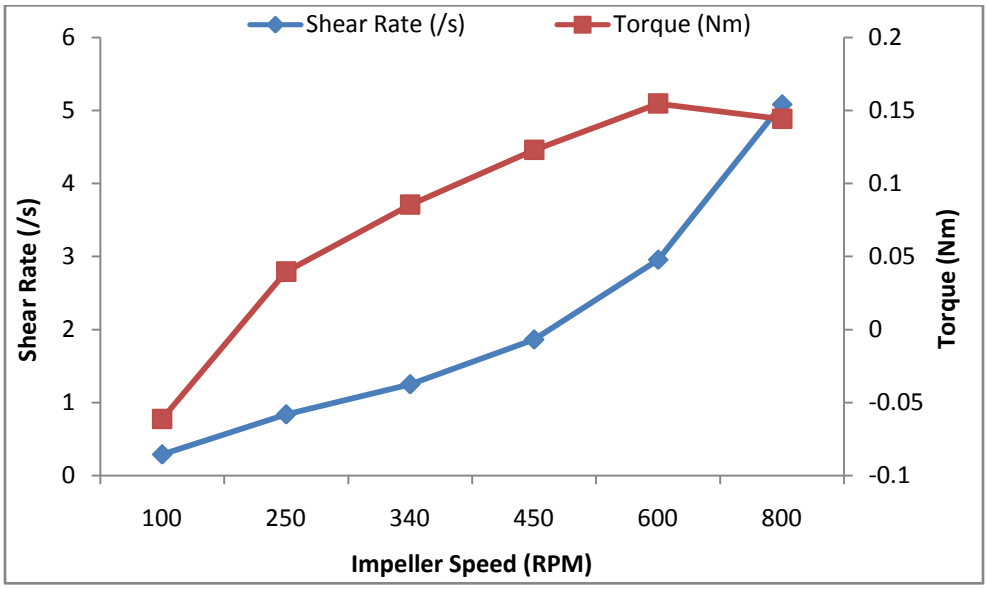

A rapid increase in torque with increase in impeller speed was reported by Carvajal et al., (2012). A comparable pattern was obtained in the present study also (Figure 7.11). A speedy increase in impeller power was observed with increase in impeller rotation speed (Figure 7.12) as observed by Zhang et al., (2014b).

Figure 7.12: Impeller power as a function of impeller rotation speed

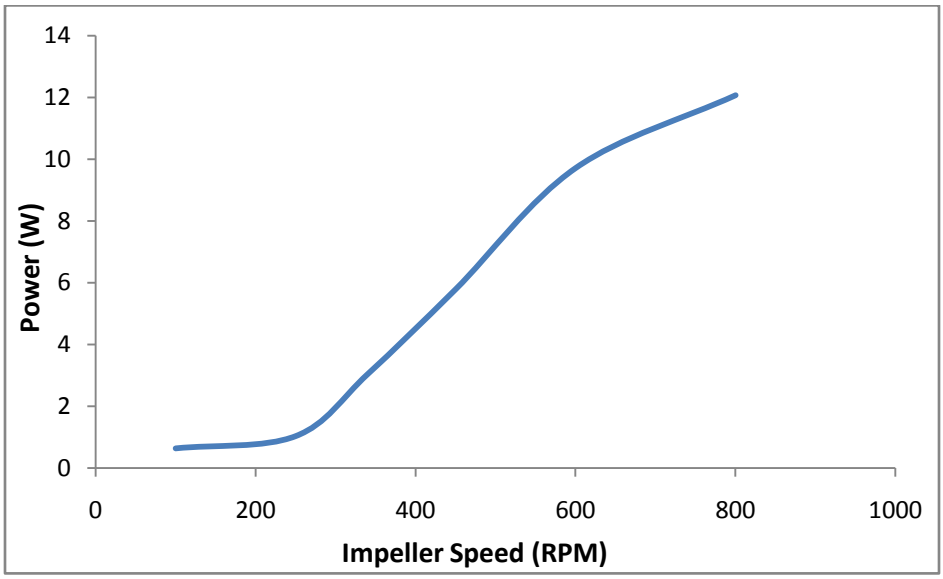

Processing of non-Newtonian slurries with high biomass loadings is challenging due to their very high viscosities and complex rheology which cause problems with mixing that results in poor mass and heat transfer. Many reactor configurations have been designed to effectively mix high solid containing slurries: a laboratory ball mill (Mohagheghi et al., 1992), a theoretical continuous tower reactor design (Nguyen, 1998), a paddle-impeller reactor of Tengborg et al. (2001) and an attrition bioreactor (ABR) (Jones and Lee, 2004). These reactors suffer from a major drawback that they require high power for agitation, which make their scalability a challenge. Zhang et al., (2009a) reports mixing energy requirements equal to as high as 59% of the higher heating value of the ethanol produced at 30% biomass loading, corresponding to a mean power input of 3.9 kW/ton slurry.

Dasari et al. (2009) achieved adequate mixing at only 2 rpm. They used a horizontal scraped surface bioreactor for their studies and hence the required power input was greatly reduced to a maximum of 0.56 kW/m^3 slurry at 25% solids loading. He et al., (2014) used helically agitated impellers for pretreatment of biomass with very high loadings up to 50% and have carried out CFD simulations to determine mixing efficiency. They reported higher pretreatment efficiency and lower inhibitor generation due to mixing with helical agitators. They could achieve a high heat and mass transfer efficiency with just 50 rpm impeller speed as per CFD modeling results.

Many studies have been carried out to determine the efficacy of helical impellers on highly viscous liquids mixing. Usually, close clearance impellers are used to obtain adequate mixing under laminar flow regimes. For agitation with helical impellers, mixing first occurs in the region near impeller blades and the vessel wall where the shear strain is very high. Uniformity in mixing is then attained by the

axial vortex flow induced by the rotation of the helical ribbon impeller. It has been shown that this kind of impeller is very effective in mixing high viscous fluids (Tsui and Hu, 2011).

Robinson and Cleary (2012) analyzed the helical ribbon mixer and designed various impeller configurations for a high viscous mixing system. Wu (2012) compared 6 different impeller types for mixing high solids anaerobic digestion system and found that helical impeller performed the best. Many studies report the usage of helical impellers for enzymatic hydrolysis of lignocellulosic biomass and subsequent fermentation. Helical impellers have also been applied in pretreatment reactors for dry dilute acid pretreatment (Zhang et al., 2010; Liu et al., 2012; Zhao et al., 2013). The results were found to be promising and showed that the enzymatic conversion yield and pretreatment efficiency significantly improved.

Computational fluid dynamics (CFD) has been used for simulating the mixing performance of high solids loading systems (Renzo and Maio, 2007; Habla, 2011). Yu et al. (2011) developed a numerical method to simulate mixing in high solids digesters using helical ribbon mixers. In their studies, the slurry contained only 5% solids content and the Newtonian fluid was assumed for the CFD modeling. Giuseppina et al., (2005) studied the stirred Newtonian and pseudo plastic liquids by CFD simulations and validated the mixing times experimentally. A CFD model was developed based on the rheological model and was used to simulate the power consumption and mixing efficiency of corn stover–water system under helical ribbon agitated mixing, for dilute acid pretreatment of corn stover (Zhang et al., 2014b).

Ameur et al., (2013) have used CFD to compare the efficiency and performance of helical and double helical impellers. They have determined the effect of impeller speed, fluid rheology, impeller off bottom clearance etc. on the mixing efficiency. CFD was used to compute the Metzner constant, k in a double helical impeller with a non – Newtonian flow (Zhang et al., 2008). A dual coaxial mixer system containing Rushton turbine and helical ribbon was used to determine the ungassed power measurements for non Newtonian fluids. The experimentally predicted and CFD given values were compared (Espinosa – Solares et al., 1997).

7.4. Conclusions

Experimentally verifying the efficacy of different impeller types is a costly and time consuming process. CFD offers the advantage of accurately predicting the mixing profiles, velocity profiles, viscosity profiles etc., of the biomass slurry at any point of time in any part of the reactor. CFD thus makes it easier in predicting the best impeller geometry for high solid loading lignocellulosic enzymatic hydrolysis. A large number of trials can be done simultaneously and hence requirement of experimentation reduces to

validation checks of predicted outcomes. From the results of the present study, it can be concluded that stirred tank with conventional Rushton turbine is not suited for enzymatic saccharification due to the inefficiency in mixing and formation of large number of stagnant zones. On the other hand, double helical impeller mixes the slurry with a laminar flow regime and mixing is uniform throughout the reactor. Maximum velocity is observed at the edges of reactor wall and impeller blades. One drawback of this impeller type could be lower efficiencies in mixing liquids with lower viscosity. Hence after the initial liquefaction period, the reaction contents may need to be shifted to a conventional STR with turbines for higher sugar yields. This has to be verified with varying concentration and time in the simulation.

Chapter 8
Summary and Conclusions

8.1. Summary

Bioethanol production from lignocellulosic biomass is not yet a commercial reality due to the huge costs involved. The most energy and cost intensive unit operation in the second generation alcohol production is enzymatic saccharification of biomass. The major problems involved here are the high costs of enzymes, long reaction durations, inefficient enzyme mixtures, lack of knowledge on exact mechanism of action of cellulase enzymes, lower substrate loadings, unavailability of reactors capable of handling high substrate loadings etc. Hence, an attempt to address some of these issues was made in this study.

Investigations on the optimization of BGL and cellulase loadings for efficient enzymatic hydrolysis of lignocellulosic biomass carried out in this work lead to the conclusion that the effectiveness of hydrolysis strongly depends upon the cellulase and beta-glucosidase loadings. In the initial studies, overall sugar yields were found to be lower than optimum efficiencies previously reported. Hence studies were carried out with higher loadings of BGL and other accessory enzymes to maximize hydrolysis efficiencies. In the kinetics experiments with both xylanase and BGL, maximum efficiency achieved was 87% with 20 FPU/g cellulase, 10 IU/g BGL and 7500 U/g xylanase upon 48 h of incubation. It was observed that majority of the reaction was over by 12 h. Of the three enzymes, xylanase had a most profound effect on sugar yield. The cocktail studied, performed much better than the commercial enzymes. The maximum efficiency for the commercial cellulase -Zytex was 40% after 48 h. SacchariCEB C6 being designed as a biomass hydrolyzing enzyme, gave an efficiency of 54%. Cellic CTec 2® one of the world's best enzymes for biomass hydrolysis was only marginally better in hydrolysis efficiency than the optimized cocktail. The combination recommended for hydrolysis of alkali pretreated rice straw was 10 FPU/g cellulase, 5 IU/g BGL and 7500 U/g xylanase.

It was found that particle size did not have a significant impact on sugar yield and hence mixed particle size (as obtained from knife mill with 1mm pore size sieve) was recommended. The variation in sugar yield upon increase in biomass loading was profound. Higher biomass loading led to a decrease in yield and hence lower efficiency of hydrolysis. At 18% solids loading, a hydrolysate with around 133 mg/mL total sugars was obtained which contained 78 mg glucose. This hydrolysate needs to be concentrated only twice to yield enough sugars to be fermented to produce adequate alcohol that can be separated by distillation.

The high regression values close to unity indicate the adequacy of the ANN models developed in all the cases to predict the reducing sugar yields upon different enzyme loadings. This model can predict

not only the reducing sugar yield profiles, but can also determine the optimum range of enzyme loadings and biomass loadings to obtain optimum reducing sugar yields. The optimum hydrolysis condition for rice straw was determined as 10 FPU/g Cellulase, 5 IU/g BGL, 7500 U/g Xylanase, 18% solid loading by weight and a mixed particle size with reaction time between 12-28 hours.

Cellulase adsorption plays a major role in efficient enzymatic hydrolysis. During hydrolysis, it was found that activity of all enzymes bound to biomass is much lower than the activity in free liquid. This might be due to the excess addition of enzymes. Activity of enzymes in free liquid and in bound state increases during initial hours of hydrolysis. Later it starts decreasing. From the fluorescence assay with FITC labeled antibody against endoglucanase, it was confirmed that binding of enzyme to biomass reduces as hydrolysis proceeds and becomes constant after about 12 h of reaction. Adsorbed endoglucanase activity follows a similar trend as that of fluorescence assay of biomass. It increases in the initial hours of hydrolysis and then reduces/stabilizes towards the end. The relative ash content and acid insoluble lignin content of biomass increases till 24 h of hydrolysis. Also, the cellulose content reduces from around 58% to 10% of biomass during hydrolysis.

Particle size of biomass continuously decreased as hydrolysis progressed. The distribution shifts towards lower particle size range toward the end of hydrolysis. The IR spectrum showed decrease in transmittance at wavenumbers that are specific for lignin and phenolics which implies that the lignin content of the biomass relatively increases as hydrolysis proceeds. The crystallinity of the biomass decreased and amorphous region increased with time during hydrolysis. This symbolized cellulose removal from biomass and increase in lignin (lignin content makes biomass amorphous). SEM images proved that the structure of biomass gets disrupted upon enzyme action.

For relatively smaller loadings up to 10%, batch or semi batch operation gave similar yields. For higher loadings, batch operations are not feasible, particularly above 17.5% due to inefficient mixing. For higher loadings up to 25%, semi batch operation with intermittent enzyme and biomass loadings was optimum due to higher glucose yields. Loadings higher than 25% were difficult to mix and hence efficiencies were much lower. Maximum concentration of 136 mg/mL glucose was obtained with 30% loading and 48 h incubation.

Enzyme recycling was attempted using magnetic nanoparticle (MNP) immobilized BGL. The synthesized magnetic nanoparticle was confirmed to be magnetite using various techniques. The size of MNPs was between 50 – 55 nm as per DLS and AFM studies. The MNPs were silica coated which was confirmed through XRD and FTIR analyses. Enzymatic hydrolysis with free and immobilized BGL yielded similar results. Immobilized BGL retained up to 69% activity after 5 cycles of hydrolysis. Upon hydrolysis with 30 IU/g BGL, it was found that sugar release was higher. When hydrolysis was carried out with 60 IU/g BGL, the sugar release maximized at around 12 h and then started gradually decreasing.

MNP immobilized BGL can be effectively used to economize the hydrolysis process owing to its reusability. Also, higher BGL loadings are possible with MNP-BGL which maximizes sugar release in lesser hydrolysis times.

High solid loading reactors are significant in enhancing the efficiency of enzymatic hydrolysis of lignocellulosic biomass. CFD approach reduces the time and investment required to design such reactors. From the present study, it was found that even at very high impeller rotation speeds like 2000 rpm, Rushton turbine was not efficient in mixing biomass slurries. Mixing in this case was observed only near the impeller blades. Thus, it could not be used for enzymatic saccharification upon higher solid loadings. Double helical impeller was found to have a better mixing pattern compared to Rushton turbine. Mixing was observed throughout the reactor and higher mixing velocities were found near the impeller blades and reactor walls. As the rotation speed increased, apparent viscosity decreased and shear rate increased. Power consumption also rose with higher mixing speeds. The relation between power number and Reynolds number obtained in the present study was comparable with that of literature reported relations. Thus, double helical impeller could be used to obtain higher saccharification yields during high solid loading enzymatic hydrolysis of biomass.

8.2. Conclusions

This study is focused on developing various strategies for enhancement of the efficiency of enzymatic hydrolysis process to make it a cost effective unit operation. Artificial Neural network (ANN) models were developed to optimize the enzyme cocktail for saccharification as well as to predict the sugar yields during hydrolysis at different substrate factors and enzyme loadings. Supplementation with accessory enzymes enhances the hydrolytic efficiency. Adequate supplementation can reduce the reaction time economizing the overall unit operation.

During hydrolysis, activity of all enzymes bound to biomass is much lower than the activity in free liquid. This indicates that lower protein loadings might be sufficient for higher hydrolysis efficiencies. Also, a significant portion of enzyme is lost due to irreversible binding on lignin. As hydrolysis proceeds, the residual biomass becomes more of lignin and less of cellulose. The most significant time for hydrolysis reaction is between 4 – 12 h. Not much change in biomass was observed physically as well as chemically after 12 h of reaction. Also, adsorption – desorption of enzymes attain equilibrium after this time. Hence hydrolysis beyond 12 h does not yield higher sugars and reaction can be terminated at 12 h to reduce the reaction times. Further studies need to be carried out to determine the adsorption and desorption pattern of cellulase from biomass.

Semi batch process is more efficient in keeping the reaction rates higher. Immobilized BGL can be recycled without loss in activity. Thus higher loadings of BGL can be used that can enhance reaction rates and efficiency. Significantly higher BGL loadings aids in further bringing down the reaction times to 8-12 h which can bring significant savings in hydrolysis operation. CFD studies proved the inefficiency of conventional Rushton turbine impellers to efficiently mix high solid biomass slurries during hydrolysis. Hence, double helical impeller is proposed as alternate impeller geometry for efficient hydrolysis.

8.3. Future Perspectives

In the present work, separate ANN models were developed to predict the sugar yields upon a) varying enzyme loadings and time; b) varying biomass loadings, particle size and time. An integrated ANN model that includes all the factors affecting enzymatic hydrolysis like enzymes loading, biomass loading, particle size of biomass, time, hydrolysis temperature, pH etc. needs to be developed. Such a model can be an efficient tool to predict the sugar yields at different reaction conditions.

From the adsorption studies, it was found that maximum amount of enzymes added to the hydrolysis mixture was free in the supernatant. So, adsorption studies with lower loadings need to be carried out to determine the minimum enzyme loading that can achieve high sugar yields. Also, enzyme adsorption – desorption dynamics study needs to be carried out to better reveal the mechanism of cellulose hydrolysis. Adsorption dynamics of xylanase also needs to be studied to understand the role and significance of xylanases in cellulose hydrolysis.

Feeding times for enzymes and biomass needs to be optimized for high solid loading lignocellulosic biomass enzymatic hydrolysis.

Apart from BGL, immobilization studies needs to be carried out for cellulases and xylanases as well, so that these enzymes can be recycled after hydrolysis. This could then lead to a more economic hydrolysis process. Magnetic nanoparticle immobilization process needs to be optimized to increase the efficiency of immobilization.

CFD studies with conventional Rushton turbine and double helical impeller could only be carried out to predict the best impeller type for high solid loading reactors. In addition to the helical impeller, fluid dynamics studies needs to be carried out with other impeller models like anchor impeller, segmented helical impeller etc. With the impeller that is found best suited for high loading hydrolysis, a reactor prototype needs to be fabricated and all the experimental data can be validated in here. CFD studies also need to be carried out for determining mixing efficiency and power requirements throughout the course of reaction so as to determine the rheological behavior of rice straw.

References

Abraham, R.E., Verma, M.L., Barrow, C.J., Puri, M., 2014. Suitability of magnetic nanoparticle immobilized cellulases in enhancing enzymatic saccharification of pretreated hemp biomass. Biotechnol. Biofuels, 7, 90.

Aden, A., Ruth, M., Ibsen, K., Jechura, J., Neeves, K., Sheehan, J., Wallace, B., Montague, L., Slayton, A., Lukas, J., 2002. Lignocellulosic biomass to ethanol process design and economics utilizing co-current dilute acid prehydrolysis and enzymatic hydrolysis for corn stover. Technical Report: TR-510-32438. NREL.

Ahmad, R., Sardar, M., 2014. Immobilization of cellulase on TiO_2 nanoparticles by physical and covalent methods: A comparative study. Indian J. Biochem. Biophys., 51, 314-320.

Aissaoui, N., Bergaoui, L., Boujday, S., Lambert, J.F., Méthivier, C., Landoulsi, J., 2014. Enzyme immobilization on silane-modified surface through short linkers: Fate of interfacial phases and impact on catalytic activity. Langmuir, 30, 4066–4077.

Alasepp, K., Borch, K., Cruys-Bagger, N., Badino, S., Jensen, K., Sørensen, T.H., Windahl, M.S., Westh, P., 2014. In Situ Stability of Substrate-Associated Cellulases Studied by DSC. Langmuir, 30, 7134−7142.

Alex, D., Mathew, A., Sukumaran, R.K., 2014. Esterases immobilized on amino-silane modified magnetic nanoparticles as a catalyst for biotransformation reactions. Bioresour. Technol., 167, 547–550.

Alftre´n, J., Hobley, T.J., 2014. Immobilization of cellulase mixtures on magnetic particles for hydrolysis of lignocellulose and ease of recycling. Biomass Bioenergy, 65, 72 -78.

Alvira, P., Negro, M.J., Ballesteros, M., 2011. Effect of endoxylanase and a-L-arabinofuranosidase supplementation on the enzymatic hydrolysis of steam exploded wheat straw. Bioresour. Technol., 102, 4552 - 4558.

Ameur, H., Bouzit, M., Ghenaim, A., 2013. Hydrodynamics in a vessel stirred by simple and double helical impellers. Cent. Eur. J. Eng., 3, 87 – 98.

Andrić, P., Meyer, A.S., Jensen, P.A., Dam-Johansen K. 2010. Effect and modeling of glucose inhibition and in situ glucose removal during enzymatic hydrolysis of pretreated wheat straw. Appl. Biochem. Biotechnol., 160, 280–97.

Anwar, Z., Gulfraz, M., Irshad, M., 2014. Agro-industrial lignocellulosic biomass a key to unlock the future bio-energy: A brief review. J. Rad. Res. Appl. Sci., 7, 163-173.

Arantes, V., Saddler, J.N., 2010. Access to cellulose limits the efficiency of enzymatic hydrolysis: the role of amorphogenesis. Biotechnol. Biofuels, 3:4.

Arantes, V., Saddler, J.N., 2011. Cellulose accessibility limits the effectiveness of minimum cellulase loading on the efficient hydrolysis of pretreated lignocellulosic substrates. Biotechnol. Biofuels, 4, 3.

Bailey, M.J., Biely, P., Poutanen, K., 1992, Inter laboratory testing of methods for assay of xylanase activity. J. Biotech., 23, 257-270.

Ballesteros, I., Negro, M.J., Oliva, J.M., Cabanas, A., Manzanares, P., Ballesteros, M., 2006. Ethanol production from steam-explosion pretreated wheat straw. Appl. Biochem. Biotechnol. 129, 496-508.

Banerjee, G., Car, S., Scott – Craig, J.S., Borrusch, M.S., Walton, J.D., 2010a. Rapid optimization of enzyme mixtures for deconstruction of diverse pretreatment/biomass feedstock combinations. Biotechnol. Biofuels, 3, 22.

Banerjee, G., Scott-Craig, J.S,, Walton, J.D., 2010b. Improving enzymes for biomass conversion: a basic research perspective. Bioenerg. Res., 3, 82–92.

Bas, D., Boyaci, I.H., 2007. Modeling and optimization II: comparison of estimation capabilities of response surface methodology with artificial neural networks in a biochemical reaction. J. Food Eng., 78, 846-854.

Beg, Q.K., Kapoor, M., Mahajan, L., Hoondal, G.S., 2001. Microbial xylanases and their industrial applications: A review. Appl. Microbiol. Biotechnol., 56, 326–338.

Beldman, G., Voragen, A.G.J., Rombouts, F.M., Searle-van-Leeuwen, M.F., Pilnik, W., 1987. Adsorption and kinetic behavior of purified endoglucanases and exoglucanases from *Trichoderma viride*. Biotechnol. Bioeng, 30, 251–257.

Bell, J.L., Attfield, P.V., 2006. Breakthrough in yeast for making bio-ethanol from lignocellulosics. Sydney, NSW2109, Australia: Microbiogen Pty LTD, Macquarie University Campus.

Bendl, R.F., Kandel, J.M., Amodeo, K.D., Ryder, A.M., Woolridge, E.M., 2008. Characterization of the oxidative inactivation of xylanase by laccase and a redox mediator. Enzym. Microb. Technol., 43, 149–156.

Berger, P., Adelman, N.B., Beckman, K.J., Campbell, D.J., Ellis, A.B., Lisensky, G.C., 1999. Preparation and properties of an Aqueous Ferrofluid. J. Chem. Educ., 76, 943-948.

Berlin, A., Balakshin. M., Gilkes, N., Kadla, J., Maximenko, V., Kubo, S., 2006. Inhibition of cellulase, xylanase and β-glucosidase activities by softwood lignin preparations. J. Biotechnol. 125, 198–209.

Berlin, A., Maximenko, V., Gilkes, N., Saddler, J. 2007. Optimization of enzyme complexes for lignocellulose hydrolysis. Biotechnol. Bioeng., 97, 287–296.

Billard, H., Faraj, A., Ferreira, N.L., Menir, S., Heiss-Blanquet, S., 2012. Optimization of a synthetic mixture composed of major *Trichoderma reesei* enzymes for the hydrolysis of steam-exploded wheat straw. Biotechnol. Biofuels, 5, 9.

Binder J.B., Raines, R.T., 2010. Fermentable sugars by chemical hydrolysis of biomass. Proc. Natl. Acad. Sci. U.S.A., 107, 4516–4521.

Bird, R. B., Warren, W. S., Lightfoot, E. N. 2002. Transport phenomena, 2nd edition, John Wiley & Sons, Inc., New York.

Blanchard, C.R., 1996. Atomic Force Microscopy. The Chemical Educator, 1, 1-8.

Bo, Z., Jian-Min, X., Yu-Qi, L., Hui-Zhou, L., 2008. Synthesis of amino-silane modified magnetic silica adsorbents and application for adsorption of flavonoids from *Glycyrrhiza uralensis* Fisch. Sci. China Ser. B Chem., 51, 145-151.

Bommarius, A.S., Katona, A., Cheben, S.E., Patel, A.S., Ragauskas, A.J., Knudson, K., 2008. Cellulase kinetics as a function of cellulose pretreatment. Metab. Eng., 10, 370-381.

Bonnin, E., Clavurier, K., Daniel, S., Kauppinen, S., Mikkelsen, J.D., Thibault, J.F., 2008. Pectin acetylesterases from Aspergillus are able to deacetylate homogalacturonan as well as rhamnogalacturonan. Carbohydr. Polym., 74, 411–418.

Borges, D.G., Baraldo, A., Farinas, C.S., Giordano, R.L.C., Tardioli, P.W., 2014. Enhanced saccharification of sugarcane bagasse using soluble cellulase supplemented with immobilized b-glucosidase. Bioresour. Technol., 167, 206–213.

Boussaid, A., Saddler, J.N., 1999. Adsorption and activity profiles of cellulases during the hydrolysis of two Douglas fir pulps. Enzyme Microb. Technol., 24, 138–143.

Bozell, J.J., Petersen, G.R., 2010. Technology development for the production of biobased products from biorefinery carbohydrates-The US Department of Energy's "Top10" revisited, Green Chem., 12, 525-728.

Bradford, M.M., 1976. A rapid and sensitive method for the quantization of microgram quantities of protein utilizing the principle of protein dye binding. Anal. Biochem., 72, 242-254.

Bura, R., Chandra, R., Saddler, J., 2009. Influence of xylan on the enzymatic hydrolysis of steam-pretreated corn stover and hybrid poplar. Biotechnol. Prog., 25, 315-322.

Bustamante, C., Rivetti, C., Keller, D.J., 1997. Scanning force microscopy under aqueous solutions. Curr. Opin. Struct. Bio., 7,709-716.

Byung-Hwan, U., Hanley, T.R., 2008. High-Solid Enzymatic Hydrolysis and Fermentation of Solka Floc into Ethanol. J. Microbiol. Biotechnol., 18, 1257–1265.

Caledria, K., Jain, A.K., Hoffert, M.I., 2003. Climate sensitivity uncertainty and the need for energy without CO_2 emission. Sci., 299, 2052 - 2054.

Campbell, C.J., Laherrere, J.H., 1998. The end of cheap oil. Sci. Am. 3, 78–83.

Can, K., Ozmen, M., Ersoz, M., 2009. Immobilization of albumin on aminosilane modified superparamagnetic magnetite nanoparticles and its characterization. Colloids Surf. B:, 71, 154-159.

Cardona, C.A., Sanchez, O.J., 2007. Fuel ethanol production: process design trends and integration opportunities. Bioresour. Technol., 98, 2415 - 2457.

Carrasco, F., Roy, C., 1992. Kinetic study of dilute-acid prehydrolysis of xylan containing biomass. Wood Sci. Technol., 26, 189–208.

Carvajal, D., Marchisto, D.L., Bensaid, S., Fino, D., 2012. Enzymatic hydrolysis of lignocellulosic biomasses via CFD and experiments. Ind. Eng. Chem. Res, 51, 7518–7525.

Caspeta, L., Caro-Bermúdez, M. A., Ponce-Noyola, T., Martinez, A., 2014. Enzymatic hydrolysis at high-solids loadings for the conversion of agave bagasse to fuel ethanol. Appl. Energy. 113, 277–286.

Cavaco-Paulo, A., Almeida, L., 1994. Cellulase hydrolysis of cotton cellulose: the effects of mechanical action, enzyme concentration and dyed substrates. Biocatal., 10, 353–360.

Chandra, R.P., Au-Yeung, K., Chanis, C., Roos, A.A., Mabee, W., Chung, P.A., 2011. The influence of pretreatment and enzyme loading on the effectiveness of batch and fed-batch hydrolysis of corn stover. Biotechnol. Prog., 27, 77-85.

Chandra, R.P., Bura, R., Mabee, W.E., Berlin, A., Pan, X., Saddler, J.N., 2007. Substrate pretreatment: the key to effective enzymatic hydrolysis of lignocellulosics. Adv. Biochem. Eng. Biotechnol. 108, 67–93.

Chang, Q., Tang, H., 2014. Immobilization of Horseradish Peroxidase on NH_2-Modified Magnetic Fe_3O_4/SiO_2 Particles and Its Application in Removal of 2,4-Dichlorophenol. Molecules, 19, 15768-15782.

Chang, V.S., Holtzapple, M.T., 2000. Fundamental factors affecting biomass enzymatic reactivity. Appl. Biochem. Biotechnol. 37, 84–86.

Chen, J.P., Yang, P.C., Ma, Y.H., Tu, S.J., Lu, Y.J., 2012. Targeted delivery of tissue plasminogen activator by binding to silica-coated magnetic Nanoparticle. Int. J. Nanomed., 7, 5137–5149.

Chen, X.A., Ishida, N., Todaka, N., Nakamura, R., Maruyama, J., Takahashi, H., Kitamoto, K., 2010. Promotion of efficient saccharification of crystalline cellulose by *Aspergillus fumigatus* Swo1. Appl. Environ. Microbiol., 76, 2556–2561.

Cheng, J., Li, Q.S., Xiao, R.C., 2008a. A new artificial neural network-based response surface method for Structural reliability analysis. Probab. Eng. Mech. 23, 51-63.

Cheng, K.K., Cai, B.Y., Zhang, J.A., Ling, H.Z., Zhou, Y.J., Ge, J.P., 2008b. Sugarcane bagasse hemicelluloses hydrolysate for ethanol production by acid recovery process. Biochem. Eng. J. 38, 105 – 109.

Cheng, Y. S., Zheng, Y., Yu, C. W., Dooley, T. M., Jenkins, B. M., VanderGheynst, J. S., 2010. Evaluation of high solids alkaline pretreatment of rice straw. Appl. Biochem. Biotechnol., 162, 1768 -1784.

Cherubini, F., Ulgiati S., 2010. Crop residues as raw materials for biorefinery systems –A LCA case study. Appl. Energy, 87, 47-57.

Chew, T.L., Bhatia, S., 2008. Catalytic processes towards the production of biofuels in a palm oil and oil palm biomass-based biorefinery. Bioresour. Technol., 99, 7911–7922.

Chundawat, S.P., Venkatesh, B., Dale, B.E., 2007. Effect of particle size based separation of milled corn stover on AFEX pretreatment and enzymatic digestibility. Biotechnol. Bioeng. 96, 219–231.

Corpstein, R.R., Fasano, J.B., Myers, K.J., 1994. The high efficiency road to liquid-solid agitation. Chem. Eng. J., 138–144.

Couper, J.R., Penney, W.R., Fair, J.R., Walas, S.H., 2005. Chemical Process Equipment. Second Edition. Elsevier Inc. 277-327.

Cui, M., Zhang, Y., Huang, R., Su, R., Qia, W., Hea, Z., 2014. Enhanced enzymatic hydrolysis of lignocellulose by integrated decrystallization and fed-batch operation. RSC Adv., 4, 44659 – 44665.

Dasari, R. K., Dunaway, K., Ye, Z., Berson, R. E., 2007a. Power consumption in a scraped surface bio-reactor for batch and fed-batch enzymatic hydrolysis of pretreated corn stover slurries. The 29th Symposium on Biotechnology for Fuels and Chemicals. Denver. CO. U.S.A.

Dasari, R.K., Berson, R.E., 2007b. The Effect of Particle Size on Hydrolysis Reaction Rates and Rheological Properties in Cellulosic Slurries. Appl. Biochem. Biotechnol., ABAB Symposium, 289-299.

Dasari, R.K., Dunaway, K., Berson, R.E., 2008. A scraped surface bioreactor for enzymatic saccharification of pretreated corn stover slurries. Energy Fuels, 23, 492–497.

Del Pozo, M.V., Fernández-Arrojo, L., Gil-Martínez, J., Montesinos, A., Chernikova, T.N., 2012. Microbial β-glucosidases from cow rumen metagenome enhance the saccharification of lignocellulose in combination with commercial cellulase cocktail. Biotechnol. Biofuels, 5, 73.

Demain, A.L., Newcomb, M., Wu, J.D., 2005. Cellulase, clostridia and ethanol. Microbiol. Mol. Rev., 69, 124-154.

Demirabas, A., 2008. Products from lignocellulosic materials via degradation processs, Energy Sources Part A, 30, 27-37.

Demirbas, A., 2003. Energy and environmental issues relating to greenhouse gas emissions in Turkey. Energy Convers. Manage., 44, 201-213.

den Haan, R., van Zyl, J.M., Harms, T.M., van Zyl, W.H., 2013. Modeling the minimum enzymatic requirements for optimal cellulose conversion. Environ. Res. Lett., 8, 11 – 22.

Department of Energy. 2009. Biomass multi-year program plan. Office of the Biomass Program. US DOE. At website, http://www1.eere.energy.gov/biomass/pdfs/algal_biofuels_roadmap.pdf.

Desai, S.G., Converse, A.O., 1997. Substrate reactivity as a function of the extent of reaction in the enzymic hydrolysis of lignocellulose. Biotechnol. Bioeng., 56, 650–655.

Dijkerman, R., Bhansing, D.C., Op den Camp, H.J., van der Drift, C., Vogels, G.D., 1997. Degradation of structural polysaccharides by the plant cell-wall degrading enzyme system from anaerobic fungi: an application study. Enzyme Microb. Technol., 21, 130–136.

Dourado, F., Bastos, M., Mota, M., Gama, F.M., 2002. Studies on the properties of Celluclast/Eudragit L-100 conjugate. J. Biotechnol., 99, 121-131.

Duff, S.J.B., Murray, W.D., 1996. Bioconversion of forest products industry waste cellulosics to fuel ethanol: A review. Bioresour. Technol., 55, 1–33.

Duncan, S.M., Schilling, J.S., 2010. Carbohydrate-hydrolyzing enzyme ratios during fungal degradation of woody and non-woody lignocellulose substrates. Enzyme Microb. Technol., 47, 363–371.

Dutcher, D.D., Stolzenburg, M.R., Thompson, S.L., Medrano, J. M., Gross, D. S., Kittelson, D. B., McMurry, P. H. 2011. Emissions from ethanol-gasoline blends: A single particle perspective. Atmosphere, 2, 182-200.

Eggeman, T., Elander, R.T., 2005. Process and economic analysis of pretreatment technologies. Bioresour. Technol., 96, 2019–2025.

Ehrhardt, M., 2008. In: MS thesis: Rheology of Biomass, Chemical and Biological Engineering. University of Wisconsin, Madison. pp. 102.

Ehrhardt, M.R., Monz, T.O., Root, T.W., Connelly, R.K., Scott, C.T., Klingenberg, D.J., 2010. Rheology of dilute acid hydrolyzed corn stover at high solids concentration. Appl. Biochem. Biotechnol., 160, 1102–1115.

Ehrman, T., 1994. Determination of acid-soluble lignin in biomass. In: Laboratory analytical procedure-LAP 004, NREL.

EISA. 2007. Energy independence and security act. Federal and State incentives and Laws, http://www.afdc.energy.gov/afdc/laws/eisa; 2007.

El-Naggar, N.E., Deraz, S., Khalil, A., 2014. Bioethanol production from lignocellulosic feedstocks based on enzymatic hydrolysis: Current status and recent developments. Biotechnol, 13, 1-21.

Emmel, A., Mathias, A.L., Wypych, F., Ramos, L.P., (2003) Fractionation of Eucalyptus grandis chips by dilute acid- catalysed steam explosion. Bioresour. Technol., 2003, 86, 105-115.

Eriksson, K.E.L., Bermek, H., 2009. Lignin, lignocellulose, ligninase. Appl. Microbiol., Ind. 373–84.

Eriksson, T., Borjesson, J., Tjerneld, F., 2002. Mechanism of surfactant effect in enzymatic hydrolysis of lignocellulose. Enzyme Microb. Technol., 31, 353–364.

Espinosa-Solares, T., La-Fuente, E.B.D., Tecante, A., Tanguy, P.A., 1997. Power consumption of a dual turbine – helical ribbon impeller mixer in ungassed conditions. Chem. Eng. J., 67, 215-219.

Esteghlailian, A., 1997. Modeling and optimization of the dilute sulphuric-acid pretreatment of corn stover, poplar and switchgrass. Bioresour. Technol., 59, 129-136.

Esteghlalian, A.R., Bilodeau, M., Mansfeld, S.D., Saddler, J.N., 2001. Do enzymatic hydrolyzability and simons' stain reflect the changes in the accessibility of lignocellulosic substrates to cellulase enzymes? Biotechnol. Prog., 17, 1049–1054.

European Union. 2009. Directive on the promotion of the use of energy from renewable sources. Official J. Eur. Union.

Fan, Z. L., South, C., Lyford, K., Munsie, J., van Walsum, P., Lynd, L. R. 2003. Conversion of paper sludge to ethanol in a semi continuous solids-fed reactor. Bioprocess Biosyst. Eng., 26, 93– 101.

Faraji, M., Yamini, Y., Rezaee, M., 2010. Magnetic Nanoparticles: Synthesis, stabilization, functionalisation, characterization and applications. J. Iran. Chem. Soc., 7, 1-37.

Farrell, A.E., Plevin, R.J., Turner, B.T., Jones, A.D., O'Hare, M., Kammen, D.M., 2006. Ethanol can contribute to energy and environmental goals. Sci., 311, 506-508.

Fernando, S., Adhikari, S., Chandrapal, C., Murali, N., 2006. Biorefineries: current status challenges and future direction. Energy Fuel, 20, 1727–1737.

FitzPatrick, M., Champagne, P., Cunningham, M.F., Whitney, R.A., 2010. A biorefinery processing perspective: Treatment of lignocellulosic materials for the production of value-addued products, Bioresour. Technol., 101, 8915-8922.

Fondy, P.L., Bates, R.L., 1963. Agitation of liquid systems requiring a high shear characteristic, AIChE J., 9, 338–342.

Fontes, C., Gilbert, H., 2010. Cellulosomes: highly efficient nanomachines designed to deconstruct plant cell wall complex carbohydrates. Ann. Rev. Biochem., 79, 655–681.

Franzreb, M., Herzberg, S.M., Hobley, T.J., Thomas, O.R.T., 2006. Protein purification using magnetic adsorbent particles. Appl. Microbiol. Biotechnol., 70, 505-516.

Galbe, M., Zacchi, G., 2002. A review of the production of ethanol from softwood. Appl. Microbiol. Biotechnol., 59, 618–628.

Gan, Q., Allen, S., Taylor, G., 2005. Analysis of process integration and intensification of enzymatic cellulose hydrolysis in a membrane bioreactor. J. Chem. Technol. Biotechnol., 80, 688-698.

Gan, Q., Allen, S.J., Taylor, G., 2003. Kinetic dynamics in heterogeneous enzymatic hydrolysis of cellulose: An overview, an experimental study and mathematical modeling. Process. Biochem., 38, 1003–1018.

Gao, D., Chundawat, S.P., Krishnan, C., Balan, V., Dale, B.E., 2010. Mixture optimization of six core glycosyl hydrolases for maximizing saccharification of ammonia fiber expansion (AFEX) pretreated corn stover. Bioresour. Technol., 101, 2770–2781.

Gao, D., Uppugundla, N., Chundawat, S.P., Yu, X., Hermanson, S., Gowda, K., 2011. Hemicellulases and auxiliary enzymes for improved conversion of lignocellulosic biomass to monosaccharides. Biotechnol. Biofuels, 4, 5.

Gao, S., You, C., Renneckar, S., Bao, J., Zhang, Y.H.P., 2014. New insights into enzymatic hydrolysis of heterogeneous cellulose by using carbohydrate binding module 3 containing GFP and carbohydrate-binding module 17 containing CFP. Biotechnol. Biofuels, 7, 24.

Gargouri, M., Smaali, I., Maugard, T., Legoy, M.D., Marzouki, N., 2004. Fungus β-glycosidases: immobilization and use in alkyl-β-glycoside synthesis. J. Mol. Catal. B: Enzym., 29, 89-94.

Gervais, P., Bensoussan, M., Grajek, W., 1988. Water activity and water content comparative effects on the growth of *Penicillium roqueforti* on solid substrate. Appl. Microbiol. Biotechnol., 27, 389-392.

Ghaffari, A., Abdollahi, H., Khoshayand, M.R., Soltani, B.I., Dadgar, A., Rafiee, T.M., 2006. Performance comparison of neural Network training algorithms in modeling of bimodal drug delivery. Int. J. Pharm., 327, 126-138.

Ghosh, T.K., 1987. Measurement of cellulase activities. Pure Appl. Chem., 59, 257–268.

Ghosh, T.K., Bisaria, V.S., 1987. Measurement of Hemicellulase Activities, Part I- Xylanases. Pure Appl. Chem., 59, 1739—1752.

Giuseppina, M., Michal, M., Milan, J., Franco, M., 2005. CFD simulations and experimental validation of homogenization curves and mixing time in stirred Newtonian and pseudoplastic liquids. Chem. Eng. Sci., 60, 2427–2437.

Gnansounou, E., 2010. Production and use of lignocellulosic bioethanol in Europe: current situation and perspectives. Bioresour. Technol., 101, 4842-4850.

Goldemberg, J., 2007. Ethanol for a sustainable energy future. Science, 315, 808-810.

Graham, L.A., Belisle, S.L., Baas, C.L., 2008. Emissions from light duty gasoline vehicles operating on low blend ethanol gasoline and E85. Atmos. Environ., 42, 4498-4516.

Gregg, D., Saddler, J.N., 1996. Factor affecting cellulose hydrolysis and the potential of enzyme recycle to enhance the efficiency of an integrated wood to ethanol process. Biotechnol. Bioeng., 51, 375-383.

Grethlein, H.E., 1985. The effect of pore size distribution on the rate of enzymatic hydrolysis of cellulosic substrates. Nature Biotechnol, 2, 155-160.

Güllü, D., 2010. Effect of catalyst on yields of liquid products from biomass via pyrolysis. Energy sources, 25, 753-756.

Gupta, A.K., Gupta, M., 2005. Cytotoxicity suppression and cellular uptake enhancement of surface modified magnetic nanoparticles. Biomaterials, 26, 1565–1573.

Gupta, R., Kumar, S., Gomes, J., Kuhad, R.C., 2012. Kinetic study of batch and fed-batch enzymatic saccharification of pretreated substrate and subsequent fermentation to ethanol. Biotechnol. Biofuels, 5, 16.

Gupta, R., Lee, Y.Y., 2009. Mechanism of cellulase reaction on pure cellulosic substrates. Biotechnol. Bioeng., 102, 1570–1581.

Gurunathan, B., Sahadevan, R., 2011. Design of Experiments and artificial neural network linked genetic algorithm for modeling and optimization of L-asparaginase production by *Aspergillus terreus* MTCC 1782. Biotechnol. Bioprocess Eng., 16, 50-58.

Habla, F., Marschall, H., Hinrichsen, O., Dietsche, L., Jasak, H., Favero, J.L., 2011. Numerical simulation of viscoelastic two-phase flows using open FOAM, Chem. Eng. Sci., 66, 5487–5496.

Han, Y., Chen, H., 2007. Plant cell wall proteins & enzymatic hydrolysis of lignocellulose. Prog. Chem., 19, 1154–1158.

Harris, P.V., Welner, D., McFarland, K.C., Re, E., Navarro Poulsen, J.C., Brown, K., Salbo, R., Ding, H., Vlasenko, E., Merino, S., Xu, F., Cherry, J., Larsen, S., Lo Leggio, L., 2010. Stimulation of lignocellulosic biomass hydrolysis by proteins of glycoside hydrolase family 61: structure and function of a large, enigmatic family. Biochem., 49, 3305–3316.

Hatti-Kaul, R., Törnvall, U., Gustaffson, L., Börjesson, P., 2007. Industrial biotechnology for the production of bio-based Chemicals: A cradle-to-perspective. Trends Biotechnol., 25, 119-124.

Haven, M.O., Jorgensen, H., 2013. Adsorption of β-glucosidases in two commercial preparations onto pretreated biomass and lignin. Biotechnol. Biofuels, 6, 165.

Haykir, N.I., Bakir, U., 2013. Ionic liquid pretreatment allows utilization of high substrate loadings in enzymatic hydrolysis of biomass to produce ethanol from cotton stalks. Ind. Crops Prod., 51, 408– 414.

He, Y., Zhang, L., Zhang, J., Bao, J., 2014. Helically agitated mixing in dry dilute acid pretreatment enhances the bioconversion of corn stover into ethanol. Biotechnol. Biofuels, 7, 1.

Hendriks, A.W., Zeeman, G., 2009. Pretreatments to enhance the digestibility of lignocellulosic biomass. Bioresour. Technol., 100, 10–18.

Hill, J., Nelson, E., Tilman, D., Polasky, S., Tiffany, D., 2006. Environmental, economic and energetic costs and benefits of biodiesel and ethanol biofuels. Proc. Nat. Acad. Sci., 103, 11206 - 11210.

Himmel, M.E., Ding, S.Y., Johnson, D.K., Adney, W.S., Nimlos, M.R., Brady, J.W., Foust, T.D., 2007. Biomass recalcitrance: engineering plants and enzymes for biofuel production. Sci., 315, 804-807.

Himmel, M.E., Karplus, P.A., Sakon, J., Adney, W.S., Baker, J.O., Thomas, S.R., 1997. Polysaccharide hydrolase folds diversity of structure and convergence of function. Appl. Biochem. Biotechnol., 63, 315–325.

Hodge, D.B., Karim, M.N., Schell, D.J., McMillan, J.D., 2006. Control of high-solids saccharification using a model-based methodology for fed-batch operation. Proceedings of ADCHEM 2006 - International Symposium on Advanced Control of Chemical Processes Gramado, Brazil – April 2-5, 2006, 177-182.

Hodge, D.B., Karim, M.N., Schell, D.J., McMillan, J.D., 2008. Soluble and insoluble solids contributions to high-solids enzymatic hydrolysis of lignocellulose. Bioresour. Technol., 99, 8940–8948.

Hodge, D.B., Karim, M.N., Schell, D.J., McMillan, J.D., 2009. Model-based fed-batch for high-solids enzymatic cellulose hydrolysis. Appl. Biochem. Biotechnol., 152, 88-107.

Hogan, C.H., Mes-Hartree, M., Saddler, J.N., Kushner, D., 1990. Assessment of methods to determine minimal cellulase concentrations for efficient hydrolysis of cellulose. Appl. Microbiol. Biotechnol., 32, 614-620.

Howard, R.L., Abotsi, E., Jansen, V.R.E.L., Howard, S., 2003. Lignocellulose biotechnology: issues of bioconversion and enzyme production. Afr. J. Biotechnol., 2, 602-619.

Hoyer, K., Galbe, M., Zacchi, G., 2010. Effects of enzyme feeding strategy on ethanol yield in fed-batch simultaneous saccharification and fermentation of spruce at high dry matter. Biotechnol. Biofuels, 3, 14.

Hu, J., Arantes, V., Saddler, J.N., 2011. The enhancement of enzymatic hydrolysis of lignocellulosic substrates by the addition of accessory enzymes such as xylanase: is it an additive or synergistic effect? Biotechnol. Biofuels, 4, 36.

Hussain, M., Bedi, J.S., Singh, H., 1992. Determining number of neurons in hidden layers for binary error correcting codes. In: Proceedings of Applications of Artificial Neural Networks III (21st April, 1992, Orlando, FL, USA). SPIE, 1015-1022.

Idi, A., Mohamad, S.E., 2011. Bioethanol from second generation feedstock (lignocellulose biomass). Int. J. Contemp. Res. Bus., 3, 919 -935.

IEA. 2012a. CO2 Emissions from Fuel Combustion. Paris, France: OECD Publishing.

IEA. 2012b. World Energy Outlook 2012. Paris: OECD-IEA. 92

Ingesson, H., Zacchi, G., Yang, B., Esteghlalian, A.R., Saddler, J.N., 2001. The effect of shaking regime on the rate and extent of enzymatic hydrolysis of cellulose. J. Biotechnol., 88, 177–182.

Ioelovich, M., Morag, E., 2012. Study of enzymatic hydrolysis of pretreated biomass at increased solids loading. BioResour., 7, 4672-4682.

Iqbal, H.M.N., Kyazze, G., Keshavarz, T., 2013. Advances in valorization of lignocellulosic materials by bio-technology: An overview. BioResour., 8(2), 3157-3176.

Ishizawa, C.I., Davis, M.F., Schell, D.F., Johnson, D.K., 2007. Porosity and its effect on the digestibility of dilute sulfuric acid pretreated corn stover. J. Agric. Food Chem., 55, 2575–2581.

Jäger, G., Girfoglio, M., Dollo, F., Rinaldi, R., Bongard, H., Commandeur, U., Fischer, R., Spiess, A.C., Büchs, J., 2011. How recombinant swollenin from *Kluyveromyces lactis* affects cellulosic substrates and accelerates their hydrolysis. Biotechnol. Biofuels., 23, 33.

Jayani, R.S., Saxena, S., Gupta, R., 2005. Microbial pectinolytic enzymes: A review. Proc. Biochem., 40, 2931–44.

Jeoh, T., Ishizawa, C.I., Davis, M.F., Himmel, M.E., Adney, W.S., Johnson, D.K., 2007. Cellulase digestibility of pretreated biomass is limited by cellulose accessibility. Biotechnol. Bioeng., 98, 112–122.

Jervis, E.J., Haynes, C.A., Kilburn, D.G., 1997. Surface diffusion of cellulases and their isolated binding domains on cellulose**.** J. Biol. Chem., 272, 24016-24023.

Jing, X., Zhang, X., Bao, J., 2009. Inhibition performance of lignocellulose degradation products on industrial cellulase enzymes during cellulose hydrolysis. Appl. Biochem. Biotechnol. 159, 696–707.

Jones, E. O., Lee, J. M. 2004. Kinetic analysis of bioconversion of cellulose in attrition bioreactor. Biotechnol. Bioeng. 31, 35 - 40.

Jørgensen, H., Kristensen, J.B., Felby, C., 2007b. Enzymatic conversion of lignocellulose into fermentable sugars: challenges and opportunities. Biofuels, Bioprod. Bioref., 1,119–134.

Jørgensen, H., Vibe-Pedersen, J., Larsen, J., Felby, C., 2007a. Liquefaction of lignocellulose at high solids concentrations**.** Biotechnol. Bioeng,, 96, 862-870.

Jorjani, E., Chehreh, C.S., Mesroghli, S.H., 2008. Application of artificial neural Networks to predict chemical desulfurization of Tabas coal. Fuel. 87, 2727-2734.

Jung, H.J.G., Jorgensen, M.A., Linn, J.G., Engels, F.M., 2000. Impact of accessibility and chemical composition on cell wall polysaccaride degradability of maize and lucerne stems. J. Sci. Food Agric., 80, 419–427.

Jungmeier, G., 2010. Classification and assessment of biorefinery concepts in IEA Bioenergy Task 42 "Biorefineries", ICPS Conference, Leipzig.

Kadam, K.L., McMillan, J.D., 2003. Availability of corn stover as a sustainable feedstock for bioethanol production. Bioresour. Technol., 88, 17-25.

Kamm, B., Gruber, P.R., Kamm, M., 2006. Biorefinery industrial processes and products. Status and future direction, volumes 1 and 2. Weinheim, Wiley-Verlay Gmbtt and Co.

Kang, Q., Appels, L., Baeyens, J., Dewil, R., Tan, T., 2014. Energy efficient production of cassava-based bio-ethanol," Adv., Biosci, Biotechnol., 5, 925–939.

Karimi, K., Emtiazi, G., Taherzadeh, M.J., 2006. Ethanol production from dilute acid pretreated rice straw by simultaneous saccharification and fermentation with *Mucor indicus, Rhizopus oryzae* and *S. cerevisiae*. Enzyme Mocrobial. Technol., 40, 138-144.

Karlsson, J., Medve, J., Tjerneld, F., 1999. Hydrolysis of steam-pretreated lignocellulose. Appl. Biochem. Biotechnol., 82, 243–258.

Khullar, E., Dienb, B.S., Rauscha, K.D., Tumblesona, M.E., Singh, V., 2013. Effect of particle size on enzymatic hydrolysis of pretreated *Miscanthus*. Ind. Crop. Prod., 44, 11– 17.

Kim, D.W., Hong, Y.G., 2000. Ionic strength effect on adsorption of cellobiohydrolases I and II on microcrystalline cellulose. Biotechnol. Lett., 22, 1337–1342.

Kim, D.W., Kim, T.S., Jeong, Y.K., Lee, J.K., 1992. Adsorption kinetics and behaviors of cellulase components on microcrystalline cellulose. J. Ferment. Bioeng., 73, 461–466.

Kim, E., Irwin, D.C., Walker, L.P., Wilson, D.B, 1998. Factorial optimization of a six cellulase mixture. Biotechnol. Bioeng., 58, 494-501.

Kim, J., Grate, J.W., Wang, P., 2006. Nanostructures for enzyme stabilization. Chem. Eng. Sci., 61, 1017–1026.

Kim, J., Grate, J.W., Wang, P., 2008. Nanobiocatalysis and its potential applications. Trends Biotechnol., 26, 639–646.

Kim, J.S., Lee, Y.Y., Torget, R., 2001. Cellulose hydrolysis under extremely low sulphuric acid and high temperature conditions. Appl. Biochem. Biotechnol., 91, 331-340.

Kim, M.I., Kim, J., Lee, J., Jia, H., Na, H.B., Youn, J.K., Kwak, J.H., Dohnalkova, A., Grate, J.W., Wang, P., Hyeon, T., Park, H.G., Chang, H.N., 2007. Cross linked enzyme aggregates in

hierarchically ordered mesoporous silica: a simple and effective method for enzyme stabilization. Biotechnol. Bioeng., 96, 210–218.

Kim, S., Dale, B.E., 2005. Global potential bioethanol production from wasted crops and crops residues. Biomass Bioenergy, 29, 361-375.

Klinke, H.B., Thomsen, A.B., Ahring, B.K., 2004. Inhibition of ethanol-producing yeast and bacteria by degradation products produced during pre-treatment of biomass. Appl. Microbiol. Biotechnol., 66, 10–26.

Knauf, M., Moniruzzaman, M., 2004. Lignocellulosic biomass processing. Persp. Int. Sugar. J., 106, 147-150.

Knutsen, J.S., Liberatore, M.W., 2009. Rheology of high-solids biomass slurries for biorefinery applications. J. Rheol., 53, 877–892.

Koppram, R., Olsson, L., 2014. Combined substrate, enzyme and yeast feed in simultaneous saccharification and fermentation allow bioethanol production from pretreated spruce biomass at high solids loadings. Biotechnol. Biofuels, 7, 54.

Kose, E., 2008. Modelling of colour perception of different age groups using artificial neural networks. Expert Syst. Appl., 34, 2129-2139.

Kotiranta, P., Karlsson, J., Siika-Aho, M., Medve, J., Viikari, L., Tjerneld, F., Tenkanen, M., 1999. Adsorption and activity of *Trichoderma reesei* cellobiohydrolase I, endoglucanase II, and the corresponding core proteins on steam pretreated willow. Appl. Biochem. Biotechnol., 81, 82–90.

Koukiekolo, R., Cho, H.Y., Kosugi, A., Inui, M., Yukawa, H., Doi, R.H., 2005. Degradation of corn fiber by *Clostridium cellulovorans* cellulases and hemicellulases and contribution of scaffolding protein CbpA. Appl. Environ. Microbiol. 71, 3504–3511.

Koutinas, A.A., Wang, R.H., Webb, C., 2007. The biochemurgist—bioconversion of agricultural raw materials for chemical production. Biofuel Bioprod. Bioref. 1, 24–38.

Krishna, S.H., Reddy, T.J., Chowdary, G.V., 2001. Simultaneous saccharification and fermentation of lignocellulosic wastes to ethanol using a thermo tolerant yeast. Bioresour. Technol., 77, 193-196.

Kristensen, J.B., Borjesson, J., Bruun, M.H., Tjerneld, F., Jorgensen, H., 2007. Use of surface active additives in enzymatic hydrolysis of wheat straw lignocellulose. Enzyme Microb. Technol., 40, 888–895.

Kristensen, J.B., Felby, C., Jorgensen, H., 2009a. Yield-determining factors in high-solids enzymatic hydrolysis of lignocellulose. Biotechnol. Biofuels, 2, 11.

Kristensen, J.B., Felby, C., Jorgensen, H., 2009b. Determining yields in high solids enzymatic hydrolysis of biomass. Appl. Biochem. Biotechnol., 156, 127-132.

Kubicek, C., Mikus, M., Schuster, A., Schmoll, M., Seiboth, B., 2009. Metabolic engineering strategies for the improvement of cellulase production by *Hypocrea jecorina*. Biotechnol. Biofuels, 2, 19

Kumar R. 2008. Ph.D. Thesis: Enzymatic Hydrolysis of Cellulosic Biomass Solids Prepared by Leading Pretreatments and Identification of Key Features Governing Performance. Hanover, NH, USA: Thayer School of Engineering, Dartmouth College.

Kumar, P., Barrett, D.M., Delwiche, M.J., Stroeve, P., 2009. Methods for pretreatment of lignocellulosic biomass for efficient hydrolysis and biofuel production. Ind. Eng. Chem. Res., 48, 3713-3729.

Kumar, R., Wyman, C.E., 2008. An improved method to directly estimate cellulase adsorption on biomass solids. Enzyme. Microb. Technol., 42, 426–433.

Kumar, R., Wyman, C.E., 2009a. Effects of cellulase and xylanase enzymes on the deconstruction of solids from pretreatment of poplar by leading technologies. Biotechnol. Prog., 25, 302-314.

Kumar, R., Wyman, C.E., 2009b. Cellulase adsorption and relationship to features of corn stover solids produced by leading pretreatments. Biotechnol. Bioeng,, 103, 252–267.

Kumar, R., Wyman, C.E., 2009c. Effect of xylanase supplementation of cellulase on digestion of corn Stover solids prepared by leading pretreatment technologies. Bioresour. Technol., 100, 4203-4213.

Kumar, R., Wyman, C.E., 2009d. Effect of enzyme supplementation at moderate cellulase loadings on initial glucose and xylose release from corn stover solids pretreated by leading technologies. Biotechnol. Bioeng., 102, 457–467.

Laemmli, U. K. 1970. Cleavage of structural proteins during the assembly of the head of bacteriophage T4. Nature, 227, 680-685.

Lagaert, S., Beliën, T., Volckaerta, G., 2009. Plant cell walls: Protecting the barrier from degradation by microbial enzymes. Semin. Cell. Dev. Biol., 20, 1064–1073.

Larsen, J., Petersen, M.O., Thirup, L., Li, H.W., Iversen, F.K., 2008. The IBUS process – Lignocellulosic bioethanol close to a commercial reality. Chem. Eng. Techno., 31, 765-772.

Laureano-Perez, L., Teymouri, F., Alizadeh, H., Dale, B.E., 2005. Understanding factors that limit enzymatic hydrolysis of biomass-characterization of pretreated corn stover. Appl. Biochem. Biotechnol. 121, 1081–1099.

Lee, D., Yu, A.H.C., Saddler, J.N., 1995. Evaluation of cellulase recycling strategies for the hydrolysis of lignocellulosic substrates. Biotechnol. Bioeng., 45, 328–336.

Lee, S.M., Jin, L.H., Kim, J.H., Han, S.O., Na, H.B., Hyeon, T., Koo, Y.M., Kim, J., Lee, J.H., 2010. β-Glucosidase coating on polymer nanofibers for improved cellulosic ethanol production. Bioprocess Biosyst. Eng., 33, 141–147.

Lee, S.Y., Park, J.H., Jang, S.H., Nielsen, L.K., Kim, J., Jung, K.S., 2008. Fermentative butanol production by Clostridia, Biotechnol. Bioeng., 101, 209-228.

Lee, Y., Wu, Z., Torget, R., 2000. Modeling of countercurrent shrinking bed reactor in dilute acid total hydrolysis of lignocellulosic biomass. Bioresour. Technol., 71, 29-39.

Lee, Y.H., Fan, L.T., 1981. Kinetics of enzymic hydrolysis of insoluble cellulose: Experimental observation on initial rates. Adv. Biotechnol. Proc. Int. Ferment. Symp. 2, 9–14.

Lenting, H.B.M., Warmoeskerken, M.M.C.G., 2001. Mechanism of interaction between cellulase action and applied shear force: A hypothesis. J. Biotechnol., 89, 217–226.

Li, C., Yoshimoto, M., Fukunaga, K., Nakao, K., 2007a. Characterization and immobilization of liposome-bound cellulase for hydrolysis of insoluble cellulose. Bioresour. Technol., 98, 1366-1372.

Li, X.L., Špániková, S., de Vries, R.P., Biely, P., 2007b. Identification of genes encoding microbial glucuronoyl esterases. FEBS Lett., 581, 4029–4035.

Lin, Z.X., Zhang, H.M., Ji, X.J., Chen, J.W., Huang, H., 2011. Hydrolytic Enzyme of Cellulose for complex Formulation Applied Research. Appl. Biochem. Biotechnol., 164, 23-33.

Lindedam, J., Haven, M., Chylenski, P., Jørgensen, H., Felby, C., 2013. Recycling cellulases for cellulosic ethanol production at industrial relevant conditions: potential and temperature dependency at high solid processes. Bioresour. Technol., 148, 180–188.

Liu, K., Lin, X., Yue, J., Li, X., Fang, X., Zhu, M., Lin, J., Qua, Y., Xiao, L., 2010. High concentration ethanol production from corncob residues by fed-batch strategy. Bioresour. Technol., 101, 4952–4958.

Liu, W., Wang, Y.M., Yu, Z.C., Bao, J., 2012. Simultaneous saccharification and microbiallipid fermentation of corn stover by oleaginous yeast *Trichosporon cutaneum*. Bioresour. Technol., 118, 13–18.

Lu, A.H., Salabas, E.L., Schuth, F., 2007. Magnetic Nanoparticles: Synthesis, protection, functionalization, and application. Angew. Chem., 46, 1222 - 1244.

Lu, Y., Wang, Y., Xu, G., Chu, J., Zhuang, Y., Zhang, S., 2010. Influence of high solid concentration on enzymatic hydrolysis and fermentation of steam-exploded corn stover biomass. Appl. Biochem. Biotechnol., 160, 360–369.

Lu, Y., Yang, B., Gregg, D., Saddler, J.N., Mansfield, S.D., 2002a. Cellulase adsorption and an evaluation of enzyme recycle during hydrolysis of steam-exploded softwood residues. Appl. Biochem. Biotechnol., 98, 641- 654

Lu, Y., Yin, Y.D., Mayers, B.T., 2002b. Modifying the surface of super paramagnetic iron oxide nanoparticles through a sol-gel approach. Nano Lett., 2, 183 - 186.

Ludwig, D., Michael, B., Hirth, T., Rupp, S., Zibek, S., 2014. High solids enzymatic hydrolysis of pretreated lignocellulosic materials with a powerful stirrer concept. Appl. Biochem. Biotechnol., 172, 1699–1713.

Luterbacher, J.S., Moran – Mirabal, J.M., Burkholder, E.W., Walker, L.P., 2015. Modeling enzymatic hydrolysis of lignocellulosic substrates using fluorescent confocal microscopy II: pretreated biomass. Biotechnol. Bioeng., 112, 32–42.

Lynd, L., Weimer, P., van Zyl, W., Pretorius, I., 2002. Microbial cellulose utilization: fundamentals and biotechnology. Microbiol. Mol. Biol. Rev. 66, 506–577.

Lynd, L.R., Zyl, W.H.V., McBride, J.E., Laser, M., 2005. Consolidated bioprocessing of cellulosic biomass: An update. Curr. Opin. Biotechnol., 16, 577-583.

Ma, X.X., Yue, G.J., Yu, J.L., Zhang, X., Tan, T.W., 2011. Enzymatic hydrolysis of cassava bagasse with high solid loading. J Biobased Mater. Bioenergy, 5, 275-281.

Mabee, W.E., Gregg, D.J., Saddler, J.N., 2005. Assessing the emerging biorefinery sector in Canada. Appl. Biochem. Biotechnol., 121, 765–778.

Manohar, B., Divakar, S., 2005. An artificial neural network analysis of porcine pancreas lipase catalysed esterification of anthranilic acid with methanol. Process Biochem., 40, 3372-3376.

Mansfield, S.D., Mooney, C., Saddler, J.N., 1999. Substrate and enzyme characteristics that limit cellulose hydrolysis. Biotechnol. Prog., 15, 804–816.

Mashhadizadeh, M.H., Amoli-Diva, M., 2012. Drug-carrying amino silane coated magnetic nanoparticles as potential vehicles for delivery of antibiotics. J. Nanomed. Nanotechol., 3, 4.

Mateo, C., Grazu, V., Palomo, J.M., Lopez-Gallego, F., Fernandez-Lafuente, R., Guisan, M.J., 2007. Immobilization of enzymes on heterofunctional epoxy supports. Nature Protoc., 2, 1022-1033.

Maurer, S.A., Bedbrook, C.N., Radke, C.J., 2012. Cellulase adsorption and reactivity on a cellulose surface from flow ellipsometry. Ind. Eng. Chem. Res., 51, 11389−11400.

McMillan, J.D., 1994. Pretreatment of lignocellulosic biomass. In: Enzymatic Conversion of Biomass for Fuels Production, ed by Himmel M.E., Baker, J.O., Overend, R.P., American Chemical Society, Washington, DC, USA, 292–324.

Meng, X., Ragauskas, A.J., 2014. Recent advances in understanding the role of cellulose accessibility in enzymatic hydrolysis of lignocellulosic substrates. Curr. Opin. Biotechnol., 27, 150–158.

Menon, V., Rao, M., 2012. Trends in bioconversion of lignocellulose: biofuels, platform chemicals & biorefinery concept. Prog. Energy Combust. Sci., 38, 522-550.

Merino, S.T., Cherry, J., 2007. Progress and challenges in enzyme development for biomass utilization. Adv. Biochem. Eng .Biotechnol. 108, 95-120.

Meyer, A.S., Rosgaard, L., Sorensen, H.R., 2009. The minimal enzyme cocktail concept for biomass processing. J. Cereal Sci., 50, 337–344.

Michaud, P., Da Costa, A., Courtois, B., Courtois, J., 2003. Polysaccharide lyases: recent developments as biotechnological tools. Crit. Rev. Biotechnol., 23, 233–266.

Miller, G.M., 1959. Use of dinitrosalicylic acid reagent for determination of reducing sugar. Anal. Chem., 31, 426–428.

Modenbach, A.A., Nokes, S.E., 2013. Enzymatic hydrolysis of biomass at high-solids loadings: A review. Biomass Bioenergy., 56, 526 – 544.

Moghaddam, M.G., Ghaffari, M., Ahmad, F.B.H., Rahman, M.B.A., 2010. Artificial neural network modeling studies to predict the yield of enzymatic synthesis of betulinic acid ester. Electron. J. Biotechnol., 13, 3-14.

Mohagheghi, A., Tucker, M., Grohmann, K., Wyman, C., 1992. High solids simultaneous saccharification and fermentation of pretreated wheat straw to ethanol. Appl. Biochem. Biotechnol., 33, 67-81.

Mohanraj, V.J., Chen, Y., 2006. Nanoparticles - A review. Tropical J. Pharm. Res., 5, 561-573.

Mooney, C.A., Mansfield, S.D., Touhy, M.G., Saddler, J.N., 1998. The effect of initial pore volume and lignin content on the enzymatic hydrolysis of softwoods. Bioresour. Technol., 64, 113–119.

Morales-Rodríguez, R., Capron , M., Huusom, J.K., Sin, G., 2010. Controlled fed-batch operation for improving cellulose hydrolysis in 2G bioethanol production. Proceedings of '20th European Symposium on Computer Aided Process Engineering – ESCAPE20'.

Mores, W.D., Knutsen, J.S., Davis, R.H., 2001. Cellulase recovery via membrane filtration. Appl. Biochem. Biotechnol., 91, 297-309.

Morrison, D., Van Dyk, J.S., Pletschke, B.I., 2011. The effects of alcohols, lignin and phenolic compounds on the enzyme activity of *Clostridium cellulovorans* XynA. Bioresour. 6, 3132–3141.

Mussatto, S.I., Fernandes, M., Milagres, A.M.E., Roberto, I.C., 2008. Effect of hemicellulose and lignin on enzymatic hydrolysis of cellulose from brewer's spent grain. Enzyme Microb. Technol. 43, 124–129.

National Policy on Biofuels. 2015. Ministry of New and Renewable energy, Government of India. http://mnre.gov.in/file-manager/UserFiles/biofuel_policy.pdf

Nguyen Q. A. 1998. Tower reactors for bioconversion of lignocelluose material. US patent no. 5733758.

Nidetzky, B., Steiner, W., Hayn, M., Claeyssens, M. 1994. Cellulose hydrolysis by the cellulases from *Trichoderma reesei*: a new model for synergistic interaction. Biochem. J., 298, 705–710.

Nieves, R.A., Ehrman, C.I., Adney, W.S., Elander, R.T., Himmel, M.E., 1998. Technical communication: Survey and analysis of commercial cellulase preparations suitable for biomass conversion to ethanol. World J. Microbiol. Biotechnol., 14, 301–304.

O'Dwyer, J.P., Zhu,L., Granda, C.B., Chang, V.S., Holtzapple, M.T., 2008. Neural network prediction of biomass digestibility based on structural features. Biotechnol. Progr., 24, 283-292.

Official Nebraska government website. 2009. Washington, DC/Lincoln, NE: Renewable Fuels Association/Nebraska Energy Office, http://www.neo.ne.gov/statshtml/121_200912.htm.

Ohgren, K., Bura, R., Saddler, J., Zacchi, G., 2007. Effect of hemicellulose and lignin removal on enzymatic hydrolysis of steam pretreated corn stover. Bioresour. Technol., 98, 2503-2510.

Olofsson, K., Bertlisson, M., Liden, G.A., 2008. Short review on SSF: an interesting process option from lignocellulosic feedstocks. Biotechnol. Biofuels, 1, 1-7.

Olofsson, K., Palmqvist, B., Lidén, G., 2010. Improving simultaneous saccharification and co-fermentation of pretreated wheat straw using both enzyme and substrate feeding. Biotechnol. Biofuels, 3, 17.

Olsson, L., Soerensen, H.R., Dam, B.P., Christensen, H., Krogh, K.M., Meyer, A.S., 2006. Separate and simultaneous enzymatic hydrolysis and fermentation of wheat hemicellulose with recombinant xylose utilizing *Saccharomyces cerevisiae*. Appl. Biochem. Biotechnol., 129, 117-129.

Ooshima, H., Sakata, M., Harano, Y., 1983. Adsorption of cellulase from *Trichoderma viride* on cellulose. Biotechnol. Bioeng., 25, 3103– 3114.

Palonen, H., Tjerneld, F., Zacchi, G., Tenkanen, M., 2004. Adsorption of *Trichoderma reesei* CBHI and EGII and their catalytic domains on steam pretreated softwood and isolated lignin. J. Biotechnol., 107, 65–72.

Pan, L.H., Luo, J.P., Wang, G.J., Xu, X.L., Wan, W., 2008. Properties of beta-Glucosidase immobilized on magnetic nanoparticles of aluminum nitride. Chin. J. Catal., 29, 1021-1026.

Pan, X., Xie, D., Gilkes, N., Gregg, D.J., Saddler, J.N., 2005. Strategies to enhance the enzymatic hydrolysis of pretreated softwood with high residual lignin content. Appl. Biochem. Biotechnol., 121, 1069–1079.

Pandey, A., Biswas, S., Sukumaran, R.K., Kaushik, N., 2009. Study on availability of Indian biomass resources for exploitation, a report based on a nation-wide survey. TIFAC, New Delhi.

Pellegrini, V.O.A., Lei, N., Kyasaram, M., Olsen, J.P., Badino, S.F., Windahl, M.S., Colussi, f., Cruys – Bagger, N., Borch, K., Westh, P., 2014. Reversibility of Substrate Adsorption for the Cellulases Cel7A, Cel6A, and Cel7B from *Hypocrea jecorina*. Langmuir, 30, 12602−12609.

Perry, R.H., Green, D.W., Chemical Engineers' Handbook. 1997. Seventh Edition. McGraw Hill.

Policy energy act. 2005. Public Law, <http://www.gpo.gov/fdsys/pkg/PLAW-109publ58/content-detail.html>

Pramanik, K., 2004. Use of Artificial Neural Networks for Prediction of Cell Mass and Ethanol Concentration in Batch Fermentation using *Saccharomyces cerevisiae* Yeast. IE (I) Journal. CH., 85, 31-35.

Pribowo, A., Arantes, V., Saddler, J.N., 2012. The adsorption and enzyme activity profiles of specific *Trichoderma reesei* cellulose/xylanase components when hydrolysing steam pretreated corn stover. Enzyme. Microb. Technol., 50, 195–203.

Pryor, S.W., Nahar, N., 2010. Deficiency of cellulase activity measurements for enzyme evaluation. Appl. Biochem. Biotechnol., 162, 1737–1750.

Puri, D.J., Heaven, S., Banks, C.J., 2013. Improving the performance of enzymes in hydrolysis of high solids paper pulp derived from MSW. Biotechnol. Biofuels, 6, 107.

Qi, B., Chen, X., Su, Y., Wan, Y., 2011. Enzyme adsorption and recycling during hydrolysis of wheat straw lignocellulose. Bioresour. Technol., 102, 2881–2889.

Qing, Q., Wyman, C.E., 2011. Supplementation with xylanase and b-xylosidase to reduce xylo-oligomer and xylan inhibition of enzymatic hydrolysis of cellulose and pretreated corn stover. Biotechnol. Biofuels, 4, 18.

Qing, Q., Yang, B., Wyman, C.E., 2010. Xylooligomers are strong inhibitors of cellulose hydrolysis by enzymes. Bioresour. Technol., 101, 9624-9630.

Ragauskas, A.J., Williams, C.K., Davison, B.H., Britovsek, G., Cairney, J., Eckert, C.A., 2006. The path forward for biofuels and biomaterials. Sci., 311, 484-489.

Ranade, V.V., 2002. Computational Flow Modeling for Chemical Reactor Engineering, Academic Press, San Diego.

Ratanakhanokchai, K., Waeonukul, R., Pason, P., Tachaapaikoon, C., Kyu, K.L., Sakka, K., Kosugi, A., Mor, Y., 2013. Paenibacillus curdlanolyticus Strain B-6 Multienzyme Complex: A Novel System for Biomass Utilization. In: Biomass now – Cultivation and Utilization, INTECH, 369- 394.

Raven, P.H., Evert, R.F., Eichhorn, S.E., 1999. Biology of plants. New York: W.H. Freeman and company.

Razavi, M.A., Mortazavi, A., Mousavi, M., 2003. Dynamic modeling of milk Ultrafiltration by artificial neural network. J. Membr. Sci., 220, 47-58.

Redding, A.P., Wang, Z., Keshwani, D.R., Cheng, J.J., 2011. High temperature dilute acid pretreatment of coastal Bermuda grass for enzymatic hydrolysis. Bioresour. Technol., 102, 1414-1422.

Reese, E. T., Ryu, D. Y., 1980. Shear inactivation of cellulase of *Trichoderma reesei*. Enzyme Microb. Technol., 2, 239–240.

Renewable Fuels Association, US fuel ethanol industry biorefineries and capacity. Washington, DC: http://www.ethanolrfa.org/industry/locations/;2010.

Renzo, A.D., Maio, D.F.P. 2007. Homogeneous and bubbling fluidization regimes in DEM-CFD simulations: hydrodynamic stability of gas and liquid beds, Chem. Eng. Sci., 62, 116–130.

Rhie, C. M., Chow, W. L., 1983. A numerical study of the turbulent flow past an isolated airfoil with trailing edge separation. AIAA J., 21,1525-1532.

Rivera, E.C., Rabelo, S.C., Garcia, D.R., Filho, R.M., da Costa, A.C., 2010. Enzymatic hydrolysis of sugarcane bagasse for bioethanol production: determining optimal enzyme loading using neural networks. J. Chem. Technol. Biotechnol.85, 983–992.

Rivers, D.B., Emert, G.H., 1988. Factors affecting the enzymatic hydrolysis of bagasse and rice straw. Biol. Wastes., 26, 85–95.

Robinson, M., Cleary, P.W., 2012. Flow and mixing performance in helical ribbon mixers, Chem. Eng. Sci., 84, 382–398.

Roche CM, Dibble CJ, Stickel JJ. 2009b. Laboratory-scale method for enzymatic saccharification of lignocellulosic biomass at high-solids loadings. Biotechnol. Biofuels, 2, 28.

Roche, C.M., Dibble, C.J., Knutsen, J.S., Stickel, J.J., Liberatore, M.W., 2009a. Particle concentration and yield stress of biomass slurries during enzymatic hydrolysis at high-solids loadings. Biotechnol. Bioeng., 104, 290–300.

Rodrigues, A.C., Felby, C., Gama, M., 2014. Cellulase stability, adsorption/desorption profiles and recycling during successive cycles of hydrolysis and fermentation of wheat straw. Bioresour. Technol., 156, 163–169

Rodrigues, A.C., Leitão, A.F., Moreira, S., Felby, C., Gama, M., 2012. Recycling of cellulases in lignocellulosic hydrolysates using alkaline elution. Bioresour. Technol., 110, 526–533.

Rollin, J.A., Zhu, Z., Sathitsuksanoh, N., Zhang, Y.H., 2010. Increasing cellulose accessibility is more important than removing lignin: a comparison of cellulose solvent-based lignocellulose fractionation and soaking in aqueous ammonia. Biotechnol. Bioeng., 108, 22–30.

Romani, A., Garrote, G., Alonso, J.L., Parajo, J.C., 2010. Bioethanol production from hydrothermally pretreated *Eucalyptus globulus* wood. Bioresour. Technol., 101, 8706–8712.

Rosgaard, L., Andric, P., Dam-Johansen, K., Pedersen, S., Meyer, A.S., 2007. Effects of substrate loading on enzymatic hydrolysis and viscosity of pretreated barley straw. Appl. Biochem. Biotechnol., 143, 27–40.

Rudolf, A., Alkasrawi, M., Zacchi, G., Lid´en, G., 2005. A comparison between batch and fed-batch simultaneous saccharification and fermentation of steam pretreated spruce. Enzyme Microb. Technol., 37, 195–204.

Ruiz, R., Ehrman, T., 1996. Determination of Carbohydrates in Biomass by High Performance Liquid Chromatography. National Renewable Energy Laboratory, Laboratory Analytical Procedure #002, Revision 12/08/1996.

Ryu, K., Kim, Y., 1998. Adsorption of a xylanase purified from Pulpzyme HC onto alkali-lignin and crystalline cellulose. Biotechnol. Lett., 20, 987-990.

Saha, B.C., Iten, L.B., Cotta, M.A., Wu, Y.V., 2005. Dilute acid pretreatment, enzymatic saccharification and fermentation of rice hulls to ethanol. Biotechnol. Prog., 21, 816-822.

Samaniuk, J.R., Scott, T., Root, T.W., Klingenberg, D.J., 2011. The effect of high intensity mixing on the enzymatic hydrolysis of concentrated cellulose fiber suspensions. Bioresour. Technol., 102, 4489–4494

Samayan, I.P., Schall, C.A., 2010. Saccharification of ionic liquid pretreated biomass with commercial enzyme mixtures. Bioresour. Technol., 101, 3561–3566.

Sampedro, J., Cosgrove, D.J., 2005. The expansin superfamily. Genome Biol., 6, 242-342.

Schell, D. 2005. OBP biennial peer review, energy efficiency and renewable energy. http://programreview.biomass.govtools.us/%5Cdocuments%5C11e80e62-6e8a-4858-a0e5-1fa75a591116.ppt

Sheehan, J., Cambreco, V., Duffield, J., Garboski, M., Shapouri, H., 1998. An overview of biodiesel and petroleum diesel life cycles. A report by US Department of Agriculture and Energy, 1-35.

Sheldon, R.A., 2007. Enzyme Immobilization: The quest for Optimum Performance, Adv. Synth. Catal., 349, 1289-1307.

Shen, J., Agblevor, F.A., 2008. Optimization of enzyme loading and hydrolytic time in the hydrolysis of mixtures of cotton gin waste and recycled paper sludge for the maximum profit rate. Biochem. Eng. J., 41, 241-250.

Shen, X.C., Fang, X.Z., Zhou, Y.H., Liang, H., 2004. Synthesis and Characterization of 3-aminopropyltriethoxysilane modified super paramagnetic magnetite nanoparticles. Chem. Lett., 33, 1468-1469.

Sills, D.L., Gossett, J.M., 2011. Assessment of commercial hemicellulases for saccharification of alkaline pretreated perennial biomass. Bioresour. Technol., 102, 1389–1398.

Singh, R., Zhang, Y., Nguyen, N., Jeya, M., Lee, J., 2011. Covalent immobilization of β-1,4-glucosidase from *Agaricus arvensis* onto functionalized silicon oxide nanoparticles. Appl. Microbiol. Biotechnol., 89, 337-344.

Singhania, R.R., Sukumaran, R.K., Rajasree, K.P., Mathew, A., Gottumukkala, L., Pandey, A., 2011. Properties of a major β-glucosidase-BGL1 from *Aspergillus niger* NII-08121 expressed differentially in response to carbon sources, Process Biochem. 46, 1521-1524.

Stickel, J.J., Knutsen, J.S., Liberatore, M.W., Luu, W., Bousfield, D.W., Klingenberg, D.J., Scott, C.T., Root, T.W., Ehrhardt, M.R., Monz, T.O., 2009. Rheology measurements of a biomass slurry: an inter-laboratory study. Rheologica Acta, 48, 1005–1015.

Sukumaran, R.K., Pandey, A., 2010. India Country report , In: Eisentraut A (ed), Potential for sustainable production of 2nd generation biofuels, IEA 2010

Sumantra, M., Sivaprasad, P.V., Venugopal, S., Murthy, K.P.N., 2009. Artificial neural network modeling to evaluate and predict the deformation behavior of stainless steel type AISI 304L during hot torsion. Appl. Soft Comput., 9, 237-244.

Sun, J.L., Sakka, K., Karita, S., Kimura, T., Ohmiya, K., 1998. Adsorption of clostridium stercorarium xylanase A to insoluble xylan and the importance of the CBDs to xylan hydrolysis. J. Ferment. Bioeng., 85, 63–68.

Sun, Y., Cheng, J., 2002. Hydrolysis of lignocellulosic materials for ethanol production: A review. Bioresour. Technol., 83, 1-11.

Suurnakki, A., Tenkanen, M., Siika-aho, M., Niku-Paavola, M.L., Viikari, L., Buchert, J., 2000. *Trichoderma reesei* cellulases and their core domains in the hydrolysis and modification of chemical pulp**.** Cellulose, 7, 189-209.

Swart, J.A.A., Jiang, J., Ho, P., 2008. Risk perceptions and GM crops: the case of China. Tailoring Biotechnol. Soc. Sci. Technol., 33, 11-28.

Sweeney, M.D., Xu, F., 2012. Biomass converting enzymes as industrial biocatalysts for fuels and chemicals: Recent developments. Catalysts, 2, 244-263.

Taherzadeh, M.J., 1999. Ethanol from lignocellulose: physiological effects of inhibitors and fermentation strategies. Chemical reaction engineering. Chalmers University of Technology. Göteborg, Sweden. Doctoral thesis Nr. 1247.

Taherzadeh, M.J., Karimi, K., 2007. Enzymatic based hydrolysis process for ethanol from lignocellulosic materials: A review. Bioresour., 2, 707-738.

Tan, I.S., Lee, K.T., 2015. Immobilization of b-glucosidase from *Aspergillus niger* on j-carrageenan hybrid matrix and its application on the production of reducing sugar from macro algae cellulosic residue. Bioresour. Technol., 184, 386-394.

Teeri, T.T., 1997. Crystalline cellulose degradation: new insight into the function of cellobiohydrolases. Tibtech, 15, 160–167.

Teixeira, L.C., Linden, J.C., Schroeder, H.A., 2000. Simultaneous saccharification and cofermentation of peracetic acid pretreated biomass. Appl. Biochem. Biotechnol., 84, 111-127.

Templeton, D., Ehrman, T., 1995. Determination of acid-insoluble lignin in biomass. In: Laboratory analytical procedure-LAP 003, NREL.

Tengborg, C., Galbe, M., Zacchi, G., 2001. Influence on enzyme loading and physical parameters on the enzymatic hydrolysis of steam-pretreated softwood. Biotechnol. Prog., 17, 110–117.

Teugjas, H., Väljamäe, P., 2013. Selecting β-glucosidases to support cellulases in cellulose saccharification. Biotechnol. Biofuels, 6, 105.

Thompson, D., Grethlein, E., 1979. Design and evaluation of a plug flow reactor for acid hydrolysis of cellulose. Ind. Eng. Chem. Prod. Res. Dev., 18, 371-378.

Torget, R., Hsu, T.A., 1994. Temperature dilute acid prehydrolysis of hardwood xylan using a percolation process. Appl. Biochem. Biotechnol., 45, 5-22.

Tsui, Y.Y., Hu, Y.C., 2011. Flow characteristics in mixers agitated by helical ribbon blade impeller. Eng. Appl. Comp. Fluid Mech., 5, 416-429

Tu, M., Pan, X., Saddler, J.N., 2009a. Adsorption of cellulase on cellulolytic enzyme lignin from lodgepole pine. J. Agric. Food Chem., 57, 7771–7778.

Tu, M., Zhang, X., Kurabi, A., Gilkes, N., Mabeel, W., Saddler, J., 2006. Immobilization of *b*-glucosidase on Eupergit C for lignocellulose hydrolysis. Biotechnol. Lett., 28, 151–156.

Tu, M., Zhang, X., Paice, M., MacFarlane, P., Saddler, J.N., 2009b. The potential of enzyme recycling during the hydrolysis of a mixed softwood feedstock. Bioresour. Technol., 100, 6407–6415.

Uhl, V., Gray. 1966. Mixing: Theory and Practice.-1, Chapter 5. Academic Press. London.

Um, B.H., Hanley, T.R., 2008. High-solid enzymatic hydrolysis and fermentation of Solka Floc into ethanol. J. Microbiol. Biotechnol. 18, 1257–1265.

Valenzuela, R., Castro, J.F., Parra, M.C., Baeza, J., Free, J., 2011. Beta-glucosidase immobilization on synthetic superparamagnetic magnetite nanoparticles and their application in saccharification of wheat straw and *Eucalyptus globulus* pulps. Nanotech., 3, 665-668.

Van Dyk, J.S., Pletschke, B.I., 2012. A review of lignocellulose bioconversion using enzymatic hydrolysis and synergistic cooperation between enzymes—Factors affecting enzymes, conversion and synergy. Biotechnol. Adv., 30, 1458–1480.

Varnai, A., Siika-aho, M., Viikari, L., 2010. Restriction of the enzymatic hydrolysis of steam-pretreated spruce by lignin and hemicellulose. Enzyme Microb. Technol., 46, 185–193.

Verma, M.L., Chaudhary, R., Tsuzuki, T., Barrow, C.J., Puri, M., 2013. Immobilization of b-glucosidase on a magnetic nanoparticle improves thermostability: Application in cellobiose hydrolysis. Bioresour. Technol., 135, 2–6.

Vidal Jr., B.C., Dien, B.S., Ting, K.C., Singh, V., 2011. Influence of feedstock particle size on lignocellulose conversion - A review. Appl. Biochem. Biotechnol., 164, 1405–1421.

Wahlström, R.M., Suurnäkki, A., 2015. Enzymatic hydrolysis of lignocellulosic polysaccharides in the presence of ionic liquids, Green Chem., 17, 694- 714.

Wang, M., Wu, M., Huo, H., 2007. Life-cycle energy and greenhouse gas emission impacts of different corn ethanol plant types. Environ. Res. Lett. 2, 1-13.

Wang, Q.Q., He, Z., Zhu, Z., Zhang, Z.H.P., Ni, Y., Luo, X.L., Zhu, J.Y., 2012. Evaluations of cellulose accessibilities of lignocelluloses by solute exclusion and protein adsorption techniques. Biotechnol. Bioeng., 109, 381-389.

Wang, W., Kang, L., Wie, H., Arora, R., Lee, Y.Y., 2011a. Study on the decreased sugar yield in enzymatic hydrolysis of cellulosic substrate at high solid loading. Appl. Biochem. Biotechnol., 164, 1139–1149.

Wang, Y.M., Cao, X., Liu, G.H., Hong, R.Y., Chen, Y.M., Chen, X.F., Li, H.Z., Xu, B., Wei, D.G., 2011b. Synthesis of Fe_30_4 magnetic fluid used for magnetic resonance imaging and hyperthermia, J. Magn. Magn. Mater., 323, 2953-2959.

Wei, H., Xu, Q., Taylor, L. E., Baker, J. O., Tucker, M. P., Ding, S. Y. 2009. Natural paradigms of plant cell wall degradation. Curr. Opin. Biotechnol., 20, 330–338.

Weiss, N., Borjesson, J., Pedersen, L.S., Meyer, A.S., 2013. Enzymatic lignocellulose hydrolysis: Improved cellulase productivity by insoluble solids recycling. Biotechnol. Biofuels, 6, 5.

Werpy, T., Petersen, G., Aden, A., Bozell, J., Holladay, J. White, J. Manheim, A., Eliot, D., Lasure, L., Jones, S., 2004. Top value added chemicals from biomass: results of screening for potential candidates from sugars and synthesis gas. Report -August, 2004, Department of Energy, Oak Ridge, TN

Wheals, A.E., Basso, L.C., Alves, D.M.G., Amorim, H.V., 1999. Fuel ethanol after 25 years. Trends Biotechnol., 17, 482-487.

Wu, B.X., 2012. CFD simulation of mixing for high-solids anaerobic digestion, Bio-technol. Bioeng., 109, 2116–2126.

www.NREL.com

Wyman, C. E., 1999. Biomass ethanol: technical progress, opportunities and commercial challenges. Annu. Rev. Energy Env., 24, 189-226.

Wyman, C.E., 2001. Twenty years of trials, tribulations and research progress in bioethanol technology: Selected key events along the way. Appl. Biochem. Biotechnol., 5, 91-93.

Wyman, C.E., Balan, V., Dale, B.E., Elander, R.T., Falls, M., Hames, B., 2011. Comparative data of effects of leading pretreatments and enzyme loadings and formulations on sugar yields from different switchgrass sources. Bioresour. Technol., 102, 11052–11062.

Wyman, C.E., Dale, B.E., Elander, R.T., Holtzapple, M., Ladisch, M.R., Lee, Y.Y., 2005. Coordinated development of leading biomass pretreatment technologies. Bioresour. Technol, 96, 1959-1966.

Ximenes, E., Kim, Y., Felix, S., Mosier, N.S., Ladisch, M.R., 2010. Inhibition of cellulolytic enzymes due to products of hemicelluloses hydrolysis. A Special Conference on the Society for Industrial Microbiology: 32nd Symposium on biotechnology for fuels and chemicals, Clear Water Beach, FL.

Xu, F., Ding, H., Osborn, D., Tejirian, A., Brown, K., Albano, W., Sheehy, N., Langston, J., 2008. Partition of enzymes between the solvent and insoluble substrate during the hydrolysis of lignocellulose by cellulases. J. Mol. Catal. B: Enzym., 51, 42--48.

Xu, F., Ding, H., Tejirian, A., 2009. Detrimental effect of cellulose oxidation on cellulose hydrolysis by cellulase. Enzym. Microb. Technol., 45, 203–209.

Xu, F., Ding, H.S., 2007. A new kinetic model for heterogeneous (or spatially confined) enzymatic catalysis: contributions from the fractal and jamming (overcrowding) effects. Appl. Catal. A: General, 317, 70-81.

Yang, B., Dai, Z., Ding, S.Y., Wyman, C.E., 2011. Enzymatic hydrolysis of cellulosic biomass. Biofuels, 2, 421–450.

Yang, B., Wyman, C.E., 2004. Effect of xylan and lignin removal by batch and flow through pretreatment on the enzymatic digestibility of corn stover cellulose. Biotechnol. Bioeng., 86, 88–95.

Yang, B., Wyman, C.E., 2006. BSA treatment to enhance enzymatic hydrolysis of cellulose in lignin containing substrates. Biotechnol. Bioeng., 94, 611--617.

Yang, B., Wyman, C.E., 2008. Pre-treatment: the key to unlocking low-cost cellulosic ethanol. Biofuel Bioprod. Bioref., 2, 26-40.

Yang, J., Zhang, X., Yong, Q., Yu, S., 2010. Three-stage hydrolysis to enhance enzymatic saccharification of steam-exploded corn stover. Bioresour. Technol., 101, 4930–4935.

Yang, J., Zhang, X.P., Yong, Q.A., Yu, S.Y., 2011. Three-stage enzymatic hydrolysis of steam-exploded corn stover at high substrate concentration. Bioresour. Technol., 102, 4905-4908.

Yang, S., Ding, W., Chen, H., 2006. Enzymatic hydrolysis of rice straw in a tubular reactor coupled with UF membrane. Process Biochem., 41, 721–725.

Yang, S., Ding, W., Chen, H., 2009. Enzymatic hydrolysis of corn stalk in a hollow fiber ultrafiltration membrane reactor. Biomass Bioenergy., 33, 332-336.

Yeh, A.I., Huang, Y.C., Chen, S.H., 2010. Effect of particle size on the rate of enzymatic hydrolysis of cellulose. Carbohyd. Polym., 79, 192–199.

Yu, L., Ma, J., Chen, S., 2011. Numerical simulation of mechanical mixing in high solid anaerobic digester. Bioresour. Technol., 102, 1012–1018.

Zacchi, G., Axelsson, A., 1989. Economic evaluation of pre concentration in production of ethanol from dilute sugar solutions. Biotechnol. Bioeng., 34, 223-233.

Zhang, J., Chu, D., Huang, J., Yu, Z., Dai, G., Bao, J., 2010. Simultaneous saccharification and ethanol fermentation at high corn stover solids loading in a helical stirring bioreactor. Biotechnol. Bioeng., 105, 718–728.

Zhang, L., Qiu, J., Wu, X., Zhang, W., Sakai, E., Wei, Y., 2014a. Preparation of magnetic chitosan nanoparticles as support for cellulase immobilization. Ind. Eng. Chem. Res., 53, 3448−3454.

Zhang, L.P., Zhang, J., Li, C.H., Bao, J., 2014b. Rheological characterization and CFD modeling of corn stover–water mixing system at high solids loading for dilute acid pretreatment. Biochem. Eng. J., 90, 324–332.

Zhang, M., Eddy, M.C., Deanda, K., Finkelstein, M., Picataggio, S., 1995. Metabolic engineering of a pentose metabolism pathway in ethanologenic *Zymomonas mobilis*. Sci., 267, 240-243.

Zhang, M., Zhang, L., Jiang, B., Yin, Y., Li, X., 2008. Calculation of Metzner Constant for Double Helical Ribbon Impeller by Computational Fluid Dynamic Method. Chin. J. Chem. Eng., 16, 686-692.

Zhang, X., Qin, W., Paice, M.G., Saddler, J.N., 2009a. High consistency enzymatic hydrolysis of hardwood substrates. Bioresour. Technol., 100, 5890–5897.

Zhang, Y., Liu, Y.Y., Xu, J.L., Yuan, Z.H., Qi, W., Zhuang, X.S., 2012. High solid and low enzyme loading based saccharification of agriculutural biomass. BioResour, 7, 345-353.

Zhang, Y., Xu, J.L., Yuan, Z.H., 2009b. Modeling and prediction in the enzymatic hydrolysis of cellulose using artificial neural network. Fifth Intern. Conf. Natural Comput., Tianjin, China.

Zhang, Y.H., Lynd, L.R., 2004. Towards an aggregated understanding of enzymatic hydrolysis of cellulose: Noncomplexed cellulase systems. Biotechnol. Bioeng., 88, 797–824.

Zhang, Y.H., Lynd, L.R., 2006. A functionally based model for hydrolysis of cellulose by fungal cellulase. Biotechnol. Bioeng., 94, 888–898.

Zhang, Y.H.P., Ding, S.Y., Mielenz, J.R., Cui, J.B., Elander, R.T., Laser, M., 2007. Fractionating recalcitrant lignocellulose at modest reaction conditions. Biotechnol. Bioeng., 97, 214–223.

Zhao, K., Qiao, Q.A., Chu, D.Q., Gu, H.Q., Dao, T.H., Zhang, J., Bao, J., 2013. Simultaneous saccharification and high titer lactic acid fermentation of corn stover using a newly isolated lactic acid bacterium *Pediococcus acidilactici* DQ2, Bioresour. Technol., 135, 481–489.

Zhao, X., Liu, D., 2011. Fractionating pretreatment of sugarcane bagasse for increasing the enzymatic digestibility of cellulose. Chinese J. Biotechnol., 27, 384–392.

Zhao, X., Wang, L., Liu, D., 2008. Peracetic acid pretreatment of sugarcane bagasse for enzymatic hydrolysis: a continued work. J. Chem. Technol. Biotechnol., 83, 950–956.

Zhao, X., Zhang, L., Liu, D., 2012. Biomass recalcitrance. Part I: the chemical compositions and physical structures affecting the enzymatic hydrolysis of lignocellulose. Biofuels, Bioprod. Bioref. DOI: 10.1002/bbb

Zheng, Y., Pan, Z., Zhang, R., 2009. Overview of biomass pretreatment for cellulosic ethanol production. Int. J. Agric. Biol. Eng., 2, 51–68.

Zhou, J., Wang, Y.H., Chu, J., Luo, L.Z., Zhuang, Y.P., Zhang, S.L., 2009. Optimization of cellulase mixture for efficient hydrolysis of steam-exploded corn stover by statistically designed experiments. Bioresour. Technol., 100, 819–825.

Zhu, J.Y., Wang, G.S., Pan, X.J., Gleisner, R., 2009. Specific surface to evaluate the efficiencies of milling and pretreatment of wood for enzymatic saccharification. Chem. Eng. Sci., 64, 474–485.

Zhu, L., O'Dwyer, J.P., Chang, V.S., Granda, C.B., Holtzapple, M.T., 2008. Structural features affecting biomass enzymatic digestibility. Bioresour. Technol., 99, 3817–3828.

Zhu, P., Moran-Mirabal, J.M., Luterbacher, J.S., Walker, L.P., Craighead, H.G., 2011. Observing *Thermobifida fusca* cellulase binding to pretreated wood particles using time-lapse confocal laser scanning microscopy. Cellulose, 18, 749–758.

Zilliox, C., Debeire, P., 1998. Hydrolysis of wheat straw by a thermostable endoxylanase: Adsorption and kinetic studies. Enzyme Microb. Technol., 22, 58–63.

Zimbardi, F., Viola, E., Gallifuoco, A., de Bari, I., Cantarella, M., Barisano, D., Braccio, G., 2002. Overview of the ethanol production, Report ENEA and University of L'Aquila.

Luo, J.Y., Gosman, A.D., Issa, R.L., Middleton, J.C., Fitzgerald, M.K., 1993. Full flow fields computation of mixing in baffle stirred vessels. Chem. Eng. Res. Des., 71. 342-344.

APPENDIX 1

LIST OF ABBREVIATIONS

µ	Micron
µl	microliter
µm	micrometer
^{0}C	Degree Celsius
Å	Angstrom
Ab	Antibody
AFEX	Ammonia Fiber Explosion
AFM	Atomic Force Microscopy
ANN	Artificial Neural Network
APL	Acid Pretreated Liquor
APTES	3- amino propyl- tri ethoxysilane
ASA	Accessible Surface Area
BET	Brunauer, Emmett and Teller
BGL	β- Glucosidase
BSA	Bovine Serum Albumin
CBD	Cellulose Binding Domain
CBH	Cellobiohydrolase
CBU	Cellobiose Unit
CD	Catalytic Domain
CFD	Computational Fluid Dynamics
CIP	Cellulase Induced Protein
cm	Centimeter
CMC	Carboxy Methyl Cellulose
CMCase	Carboxy Methyl Cellulase
CBP	Consolidated Bioprocessing

CSIR	Council of Scientific and Industrial Research
CVD	Chemical Vapor Deposition
DLS	Dynamic Light Scattering
DNA	Deoxy Ribonucleic Acid
DNS	3,5 – Dinitro salicylic acid
DOE	Design of Experiments
DP	Degree of Polymerization
EG	Endoglucanse
EISA	Energy Independence and Security Act
ETP	Effluent Treatment Plant
FITC	Fluorescein Isothiocyanite
FPS	Foot per second
FPU	Filter Paper Units
FT Diesel	Fisher –Tropsch Diesel
FTIR	Fourier Transform Infrared
g	Gram
GA	Genetic Algorithm
gal	Gallon
GEN PLAT	Genius Ultimate Platform
GFP	Green Fluorescent Protein
GH	Glycosyl Hydrolase
GHG	Green House Gases
GT	Giga Tonnes
h	Hour
HMF	Hydroxymethyl furfural
HPLC	High Performance Liquid Chromatography
IEA	International Energy Agency
IgG	Immunoglobulin G

IPCC	Intergovernmental Panel on Climate Change
IU	International Units
kDa	KiloDalton
Kg	Kilogram
kHz	KiloHertz
KV	KiloVolt
KW	KiloWatt
L	Liter
LO	Ligninolytic Oxidoreducatses
M	Molar
m	Meter
m/s	meter/second
mA	Milliampere
mg	Milligram
min	Minutes
MJ	Mega Joule
MJ/Kg	Mega Joule/Kilogram
MJ/L	Mega Joule/Liter
mL	Milliliter
mL/min	Milliliter/ minute
MLP	Multi Layer Perceptron
mm	Millimeter
mM	Millimolar
MMT	Million Metric Tonnes
MNP	Magnetic Nanoparticle
MPa	MegaPascal
MPP	Minimum Purchase Price
MRF	Multiple Reference Frame

MSE	Mean Square Error
MSP	Minimum Support Price
MTBE	Methyl tert- butyl ether
N/m	Newton/ meter
NC	Negative control
NIIST	National Institute for Interdisciplinary Science and Technology
nm	Nanometer
Nm	Newton-meter
NREL	National Renewable Energy Laboratory
OECD	Organization for Economic Co-operation and Development
OMC	Oil Marketing Companies
Pa.s	Pascal-second
PC	Positive Control
PEA	Policy Energy Act
PEG	Poly Ethylene Glycol
PHA	Poly Hydroxy Alkanoate
pNP	p-Nitrophenol
pNPG	p-nitrophenyl –β-D glucopyranoside
R^2	Regression coefficient
RI	Refractive Index
RMS	Root Mean Square
RPM	Rotations per Minute
rps	Rotations per second
s	Second
SB	Semi Batch
SDS PAGE	Sodium Dodecyl Sulphate Polyacrylamide Gel Electrophoresis

SEM	Scanning Electron Microscope
SHF	Separate Hydrolysis and Fermentation
SS	Stainless Steel
SSA	Specific Surface Area
SSCF	Simultaneous Saccharification and Co-Fermentation
SSF	Simultaneous Saccharification and Fermentation
STR	Stirred Tank Reactor
TGA	Thermo Gravimetric Analysis
TIFAC	Technology Information, Forecasting and Assessment Council
TRS	Total Reducing Sugar
U	Units
USA	United States of America
UV	Ultra Violet
v/v	Volume by Volume
VOC	Volatile Organic Compounds
w/v	Weight by Volume
w/w	Weight by weight
XRD	X-Ray Diffraction

APPENDIX 2

LIST OF SYMBOLS

W_{kj}	weight connecting the j^{th} neuron in the hidden layer to the k^{th} neuron in the output layer
b_k	bias of the k^{th} neuron in the output layer
d_k	experimental output
g_k	predicted output of neural network
θ_j	bias of the j^{th} neuron in the hidden layer
μ	Apparent viscosity
b	Bias of model
D	Rate of strain tensor
D	Tank Diameter
D_i	Impeller Diameter
F	External Force
$f(\cdot)$	activation functions of j^{th} neuron in the hidden layer
$F(\cdot)$	activation functions of k^{th} neuron in output layer
g	Gravity
H	Tank Diameter
I	Unit tensor
K	Number of neurons in output layer
K	Flow consistency index
M	Number of neurons in hidden layer
N	Number of neurons in input layer
n	Flow behavior index
N_i	Tip Speed
N_P	Power Number
N_{Re}	Reynold's Number

P	Impeller power
p	Pressure
u_r	whirl velocity due to the moving frame
v	Velocity
w	Weights of neural network model
w_{ji}	weight connecting i^{th} neuron in the input layer to the j^{th} neuron in the hidden layer
γ	Shear stress rate
λ	Wave length
ρ	Density
τ	Shear stress
τ_r	the stress tensor based on v_r
υ_r	relative velocity viewed from the rotating frame
ω	Angular velocity
$\partial u/\partial y$	Shear rate

APPENDIX 1

LIST OF TABLES

APPENDIX 4

LIST OF FIGURES